FAK and SRC Kinases Maintain Integrin Activation During Endocytic Recycling to Polarize Adhesion Formation

Guilherme Pedreira de Freitas Nader

Submitted in partial fulfillment of the

requirements for the degree of

Doctor of Philosophy

under the Executive Committee

of the Graduate School of Arts and Sciences

COLUMBIA UNIVERSITY

2015

ABSTRACT

FAK and SRC Kinases Maintain Integrin Activation During Endocytic Recycling to Polarize Adhesion Formation

Guilherme Pedreira de Freitas Nader

Integrin recycling has been generally assumed to be important for cell migration but the trafficking pathways and the molecules regulating integrin trafficking remain poorly characterized. Furthermore, little is known about the activation status of endocytosed integrins and how it affects the recycling of these receptors. It is likely that FA-engaged integrins will follow different trafficking pathways than bulk integrins and here I sought to study the endocytic fate of this particular integrin pool using the MT-induced FA disassembly assay. I found that integrins previously resident at FAs travel through different Rab compartments after FA disassembly and that their return to the plasma membrane is Rab11- and Src-dependent. Strikingly, I unveiled new functions for FAK and Src family kinases in this process by showing that these kinases are critical to keep integrins active during endocytic trafficking. This finding is unprecedented since it was not known whether endocytosed integrins were kept active during their trafficking. Interestingly, reassembly of FAs from endocytosed integrin occurred preferentially at the leading edge of migrating cells suggesting that integrins are trafficked in a polarized fashion. Furthermore, the recycling of integrins from the Rab11-positive compartment to the plasma membrane is a long-range transport implying the existence of a MT motor committed to this task. Consistently, I identified that a kinesin-II motor, Kif3AC, is engaged in

this process. My work establishes a FAK- and Src family kinases-based mechanism for integrin "adhesion memory" during endocytic trafficking and identifies a direct link between FA disassembly and reassembly through an endocytic recycling pathway involving Rab5 and Rab11 and a kinesin-II family member.

TABLE OF CONTENTS

LIST OF FIGURES ..... **iv**

ACKNOWLEDGEMENTS ..... **vii**

INTRODUCTION **1**

Cell Migration 1

Integrins and Adhesion During Cell Migration 2

Complexity of Focal Adhesions 3

Focal adhesion assembly 5

Focal Adhesion Disassembly 7

Focal Adhesion Kinase 10

Integrin Activation 13

Integrin Trafficking 16

Role of Microtubule Motors in Endocytic Recycling and Polarized Trafficking 21

Chapter 1: FAK and Src Kinases Maintain Activation of Endocytosed Integrin for Rapid and Polarized Reformation of Adhesions **26**

Abstract 27

Introduction 28

Results 32

Discussion 43

Figures 47

Material And Methods 91

Chapter 2: The Heterodimer Kif3AC is a Microtubule Motor for Polarized Integrin Trafficking in Migrating Cells **97**

Abstract 98

Introduction 99

Results 101

Discussion 103

Figures 106
Material And Methods 119
Chapter 3: Talin but not Other Integrin Activation Regulators is Required for Focal Adhesion Reassembly 122
Introduction 123
Results And Discussion 124
Figures 129
Material And Methods 150
Chapter 4: Kif4 Interacts with EB1 and Stabilizes Microtubules Downstream of Rho-mDia in Migrating Fibroblasts 154
Abstract 155
Introduction 156
Results 160
Discussion 166
Figures 170
Material And Methods 199
DISCUSSION 204
BIBLIOGRAPHY 220

LIST OF FIGURES

Figure 1. Model system to study FA turnover and integrin recycling. 22

Figure 2. Focal adhesion kinase domain structure and phosphorylation sites. 24

Figure 3. FA reassembly occurs with a lag of 30 minutes after disassembly. 48

Figure 4. FA reassembly as assayed with additional FA markers. 50

Figure 5. Characterization of paxillin-EGFP NIH3T3 fibroblast cell line. 52

Figure 6. FA reassembly involves endocytic recycling. 54

Figure 7. Analysis of total integrin levels and of dominant negative Rab5 during MT induced FA disassembly. 56

Figure 8. Localization of α5 integrin-GFP in the Rab11 ERC after FA disassembly. 58

Figure 9. FAK kinase activity is dispensable for FA disassembly but critical for FA reassembly. 60

Figure 10. FAK and SFKs activities are required for FA adhesion reassembly. 62

Figure 12. Biochemical analysis of FA disassembly and reassembly after inhibition of FAK or SFKs. 66

Figure 13. Src localizes to the Rab11 ERC after FA disassembly. 68

Figure 14. SFKs mediate integrin trafficking from the ERC. 70

Figure 15. FAK inhibitor causes impaired cell adhesion and blocks FA reassembly by affecting integrin activation. 72

Figure 16. Manganese does not rescue FA reassembly in Rab11-depleted cells. 74

Figure 17. FAK inhibitor blocks FA reassembly without interfering with FA disassembly in HT1080 fibrosarcoma cells. 76

Figure 18. FAK kinase activity maintains integrin in an active state after FA disassembly and during endocytic recycling. 78

Figure 19. FAK-pY397 colocalizes with active integrin following FA disassembly in HT1080 fibrosarcoma cells. 81

Figure 20. Dynasore blocks FA disassembly in HT1080 fibrosarcoma cells. 83

Figure 21. FAK and SFKs inhibitors mitigate migration. 85

Figure 22. The effects of FAK and SFK inhibitors on migrating NIH3T3 fibroblasts are consistent with their role in regulating integrin activation and recycling. 87

Figure 23. Proposed model for polarized FA reassembly mediated by recycling of integrins previously resident at FAs. 89

Figure 24. Kif3A depleted NIH3T3 fibroblasts exhibit small FAs. 107

Figure 25. Kif3A and Kif3C but not Kif 3B are required for FA reassembly. 109

Figure 26. KAP3 is not required for FA reassembly. 111

Figure 27. Kif3A-tail-microinjected NIH3T3 fibroblasts display impaired FA reassembly. 113

Figure 28. Kif3A localizes to the ERC after FA disassembly and during cell migration. 115

Figure 29. Kif3A is a motor for integrin trafficking and is important for cell migration. 117

Figure 30. Models for integrin (re)activation during endocytic recycling. 130

Figure 31. Talin1 is required for FA reassembly. 132

Figure 32. Kindlin is not required for FA reassembly. 134

Figure 33. Overexpression of full length talin or talin head (1-405) does not rescue FA reassembly in FAK-inhibited cells. 136

Figure 34. Talin binding to FAK is not required for FA reassembly. 138

Figure 35. Overexpression of PIPK1 γ 90 rescues FA reassembly in FAK-inhibited cells. 140

Figure 36. The phospholipid PI(4,5)P_2 rescues FA reassembly in FAK-inhibited cells but PI(4,5)P_2 levels remain unchanged. 142

Figure 37. Rho activator rescues FA reassembly in FAK-inhibited cells. 144

Figure 38. SHARPIN depletion does not rescue FA reassembly in FAK-inhibited cells. 146

Figure 39. Migfilin (1-85aa) overexpression does not rescue FA reassembly in FAK-inhibited cells. 148

Figure 40. Kif4 motor domain induces the formation of stable Glu MTs in starved NIH3T3 fibroblasts. 171

Figure 41. Analysis of Kif17 expression in NIH3T3 fibroblasts. 173

Figure 42. Knockdown of Kif4 inhibits LPA-induced formation of Glu MTs in NIH3T3 fibroblasts. 175

Figure 43. Western blot of Kif4 knockdown using a second siRNA. 177

Figure 44. LPA stimulates normal actin fiber formation in Kif4 siRNA-treated NIH3T3 fibroblasts..... 179

Figure 45. Localization of endogenous Kif4 in interphase cells. 181

Figure 46*. Immunofluorescence images of Kif4 and Tyr MTs in noncoding (NC) and Kif4 siRNA-treated cells. 183

Figure 47. Kif4 localization on Glu MT ends in TC-7 cells..... 185

Figure 48. Kif4 functions downstream of mDia in the Rho-mDia-EB1 MT stabilization pathway..... 187

Figure 49*. GFP-Kif4 motor expression does not change the distribution of mDia1 or EB1. 189

Figure 50. Expressed Kif4 and EB1 require each other to induce Glu MTs. 191

Figure 51*. Western blot of EB1 knockdown using EB1 siRNA. 193

Figure 52. Kif4 interacts directly with EB1. 195

Figure 53*. Kif4 knockdown inhibits cell migration into wounded monolayers. 197

Figure 54. Proposed model for polarized FA reassembly mediated by a kinesin II-driven integrin trafficking. 216

Figure 55. Different FA markers localize to the ERC following FA disassembly. 218

ACKNOWLEDGEMENTS

I have no words to describe my gratitude for the mentorship provided by Gregg. He was always available to talk and provided me guidance on scientific writing, experimental design and troubleshooting. Moreover, his excitement for science is contagious and certainly had a huge impact on the admiration and passion that I have today for science. I definitely could not have chosen a better lab to develop my thesis research. Also I would like to thank all the current and former lab members: Wakam, Claire, Susumu, Francesca, Nagendran, Ellen, Safiya, Ruijun, Anna, Sara, Alba, Lily and Frank for the support and guidance and for providing a very pleasant working environment.

I am also thankful to all of my committee members: Dr. Gil DiPaolo, Dr. Eugene Marcantonio and Dr. Jan Kitajewski for the valuable advices and guidance throughout my tenure as a graduate student. I also would like to thank Dr. Ellen Ezratty for providing the initial "spark" for this work and agreeing to be part of my thesis committee.

I would like to thank Dr. Zaia Sivo for the all the help and support during my PhD and also Dr. Richard Kessin for helping me during my preparation for my talk at the ASCB in San Francisco. Additionally I would like to thank Dr. Ron Liem for believing in my potential and for the constant support during my PhD.

Lastly I would like to thank my parents, family and friends for their unconditional support through the pursuit of my PhD degree.

INTRODUCTION

CELL MIGRATION

Cell migration is an evolutionary conserved physiological mechanism that orchestrates embryonic development and functioning and continues to play critical role through life. For instance, migration constitutes a prominent component of tissue repair and immune surveillance and contributes to several important pathological processes, including vascular disease, osteoporosis, chronic inflammatory diseases, cancer and mental retardation (Ridley et al., 2003).

Migration is a cyclical process and the general mechanism involves the repetition of four basic steps: (a) leading edge protrusion, (b) adhesion, (c) cell body contraction, and (d) rear retraction (Vicente-Manzanares et al., 2009). A hallmark of cell migration is that these different steps must be coordinated in time and space. Membrane protrusion is driven by actin polymerization via the small Rho GTPases Rac and Cdc42 (Borisy and Svitkina, 2000; Etienne-Manneville and Hall, 2001) and is required for the formation of new adhesions, which transmit propulsive forces and serve as traction points over which the cell moves.

Polarity is intrinsic to a migrating cell and spatial regulation must prevent protrusions from occurring along the entire cell periphery and contraction from developing randomly to avoid disorganized cell motility and stalling of the cell body displacement (Etienne-Manneville, 2013). The polarized organization of a migrating cell results from directed vesicle trafficking towards the leading edge, organization of microtubules (MTs), and the localization of the MT organizing centre (MTOC) and Golgi apparatus in front of the nucleus. Importantly, these events are paralleled by the polarized distribution of active signaling molecules (Etienne-Manneville, 2013).

One model for how migrating cells maintain polarity is based on the fact that the members of the family of small Rho GTPases, Rho and Rac, are mutually antagonistic, each suppressing the other's activity (Evers et al., 2000). Active Rac at the leading edge of cells would suppress Rho activity, whereas Rho would be more active at the sides and rear of the cell and suppress Rac activity, thereby preventing Rac-mediated protrusion at sites other than the leading edge (Worthylake and Burridge, 2003; Xu et al., 2003). Despite this model of Rac-Rho antagonism, measurements of active GTPases show that Rho is also active at the leading edge (Pertz et al., 2006) and actually precedes Rac and Cdc42 activation (Machacek et al., 2009). These results suggest that the activity of Rac/Rho must be tightly coordinated during migration.

INTEGRINS AND ADHESION DURING CELL MIGRATION

Although many different receptors are involved in the migration of different cell types, the integrins are a major family of migration-promoting receptors that act as the "feet" of a migrating cell by supporting adhesion to the extracellular matrix (ECM) by linking with actin filaments on the inside of the cell via adapters such as talin1 (Critchley, 2005; Geiger et al., 2001). Integrins are glycoproteins that play central roles in the biology of metazoan by controlling cell adhesion and cell migration, growth, differentiation and apoptosis. They constitute heterodimeric αβ receptors with large ligand-binding extracellular domains, a single transmembrane domain and a generally short cytoplasmic tail. In mammals, they consist of 18 α-subunits and 8 β-subunits that assemble into 24 different integrins capable of binding several ECM substrates such as laminin, fibronectin (FN), collagen, and vitronectin (Hynes, 2002; van der Flier and Sonnenberg, 2001).

Although integrins themselves do not have intrinsic catalytic activity, signals are transmitted through direct and indirect interactions with many partners at sites termed focal adhesions (FAs),

which are sites of clustered integrins and associated proteins that mediate connection to the actin cytoskeleton and transmit signals. Thus by connecting the ECM to the intracellular cytoskeleton, integrins serve as both traction sites over which the cell moves and as mechanosensors, transmitting information about the physical state of the ECM into the cell and altering cytoskeletal dynamics (Beningo et al., 2001; Galbraith et al., 2002; Lauffenburger and Horwitz, 1996). The binding of ligands to the extracellular portion of integrins leads to conformational changes in the receptors by changing interactions between the α- and β-chain transmembrane and cytoplasmic domains leading to integrin clustering (Emsley et al., 2000). This combination of occupancy and clustering initiates intracellular signals ("outside-in" signaling) such as protein tyrosine phosphorylation, activation of small GTPases and changes in phospholipid biosynthesis that regulate the formation and strengthening of adhesion sites, the organization and dynamics of the cytoskeleton and cell polarity during migration (Geiger et al., 2001). Likewise, cytoplasmic signals can also influence the activation status and ligand-binding competency of integrins ("inside-out" signaling). Thus integrins are known as receptors that transduce signals in a bidirectional fashion (Hynes, 2002; Schwartz, 2001; Shattil et al., 2010).

COMPLEXITY OF FOCAL ADHESIONS

FAs have been the objects of intense study and much has been learned about many of their major components, structure, dynamics and the signaling pathways that emanate from them. Adhesions of fibroblasts to the underlying substratum were first observed by electron microscopy, where they were described as "dense plaques" which appeared to anchor "bundles of microfilaments" (today known as stress fibers) at the ventral plasma membrane (Abercrombie and Dunn, 1975; Abercrombie et al., 1971; Izzard and Lochner, 1976; Izzard and Lochner, 1980). At the light microscope level, the technique of interference reflection microscopy (IRM)

(Curtis, 1964) was used to show that these dense adhesion plaques seen by electron microscopy coincided with regions that came closest to the substratum, appearing most dark by IRM. They called these structures “feet” and through many observations concluded that they were sites of cell adhesion and therefore must play critical role on cell locomotion (Abercrombie, 1978; Abercrombie and Dunn, 1975; Abercrombie et al., 1977; Abercrombie et al., 1971).

The classification of adhesions is based on morphology, composition and method of formation and include, FAs, focal complexes (FCs), fibrillar adhesions and podosomes (Webb et al., 2002). FAs are large integrin clusters that are composed of numerous proteins, including paxillin, vinculin, talin, focal adhesion kinase (FAK) and high levels of tyrosine-phosphorylated proteins, whereas FCs are small adhesions near the leading edge of a protrusion that are induced by Rac activation and can mature into FAs (Nobes and Hall, 1995; Rottner et al., 1999). Fibrillar adhesions are elongated, central structures, which contain tensin but have low levels of paxillin, vinculin and tyrosine-phosphorylated proteins (Katz et al., 2000; Pankov et al., 2000; Zamir and Geiger, 2001). Lastly, podosomes are actin-based dynamic protrusions of the plasma membrane that represent sites of attachment to — and degradation of — the ECM. Key players include the actin regulators cortactin and neural Wiskott-Aldrich syndrome protein (N-WASP), the tyrosine kinase Src and the transmembrane membrane type 1 matrix metalloprotease (MMP1) (Murphy and Courtneidge, 2011).

Currently more than 150 proteins have been reported to be associated with FAs and related ECM adhesions (Zaidel-Bar et al., 2007). Most of these contain multiple domains through which they can interact with other molecular partners, potentially forming a dense and heterogeneous protein network at the cytoplasmic faces of the adhesion site (Zamir and Geiger, 2001). Since most components of FAs contain multiple binding sites for other components, the molecular

ensemble can, theoretically, assemble in alternative ways, thus giving rise to different supramolecular structures and signaling platforms (Zamir and Geiger, 2001). Sorting these structures according to their presumed functions reveals cytoskeletal proteins (e.g. tensin, vinculin, paxillin, α-actinin and talin), tyrosine kinases (e.g. Src, FAK, PYK2, Csk and Abl), serine/threonine kinases (e.g. Integrin Linked Kinase-ILK, PKC and PAK), modulators of small GTPases (e.g. ASAP1 and GRAF) and tyrosine phosphatases (e.g. SHP-2). Some of these proteins can directly bind, cap, bundle or nucleate actin filaments (e.g. vinculin, tensin, α-actinin and VASP,) and/or directly bind to the cytoplasmic tails of integrins (e.g. talin, tensin, FAK, ILK and α-actinin) (Zamir and Geiger, 2001).

FOCAL ADHESION ASSEMBLY

Cell migration is a physically integrated molecular process. In order to migrate cells need to constantly assemble and disassemble their FAs, a process called FA turnover. The signaling cascades involved in FA assembly are well understood and most of the findings came from adhesion and spreading assays performed on different matrices. Moreover, since Rho GTPase was known to be activated by growth factors and to be required for adhesion formation following integrin activation, additional findings came from studies where serum-starved cells were treated with growth factors to activate this pathway (Ridley and Hall, 1992; Ridley et al., 1992).

The formation of the adhesion complexes occurs underneath the lamellipodia, a thin, veil-like structure filled with a dynamic branching actin network generated by actin nucleation mediated by the actin-related protein 2/3 (Arp2/3) complex (Small et al., 2002). The small GTPases Rac and Ccd42 are critical players in the first steps of adhesion formation (Guo et al., 2006). They contribute to cell migration by mediating the formation of FCs thus allowing the attachment of the protruding lamellipodium to the ECM. Interestingly, FCs depend on actin

polymerization but they do not require myosin II activity (Choi et al., 2008). Subsequently, these sites can either undergo a rapid turnover at the rear of the lamellipodium or grow into FAs in the lamella (Parsons et al., 2010). Maturation occurs along an α-actinin–actin template that elongates centripetally from nascent adhesions (Choi et al., 2008) and relies on both the formation of actin filaments mediated by the formin mDia (Geneste et al., 2002; Li and Higgs, 2003) and on the force transmitted to these sites derived from Rho-mediated acto-myosin contractility (Amano et al., 1996). The key player in the FA-maturation signaling pathway is the Rho effector Rho kinase (ROCK). This kinase promotes myosin-II activity by phosphorylating and inhibiting MLC phosphatase and perhaps by directly phosphorylating myosin light-chain (MLC) (Amano et al., 1996; Kimura et al., 1996). This in turn leads to crosslinking of actin filaments and increased tension at the adhesion sites (Vicente-Manzanares et al., 2009). Ultimately, the cooperation between the two Rho effectors mDia and ROCK leads to augmented contractility and adhesion maturation (Nakano et al., 1999). Interestingly, while integrin activation plays a central role in adhesion formation during platelet aggregation (see below), models for FA assembly do not specifically indicate a separate step of integrin activation. They assume either that the integrin is activated by ECM binding or that it is constitutively active. The ensuing steps in FA formation include the recruitment of additional components that promote integrin clustering and reinforcement of the integrin–cytoskeleton bonds. In particular, the binding of vinculin to talin triggers the clustering of activated integrins (Humphries et al., 2007) and, through the vinculin tail, their association with actin, thereby strengthening the actin–integrin link (Galbraith et al., 2002).

FOCAL ADHESION DISASSEMBLY

The application of traction forces to the substrate is the result of the force-producing actin–myosin network interacting with force-transmitting FAs. In this way, cellular tractions can be considered as a function of both actin flow and FA turnover (Gardel et al., 2010; Hu et al., 2007; Lapierre et al., 2001). FA turnover has been described as a key component for cell migration and the dynamics of FA disassembly and reassembly and the regions where these events take place in a migrating cell have been characterized (Berginski et al., 2011; Mohl et al., 2012; Smilenov et al., 1999). Assembling FAs are exclusively found at the leading edge, which is also the zone of pronounced FA nucleation. Directly behind the leading edge, there is a sharp change from assembling to disassembling FAs. Disassembly of FAs, however, occurs in the front and rear parts of the cell (Mohl et al., 2012; Smilenov et al., 1999). The next two sections consider the mechanisms underlying FA disassembly.

Microtubules

Well known for its key role during cell division and in vesicular transport, the MT cytoskeleton has also been revealed as an essential component of migration (Vasiliev et al., 1970). Low concentrations of nocodazole (NZ) or taxol block cell migration by inhibiting MT dynamic instability without affecting MT polarity or abundance (Liao et al., 1995; Mikhailov and Gundersen, 1998; Tanaka et al., 1995). Interestingly, MTs have also been linked to FA dynamics and signaling. For instance, it was shown that MT destabilization in serum-starved cells is associated with contractility- and ECM-dependent growth of FAs via assembly of the FA proteins vinculin and paxillin into primordial adhesion sites. This was shown to be accompanied by initiation of signal transduction events, including the tyrosine phosphorylation of FAK and paxillin (Bershadsky et al., 1996; Musse et al., 2012; Pletjushkina et al., 1998).

Further evidence supporting the involvement of MTs in adhesion dynamics came from studies performed by Vic Small's group. They observed that in migrating fibroblasts some FAs are targeted for disassembly by contact with the dynamic ends of MTs in a process sometimes referred to as the "kiss of death" (Kaverina et al., 1999; Kaverina et al., 1998). As multiple MT targeting events were required, and MTs did not need to remain in contact with the disassembling FA, they proposed that MTs delivered a "relaxing factor" to FAs in a precise, site-specific manner (Kaverina et al., 1999). Based on these observations, the Gundersen laboratory developed an assay where MT regrowth after NZ washout synchronously induces FA disassembly and integrin endocytosis allowing the temporal segregation (and study) of both FA disassembly and reassembly (Figure 1) (Ezratty et al., 2009; Ezratty et al., 2005). Using this assay, the Gundersen laboratory and others have shown that FA disassembly constitutes an endocytic process that involves dynamin, clathrin, clathrin adaptors (Dab2, ARH and AP-2) and FAK (Chao and Kunz, 2009; Ezratty et al., 2009; Ezratty et al., 2005; Wang et al., 2011b). Another clathrin adaptor protein, Numb, was shown to bind to integrin and to affect integrin endocytosis in migrating cells, but it may function in endocytosis of unengaged integrins (Nishimura and Kaibuchi, 2007).

Alternatively, MT-dependent transport processes directly contribute to the delivery of proteases to sites of degradation (Steffen et al., 2008; Wiesner et al., 2010). Degradation of the ECM by matrix metalloproteases such as MT1-MMP/MMP-14 alters integrin engagement with the ECM and facilitates FA turnover (Takino et al., 2006). Accordingly, MT1-MMP was shown to be exocytosed in proximity to FAs and promote local ECM degradation and integrin endocytosis (Shi and Sottile, 2011; Stehbens et al., 2014; Takino et al., 2007; Wang and McNiven, 2012). Interestingly, the identity of the "relaxing factor" is still unknown although it

has been suggested that it might be some component that stimulates clathrin- and dynamin-dependent endocytosis (Chao and Kunz, 2009; Ezratty et al., 2009; Ezratty et al., 2005; Wang et al., 2011b). Additionally, kinesin-I has been proposed to be the motor for the "relaxing factor" since interfering with it led to increased FA size (Krylyshkina et al., 2002). However, in direct tests of kinesin-I in the MT-induced FA disassembly assay no effect was observed when this motor was inhibited (Ezratty, E.J., unpublished results).

Tension and retraction at the rear

At the rear of migrating cells, adhesions must also disassemble. In fibroblasts, the rearmost adhesions often tether the cell strongly to the substratum. Increased contractility and transmission of tension to sites of adhesion can be sufficient to physically break the linkage between integrin and the actin cytoskeleton, with the result that integrin is left behind while the rest of the cell moves on (Ridley et al., 2003). In addition, the tension generated in migrating cells by strong adhesions in the rear can be sufficient to open stretch-activated calcium channels (Lee et al., 1999). Potential targets for calcium are the calcium-regulated phosphatase calcineurin and the calcium-activated protease calpain, which is also activated by ERK and has the potential to cleave several FA proteins, including integrins, talin, vinculin, and FAK (Glading et al., 2002; Hendey et al., 1992).

Regulated-FA assembly and disassembly is a critical component of the front-to-rear polarity of the cell, most apparently by formation of a lamellipodium at the front and contractile actin bundles at the rear. Thus, it is likely that signaling pathways controlling FA dynamics will influence cell polarization. In line with this hypothesis, FAK has been shown to promote the reorganization of the cytoskeleton and to induce stress fiber assembly (Mitra et al., 2005).

FOCAL ADHESION KINASE

FAK is a ubiquitously expressed 125-kDa cytoplasmic tyrosine kinase that regulates migration and proliferation (Mitra et al., 2005). It plays an essential role during embryonic development and in the pathogenesis of human disease, including cancer and cardiovascular disease (Golubovskaya et al., 2009; Vadali et al., 2007). Interestingly, FAK has been described as both a signaling kinase and as an adaptor/scaffold protein, which places FAK in a position to modulate various intracellular signaling pathways. Additionally, a kinase related to FAK, PYK2, has been shown to play a redundant role (Mitra et al., 2005).

Molecular structure of FAK

Sequence and structural analysis reveals four distinct domains within FAK: an N-terminal FERM (protein 4.1, ezrin, radixin and moesin homology) domain, a central kinase domain, a proline-rich region and a C-terminal FA targeting (FAT) domain (Mitra et al., 2005) (Figure 2). The FERM domain of FAK has been shown to be involved in signaling from receptor tyrosine kinases such as the epidermal growth factor receptor (EGFR) and the platelet-derived growth factor receptor (PDGFR) (Sieg et al., 2000). It can also bind to and promote the integrin- and FAK-mediated activation of other non-receptor tyrosine kinases (Chen et al., 2001). The C-terminal domain contains two proline-rich regions that function as binding sites for Src-Homology (SH)3-domain-containing proteins. SH3-domain-mediated binding of the adaptor protein p130Cas to FAK is important in promoting cell migration through the coordinated activation of Rac at membrane extensions (Hanks et al., 2003; Wozniak et al., 2005). The SH3-mediated binding of other proteins, such as GRAF and ASAP1 connects FAK to the regulation of cytoskeletal dynamics and FA assembly (Parsons, 2003). The C-terminal domain of FAK also encompasses the FAT region, which promotes the colocalization of FAK with integrins at FA.

Whereas it was first hypothesized that FAK might bind directly to the cytoplasmic tails of integrins (Schaller, 2001), accumulated evidence supports an indirect association of FAK with integrins through binding to integrin-associated proteins such as paxillin and talin (Schlaepfer et al., 2004). Additionally the tyrosine residue Y925 in the FAT domain was reported to bind the adaptor protein GRB2 (Kharbanda et al., 1995; Schlaepfer and Hunter, 1996) which in turn recruits dynamin and triggers FA disassembly (Ezratty et al., 2005; Wang et al., 2011b).

FAK activation and phosphorylation

FAK can be activated by integrin-, G-protein-coupled receptors- or growth factors-linked stimuli (Mitra et al., 2005; Sieg et al., 2000; Streblow et al., 2003). The best-characterized FAK phosphorylation event is autophosphorylation at Tyr397, which can occur in either cis or trans (Toutant et al., 2002). Another direct FAK substrate is N-WASP, which functions to activate the Arp2/3 complex to promote both actin branching and nucleation of F-actin assembly (Wu et al., 2004). Phosphorylation of FAK at Tyr397 creates a motif that is recognized by various SH2-domain-containing proteins, such as Src Family Kinases (SFKs), phospholipase Cγ (PLCγ), growth-factor-receptor-bound protein-7 (GRB7), the Shc adaptor protein, p120 RasGAP and the p85 subunit of phosphatidylinositol 3-kinase (PI3K) (Hanks et al., 2003; Parsons, 2003; Schaller, 2001; Schlaepfer et al., 2004). It is the transient recruitment of SFKs into a signaling complex with FAK that is one of the first events associated with FAK tyrosine phosphorylation and activation (Schlaepfer et al., 2004). Src-mediated transphosphorylation of FAK within the kinase domain activation loop at Tyr576 and Tyr577 promotes maximal FAK catalytic activation (Hanks et al., 2003). Within this FAK–Src complex, Src phosphorylates FAK at Tyr861, and this is associated with an increase in SH3-domain-mediated binding of p130Cas to the FAK C-terminal proline-rich regions (Lim et al., 2004). Additionally, the FA component paxillin was shown to be phosphorylated by FAK-Src-associated signaling (Bellis et al., 1995; Schaller and

Parsons, 1995). Activated Src also phosphorylates FAK at Tyr925, which creates an SH2-binding site for the GRB2 adaptor protein that recruits dynamin (Kharbanda et al., 1995; Schlaepfer and Hunter, 1996).

FAK signaling and effects on GTPases

Studies using knockout mice revealed that FAK deletion resulted in defective developmental morphogenesis (Ilic et al., 1995). As FAK-null fibroblasts show excessive, rather than decreased FA assembly, FAK signaling has been associated with the disassembly of integrin-based adhesion sites (Webb et al., 2002). Additionally, the loss of FAK expression disrupts MT polarization within cells (Palazzo et al., 2004) and $FAK^{-/-}$ cells display somewhat elevated RhoA activity (Ren et al., 2000). Altogether these findings linked FAK to the regulation of the Rho-family GTPases. In concurrence with this hypothesis, pharmacological inhibitors of ROCK partially reverse the polarization defects of $FAK^{-/-}$ cells (Chen et al., 2002) and stable FAK re-expression in $FAK^{-/-}$ cells decreased RhoA activity (Ren et al., 2000) through enhanced-p190RhoGAP tyrosine phosphorylation (which increases its GAP activity) (Arthur et al., 2000; Hsia et al., 2003). Alternatively, in other cell types, FAK activation and tyrosine phosphorylation are associated with RhoA activation and the formation of stress fibres (Schlaepfer et al., 2004). This connection is mediated by the FAK FAT domain which binds to and phosphorylates a Rho activator known as p190RhoGEF (Zhai et al., 2003). Additionally, the FAK FAT domain was shown to play a critical role in targeting dynamin to FAs and this was shown to be a critical step in FA disassembly (Ezratty et al., 2005; Wang et al., 2011b).

Importantly, FAK-Src signaling is also involved in the modification of phosphatidylinositol lipids, and differentially phosphorylated lipid function as binding sites for signaling proteins that are involved in the formation of FAs. Phosphatidylinositol-4,5-bisphosphate ($PtdIns(4,5)P_2$) binds to and controls the assembly of proteins such as α-actinin, vinculin and talin into FAs

(Ridley et al., 2003). As the binding of the talin FERM domain to β-integrin cytoplasmic tails is enhanced by PtdIns(4,5)P_2 (Calderwood, 2004a; Calderwood, 2004b), and the talin rod domain binds vinculin and actin (Papagrigoriou et al., 2004), a link between integrins, FA formation and the actin cytoskeleton is established. The type I phosphatidylinositol phosphate kinase-γ (PIPKIγ) is an enzyme that makes PtdIns(4,5)P_2 and it is targeted to FAs by an association with the talin FERM domain (Di Paolo et al., 2002). PIPKIγ is phosphorylated by a FAK-Src complex, which promotes increased PIPKIγ activity and association with talin (Ling et al., 2002). In this manner, FAK signaling is connected to the formation of FAs and the spatial regulation of PtdIns(4,5)P_2 generation. Interestingly, the integrin and PIPKIγ binding sites within the talin FERM domain overlap, which implies that PIPKIγ binding might displace talin from β-integrin tails (Barsukov et al., 2003; Ling et al., 2002). Thus, although FAK-Src activity could promote the production of PtdIns(4,5)P_2 and the formation of FAs by enhancing the activity of PIPKIγ, subsequent phosphorylation of PIPKIγ by FAK-Src signaling might break the talin-integrin linkage and promote FA turnover. Additionally, despite the canonical role for talin in integrin activation (Moser et al., 2009), it was recently demonstrated that impaired recruitment of talin to FA sites in $FAK^{-/-}$ cells did not affect FA formation during early spreading (Lawson et al., 2012). Consistently, alternative FA targeting mechanisms for talin have been porposed (Franco et al., 2006; Wang et al., 2011a).

INTEGRIN ACTIVATION

Many integrins are known to adopt low-affinity, intermediate-affinity, and high-affinity conformations, and these exist in a dynamic equilibrium with one another. The turnover of FAs that occurs during cell migration requires dynamic regulation of integrin-ligand binding affinity (Askari et al., 2009). Conformational changes in α5β1 from the bent to the extended

conformation have been observed in FAs, but the mechanism that triggers the unbending remains to be elucidated (Askari et al., 2010). It has been suggested that integrin activation in adherent cells occurs by an "outside-in" mechanism (e.g. the high concentration of available ligand in the ECM), by regulation of avidity (integrin clustering), or by force. However, the specific factors or processes regulating integrin activation remain unclear and most models of FA formation in migrating cells assume that the integrin is constitutively active.

On the basis of structural studies, it is thought that integrins are in a low-affinity state when their extracellular domains are bent and in a high-affinity state when those are extended. The exact changes that occur in the head domain when integrins move to the high-affinity state are still unclear. Mutational studies and molecular modeling suggest that interactions between the transmembrane domain of an α- and a β-integrin subunit are important in maintaining the low affinity inactive state and that activation requires separation of these transmembrane domains (Gottschalk, 2005; Hughes et al., 1996; Li et al., 2005b; Luo et al., 2005; Luo et al., 2004; Partridge et al., 2005). Integrin affinity is regulated in large part by alterations in the conformation of the integrin extracellular domains that result from interactions at the integrin cytoplasmic tail (Moser et al., 2009; Shattil et al., 2010). The relatively short α-cytoplasmic and β-cytoplasmic tails (except for β4) contain docking sites for a variety of proteins that control integrin activation, recruitment to adhesion sites, and trafficking (Margadant et al., 2011).

Almost all β tails have two well-defined motifs that are part of a canonical recognition sequence for phosphotyrosine-binding (PTB) domains (Calderwood et al., 2003), consisting of a membrane proximal NPxY (where x represents any amino acid) motif and a membrane distal NxxY motif. These NxxY motifs are binding sites for multiple integrin-binding proteins, including talin and kindlin (Moser et al., 2009). High integrin affinity is thought to be associated

with talin and kindlin binding to the membrane-proximal (MP) and -distal (MD) motifs of the β-tail, respectively, causing separation of the α and β cytoplasmic tails (Kim et al., 2003; Lau et al., 2008). Because kindlins and talin bind distinct regions of the β integrin tail, they may cooperate to regulate integrin affinity (Calderwood et al., 2002; Calderwood et al., 1999; Ma et al., 2008; Montanez et al., 2008; Moser et al., 2009; Moser et al., 2008). Although kindlins are not sufficient to shift integrins to a high-affinity state, they facilitate talin function. Conversely, talin depends on kindlins to promote integrin affinity because talin-head overexpression failed to increase αIIbβ3 affinity in CHO cells in which kindlin expression was reduced by siRNA. Thus, kindlins require talin, and talin is not sufficient to increase integrin affinity (Moser et al., 2009).

The best example of a tightly controlled integrin activation process comes from studies performed with the integrin αIIbβ3 following platelet activation with thrombin. In resting platelets, the bent, low-affinity conformation of αIIbβ3 is stabilized by a "clasp" formed between αIIb and β3 and this mechanism is thought to help prevent inappropriate platelet aggregation that could lead to thrombosis. Activation of cytoplasmic signaling downstream of the thrombin receptor leads to disruption of the salt bridge, and the subsequent separation ("unclasping") of the cytoplasmic tails. This event triggers an allosteric change to favor the extended, high-affinity integrin conformation. The last step of this inside-out mechanism is the binding of the FERM-containing head-domain of talin to the MP motif and an additional region of the β3 cytoplasmic tail (Anthis et al., 2009; Kim et al., 2011). Inside-out activation also requires kindlin-3 (Moser et al., 2009). Loss of talin or kindlin-3 from platelets prevents platelet adhesion and aggregation in mice (Moser et al., 2009; Moser et al., 2008; Nieswandt et al., 2007; Petrich et al., 2007). Likewise, gene targeting of kindlin-1 and kindlin-2 compromises integrin-mediated adhesion in mice (Margadant et al., 2010; Margadant et al., 2009; Meves et al., 2009).

For several years it has been known that adhesion receptors undergo endocytic-exocytic transport (Bretscher, 1992; Caswell and Norman, 2006). Interestingly, the NPxY motifs found in β-integrin tails are canonical signals for clathrin-mediated endocytosis of plasma membrane receptors (Traub, 2009). For instance, whereas the integrin MP domain was shown to be dispensable for integrin recycling, the MD domain (which binds to kindlin) was shown to be critical for this event (see below) (Margadant et al., 2012). Additionally, depletion of clathrin adaptors such as AP-2, Dab-2 and ARH reduces integrin endocytosis and affects cell migration (Chao and Kunz, 2009; Ezratty et al., 2009; Teckchandani et al., 2009) thus establishing a direct link between integrin trafficking and cell motility.

INTEGRIN TRAFFICKING

Over the past years, it has been established that integrin trafficking in adherent cells is important for FA turnover during cell spreading and migration and for localized integrin redistribution to new adhesion sites, for example at the leading edge of migrating cells. Trafficking mechanisms include the delivery of newly synthesized integrins via the biosynthetic-secretory pathway, integrin endocytosis and recycling of internalized integrins (Caswell et al., 2009).

Integrin Endocytosis

Integrin internalization occurs through clathrin-dependent and clathrin-independent (via caveolae or macropinocytosis) mechanisms, and many integrins can follow more than one route into the cell (Bridgewater et al., 2012; Margadant et al., 2011). As mentioned above, it is generally thought that most integrins are recruited to clathrin-coated pits by binding to clathrin adaptors. Indeed, Numb and Dab-2 bind respectively to the MP-NPxY and the MD-NxxY motifs of β-tails (Calderwood et al., 2003).

Importantly, FA disassembly was shown to involve integrin endocytosis and to require dynamin, FAK, clathrin and the clathrin adaptors ARH, Dab2 and AP-2 (Chao and Kunz, 2009; Ezratty et al., 2009; Ezratty et al., 2005). Moreover, the clathrin adaptors Numb, ARH, Dab-2 and AP-2 accumulate at FAs at the leading edge of migrating cells or shortly before their disassembly (Chao and Kunz, 2009; Ezratty et al., 2009; Nishimura and Kaibuchi, 2007). Accordingly, depletion of clathrin or any of these adaptors leads to increased integrin surface expression and reduced migration (Chao and Kunz, 2009; Ezratty et al., 2009; Teckchandani et al., 2009).

Of note, integrins have been observed in Rab5- and Rab11-positive endosomes following dynamin-dependent endocytosis after manipulations that lead to synchronous disruption of FAs (Chao and Kunz, 2009; Ezratty et al., 2009). Additionally, it was recently proposed that ligand-bound integrins are directed to lysosomes (Lobert et al. 2010). Therefore it is likely that in order to be sorted to a recycling route, i.e., the Rab11 ERC, FA-resident integrins have to be separated from their ECM ligand upon FA disassembly (and therefore are expected to be deactivated), otherwise they would be directed to the lysosomes for degradation.

Integrin Recycling and Degradation

The early endosome are the first port of call for receptors following internalization and delivers internalized receptors to the sorting endosome. It is in the sorting endosome where key decisions are made as to whether a receptor is routed to late endosomes and lysosomes for degradation or whether it is sent to recycling endosomes for return to the plasma membrane. The rate at which internalized integrins are degraded is very slow by comparison with the speed of their recycling (Bretscher, 1989; Bretscher, 1992; Dozynkiewicz et al., 2012; Lobert et al., 2010; Roberts et al., 2001). This has led to the view that integrins are so very efficiently sorted into recycling pathways that they are not trafficked to late endosomes. More recently, however, it has

become clear that this is not the case. We now know of regulatable mechanisms whose function is to control the sorting of integrin between late endosomes and recycling pathways, and these can dictate the rate of integrin degradation (Bottcher et al., 2012; Dozynkiewicz et al., 2012; Lobert et al., 2010; Steinberg et al., 2012). For instance the decision to recycle or degrade internalized α5β1 was shown to be influenced by its ubiquitinylation. In migrating fibroblasts, endocytosed α5β1 integrin associated with FN is ubiquitinated (on the α5-tail) and this is required to direct FN-α5β1 complexes to lysosomes for degradation. Therefore it was suggested that ubiquitinylation functions to prevent endosomal accumulation of ligated integrins which may interfere with cell signaling and efficient migration (Lobert et al., 2010).

Different groups have been investigating the consequences of mutating integrin NPxY motifs on their intracellular trafficking and recycling (Bottcher et al., 2012; Margadant et al., 2012; Steinberg et al., 2012). A clear consequence of disrupting the MD NPxY in β1 is that rather than being sorted to recycling endosomes, it is routed to late endosomes and lysosomes. Additionally, its half-life for degradation is reduced from several hours to less than 15 min. These observations initially pointed kindlins as regulators of integrin lysosomal sorting (Margadant et al., 2012). The mechanism by which the MD NPxY motif dictates whether integrins are sorted for recycling or degradation was revealed shortly after. First, using a proteomic approach to identify new cargoes of sorting nexins, Steinberg et al. (2012) found that knockdown of sorting nexin 17 (SNX17) leads to reduced surface expression of β1 integrins. Using a different proteomic approach, the Fassler lab identified SNX17 as a ligand for β1 integrin's MD NPxY domain (Bottcher et al., 2012). There is a common strand to the results emanating from both labs which indicates that when internalized β1 integrins arrive in early endosomes they recruit SNX17 to their MD NPxY motif. This promotes sorting of the integrin

into a Rab11-dependent recycling pathway and opposes integrin ubiquitinylation and the ensuing lysosomal-routing. Thus integrins are normally recycled efficiently and degraded very slowly. But in SNX17-depleted cells, their recycling is reduced and they are rapidly degraded. Conceptually, these studies indicate that there are sorting signals present in integrin cytoplasmic domains that directly participate in recruitment of a trafficking regulator at a stage that is critical for the delivery of integrins from sorting to recycling endosomes and, if this is disrupted integrins end up in late endosomes for degradation.

As suggested above, most internalized integrins are not degraded, but are efficiently recycled to the plasma membrane by either a Rab4-dependent short (fast)-loop or by a Rab11-dependent long (slow)-loop and a number of growth factors and kinases are now known to influence this process (Arjonen et al., 2012; Caswell and Norman, 2008; Caswell et al., 2008; Caswell and Norman, 2006; Gu et al., 2011; Jones et al., 2006; Pellinen and Ivaska, 2006; Rainero and Norman, 2013; Veale et al., 2010). For example, PDGF stimulates rapid, short-loop recycling of internalized αvβ3 from early endosomes (Roberts et al., 2001), whereas α5β1 travels from early endosomes to the endocytic recycling compartment (ERC) and is then recycled via a long-loop to the plasma membrane (Powelka et al., 2004).

Rabs contain PTB domains that recognize NPxY motifs and can thus potentially bind to β-tails. Indeed, Rab25 (Rab11c) was reported to bind directly to α5β1 integrin and contribute to the aggressiveness of breast and ovarian cancers (Cheng et al., 2004) and along with Rab-coupling protein to coordinate the delivery of endocytosed α5β1 integrin to pseudopodial tips thus promoting an invasive mode of migration (Caswell et al., 2008; Caswell et al., 2007). Furthermore it has been shown that serum-stimulation dependent recycling of β1 integrin involves ADP-ribosylation factor 6 (Arf6) and Rab11 (Powelka et al., 2004). Rab11 was also

shown to control recycling of α6β4 integrin in breast cancer cells, which may contribute to hypoxia-induced invasive migration (Yoon et al., 2005). Likewise Rab5 and Rab21 were shown to regulate cell adhesion and motility by controlling the endosomal trafficking of β1 integrin (Pellinen et al., 2006).

It has been known for some time that sorting endosomes are located near to the front of migrating cells, at their leading edge (Pierini et al., 2000). Consistently, it is now apparent that clathrin-dependent endocytosis is sharply polarized towards the leading edge (Rappoport and Simon, 2003), and more recently it has become clear that integrins are internalized at FAs near the leading edge and then transported backwards to the Rab11 ERC (Chao and Kunz, 2009; Ezratty et al., 2009; Laukaitis et al., 2001). Thus it has been suggested that integrins undertake an intracellular journey from the cell front to the Rab11 compartment and back again, thus spatially restricting a particular population of integrins to the front portion of the cell (Caswell et al., 2009). Taken together, these findings support the view that trafficking through the Rab11 ERC is the major route for large scale recycling of integrins in migrating cells. In this context, there are some important questions that remain to be addressed and that I will try to answer in the present study: Do FA-resident integrins undertake different endocytic pathways than bulk integrins? Is FA disassembly connected to FA assembly through the Rab11 ERC, which would be in this case the source of integrins for FA formation? If so, is integrin endocytic trafficking rate limiting for cell migration? Do FA components traffic with internalized integrins and affect their trafficking? And lastly, is this integrin endocytic recycling pathway coupled to a cytoskeletal component to ensure a polarized trafficking towards the cell leading edge?

ROLE OF MICROTUBULE MOTORS IN ENDOCYTIC RECYCLING AND POLARIZED TRAFFICKING

In a migrating cell MTs form a single network that spreads throughout the cytoplasm from the leading edge to the rear edge and the continuity of the network is essential for long-range intracellular traffic (Etienne-Manneville, 2013). In order to maintain a cycling pool of integrins at the front edge (as suggested above) it is reasonable to speculate that a migrating cell must have polarized trafficking of integrin-containing vesicles towards the leading edge. In concurrence with this hypothesis, a generic monoclonal antibody to integrins was shown to preferentially label the leading edge of freshly plated fibroblasts, suggesting that this receptor is recirculated to the leading edge of motile cells by an endo/exocytic cycle (Bretscher, 1989). These observations suggested that there must be a cytoskeletal component for such function and kinesins would be likely candidates. Surprisingly, direct evidence of kinesin-mediated integrin transport is very scarce. Only recently a study by Anne Straube's group shed some light on this topic. Kif1C was shown to transport α5β1-integrins to the cell rear where it is required for proper maturation of trailing adhesions and the consequent maintenance of directional persistence of migrating cells (Theisen et al., 2012). Thus polarized integrin trafficking towards the cell front still remains to be demonstrated.

It is well accepted that Rabs are major regulators of integrin trafficking and that they can associate to kinesin motors directly or via linker proteins that simultaneously bind the Rab and the kinesin motor (Horgan and McCaffrey, 2011). Although Theisen et al. identified Kif1C as an integrin-associated motor for transport to the trailing edge we think there might be distinct kinesins committed to the polarized trafficking of integrins to the leading edge and this is likely to be a critical aspect of FA assembly during cell migration.

Figure 1. Model system to study FA turnover and integrin recycling.

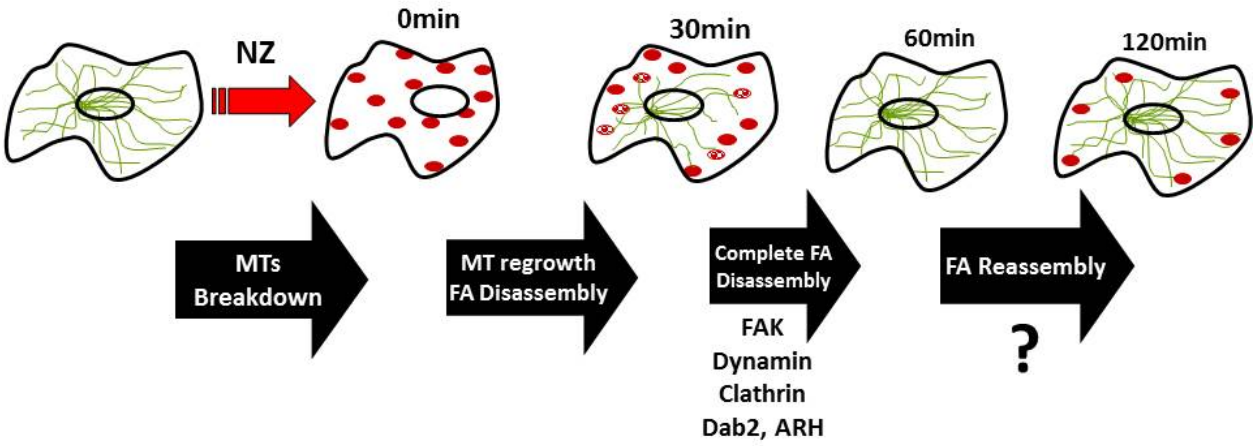
NZ
0min
30min
60min
120min
MTs
Breakdown
MT regrowth
FA Disassembly
Complete FA
Disassembly
FAK
Dynamin
Clathrin
Dab2, ARH
FA Reassembly
?

Figure 2. Focal adhesion kinase domain structure and phosphorylation sites.

Focal adhesion kinase (FAK) contains a FERM (protein 4.1, ezrin, radixin and moesin homology) domain, a kinase domain and a FA targeting (FAT) domain. The FERM domain mediates interactions of FAK with the epidermal growth factor (EGF) receptor, platelet-derived growth factor (PDGF) receptor. The FAT domain recruits FAK to focal contacts by associating with integrin-associated proteins such as talin and paxillin. It also links FAK to the activation of Rho GTPases by binding to guanine nucleotide-exchange factors (GEFs) such as p190 RhoGEF. FAK contains three proline-rich regions (PRR1–3), which bind Src homology-3 (SH3) domain-containing proteins such as p130Cas, the GTPase regulator associated with FAK (GRAF) and the Arf-GTPase-activating protein ASAP1. FAK is phosphorylated (P) on several tyrosine residues, including Tyr397, 576, 577, 861 and 925. Tyrosine phosphorylation on Tyr397 creates a Src-homology-2 (SH2) binding site for Src, phospholipase Cγ (PLCγ), suppressor of cytokine signalling (SOCS), growth-factor-receptor bound protein 7 (GRB7), the Shc adaptor protein, p120 RasGAP and the p85 subunit of phosphatidylinositol 3-kinase (PI3K). Phosphorylation of Tyr576 and Tyr577 within the kinase domain is required for maximal FAK catalytic activity, whereas the binding of FAK-family interacting protein of 200 kDa (FIP200) to the kinase region inhibits FAK catalytic activity. FAK phosphorylation at Tyr925 creates a binding site for GRB2. Modified from (Mitra et al., 2005).

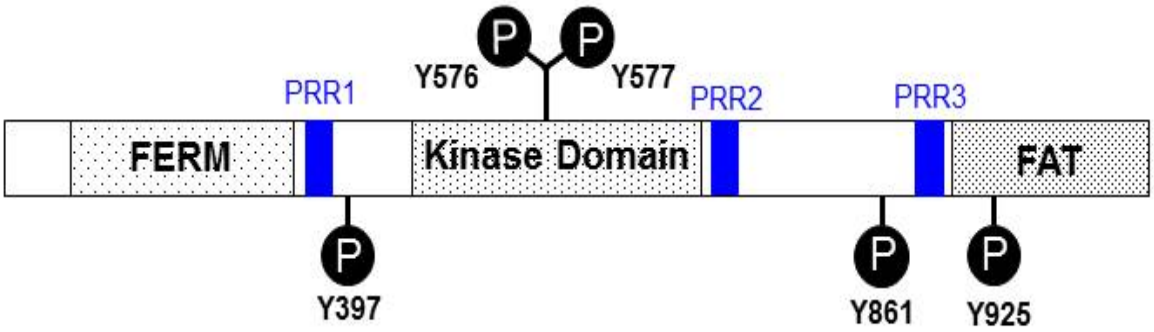
P
P
Y576
Y577
PRR1
PRR2
PRR3
FERM
Kinase Domain
FAT
P
P
P
Y397
Y861
Y925

Chapter 1: FAK and Src Kinases Maintain Activation of Endocytosed Integrin for Rapid and Polarized Reformation of Adhesions

ABSTRACT

Integrin endocytosis and recycling are critical for cell migration. While the assembly of cell surface integrins into FAs is well-understood from spreading assays, it is unclear whether recycled integrins follow the same steps to reassemble FAs. Here we developed a system to study the reassembly of recycled integrins into adhesions based on the synchronous endocytosis of integrins from FAs triggered by MT regrowth. In this system, FA reassembly required integrin recycling from the Rab11 compartment. Activated FAK and Src colocalized with the endocytosed integrin in the Rab11 compartment prompting us to test their role in reformation of adhesions. FAK kinase mutants rescued defective FA disassembly but not reassembly in $FAK^{-/-}$ cells. Consistently, FAK and Src inhibitors did not affect FA disassembly but blocked reassembly. Surprisingly, integrin recycling was blocked in Src family kinase- but not FAK-inhibited cells. Cell and fibronectin fragment binding assays showed that recycled integrin in FAK-inhibited cells was not active but could be induced to reassemble FAs by Mn^{2+} treatment. Localization studies revealed active integrin in Rab5 and Rab11 endosomes after FA disassembly and FAK kinase activity was required to maintain recycled integrins active. Studies in migrating cells revealed results consistent with those obtained with the synchronous system: both FAK and Src kinase inhibitors blocked formation of new adhesions without affecting disassembly of pre-existing ones; Src, but not FAK activity was required to maintain surface integrin level; and FAs reformed quicker after FAK compared to Src inhibitor washout. We propose that FAK and Src kinases are specifically required to maintain the activation state of endocytosed integrin after FA disassembly so that recycled integrin can be rapidly reassembled into FAs when it is returned to the cell surface.

INTRODUCTION

Directional cell migration is a multi-step process fundamental for embryonic development, immune responses, tissue repair and regeneration in multicellular organisms (Ridley et al., 2003). Abnormal cell migration contributes to cancer metastasis, atherosclerosis and inflammation. Deciphering the cellular mechanisms that contribute to migration is thus essential to understanding both physiological and disease processes.

The establishment of adhesive contacts between the cell and its ECM substratum is one of the central processes of migration. Integrins are the principal membrane receptors mediating ECM contacts in migrating cells. As a result of association with the ECM, integrins cluster into dynamic multi-component complexes, termed FCs and FAs (Burridge et al., 1997). FAs serve as points of force transmission during migration as well as cytoskeletal regulation (Geiger et al., 2009; Lauffenburger and Horwitz, 1996) and signaling that regulates cell survival, division and differentiation (Bershadsky et al., 2003; Zaidel-Bar et al., 2004; Zamir and Geiger, 2001).

Integrin association with its ECM ligands and clustering into FCs and FAs have been intensively studied and a detailed understanding of the major factors contributing to these processes has emerged (Geiger et al., 2009; Shattil et al., 2010). A much more poorly understood process is the turnover of adhesions and recycling of the "released" integrin receptors. Cell migration requires not only assembly of FAs at the leading edge but disassembly of FAs as the cell body translocates over the stationary adhesions. Although commonly (but incorrectly) described as occurring in the tail of migrating cells, maps of FA disassembly show two major regions: the tail and a region in the lamella just distal to the site of FA maturation (Mohl et al., 2012; Smilenov et al., 1999; Stehbens et al., 2014).

The mechanisms underlying FA disassembly are not fully understood. Consistent with a role of dynamic MTs in cell migration (Liao et al., 1995; Mikhailov and Gundersen, 1998), Small and colleagues (Kaverina et al., 1999; Kaverina et al., 1998) identified a mechanism whereby FA disassembly was triggered by repeated targeting of FAs by dynamic MTs. Later studies revealed that MT-induced FA disassembly required dynamin, clathrin (and its adaptors), PIPK1β and FAK (Chao et al., 2010; Chao and Kunz, 2009; Ezratty et al., 2009; Ezratty et al., 2005; Wang et al., 2011b). Surface labeling experiments showed that integrin is endocytosed during MT-induced FA disassembly and live imaging studies of integrin and clathrin showed that endocytosis occurs directly at FAs. FAK scaffolding function is implicated in FA disassembly since a GRB2 binding site that recruits dynamin to FAs was necessary for FA disassembly (Ezratty et al., 2005). A major regulator of FAK kinase activity is Src kinase, a member of the *S*rc *f*amily *k*inases (SFKs) (Mitra et al., 2005), which are important regulators of protein trafficking(Kaplan et al., 1992; Kasahara et al., 2007; Sandilands et al., 2007; Sandilands et al., 2004). Src has been reported to be involved in FA disassembly in cancer cells through its phosphorylation of dynamin 2 (Wang et al., 2011b), yet MT-induced FA disassembly occurs normally in cells lacking Src, Yes and Fyn ($SYF^{-/-}$ cells) (Yeo et al., 2006), suggesting SFKs may only be require under specific circumstances or in specific cell types. Other factors contribute to FA disassembly, including calpain-dependent cleavage of adhesion components (Franco et al., 2004a; Franco et al., 2004b), targeted ECM degradation (Stehbens et al., 2014) and in some types, enhanced contractility that literally pulls the FA from the substratum (Chrzanowska-Wodnicka and Burridge, 1996; Crowley and Horwitz, 1995; Vicente-Manzanares et al., 2009). It is unknown whether these forms of FA disassembly involve endocytosis and/or are separate mechanisms for FA disassembly.

Given the association of integrin endocytosis in FA disassembly, an important question is the fate of the endocytosed integrin. Endocytosis and recycling of integrins are necessary to maintain cell polarization and to co-ordinate FA turnover during cell migration (Caswell et al., 2009; Fletcher and Rappoport, 2010; Grant and Donaldson, 2009). Initial evidence connecting cell motility and vesicle trafficking came from the pioneering studies of Mark Bretscher who showed that integrins were constitutively endocytosed and recycled (Bretscher, 1989; Bretscher, 1992). He proposed that endocytosed integrin was directed to the leading edge to form new adhesions (Bretscher and Aguado-Velasco, 1998). The existence of such a long-range pathway has remained controversial, although newer studies have identified intracellular trafficking factors that contribute to the recycling of integrins and in many cases shown that these factors are required for efficient cell migration. For instance, bulk α5β1 integrin recycles to the plasma membrane from a perinuclear recycling compartment via a Rab11-dependent recycling pathway and this recycling is critical for cell migration (Li et al., 2005a; Powelka et al., 2004; Roberts et al., 2004). Additionally, Rab5, Rab21 and Rab-coupling protein regulate cell motility by controlling the endosomal trafficking of β1 integrin (Caswell et al., 2008; Caswell et al., 2007; Pellinen et al., 2006). Rab11 also controls the recycling of α6β4 integrin in breast cancer cells contributing to the aggressiveness of breast and ovarian cancers (Cheng et al., 2004; Yoon et al., 2005). In contrast, growth factor-stimulated recycling of αvβ3 integrin from early endosomes to the plasma membrane is Rab4 dependent and is a key upstream event in the assembly of cell-matrix contacts (Roberts et al., 2001).

These studies establish a correlation between integrin endocytosis and recycling and cell migration (Caswell and Norman, 2006; Caswell et al., 2009; Lawson and Maxfield, 1995), yet the relationship between the uptake of integrins during FA disassembly, their endosomal

recycling and the de novo formation of adhesions is still unclear. A particularly important question is whether the recycled integrin requires activation upon return to the cell surface to allow it to bind to its ECM ligands. Indeed, it might be expected that integrins disassembled from FAs would transition to an inactive state during FA disassembly to allow them to detach from the ECM. In fact, active α5β1 integrin endocytosed with soluble fibronectin is efficiently degraded rather than returned to the cell surface (Lobert et al., 2010). Here, we adapt the MT-induced FA disassembly assay to study the trafficking of endocytosed integrin and their reassembly into FAs. We find that this integrin traffics through Rab5 and Rab11 endosomal compartments before returning to the cell surface where it reforms FAs in a highly polarized manner. Surprisingly, we find that FAK and SFK activities are required for these processes and describe a new function for these kinases in maintaining integrin in an active, but unliganded state during trafficking. These results suggest that FAK and SFKs comprise a system of "activation memory" for integrins during their intracellular trafficking.

RESULTS

FA reassembly occurs with a lag after MT-induced FA disassembly

To study the fate of integrin endocytosed from FAs we adapted the system of synchronous MT regrowth after NZ washout used previously as a model system to study MT targeting and disassembly of FAs (Chao et al., 2010; Chao and Kunz, 2009; Wang et al., 2011b; Wu et al., 2008; Yeo et al., 2006). Two previous studies noted that FAs reformed with a lag after MT-induced FA disassembly (Chao et al., 2010; Yeo et al., 2006), but did not identify the nature of the lag or whether FA reformation required recycling of integrins. We reexamined FA reassembly after MT-induced FA disassembly to more precisely determine the timing of this process relative to FA disassembly. MT regrowth triggers virtually complete FA disassembly in NIH3T3 fibroblasts by 60 min following NZ washout (Figure 3A) (Ezratty et al., 2009; Ezratty et al., 2005). As assessed by immunofluorescence of vinculin, FA reassembly occurred as soon as 90 min after NZ washout, i.e., with a lag of 30 min after complete FA disassembly (Figure 3A, B). Additional FA markers gave similar results and actin stress fibers also reassembled showing that the reassembled FAs were typical FAs (Figure 4). A biochemical marker of FAs, the autophosphorylation/activation site of FAK (pY397 FAK) decreased after disassembly as previously reported (Ezratty et al., 2005), but then increased at 80-90 min, coincident with the reformation of FAs (Figure 3C). The levels of phosphorylated paxillin (pY118), a substrate of FAK, paralleled the changes in FAK-pY397 levels (Figure 3C). Quantification revealed a 1.3-1.6 fold increase in FAK-pY397 at 80-120 min relative to 60 min of NZ washout (Figure 3D).

To examine FA reassembly dynamically, we used total internal reflection (TIRF) microscopy to image FAs in a stable NIH3T3 cell line expressing paxillin-EGFP. This cell line displayed paxillin-EGFP expression levels comparable to the endogenous protein and presented FA distribution and migration rates similar to the parental cell line (Figure 5). Consistent with

the fixed cell assays, live cell imaging revealed that FA reformation began 30 min after complete FA disassembly in individual cells (compare figures 3A and 3F). Notably, by either fixed cell or live cell assays, FA reassembly occurred in a polarized fashion with most reassembled FAs localized near the cell periphery in contrast to their random localization throughout the cell before FA disassembly (Figure 3A-compare 0 and 90 min and Figure 4). Quantification revealed that reassembled FAs showed a strong bias toward a peripheral location compared to the FAs before NZ washout (Figure 3E, F). Collectively, these results show that FA reassembly occurs with a lag of 30 min after FA disassembly and is polarized towards the cell periphery.

FA reassembly requires endocytic recycling of integrin

As integrin is endocytosed during MT-induced FA disassembly (Chao and Kunz, 2009; Ezratty et al., 2009), we tested whether FA reassembly required recycling of the endocytosed integrins. After 60 min of MT regrowth surface levels of α5 integrin decreased to 40% of that in NZ-treated cells, consistent with earlier results (Ezratty et al., 2009). Coincident with the reassembly of FAs at 90-100 min after MT regrowth, integrin surface levels increased reaching approximately 80 % of the level before MT regrowth (Figure 6A). Importantly, total levels of α5 integrin assessed by western blot did not change during MT regrowth (Figure 7A). Using α5 integrin-GFP to monitor integrin trafficking, at 60 min after MT regrowth integrin was colocalized with the Rab11 perinuclear ERC (Figure 6B), but not with the Golgi (Figure 8). The level of α5 integrin-GFP in the ERC decreased at 120 min after MT regrowth, coincident with the return of surface integrin and the reappearance of FAs (Figure 6B). These results are consistent with endocytosed integrin trafficking to the Rab 11 ERC after FA disassembly and then recycling back to the cell surface to reassemble new FAs.

Previous studies of bulk integrin trafficking have identified Rabs as regulators of integrin recycling. For instance, α5β1 integrin is recycled in a Rab5 and Rab11 dependent manner

whereas αvβ3 integrin is recycled through Rab5 and Rab4 dependent pathways (Pellinen et al., 2006; Powelka et al., 2004; Roberts et al., 2001). These studies, however, did not specifically examine integrins endocytosed during FA disassembly. To test if Rabs were important for integrin recycling and FA reassembly after MT-induced FA disassembly, we transiently transfected cells with dominant negative Rab mutants (Rab5 S34N and Rab11 S25N) and assayed them for MT-induced FA disassembly and reassembly. Neither of the mutants interfered with FA disassembly, but both prevented FA reassembly (Figure 6C, D and Figure 7B). Wild type Rab11 and EGFP had no effect on either FA disassembly or reassembly. Knockdown of the major Rab11 isoforms, Rab11a and Rab11b, expressed in NIH3T3 fibroblasts with siRNA oligonucleotides (Figure 7C), confirmed that Rab11 was required for FA reassembly, but not disassembly (Figure 6E, F). MT regrowth occurred normally in Rab11-depleted fibroblasts (Figure 6E). Importantly, Rab11-depleted fibroblasts failed to restore their surface integrin levels after 90 min of MT regrowth (Figure 6G). Together, these data show that FA reassembly requires Rab11-dependent endocytic recycling of endocytosed integrin and indicates that FA reassembly is coupled to return of integrins to the cell surface.

FAK and SFK activities are required for reassembly of FAs from endocytosed integrin

After FA disassembly we detected accumulation of activated FAK (FAK-pY397) at a perinuclear site that colocalized with Rab11 (Figure 9A-top panels). When FAs reassembled at 120 min after MT regrowth, FAK-pY397 was no longer observed at the Rab11 ERC, but instead redistributed to FAs (Figure 9A-bottom panels). These results raised the possibility that FAK might be involved in the recycling of integrins or in their reassembly into FAs.

FAK scaffolding function functions in MT-induced FA disassembly by recruiting dynamin to FAs (Ezratty et al., 2005; Wang et al., 2011b). Whether FAK kinase activity is important for either FA disassembly or reassembly has not been tested. To approach this question we

expressed FAK constructs mutated in the major autophosphorylation site (Y397F) or in the kinase active site (K454R) in $FAK^{-/-}$ fibroblasts, which were previously shown to exhibit impaired MT-induced FA disassembly (Ezratty et al., 2005). As expected, reexpression of wild type FAK-GFP rescued FA disassembly and reassembly (Figure 9B, D, E). In contrast, while FAK^{Y397F}-GFP and FAK^{K454R}-HA rescued FA disassembly in $FAK^{-/-}$ fibroblasts to the same extent of wild type FAK-GFP, neither supported FA reassembly (Figure 9C-E). To confirm the requirement of FAK kinase activity for FA reassembly, we treated cells with the FAK kinase inhibitor, PF228 (Slack-Davis et al., 2007). Consistent with the reexpression experiments, PF228 blocked FA reassembly without interfering with FA disassembly (Figure 10A, B). Similar results were observed with a structurally distinct FAK inhibitor (Figure 11).

FAK and Src are major partners and Src was previously implicated in FA reassembly (Yeo et al., 2006), so we next tested whether SFK activity was also required for FA reassembly by treating cells with PP2, a selective inhibitor of SFKs (Hanke et al., 1996). PP2 had no detectable effect on FA disassembly but blocked FA reassembly (Figure 10A, B). Inhibition of FA reassembly was also evident biochemically using paxillin-pY118 as a marker for FA in FAK- and SFK-inhibited cells (Figure 12). The effects of the FAK and SFKs inhibitors on FA reassembly were reversible: within 10 min after drug wash out, FAs begin to reassemble and by 30 min FA reassembly reached the same level as that in vehicle-treated cells (Figure 10C, D). These results show that FAK and SFKs activities are required for proper FA reassembly and that FAK scaffolding and kinase functions orchestrate distinct steps in the cycle of FA disassembly and reassembly.

FAK and SFK activities function at distinct steps in FA reassembly from recycled integrin

As with FAK (Figure 9A), Src was also localized in the ERC after MT regrowth and FA disassembly (Figure 13), consistent with earlier studies showing the localization of Src in the

ERC (Kaplan et al., 1992; Sandilands et al., 2007; Sandilands et al., 2004; Sandilands and Frame, 2008). Coupled with the requirement of FAK/SFKs for FA reassembly, these data suggest that FAK and SFKs may contribute to integrin recycling from the ERC to the cell surface. To address this we measured surface levels of α5 integrin after MT-induced FA disassembly in the presence of either FAK (PF228) or SFK (PP2) inhibitors. Although neither inhibitor affected the loss of surface integrin after FA disassembly, cells treated with PP2 failed to restore integrin surface levels after 100 min of NZ washout (Figure 14A). Surprisingly, cells treated with PF228 reestablished their surface integrins at 100 min of NZ washout to levels similar to those in DMSO-treated cells (Figure 14A). Consistent with the integrin surface levels, α5 integrin-GFP accumulated in the Rab11 ERC 60 min after MT regrowth in control cells or in cells treated with either inhibitor (Figure 14B, top panels). However, at 120 min after MT regrowth, when α5 integrin-GFP left the ERC and was reassembled into FAs in control cells, in cells treated with PP2, but not PF228, it remained in the ERC (Figure 14B, bottom panels). Instead, in cells treated with PF228, the α5 integrin-GFP appeared as diffuse labeling throughout the cell at a time when FAs had reformed in the controls (Figure 14B, bottom panels-arrowheads). To quantify these findings, we measured the signal of α5 integrin-GFP in the Rab11 ERC after 60 and 120 min of MT regrowth. At 60 min of MT regrowth, at least 50% of the integrin signal colocalized with Rab11 in all conditions. At 120 min of MT regrowth, the level of α5 integrin-GFP in the Rab11 ERC was reduced in control and PF228-treated cells, but remained elevated in PP2-treated cells (Figure 14C). Thus, while both FAK and SFKs are required for the reassembly of FAs after MT-induced FA disassembly, SFKs (but not FAK) are required for return of integrins to the cell surface, whereas FAK is required for a step after the return of surface integrins.

FAK kinase is required for activation of endocytosed integrin before FA reassembly

The failure of FAs to reassemble in FAK-inhibited cells, even though surface integrins returned to control levels, suggested that FAK kinase activity might be regulating the activation state of endocytosed integrins. To test this possibility, we explored the ability of FAK- and SFK-inhibited cells to adhere to FN-coated surfaces after FA disassembly. We used cells at 90 min of MT regrowth when integrins had returned to the surface in control and FAK-inhibited cells, but not in SFK-inhibited cells. As expected because of their reduced levels of surface integrin, SFKs-inhibited cells showed reduced binding to different FN concentrations relative to controls (Figure 15A, gray bars). Interestingly, FAK-inhibited cells showed similar reduced binding to FN as the SFK-inhibited cells (Figure 15A, gray bars).

To test whether the reduced binding in FAK-inhibited cells reflected the activation state of the returned integrin, we treated cells 90 min after MT regrowth with Mn^{2+} to artificially activate integrins (Gailit and Ruoslahti, 1988). Strikingly, Mn^{2+} increased the binding of FAK-inhibited cells to FN to levels similar to controls (Figure 15A, black bars). In contrast, Mn^{2+} had no effect on SFKs-inhibited cells binding to FN, which is consistent with the inability of these cells to return integrin to the cell surface (Figure 15A). To test whether integrin activation was sufficient for FA reassembly, we added Mn^{2+} to FAK- or SFKs-inhibited adherent cells 80 min after MT regrowth. Paralleling the cell binding results, we found that Mn^{2+} stimulated FA reassembly in FAK- but not SFKs-inhibited cells (Figure 15B). Furthermore, Mn^{2+} did not rescue FA reassembly in Rab11a/b-depleted cells (Figure 16). To test directly the ligand binding state of α5β1 integrin, we quantified by FACS the binding of a fluorescent FN fragment comprising the RGD- and synergy-binding sites that mediate binding to integrins (Bouaouina et al., 2012). This analysis showed that both FAK- and SFK-inhibited cells had reduced FN binding compared to vehicle-treated control cells (Figure 15C). The reduced binding of the FN fragment

in FAK-inhibited cells was reversible as binding of the FN fragment was restored to control levels within 15 min of PF228 washout (Fig 15C). Thus, recycled integrins from disassembled FAs require FAK kinase activity for integrin activation. We showed that FAK kinase activity is not required for integrin recycling (Figure 14) and that transfection of different FAK kinase defective mutants (FAK-Y397F and FAK-K454R) into $FAK^{-/-}$ cells rescues FA disassembly but not reassembly (Figure 9). Next, we tested whether these FAK mutants prevent FA reassembly by affecting integrin recycling or activation. To exam this we transfected $FAK^{-/-}$ cells with FAK-Y397F or FAK-K454R and treated them after MT-induced FA disassembly with Mn^{2+} to artificially activate integrins. Interestingly, this cation rescued FA reassembly in these cells (Figure 15D and E) which suggests that these mutations have the same effect on integrin activation as the FAK inhibitor (PF228).

FAK maintains integrin in an active conformation after FA disassembly and during endocytic recycling

FAK may be required either for maintaining endocytosed integrins in an active state after FA disassembly and during endocytic recycling or for reactivating them once they return to the cell surface. We tested these possibilities by examining the localization of active α5β1 integrin after FA disassembly using antibodies that specifically detect active integrin epitopes. Because of the availability of multiple antibodies to active human, but not mouse integrins, we conducted these experiments in HT1080 fibrosarcoma cells, which had previously been shown to require clathrin and dynamin for MT-induced FA disassembly (Chao and Kunz, 2009). We confirmed that HT1080 cells disassemble their FAs after 60 min of NZ washout and reassemble them with a lag after disassembly and that the FAK inhibitor, PF228, did not affect FA disassembly, but strongly inhibited FA reassembly (Figure 17). Thus, multiple features of MT-induced FA

disassembly and reassembly in NIH3T3 fibroblasts are recapitulated in human HT1080 fibrosarcoma cells.

After FA disassembly, integrin traffics through Rab5 early endosomes (Ezratty et al., 2009). We tested whether active integrin accumulated in Rab5 early endosomes after FA disassembly by transfecting HT1080 cells with constitutively active Rab5 Q79L, which artificially swells early endosomes. Before NZ washout, staining of the Rab5 endosomes with 12G10 antibody, which specifically recognizes conformationally active β1 integrin (Byron et al., 2009), was barely detectable; in contrast, 30 min after NZ washout, when many FAs had disassembled, 12G10 staining was increased in most of the Rab5 endosomes (Figure 18A, B). Quantitation showed that 12G10 staining of Rab5 endosomes increased significantly after NZ washout (Figure 18C). FAK also specifically appeared in Rab5 endosomes after NZ washout (Figure 18A, B).

We next tested whether active β1 integrin would appear in the Rab 11 endocytic recycling compartment after FA disassembly. Indeed, at 60 min after FA disassembly, a strong signal of active β1 integrin was colocalized with Rab11 in the ERC (Figure 18D-bottom panel). Interestingly, active FAK-pY397 was colocalized with this active β1 integrin (Figure 19). At 120 min after NZ washout when FAs had reassembled, the active β1 integrin was nearly depleted from the Rab11 ERC (Figure 18E). To test whether the presence of active β1 integrin in the ERC depended on FA disassembly, we treated cells with the dynamin inhibitor dynasore after NZ washout. Dynasore prevented MT-induced FA disassembly (see Figure 20), as expected (Ezratty et al., 2005), and strongly prevented the accumulation of active β1 integrin in the Rab11 ERC (Figure 18D-top panels). Moreover active integrin staining in the Rab11 ERC decreased sharply during FA reassembly (Figure 18D-bottom panel). Quantitation of the active β1 integrin in the

Rab11 ERC showed that it clearly increased after FA disassembly and then decreased concomitant with the reassembly of FAs (Figure 18E).

We next tested whether FAK activity was required to maintain integrin in an active conformation during endocytic recycling after FA disassembly. We triggered FA disassembly in cells by NZ washout and then allowed integrin to accumulate in the Rab11 ERC for 60 min in the absence or presence of PF228. Whereas active β1 integrin was detected in the ERC in control cells, it was dramatically reduced in PF228 treated cells (Fig. 18F, G). The lack of active integrin in the ERC was not due to the absence of β1 integrin itself, as an antibody insensitive to conformational state of β1 integrin (K20) showed similar staining of the ERC in the absence or presence of PF228 (Figure 18F). FN-bound (and therefore presumably active) integrins have been reported to be targeted to the lysosome for degradation (Lobert et al., 2010). Thus, we wanted to test if integrins endocytosed from FAs are trafficked with FN. Prior to NZ washout FN was detected mostly in fibrillar structures and small intracellular puncta, presumably vesicles. The fibrillar FN was reduced in cells after 60 min of NZ washout (Figure 18H). Importantly, active β1 integrin in the ERC 60 min after NZ washout displayed little colocalization with FN (Figure 18I), suggesting that either FN is not endocytosed with FA-engaged integrins or that FN dissociates from integrins at some point after endocytosis. Next, we used the FN fragment comprising the RGD- and synergy-binding sites that mediate binding to integrins as an alternative way to track active integrins following FA disassembly. Post-fixation staining with this fragment revealed strong labeling of the ERC (as assessed by transferrin) and colocalization with the 12G10 antibody (which also detects active integrin) after 60 min of NZ washout (Figure 18J). In agreement with our previous findings, treatment with FAK inhibitor or inhibition of FA disassembly with dynasore strongly reduced the labeling of the ERC with the FN fragment,

confirming that the staining was dependent on endocytosis and FAK (Figure 18J). These results support the hypothesis that FA-derived integrin is uncoupled from FN after endocytosis since the FN fragment only binds to ligand-free integrins. Combined, these results show that endocytosed integrin derived from FAs travels through Rab5 and Rab11 endocytic compartments in an active unliganded conformation maintained by FAK.

FAK and SFKs orchestrate integrin recycling in migrating cells

To explore whether the results from the MT induced FA disassembly system applied to a more physiological situation, we analyzed FA dynamics in migrating cells treated with FAK or SFK inhibitors. As expected from earlier studies (Ilic et al., 1995; Lawson et al., 2012; Sieg et al., 2000; Sieg et al., 1999; Slack-Davis et al., 2007; Wang et al., 2011b; Yeo et al., 2006), both kinase inhibitors prevented migration (Figure 21). Consistent with their effects on FA reformation but not disassembly, both inhibitors allowed FAs to disassemble but blocked FA reassembly in migrating cells (Figure 22A, B). The rate of FA disassembly in cells treated with FAK and SFK inhibitors was similar to DMSO-treated cells (0.022 ± 0.007 min^{-1} for DMSO, 0.018 ± 0.004 min^{-1} for PF228 and 0.017 ± 0.005 for PP2), which are all comparable to previously reported rates for NIH 3T3 fibroblasts (Berginski et al., 2011). Because integrin recycling is unaffected in FAK-inhibited cells, but is blocked in SFK-inhibited cells (Figure 14A), reassembly of FAs after inhibitor washout should be faster in FAK-inhibited cells than SFKs-inhibited cells. Indeed, after washout of the inhibitors, FAs reassembled quicker in FAK-inhibited cells compared to SFKs-inhibited cells (Figure 22C, D). The $t_{1/2,\ FA\ reassembly}$ calculated from plots of the summed intensity of FAs, was 5 min for PF228 release and 25 min for PP2 release. The ~20 min difference in the $t_{1/2,\ FA\ reassembly}$ can be taken as an estimate of the time for recycling of integrin to the cell surface from the ERC, although other processes may contribute to these values (see Discussion). Importantly, at later times both reassembly curves reached

similar intensity levels. These levels surpassed the steady state FA level in untreated cells, presumably because of the synchronous return of activated integrins (see Discussion). Also in agreement with the results obtained from the MT regrowth system (Figure 14A), SFK but not FAK inhibitor reduced surface integrin levels in migrating cells (Figure 22E).

Next, we tested if Mn^{2+} could rescue FA assembly in FAK-inhibited migrating cells. We treated migrating cells with PF228 or PP2 for 2 h to allow for complete FA disassembly and then added Mn^{2+}. In agreement with the data from the MT-induced FA disassembly system, Mn^{2+} induced FA reassembly in FAK-inhibited cells but not in SFKs-inhibited cells (Figure 22F). Lastly, we determined where and when FA reassembly takes place after MT regrowth from NZ treatment in cells at the edge of a wounded monolayer and hence polarized for migration. Consistent with the earlier results (Figure 3E, F), FA reassembly occurred at 90-100 min after MT regrowth and was highly polarized at the leading edge (Figure 22G). Quantification revealed that FA density increased 4-fold in the leading edge 90-100 min after MT regrowth compared to before MT regrowth (Figure 22H). Collectively these results support the idea that FAK and SFKs modulate activation of endocytosed integrin and its recycling during cell migration.

DISCUSSION

Our study establishes for the first time a connection between FA disassembly and reassembly through an integrin endocytic recycling pathway and shows that this cycle is rate-limiting for cell migration. Combined with results from earlier studies, our work supports a new model for the reassembly of FAs from recycled integrins in which FAK and SFKs play previously unsuspected roles (Figure 23). The key steps of the model are as follows. MT-induced disassembly of FAs results in the endocytic uptake of FA integrin through a clathrin and dynamin-dependent process (Chao and Kunz, 2009; Ezratty et al., 2009; Ezratty et al., 2005). The endocytosed integrins travel through Rab5 early endosomes and the Rab11 ERC before returning to the cell surface where they rapidly reassemble into new FAs due to their maintenance in an active state during endocytic recycling. FAK and SFKs play key roles in this trafficking by maintaining integrin in an active state after FA disassembly and returning integrin to the cell surface from the ERC, respectively. A key implication of this model is that integrins derived from disassembled FAs have "memory" of their residence in FAs since they retain their activation state.

The functions we describe for FAK and SFKs in the recycling of active integrin represent new functions for both kinases. That SFKs participate in the return of integrin from the ERC is consistent with earlier studies reporting localization of Src to perinuclear endosomes and the regulation of SFK's activity by association with endosomal membranes (Fincham et al., 1996; Kaplan et al., 1992; Sandilands et al., 2007; Tanji et al., 2010), yet SFKs have not been shown previously to regulate the recycling of integrins. The localization of Src in the ERC during integrin recycling, the failure to restore surface integrin levels and accumulation of integrin in the ERC in SFK-inhibited cells, and the lag in the reappearance of FAs after PP2 washout

relative to PF228 washout, all strongly support a role for SFKs in regulating the trafficking of integrin from the ERC to the cell surface. Consistently, SFKs have been shown to be necessary for the trafficking of one other membrane protein, namely the FGF receptor (Belleudi et al., 2011; Auciello et al., 2013).

The function of FAK in maintaining the activity of endocytosed integrin was unexpected. FAK has not previously been shown to control integrin activation state, which may reflect the fact that previous studies did not specifically examine endocytosed integrin. Strikingly, we detect active FAK with the endocytosed integrin in at least two intracellular compartments, suggesting that FAK may travel with integrin throughout its endocytic recycling. To our knowledge, FAK is the first FA resident protein shown to have a role in integrin trafficking.

Previous studies demonstrated that the scaffolding function of FAK is required for MT-induced FA disassembly (Ezratty et al., 2005; Wang et al., 2011b). Strikingly, we found that FAK kinase activity is dispensable for this process, thus indicating that the scaffolding and kinase functions of FAK can be separated. Moreover, the scaffolding function of FAK was recently shown to be important for talin recruitment to FAs during early cell spreading (Lawson et al., 2012), which is consistent with a role for this kinase in modulating integrin activation and/or clustering in the plasma membrane. Thus it is possible that FAK might contribute to integrin activation at two stages in the life cycle of integrins: during integrin recycling back to the cell surface where FAK kinase activity is required and in the plasma membrane where FAK scaffolding function enhances talin recruitment (Lawson et al., 2012).

Curiously, while we find that FAK is essential for FA reformation, previous studies using spreading assays do not report a defect in FA formation (Ilic et al., 1995). How can our results be reconciled with the earlier studies? We suggest that there is a major difference between our assay

and that used in the earlier studies. In the MT regrowth assay, FA reformation is specifically dependent on recycled integrin, whereas in spreading assays, there is a vast pool of active integrins released into the cell membrane upon cell detachment and these would be available to engage the ECM during cell spreading.

Our study supports the idea that endocytosed integrin is trafficked to different locales depending on its activation state. Previously, inactive β1 integrin was shown to traffic through a Rab4-dependent fast-loop recycling pathway, whereas active integrin traffics predominantly along the Rab11-dependent long-loop pathway (Powelka et al., 2004; Arjonen et al., 2012) as we observed in our study. Additionally, it was demonstrated that the active β1 integrin is internalized more efficiently than the inactive conformation and that this particular integrin pool does not undergo Rab4-rapid recycling (Chao and Kunz, 2009; Arjonen et al., 2012).

The presence of ECM ligand with endocytosed integrin may also effect its trafficking. Interestingly, FN has been detected in integrin-containing endosomes (Ng et al., 1999; Pellinen et al., 2006) and it has been demonstrated that this active pool of integrins follows an alternative trafficking pathway. Active integrin (detected with conformation specific antibodies) localized to Rab7 endosomes (Arjonen et al., 2012) and FN-bound integrin was shown to be ubiquitinylated and directed to lysosomes for degradation (Lobert et al., 2010). That FN bound integrin is degraded rather than recycled may be one way to ensure that the integrin returned to the cell surface is capable of binding ECM ligands and reforming adhesions. We find that after FA disassembly, there is little FN associated with β1 integrin in the Rab11 ERC (data not shown), consistent with it being returned to the cell surface in an unliganded state.

Our results support the idea that there is a cycle of integrin recycling that contributes to polarized formation of FAs in the leading edge of migrating cells. To fully understand how this

cycle is coupled to cell migration it will be important to address new questions raised by our study, including how vesicles are trafficked from the Rab11 ERC to the cell surface and how the sites of recycled integrin exocytosis are related to sites of FA reformation. We identified FAK as one component that maintains integrin in an active state during its endocytic recycling, which raises the possibility that other FA components may also be involved. The system of synchronous FA disassembly and integrin endocytosis we have characterized here should be useful for exploring these questions.

FIGURES

Figure 3. FA reassembly occurs with a lag of 30 minutes after disassembly.

(A) Immunofluorescence images of vinculin and MTs in NIH3T3 fibroblasts after treatment with NZ for 3-4 h followed by washout for the indicated times. (B) Quantification of FA disassembly and reassembly following NZ washout. The histogram illustrates data from at least 2 independent experiments in which 25 cells per time-point were analyzed. Error bars are SD. Scale bar, 15 μm. (C) Western blot of FAK, FAK-pY397, paxillin-pY118 and tubulin after NZ washout. Starved NIH 3T3 fibroblasts were incubated with NZ (10 μM; 4 h) and the drug was then washed out and MTs were allowed to regrow for the indicated times before preparing samples for SDS–PAGE. Tubulin is a loading control. (D) Quantification of FAK-pY397 to FAK ratios from western blots such as in "C". The data represent densitometric analysis of five separate experiments. Error bars are SD. (E) FA reassembly occurs preferentially at the cell periphery. Left: diagram illustrating the methodology used to quantify the distribution of reassembled FAs: FAs located outside a 2 μm range from the cell periphery were classified as internal FAs ("Region B") whereas those inside the 2 μm range were classified as peripheral FAs ("Region A"). Right: quantification of FA area within each of the regions defined in the diagram. Data are from at least 3 independent experiments in which 15 cells were analyzed for each time-point. Error bars are SD. (F) Merged images of paxillin-EGFP at 0min (green) and 100min (red) after NZ washout showing polarized FAs reassembly. Scale bar, 5 μm. ***$p < 0.001$; **$p<0.01$.

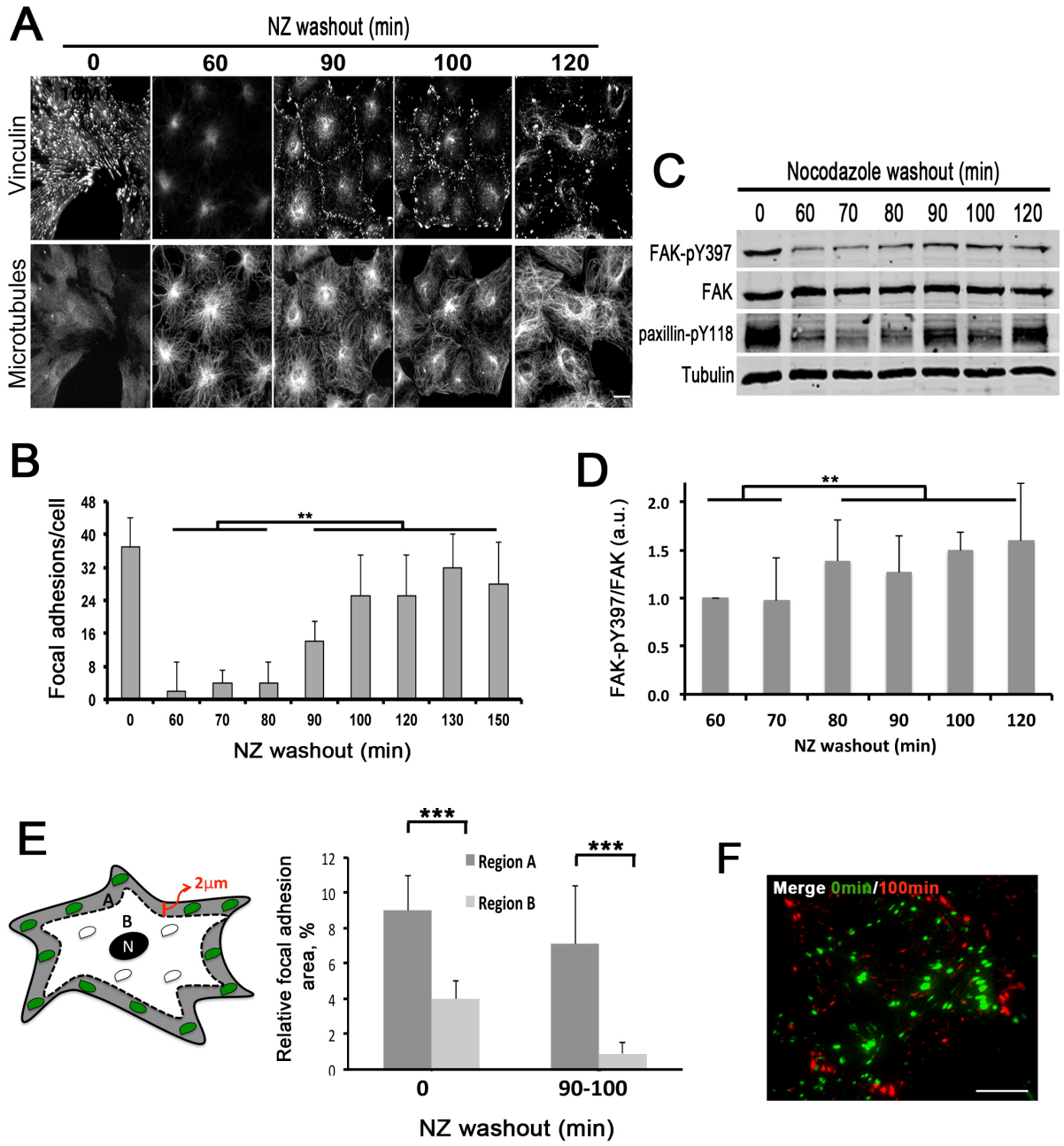
A
NZ washout (min)
0
60
90
100
120
Vinculin
Microtubules
C
Nocodazole washout (min)
0 60 70 80 90 100 120
FAK-pY397
FAK
paxillin-pY118
Tubulin
B
Focal adhesions/cell
NZ washout (min)
D
FAK-pY397/FAK (a.u.)
NZ washout (min)
E
2μm
A
B
N
Relative focal adhesion area, %
Region A
Region B
0
90-100
NZ washout (min)
F
Merge 0min/100min

Figure 4. FA reassembly as assayed with additional FA markers.

Immunofluorescence images of pY397-FAK, paxillin and Rhodamine-phalloidin staining of NIH3T3 fibroblasts after NZ treatment (3-4 h) and washout for the indicated times. Scale bar, 10 μm.

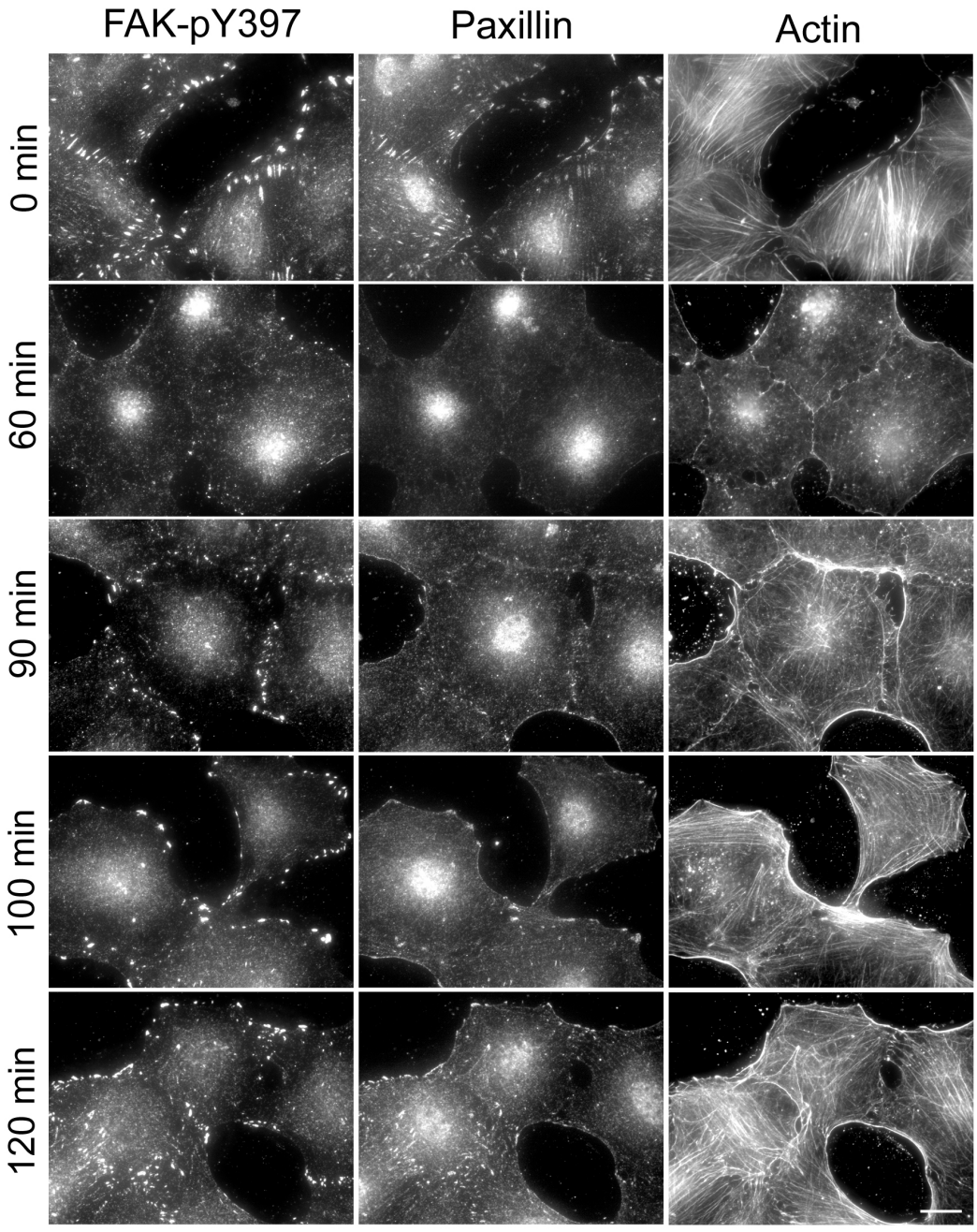
FAK-pY397
Paxillin
Actin
0 min
60 min
90 min
100 min
120 min

Figure 5. Characterization of paxillin-EGFP NIH3T3 fibroblast cell line.

(A) Immunofluorescence of Paxillin-EGFP NIH3T3 fibroblast cell line showing a similar distribution of paxillin-EGFP and endogenous FAK-pY397. (B) Immunofluorescence of NIH3T3 fibroblasts stained for paxillin and vinculin showing that FAs are similar in size, number and distribution compared to the FAs in paxillin-EGFP NIH3T3 fibroblasts. (C) Western blot analysis of paxillin levels in paxillin-EGFP NIH3T3 fibroblasts. Note that the exogenous paxillin-EGFP is expressed at levels comparable to endogenous paxillin. (D) Quantification of cell migration velocity for parental NIH3T3 fibroblasts and paxillin-EGFP NIH3T3 fibroblasts. DIC images were taken at 5 min intervals for 12 h. Error bars are SD. (A-B) Scale bars, 15 μm.

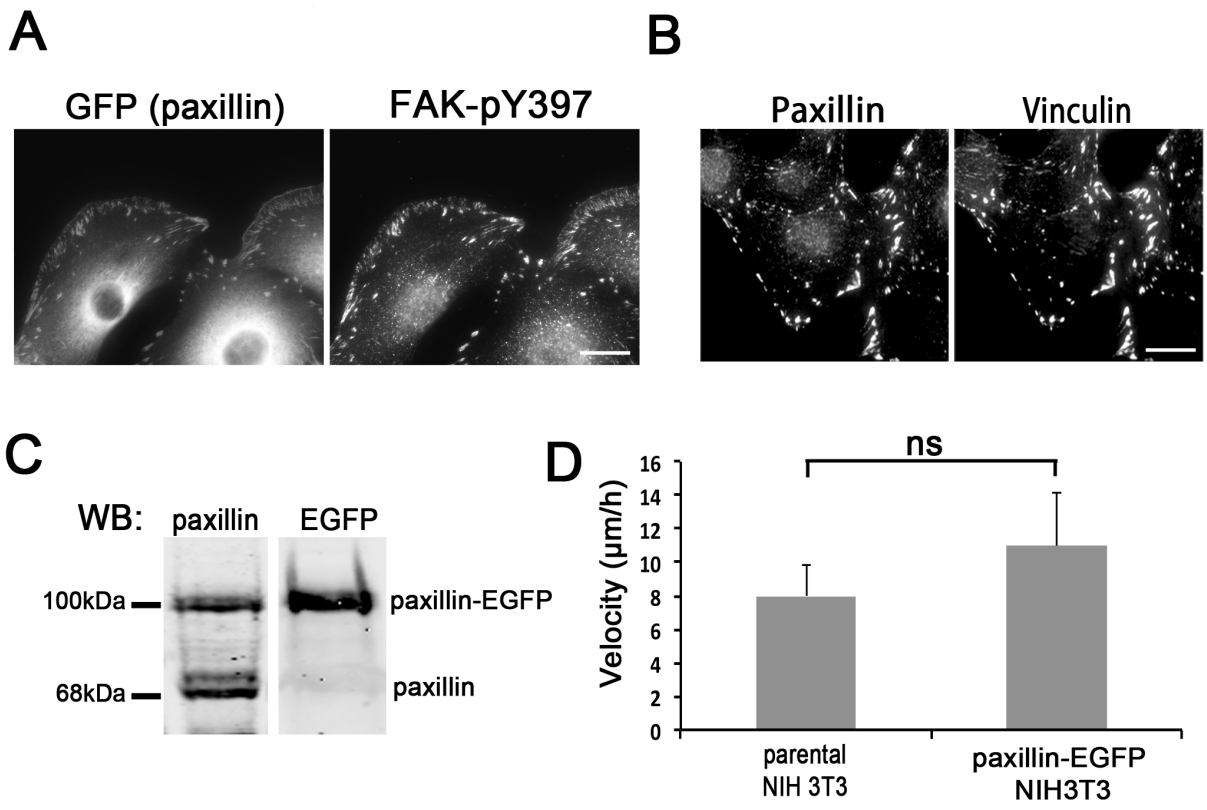
A
GFP (paxillin)
FAK-pY397
B
Paxillin
Vinculin
C
WB:
paxillin
EGFP
100kDa
68kDa
paxillin-EGFP
paxillin
D
ns
Velocity (µm/h)
16
14
12
10
8
6
4
2
0
parental
NIH 3T3
paxillin-EGFP
NIH3T3

Figure 6. FA reassembly involves endocytic recycling.

(A) Quantification of levels of surface α5 integrin measured by antibody labeling and flow cytometry for NIH3T3 fibroblasts at indicated times after NZ washout. Values represent mean fluorescent intensity normalized to the value at 0 min of NZ washout. Data are from eight independent experiments. (B) Immunofluorescence of α5 integrin-GFP and endogenous Rab11 in NIH3T3 fibroblasts at the indicated times after NZ washout. Arrows indicate colocalization of α5 integrin-GFP with the Rab11-ERC. Note the reduction and redistribution of the α5 integrin-GFP from the Rab11-positive compartment to FAs at 120 min of NZ washout. Scale bar, 15 μm. (C) Immunofluorescence images of vinculin and Rab11 in NIH3T3 fibroblasts expressing Rab11 WT-GFP or Rab11 S25N-GFP fixed at 120 min of NZ washout. Arrows indicate transfected cells. Scale bar, 20 μm. (D) Quantification of FA disassembly and reassembly in NIH3T3 fibroblasts transfected with the indicated Rab mutants. Cells were scored positive if they contained > 10 FAs. Data represent at least three independent experiments in which > 150 cells were analyzed for each condition. (E) Immunofluorescence images of vinculin and MTs in NIH3T3 fibroblasts treated with non-coding (NC) or Rab11a/b siRNAs and fixed at the indicated times after NZ washout. Scale bar, 20 μm. (F) Quantification of FA disassembly and reassembly in NIH3T3 fibroblasts treated with Rab11a/b or NC siRNAs. Cells were fixed at the indicated times after NZ washout. Data represent at least five independent experiments in which > 150 cells were analyzed for each condition. (G) Levels of surface α5 integrin at 90 min of NZ washout relative to 60 min of NZ washout in NIH3T3 fibroblasts treated with either Rab11a/b or NC siRNAs. Data represent the mean fluorescent intensity from three independent experiments. Error bars are SD. *** $p < 0.001$, ** $p < 0.01$.

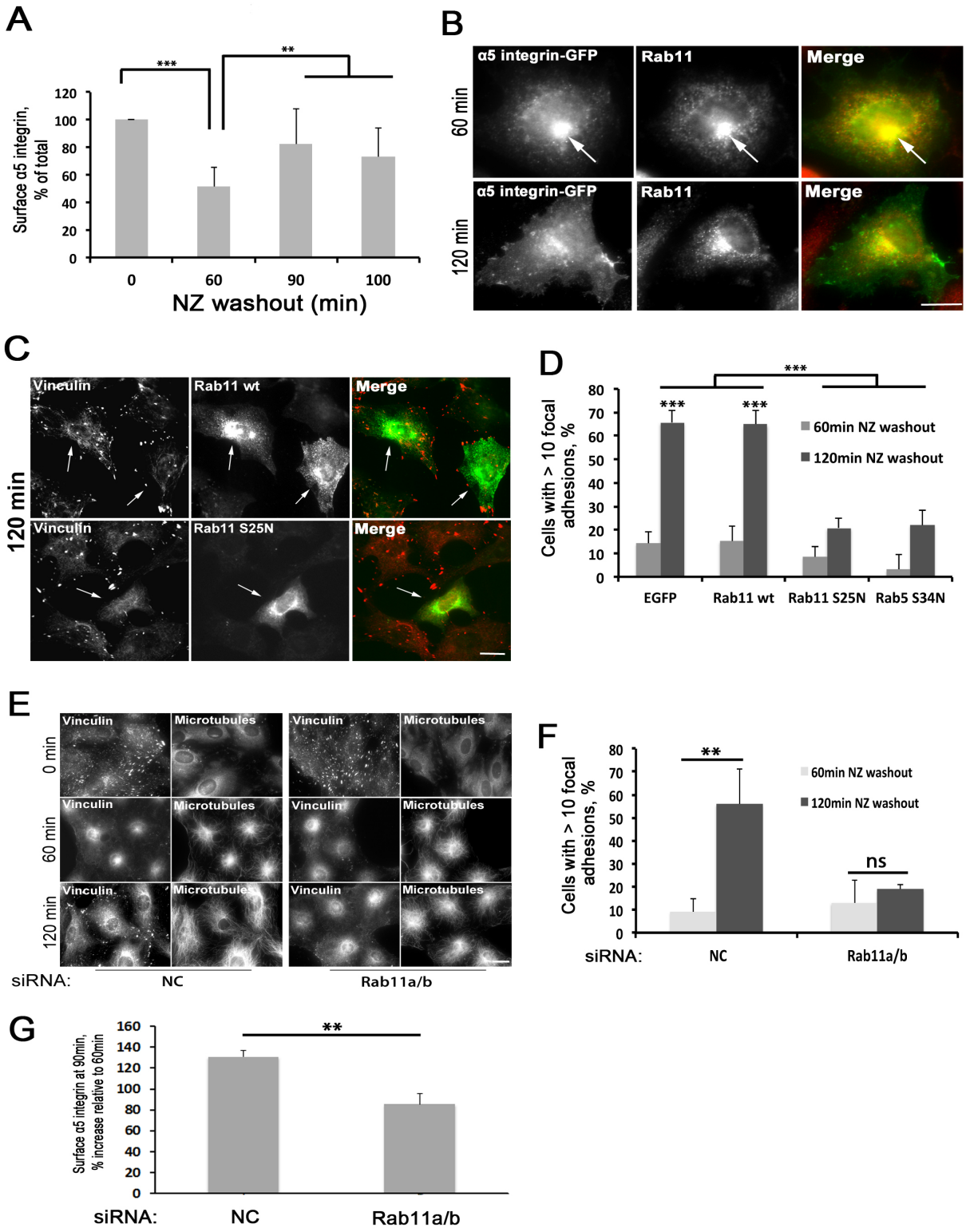
A
***
**
Surface α5 integrin, % of total
120
100
80
60
40
20
0
0
60
90
100
NZ washout (min)
B
α5 integrin-GFP
Rab11
Merge
60 min
120 min
C
Vinculin
Rab11 wt
Merge
120 min
Vinculin
Rab11 S25N
Merge
D
***
***
***
Cells with > 10 focal adhesions, %
80
70
60
50
40
30
20
10
0
60min NZ washout
120min NZ washout
EGFP
Rab11 wt
Rab11 S25N
Rab5 S34N
E
Vinculin
Microtubules
0 min
60 min
120 min
siRNA:
NC
Rab11a/b
F
**
ns
Cells with > 10 focal adhesions, %
80
70
60
50
40
30
20
10
0
60min NZ washout
120min NZ washout
siRNA:
NC
Rab11a/b
G
**
Surface α5 integrin at 90min, % increase relative to 60min
160
140
120
100
80
60
40
20
0
siRNA:
NC
Rab11a/b

Figure 7. Analysis of total integrin levels and of dominant negative Rab5 during MT induced FA disassembly.

(A) Western blot analysis of α5 integrin in NIH3T3 fibroblasts lysates at the indicated times after NZ washout. Vinculin is shown as a loading control. (B) Immunofluorescence image of zyxin and Rhodamine-phalloidin stained in a Rab5 dominant negative (Rab5 S34N)-transfected NIH3T3 fibroblast (arrow) after 120 min of NZ washout. Scale bar, 15 μm. (C) Western blot analysis of Rab11a/b in NIH3T3 fibroblasts treated with non-coding (NC) or Rab11a/b siRNAs. Tubulin is a loading control.

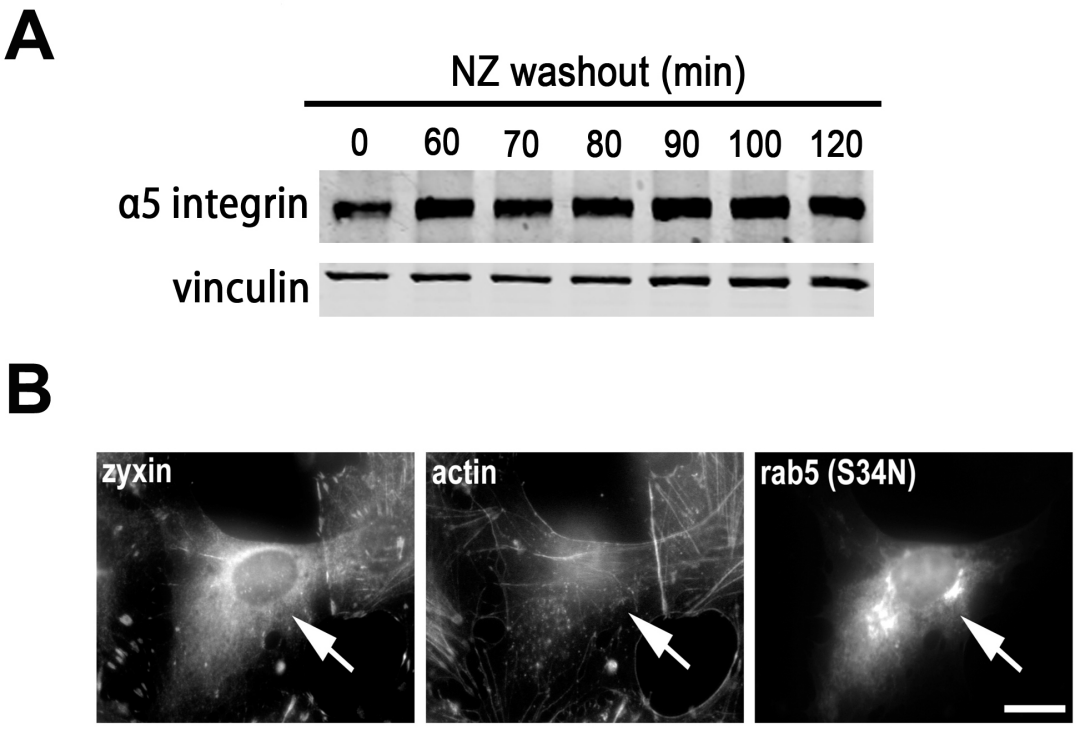
A
NZ washout (min)
0
60
70
80
90
100
120
α5 integrin
vinculin
B
zyxin
actin
rab5 (S34N)
C
siRNA
WB:
NC
Rab11a/b
Rab11a/b
tubulin

Figure 8. Localization of α5 integrin-GFP in the Rab11 ERC after FA disassembly.

Immunofluorescence images of α5 integrin-GFP, Rab11 and GM-130 (Golgi) in NIH3T3 fibroblasts expressing α5 integrin-GFP fixed at 60 min of NZ washout. Arrows indicate the Rab11 ERC; arrowhead indicates the Golgi. Note colocalization of α5 integrin-GFP with the Rab11 ERC but not the Golgi. Scale bar, 5 μm.

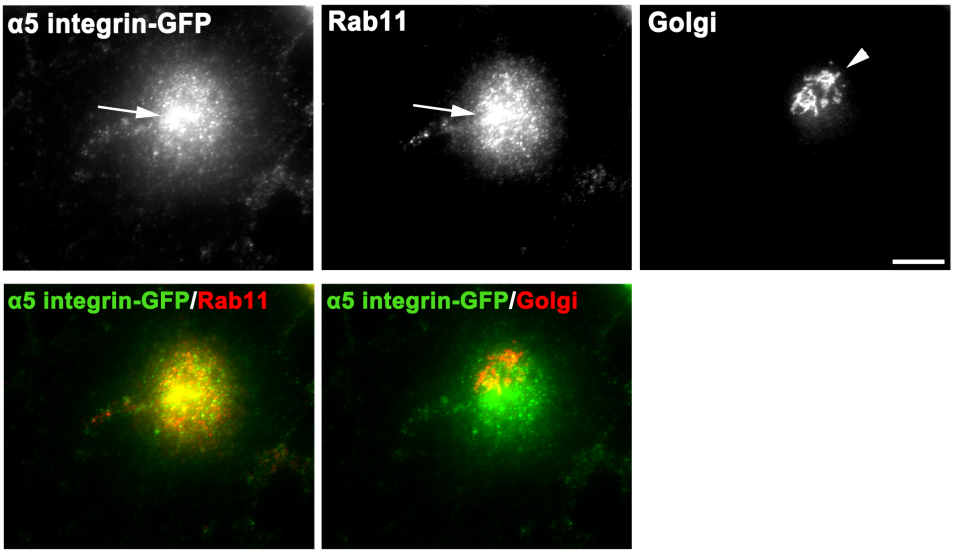
α5 integrin-GFP
Rab11
Golgi
α5 integrin-GFP/Rab11
α5 integrin-GFP/Golgi

Figure 9. FAK kinase activity is dispensable for FA disassembly but critical for FA reassembly.

(A) Immunofluorescence images of FAK-pY397 and Rab11 in NIH3T3 fibroblasts expressing Rab11 WT-GFP. Cells were fixed at the indicated times after NZ washout. Arrows indicate the Rab11 ERC. (B) Immunofluorescence images of vinculin and GFP in $FAK^{-/-}$ mouse embryo fibroblasts (MEFs) expressing FAK-WT-EGFP. Cells were fixed at the indicated times after NZ washout. Arrows indicate transfected cells. (C) Immunofluorescence images of vinculin or paxillin and GFP or HA in $FAK^{-/-}$ MEFs expressing FAK-Y397F-EGFP (autophosphorylation/Src binding site) or FAK-K454R-HA (kinase dead) variants. Cells were fixed at the indicated times after NZ washout. Arrows indicate transfected cells. (D-E) Quantification of FA disassembly (D) and reassembly (E) in $FAK^{-/-}$ MEFs expressing the indicated FAK constructs. Data represent at least five independent experiments in which > 100 cells were analyzed for each condition. Scale bars, 20 μm. Error bars are SD, *** $p < 0.001$, relative to EGFP-transfected cells.

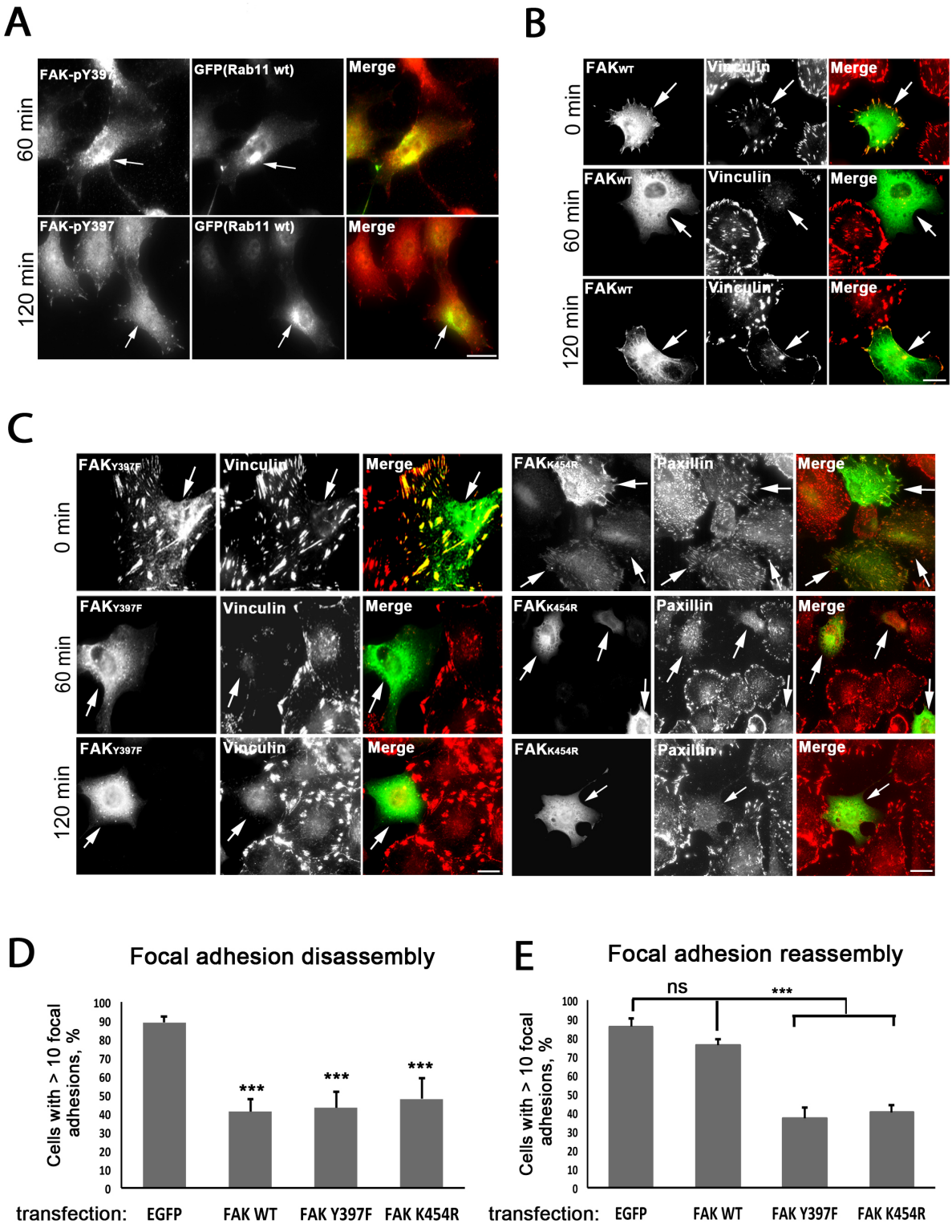
A
FAK-pY397
GFP(Rab11 wt)
Merge
60 min
120 min
B
FAKWT
Vinculin
Merge
0 min
60 min
120 min
C
FAKY397F
FAKK454R
Paxillin
0 min
60 min
120 min
D
Focal adhesion disassembly
Cells with > 10 focal adhesions, %
transfection:
EGFP
FAK WT
FAK Y397F
FAK K454R
***
E
Focal adhesion reassembly
ns
***

Figure 10. FAK and SFKs activities are required for FA adhesion reassembly.

(A) Immunofluorescence images of vinculin in NIH3T3 fibroblasts treated with NZ for 3-4 h followed by washout in the presence of the indicated drugs (DMSO, PF228 10 μM or PP2 10 μM). Cells were fixed at the indicated times. (B) Quantification of FA disassembly and reassembly in cells treated with vehicle (DMSO), PF228 or PP2. Data represent at least three independent experiments in which > 200 cells were analyzed for each condition. (C) Immunofluorescence images of vinculin and MTs in NIH3T3 fibroblasts treated with NZ for 3-4 h followed by washout in the presence of the indicated drugs (DMSO, PF228 10 μM or PP2 10 μM). Cells were fixed at the indicated times. (D) Quantification of FA reassembly following drug release. Data represent at least three independent experiments in which > 200 cells were analyzed for each condition. Error bars are SD. Scale bars, 20 μm. *** $p < 0.001$, relative to DMSO-treated cells at 120 min after NZ washout.

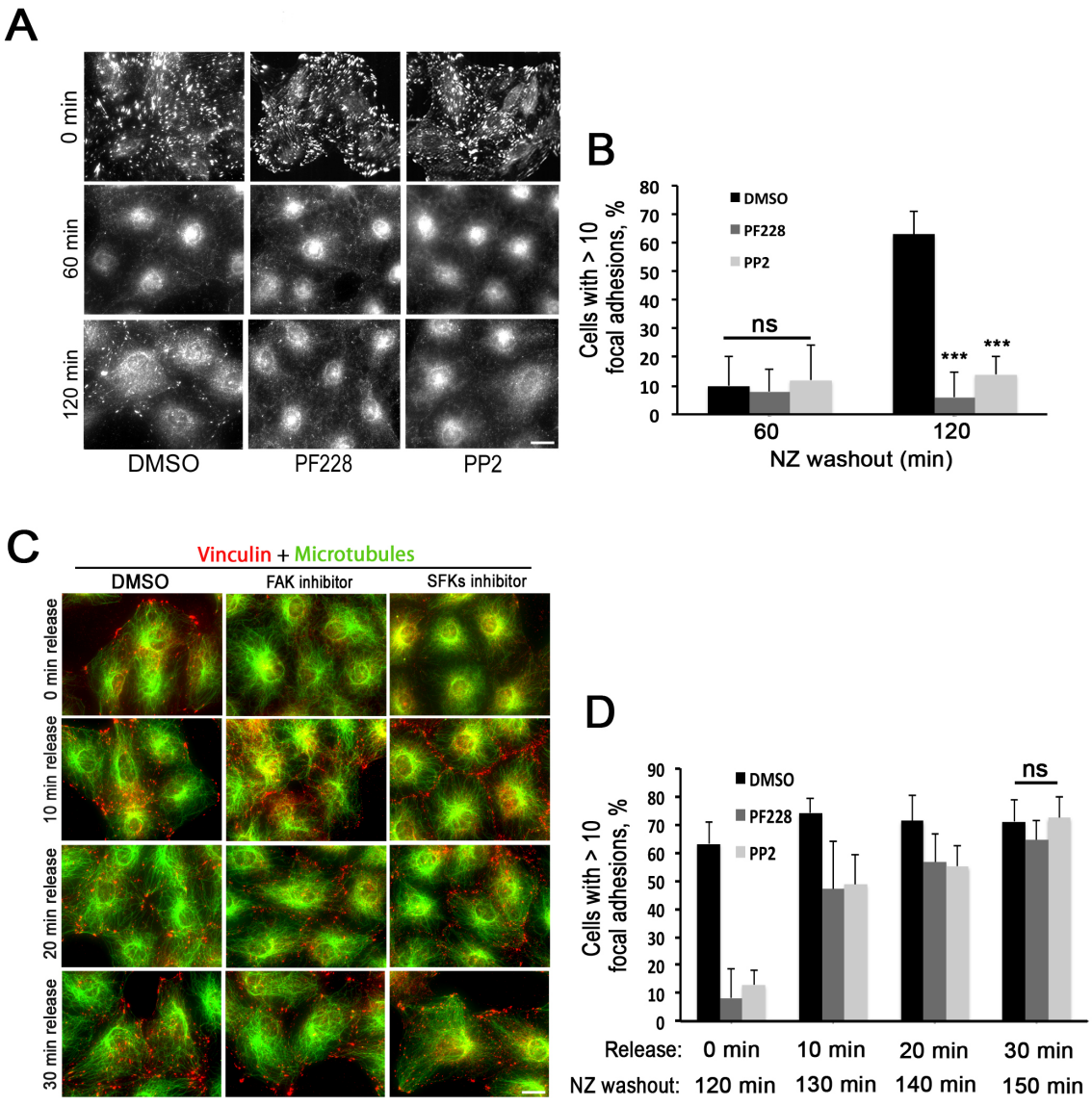
A
0 min
60 min
120 min
DMSO
PF228
PP2
B
Cells with > 10 focal adhesions, %
DMSO
PF228
PP2
ns
***
***
60
120
NZ washout (min)
C
Vinculin + Microtubules
DMSO
FAK inhibitor
SFKs inhibitor
0 min release
10 min release
20 min release
30 min release
D
Cells with > 10 focal adhesions, %
DMSO
PF228
PP2
ns
Release: 0 min 10 min 20 min 30 min
NZ washout: 120 min 130 min 140 min 150 min

Figure 11. A structurally distinct FAK inhibitor inhibits FA reassembly without affecting disassembly.

Immunofluorescence images of vinculin, paxillin and MTs in NIH3T3 fibroblasts treated with NZ for 3-4 h followed by washout in the presence of the indicated drugs (DMSO or FAK inhibitor-I 2 μM). Cells were fixed at the indicated times.

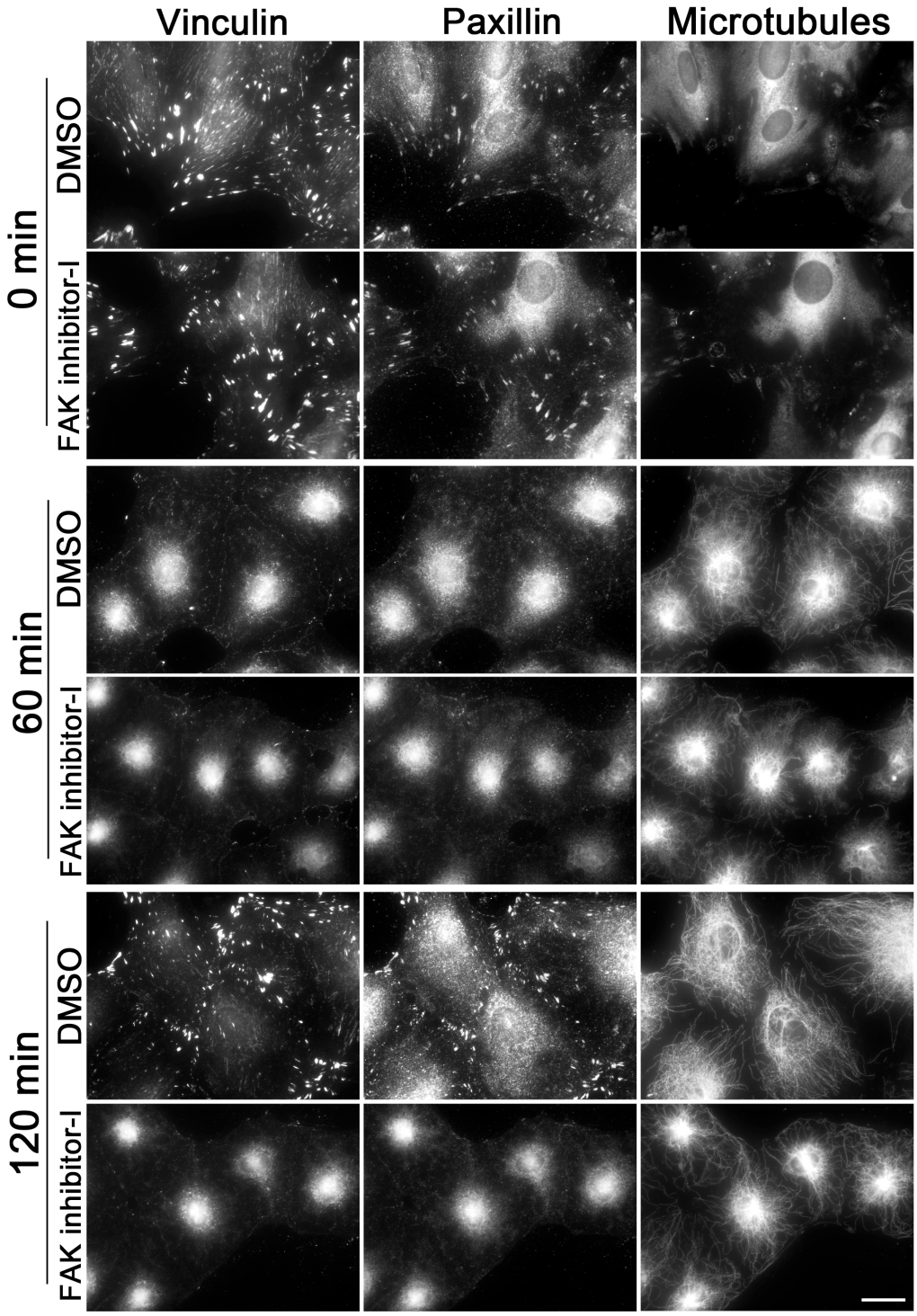
Vinculin
Paxillin
Microtubules
0 min
60 min
120 min
DMSO
FAK inhibitor-I

Figure 12. Biochemical analysis of FA disassembly and reassembly after inhibition of FAK or SFKs.

NIH3T3 fibroblasts treated with NZ for 3-4 h followed by washout in the presence of the indicated drugs (DMSO, PF228 10 μM or PP2 10 μM). Cells were lysed at the indicated times and blotted for paxillin-pY118 and paxillin antibodies. Tubulin is a loading control.

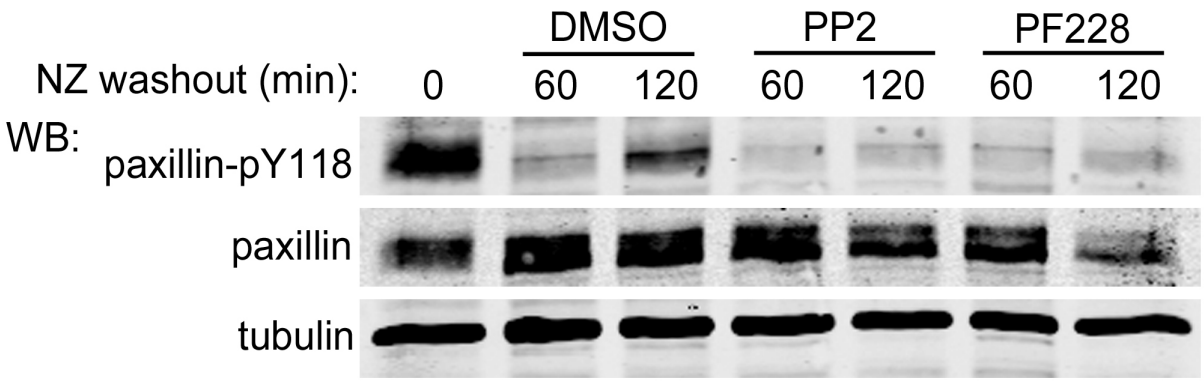
DMSO
PP2
PF228
NZ washout (min):
0
60
120
60
120
60
120
WB:
paxillin-pY118
paxillin
tubulin

Figure 13. Src localizes to the Rab11 ERC after FA disassembly.

Immunofluorescence images of Src and Rab11-EGFP in NIH3T3 fibroblasts expressing Rab11-EGFP fixed at 60 min after NZ washout. Arrows indicate the Rab11 ERC. Note colocalization of endogenous Src with the Rab11 ERC. Scale bar, 15 μm.

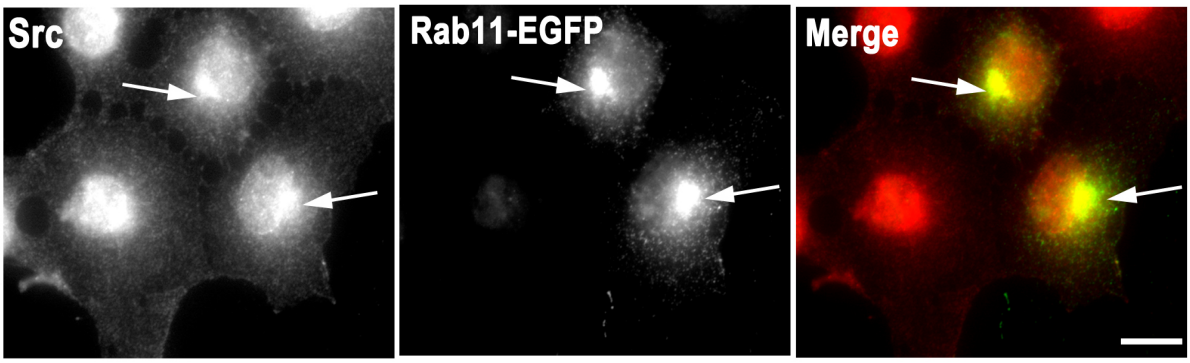
Src
Rab11-EGFP
Merge

Figure 14. SFKs mediate integrin trafficking from the ERC.

(A) NIH 3T3 fibroblasts were treated with NZ for 3-4 h and surface levels of α5 integrin were measured by flow cytometry at the indicated times after NZ washout. Data represent mean fluorescent intensity from eight independent experiments. (B) Immunofluorescence images of α5 integrin-GFP and Rab11 in NIH3T3 fibroblasts expressing α5 integrin-GFP fixed at 60 or 120 min after NZ washout. The NZ washout was performed in the presence of DMSO (vehicle), PF228 (10 μM) or PP2 (10 μM). Arrows indicate the Rab11 ERC. Note that α5 integrin-GFP accumulates in the Rab11 ERC at 60 min after NZ washout. Arrowheads indicate the redistribution of α5 integrin-GFP to FAs after 120 min of NZ washout in DMSO-treated NIH3T3 fibroblasts. Scale bar, 15 μm. (C) Quantification of α5 integrin-GFP signal in the Rab11 ERC (assessed by Rab11 staining) during FA disassembly and reassembly in the presence of DMSO (vehicle), PF228 (10 μM) or PP2 (10 μM). Data represent at least three independent experiments in which 20 cells were analyzed for each condition. Scale bars, 20 μm. Bars are SD. In "C", *** $p < 0.001$, relative to PP2-treated cells at 120 min after NZ washout.

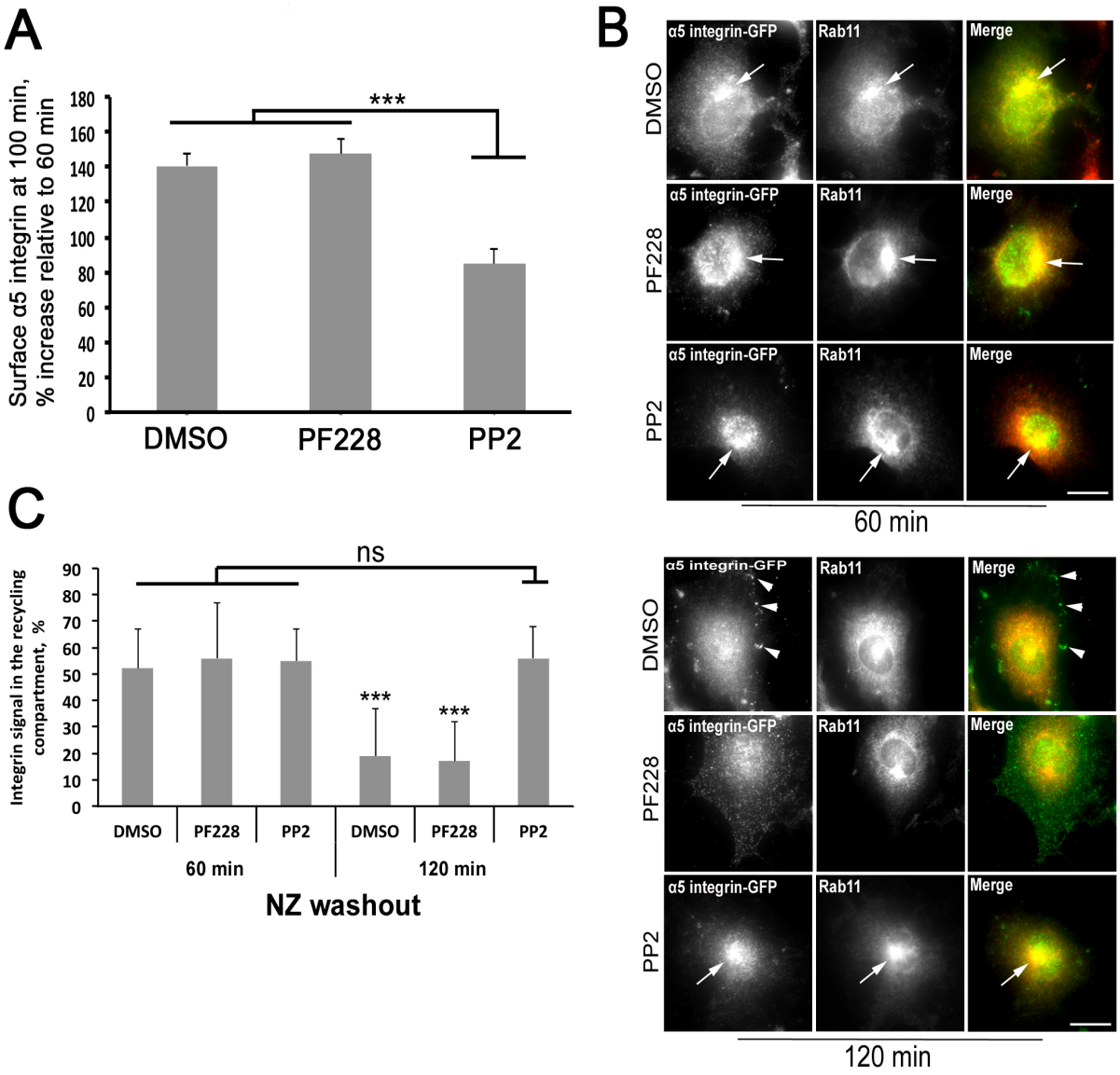
A
Surface α5 integrin at 100 min, % increase relative to 60 min
180
160
140
120
100
80
60
40
20
0
***
DMSO
PF228
PP2
B
α5 integrin-GFP
Rab11
Merge
DMSO
PF228
PP2
60 min
120 min
C
Integrin signal in the recycling compartment, %
90
80
70
60
50
40
30
20
10
0
ns
***
***
DMSO
PF228
PP2
DMSO
PF228
PP2
60 min
120 min
NZ washout

Figure 15. FAK inhibitor causes impaired cell adhesion and blocks FA reassembly by affecting integrin activation.

(A) Data represent adhesion assay performed on FN-coated surfaces. NIH3T3 fibroblasts were treated with NZ for 3-4 h and following 90 min of NZ washout in the presence of DMSO, PP2 (10 μM) or PF228 (10 μM) cells were trypsinized and replated on FN-treated coverslips for 15 min still in the presence of the drugs. Manganese was added to the indicated samples (100 μM). Nuclei were stained with DAPI to assess the number of cells adhered (for more details see Methods). (B) Immunofluorescence images of vinculin in NIH3T3 fibroblasts treated with NZ for 3-4 h and fixed at the indicated times after NZ washout. NZ washout was performed in the presence of the indicated drugs as in "A". Manganese was added to the medium at 85 min of NZ washout and cells were incubated for another 35 min. Scale bar, 10 μm. (C) Quantification of the binding of a FN fragment containing the canonical RGD- and synergy-binding sites for integrin (FN9-11). NIH3T3 fibroblasts were treated with NZ for 3-4 h and following the indicated times of NZ washout cells were harvested and the binding of the FN fragment was measured by flow cytometry (see Methods). NZ washout was performed in the presence of the indicated drugs as in "A". The histogram represents mean fluorescence intensity normalized to the value at 45 min of NZ washout. Data are from > 10 independent experiments. Error bars are SEM. (D) Immunofluorescence images of FAK (wt or different kinase mutants) and vinculin in NIH3T3 fibroblasts expressing FAK-WT-GFP, FAK-Y397F-GFP or FAK-K454R-HA and fixed at the indicated times after NZ washout. Manganese (100 μM) was added to the cells after 60 min of NZ washout. Arrows point to the transfected cells. Scale bar, 15 μm. (E) Quantification of FA disassembly and reassembly in transfected cells at the indicated times after NZ washout. At least 100 cells were analyzed in each experiment from a total of 3 independent experiments. Bars are SD. * $p < 0.05$; ** $p < 0.01$.

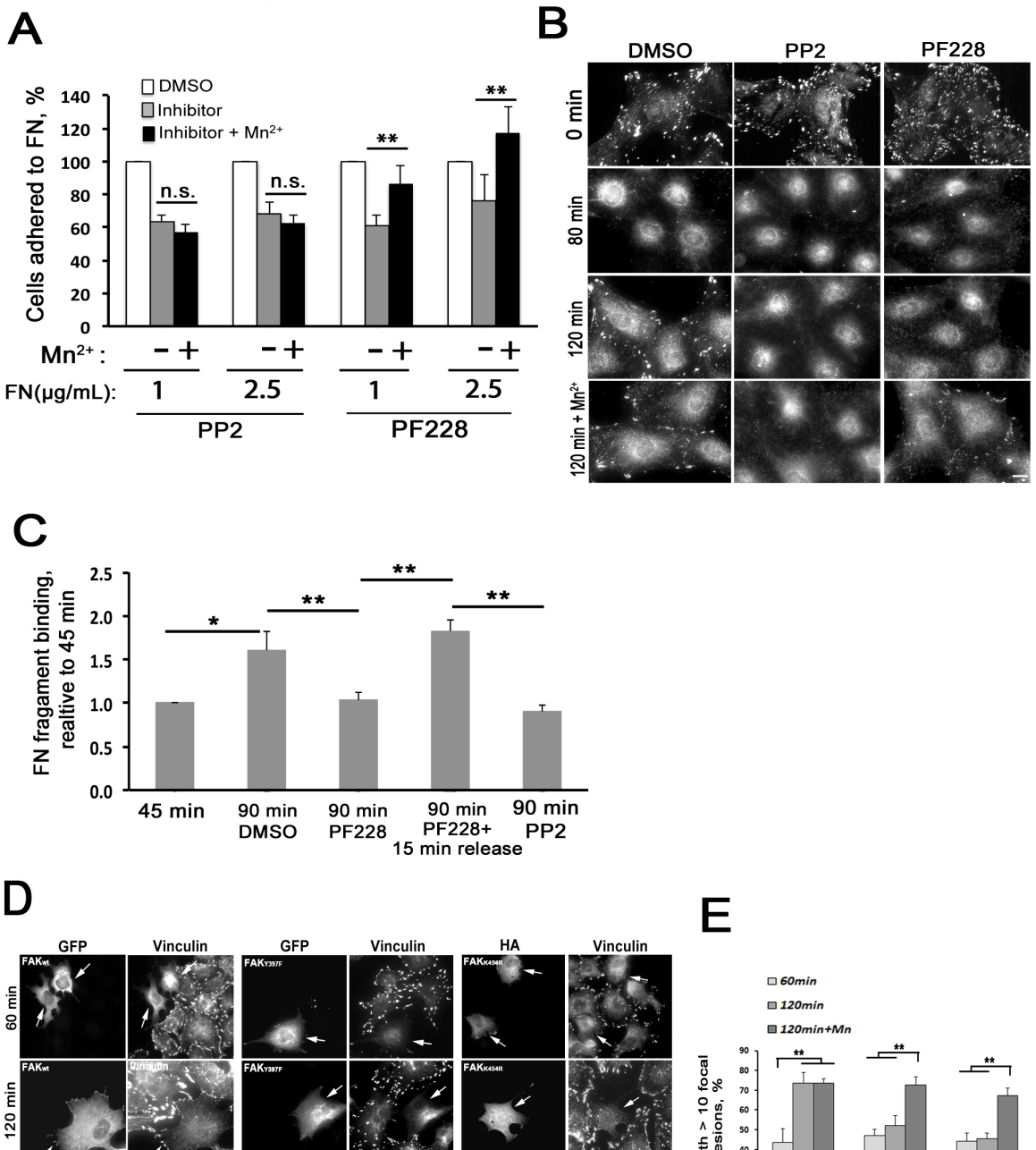
A
DMSO
Inhibitor
Inhibitor + Mn2+
Cells adhered to FN, %
n.s.
n.s.
**
**
Mn2+ :
FN(μg/mL):
1
2.5
1
2.5
PP2
PF228
B
DMSO
PP2
PF228
0 min
80 min
120 min
120 min + Mn2+
C
FN fragament binding, realtive to 45 min
45 min
90 min DMSO
90 min PF228
90 min PF228+ 15 min release
90 min PP2
D
GFP
Vinculin
GFP
Vinculin
HA
Vinculin
60 min
120 min
120 min + Mn2+
E
60min
120min
120min+Mn
Cells with > 10 focal adhesions, %
Transfection (FAK):
WT
Y397F
K454R

Figure 16. Manganese does not rescue FA reassembly in Rab11-depleted cells.

(A) Immunofluorescence images of vinculin and in NIH3T3 fibroblasts treated with non-coding (NC) or Rab11a/b siRNAs and fixed at 120 min after NZ washout. Manganese (100 μM) was added at 90 min after NZ washout. (B) Data represent the quantification of FA disassembly and reassembly in cells treated with Rab11a/b or NC siRNAs. At least two independent experiments were performed in which > 150 cells were analyzed for each condition. Scale bar, 15 μm. Error bars are SD. ***$p < 0.001$, relative to control (NC) values at 120 min after NZ washout.

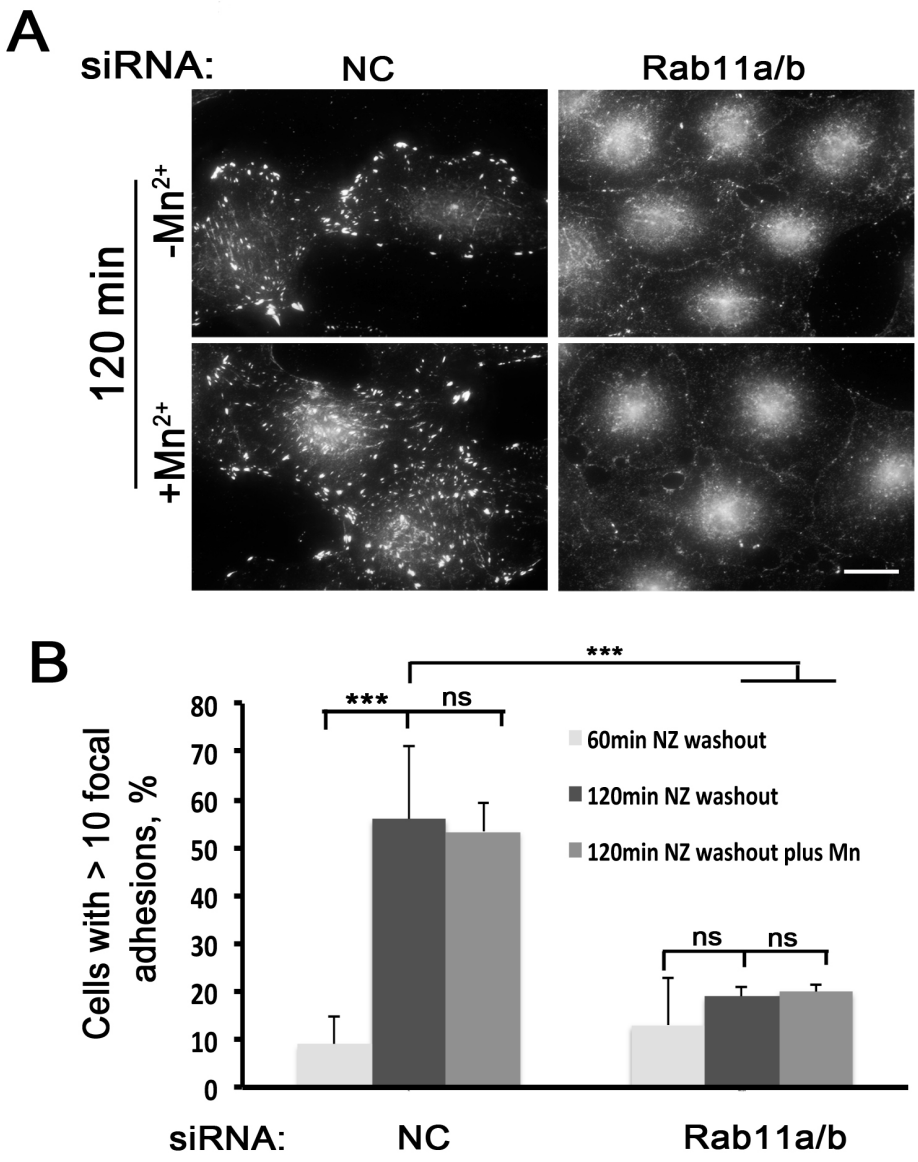
A
siRNA:
NC
Rab11a/b
120 min
-Mn2+
+Mn2+
B
***
***
ns
Cells with > 10 focal adhesions, %
80
70
60
50
40
30
20
10
0
60min NZ washout
120min NZ washout
120min NZ washout plus Mn
ns
ns
siRNA:
NC
Rab11a/b

Figure 17. FAK inhibitor blocks FA reassembly without interfering with FA disassembly in HT1080 fibrosarcoma cells.

(A) Immunofluorescence images of vinculin, paxillin-pY118 and MTs in HT1080 human fibrosarcoma cells fixed at the indicated times after NZ washout in the presence of DMSO (vehicle) or PF22 (10 μM). (B) Data represent quantification of FA disassembly and reassembly in cells treated with DMSO or PF228. Data are from at least three independent experiments in which > 200 cells were analyzed for each condition. Scale bar, 25 μm. Error bars are SD. ** $p < 0.01$.

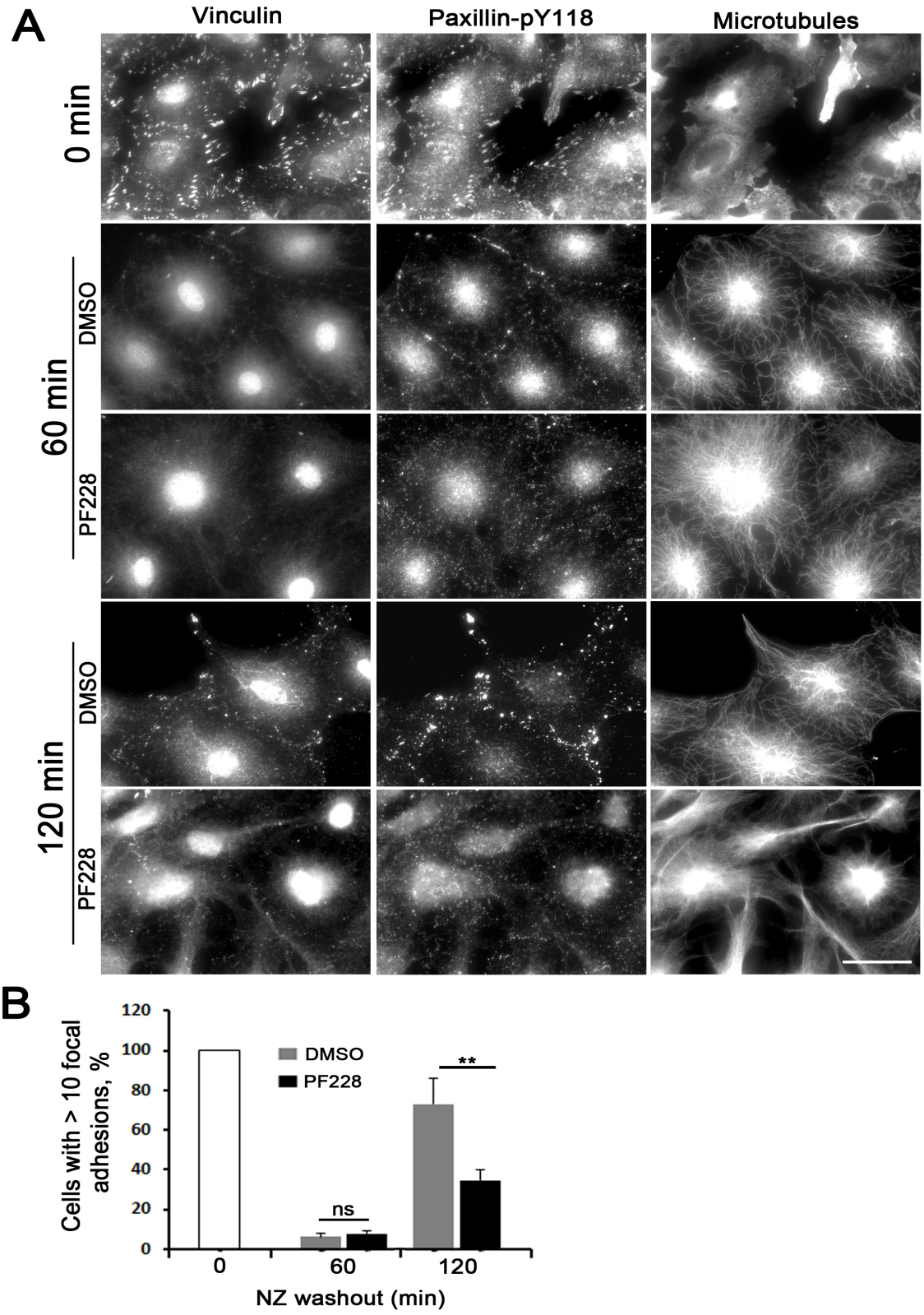
A
Vinculin
Paxillin-pY118
Microtubules
0 min
60 min
DMSO
PF228
120 min
DMSO
PF228
B
Cells with > 10 focal adhesions, %
120
100
80
60
40
20
0
DMSO
PF228
**
ns
0
60
120
NZ washout (min)

Figure 18. FAK kinase activity maintains integrin in an active state after FA disassembly and during endocytic recycling.

(A-B) Immunofluorescence images of active β1 integrin (12G10 antibody) and FAK in Rab5 constitutively active (Rab5 Q79L)-transfected HT1080 fibrosarcoma cells fixed at 0 or 30 min after NZ washout. Arrowheads indicate the Rab5 endosomes. Note the localization of active β1 integrin and FAK to the endosomes at 30 but not at 0 min after NZ washout. Scale bars, 10 μm. (C) Data represent the intensity of active β1 integrin in Rab5 endosomes. Data are from 12 cells (30 individual Rab5-positive endosomes) and this experiment was repeated at least two times. (D) Immunofluorescence images of Rab11 and active β1 integrin (12G10 antibody-insets) in HT1080 fibrosarcoma cells fixed at 60 min after NZ washout in the presence of Dynasore (80 μM) or vehicle (DMSO). Scale bars, 15 μm. (E) Data represent the intensity of active β1 integrin measured in the Rab11 ERC. Data are from 12 cells (30 individual Rab11-positive recycling compartments) and this experiment was repeated at least two times. (F) Immunofluorescence images of active β1 integrin (12G10 antibody), total β1 integrin (K20 antibody) and Rab11 in HT1080 fibrosarcoma cells fixed at 60 min after NZ washout in the presence of PF228 (10 μM) or vehicle (DMSO). Scale bars, 15 μm. (G) Data represent the intensity of active β1 integrin measured in the Rab11 ERC. Data are from 12 cells (30 individual Rab11-positive recycling compartments) and this experiment was repeated at least two times. (H) Immunofluorescence images of FN in HT1080 fibrosarcoma cells fixed at 0 and 60 min after NZ washout. Scale bar, 15 μm. (I) Immunofluorescence images of active β1 integrin (12G10 antibody), FN and Alexa 649-conjugated transferrin in HT1080 fibrosarcoma cells fixed at 60 min after NZ washout. Scale bars, 10 μm and 3 μm. (J) Immunofluorescence images of active β1 integrin [FN fragment-left row and 12G10 antibody-middle row] and Alexa 649-conjugated transferrin in HT1080 fibrosarcoma cells fixed at 60 min after NZ washout in the presence of vehicle (DMSO), PF228 (10 μM) or Dynasore (80 μM). Scale bar, 10 μm. The horizontal lines in the scatter dot plots represent the mean intensity. *** $p < 0.01$.

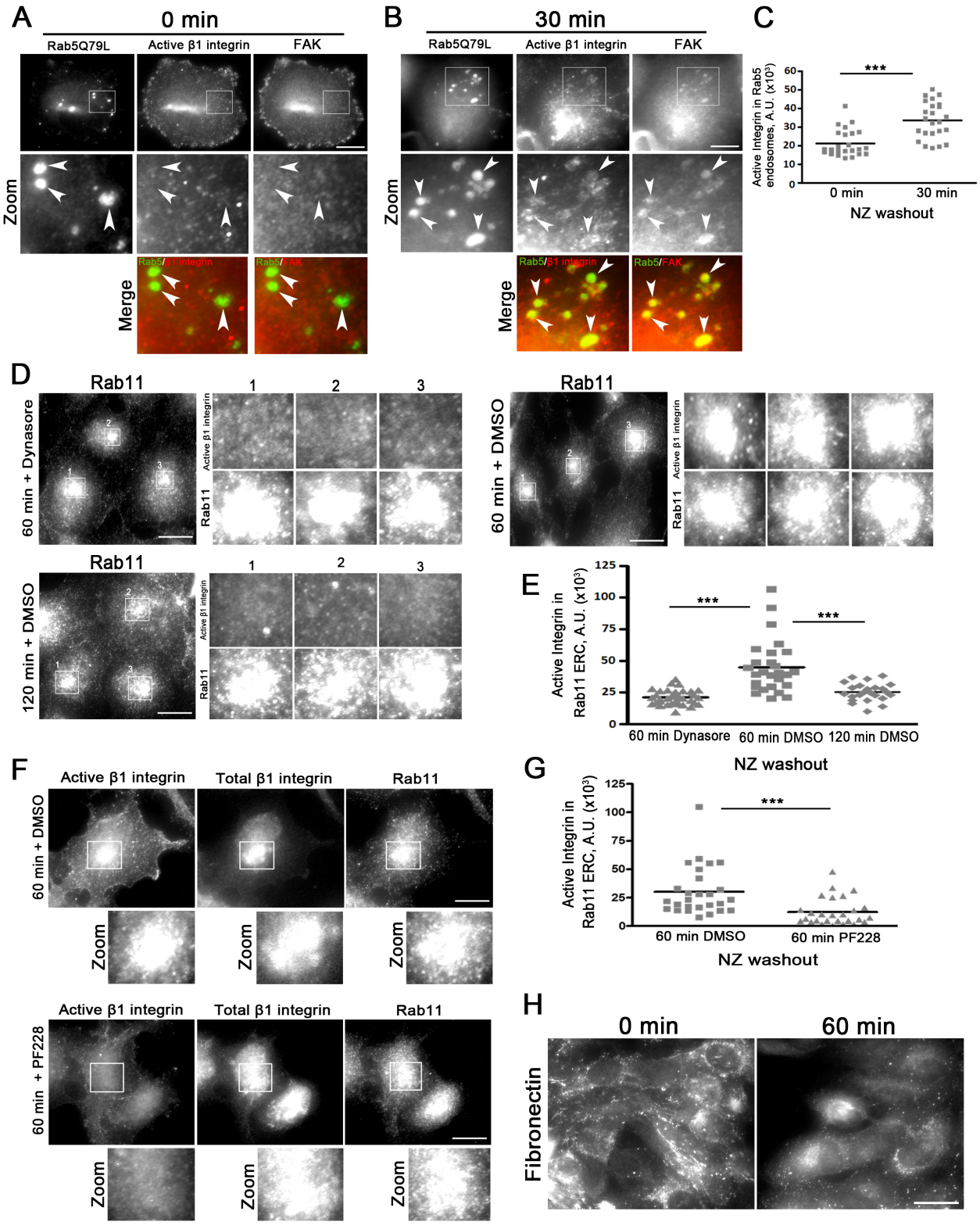
A
0 min
Rab5Q79L
Active β1 integrin
FAK
Zoom
Merge
Rab5/β1 integrin
Rab5/FAK
B
30 min
Rab5Q79L
Active β1 integrin
FAK
Zoom
Merge
Rab5/β1 integrin
Rab5/FAK
C
Active Integrin in Rab5 endosomes, A.U. (x10³)
***
0 min
30 min
NZ washout
D
Rab11
60 min + Dynasore
Active β1 integrin
Rab11
1
2
3
Rab11
60 min + DMSO
Active β1 integrin
Rab11
Rab11
120 min + DMSO
Active β1 integrin
Rab11
1
2
3
E
Active Integrin in Rab11 ERC, A.U. (x10³)
***
***
60 min Dynasore
60 min DMSO
120 min DMSO
F
Active β1 integrin
Total β1 integrin
Rab11
60 min + DMSO
Zoom
Zoom
Zoom
Active β1 integrin
Total β1 integrin
Rab11
60 min + PF228
Zoom
Zoom
Zoom
G
NZ washout
Active Integrin in Rab11 ERC, A.U. (x10³)
***
60 min DMSO
60 min PF228
NZ washout
H
0 min
60 min
Fibronectin

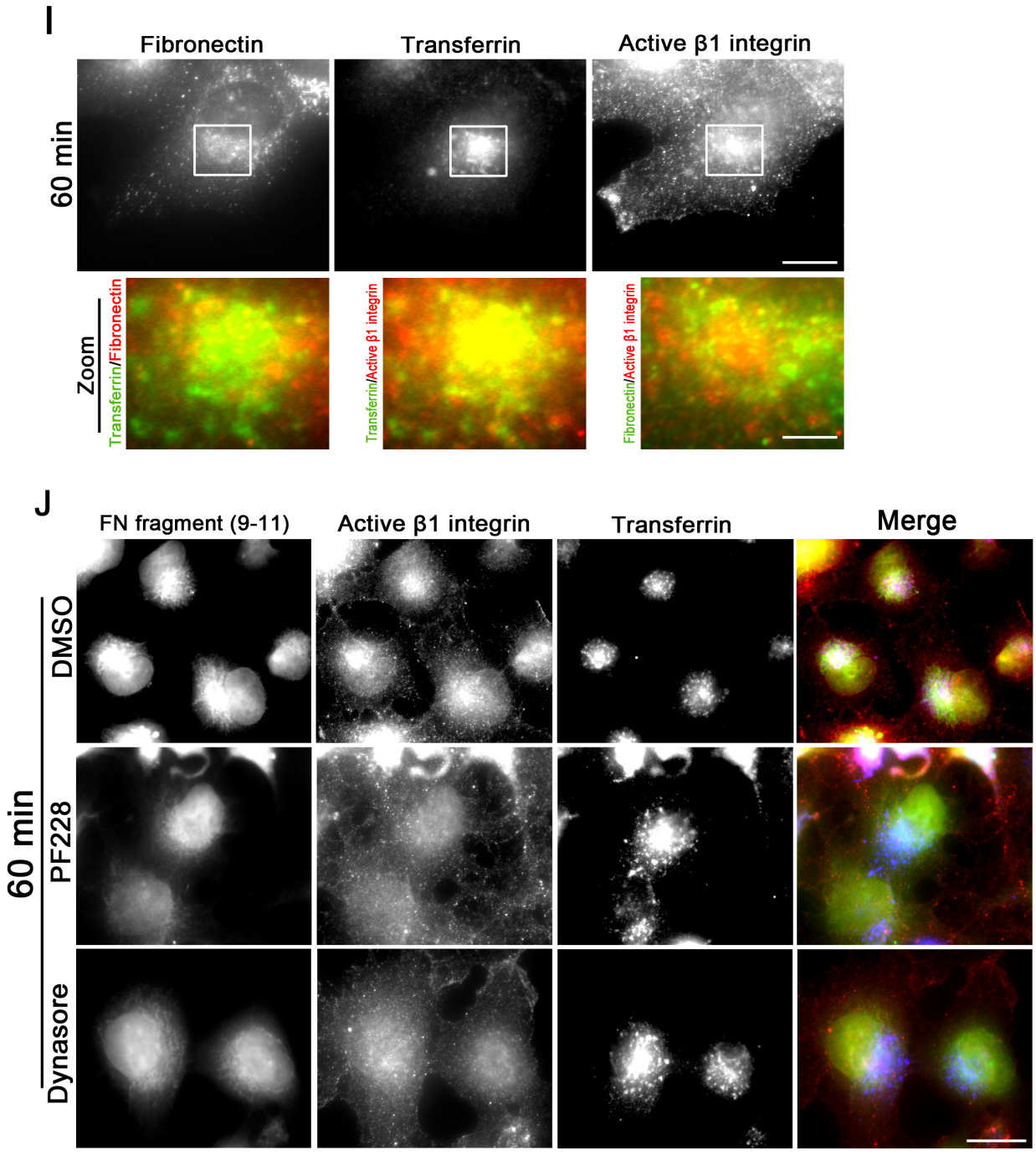
I
Fibronectin
Transferrin
Active β1 integrin
60 min
Zoom
Transferrin/Fibronectin
Transferrin/Active β1 integrin
Fibronectin/Active β1 integrin
J
FN fragment (9-11)
Active β1 integrin
Transferrin
Merge
60 min
DMSO
PF228
Dynasore

Figure 19. FAK-pY397 colocalizes with active integrin following FA disassembly in HT1080 fibrosarcoma cells.

Immunofluorescence images of active β1 integrin (12G10 antibody) and FAK-pY397 in HT1080 fibrosarcoma cells fixed at 60 min after NZ washout. Scale bar, 10 μm.

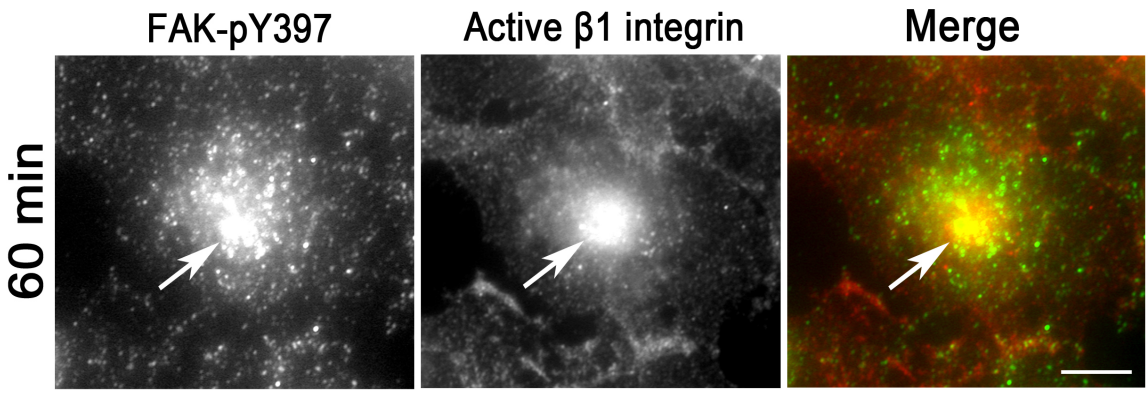
FAK-pY397
Active β1 integrin
Merge
60 min

Figure 20. Dynasore blocks FA disassembly in HT1080 fibrosarcoma cells.

Immunofluorescence images of FAK-pY397 in HT1080 fibrosarcoma cells fixed at 60 min after NZ washout in the presence of Dynasore (80 μM) or vehicle (DMSO). Scale bar, 15 μm.

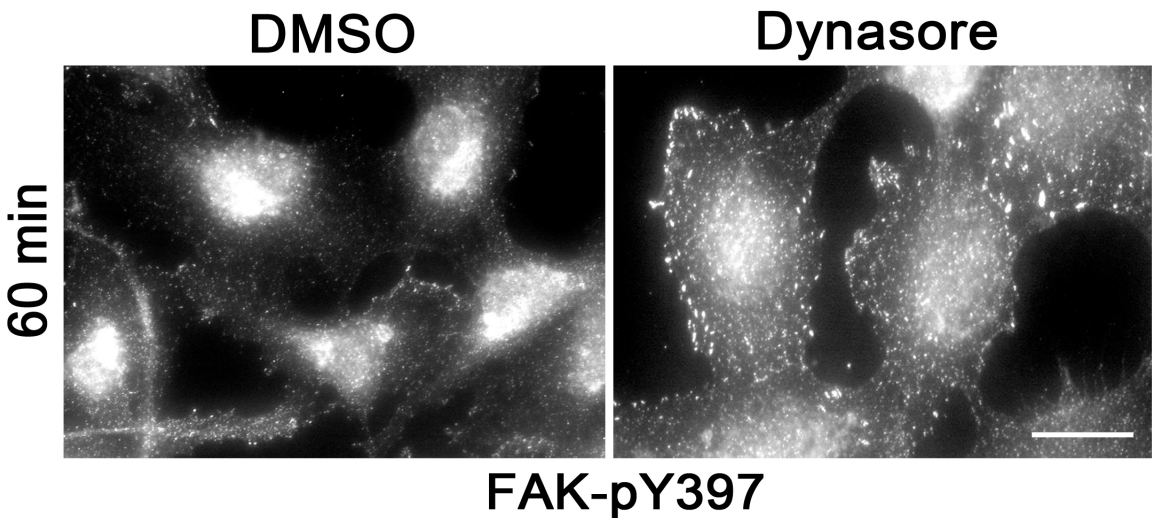
DMSO
Dynasore
60 min
FAK-pY397

Figure 21. FAK and SFKs inhibitors mitigate migration.

(A) Confluent monolayers of NIH3T3 fibroblasts were wounded and cells were imaged by DIC during 4 h in the presence of vehicle (DMSO), PF228 (10 µM) or PP2 (10 µM). Scale bar, 5 µm. (B) Data represent the quantification of cell migration for the duration of the experiment (4 hours). Results are from three independent experiments. Bars are SD. *** $p<0.001$, relative to DMSO-treated cells.

A

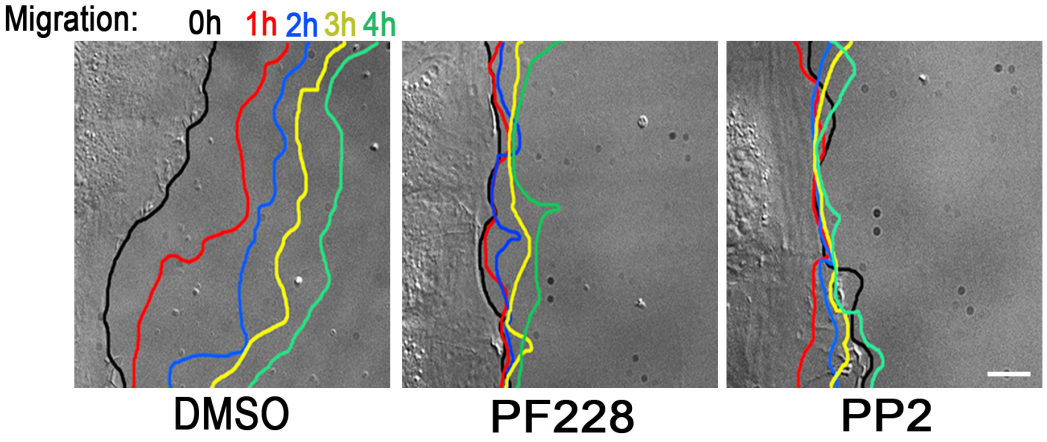
Migration:
0h 1h 2h 3h 4h
DMSO
PF228
PP2

B

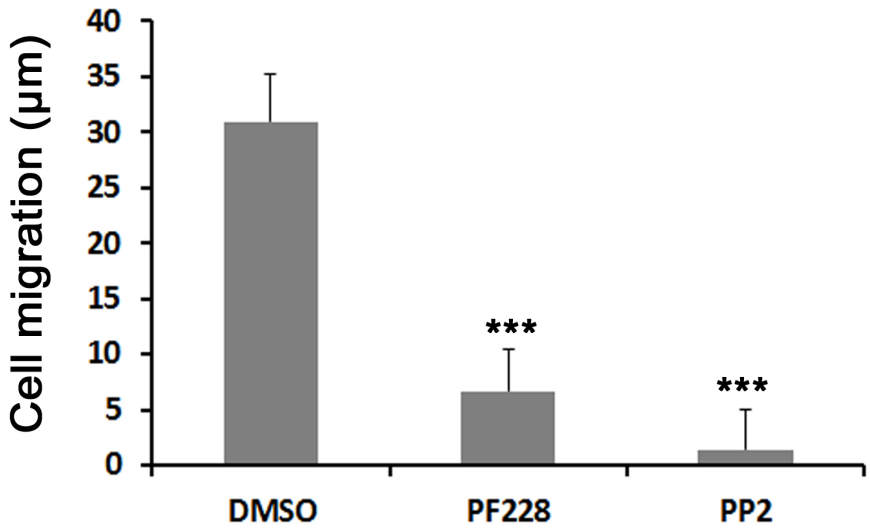
Cell migration (μm)
40
35
30
25
20
15
10
5
0
***
***
DMSO
PF228
PP2

Figure 22. The effects of FAK and SFK inhibitors on migrating NIH3T3 fibroblasts are consistent with their role in regulating integrin activation and recycling.

(A) TIRF images of a paxillin-EGFP NIH3T3 cell line incubated with DMSO (vehicle), PF228 (10 μM) or PP2 (10 μM). Scale bar, 5 μm. (B) Data represent the average sum intensity of FAs which was normalized to the time when drugs were added (see methods). Error bars are SD. (C) TIRF images of drug washout from the same cells represented in "A". Scale bar, 5 μm. (D) Data represent the average sum intensity of FAs following drug washout. Note the faster FA reformation for FAK-inhibited cells. Error bars are SD. (E) Quantification of levels of surface α5 integrin measured by antibody labeling and flow cytometry. Cells were submitted to random migration for 6 h on FN-coated dishes in the presence of DMSO (vehicle), PF228 (10 μM) or PP2 (10 μM). Error bars are SD. (F) TIRF images of a paxillin-EGFP NIH3T3 cell line incubated with PF228 (10 μM) for approximately 2 h followed by treatment with manganese (100 μM). Scale bar, 2.5 μm. (G) Immunofluorescence images of FAK in wounded monolayers of NIH3T3 fibroblasts at 0 and 90-100 min after NZ washout. Scale bar, 7.5 μm. (H) Assessment of the distribution of FAs during FA reassembly in wounded monolayers. Left: diagram illustrating the methodology used to quantify FA reassembly distribution: FAs located within a 2 μm range from the cell periphery were classified as peripheral FAs; subsequently this population was further divided in leading edge- ("Region A") or cell side/rear-located FAs ("Region B"). Right: the histogram represents the total FA area relative to each region. The data are from at least 3 independent experiments in which 15 cells were analyzed in each time-point. Error bars are SD. *** $p < 0.001$, relative to 90-100 min of NZ washout in "Region A"; **$p<0.01$.

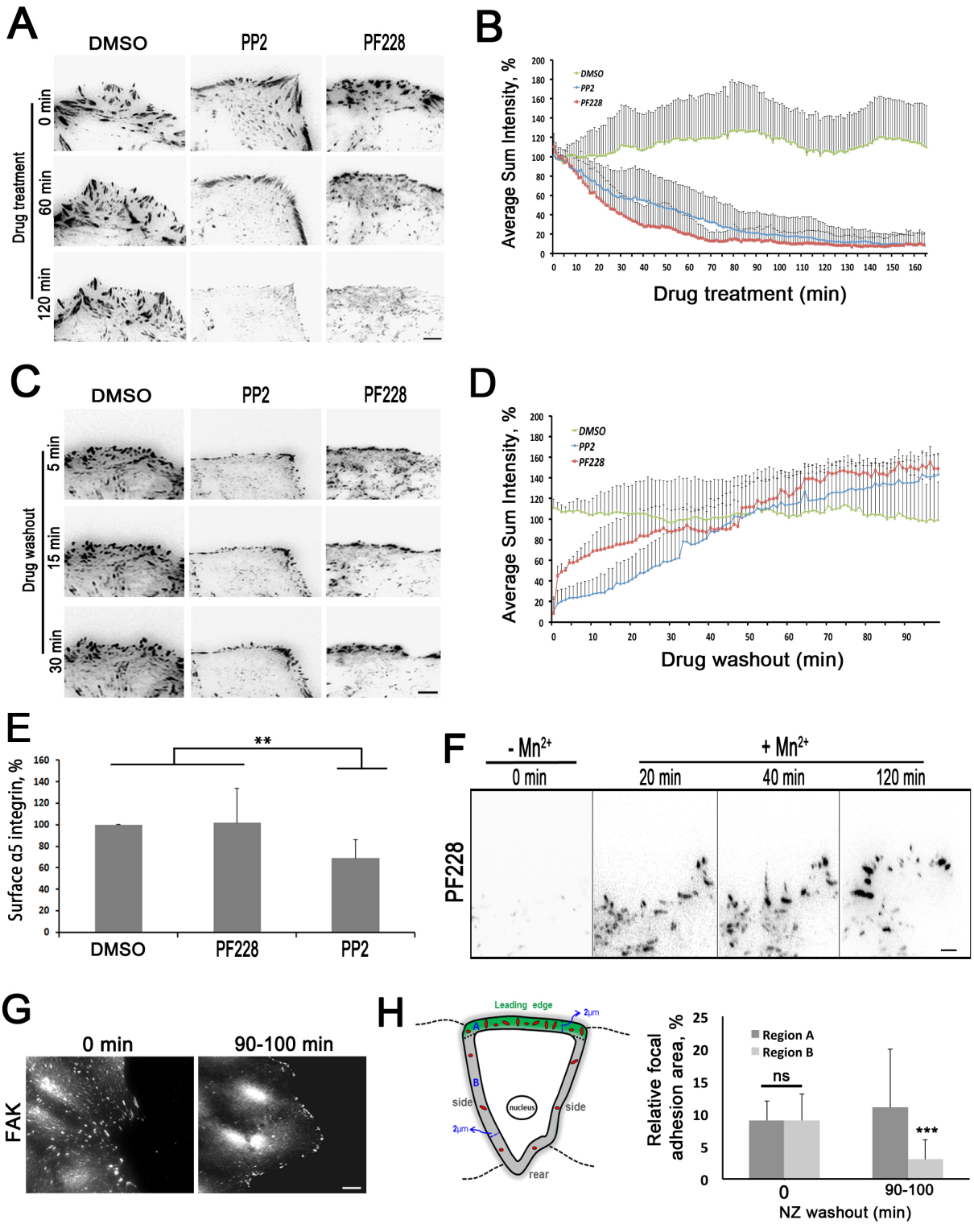
A
DMSO
PP2
PF228
Drug treatment
0 min
60 min
120 min
B
Average Sum Intensity, %
DMSO
PP2
PF228
Drug treatment (min)
C
DMSO
PP2
PF228
Drug washout
5 min
15 min
30 min
D
Average Sum Intensity, %
DMSO
PP2
PF228
Drug washout (min)
E
Surface α5 integrin, %
**
DMSO
PF228
PP2
F
- Mn2+
+ Mn2+
0 min
20 min
40 min
120 min
PF228
G
0 min
90-100 min
FAK
H
Leading edge
2μm
B
side
nucleus
side
2μm
rear
Relative focal adhesion area, %
Region A
Region B
ns
***
0
90-100
NZ washout (min)

Figure 23. Proposed model for polarized FA reassembly mediated by recycling of integrins previously resident at FAs.

MT-induced-FA disassembly is dependent on integrin endocytosis mediated by FAK, GRB2, dynamin2, clathrin, clathrin adaptors (Dab2 and ARH) and PIPk1β. Following endocytosis, integrins remain associated with Rab5-positive early endosomes that also contain FAK and possibly Src, and this maintains integrins in an active conformation. Alternatively, integrins might not remain associated with FAK/Src after endocytosis and in this case we suggest that they get deactivated. Active integrins are then trafficked to the Rab11 endocytic recycling compartment where FAK and Src are also present. The recycling of integrins back to the cell surface is dependent on Rab11 and SFKs activity and probably on a MT-associated motor given the fact that this is a long range and polarized transport. Whether these proteins function in one or multiple steps in returning integrin from the ERC is unclear. Of note, FA reassembly will rapidly occur following exocytosis of integrin-containing vesicles since recycled integrins are active and therefore ready to engage with the extracellular matrix. The labels in red represent my findings whereas those in black refer to previous findings.

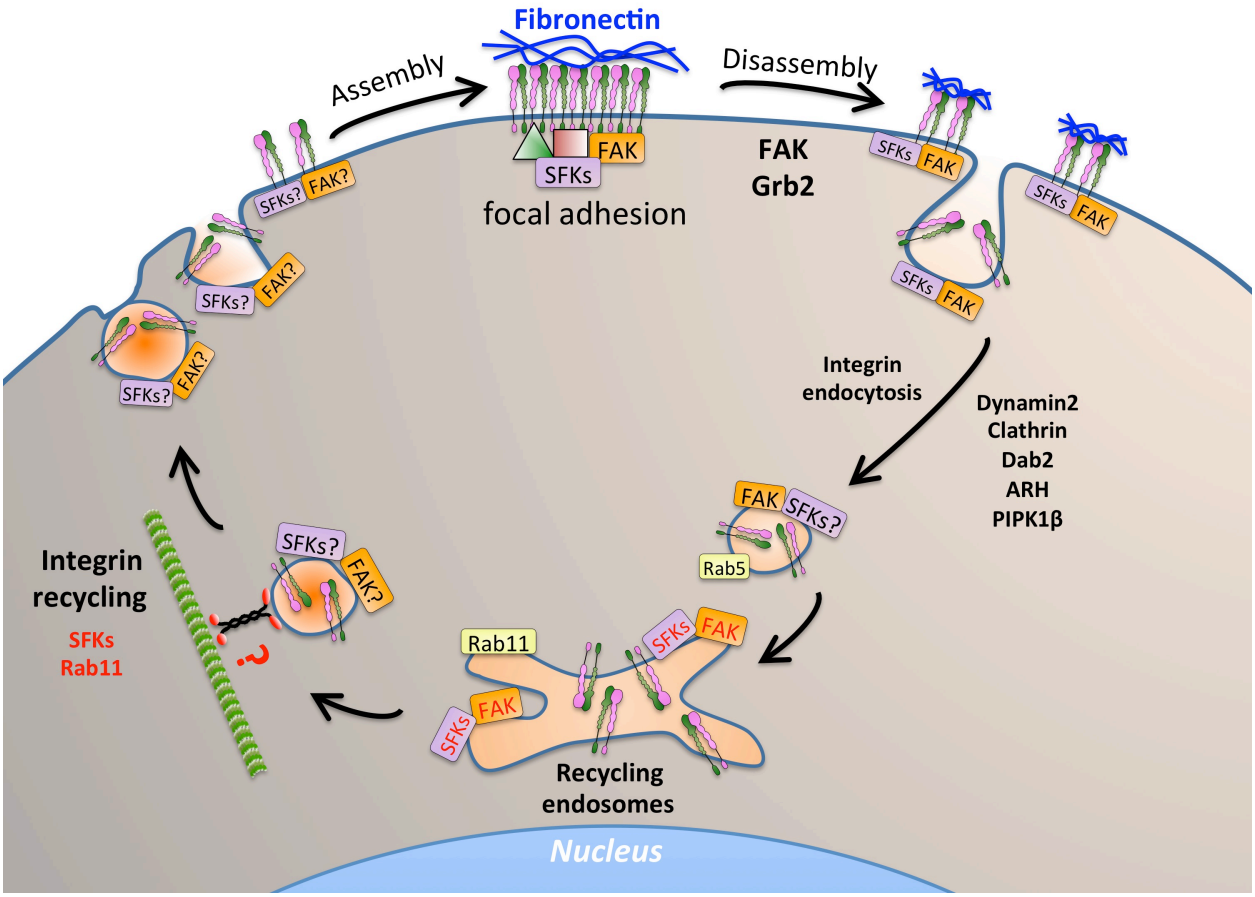
Fibronectin
Assembly
Disassembly
FAK
SFKs
focal adhesion
FAK
Grb2
SFKs?
FAK?
Integrin
endocytosis
Dynamin2
Clathrin
Dab2
ARH
PIPK1β
Rab5
Integrin
recycling
SFKs
Rab11
Rab11
Recycling
endosomes
Nucleus

MATERIAL AND METHODS

Chemicals and cell culture

Src family kinases inhibitor (PP2) was purchased from Calbiochem. FAK kinase inhibitor (PF-573228) was purchased from Tocris Bioscience and FAK Kinase inhibitor I was purchased from Chemicon. Nocodazole was purchased from Sigma-Aldrich. NIH3T3 fibroblasts were cultured in DMEM (Life Technologies, Grand Island, NY) with 10% calf serum (Gemini, West Sacramento, CA) and 10 mM HEPES (pH 7.4). For serum starvation, cells on acid-washed coverslips were grown to confluence (~2 days) and transferred to serum-free medium (DME and 10 mM Hepes, pH 7.4) for 48 hours as previously described (Ezratty et al., 2005; 2009). FAK-null mouse embryonic fibroblasts were cultured in DMEM and fetal bovine serum as previously described (Schlaepfer et al., 1999; Sieg et al., 1999). The human fibrosarcoma cell line HT1080 (ATCC) was grown in DMEM supplemented with 10% bovine serum and 10 mM HEPES (pH 7.4). All cell lines were cultured on 5% CO_2 at 37^{o}C.

Model system to study FA turnover and integrin recycling

Focal adhesion disassembly and cell migration experiments were performed as previously described (Ezratty et al., 2005; 2009). In brief, NIH3T3 cells grown on glass coverslips were treated with 10 μM NZ for 4 hours to completely depolymerize MTs. The drug was washed out with serum-free medium, and MTs were allowed to repolymerize for different intervals. Cells were either fixed in –20°C methanol for 5 min and rehydrated in TBS or fixed in 4% paraformaldehyde in PBS for 10 min, followed by permeabilization with 0.3% Triton X-100 in PBS for 5 min before immunofluorescence staining. Depending on the experiment, cells were stained with anti-HA (mouse monoclonal; 1:200; Covance), vinculin (mouse monoclonal; 1:100; Sigma-Aldrich), FAK-pY397 (rabbit polyclonal; 1:200; Invitrogen), Paxillin-pY31 (rabbit polyclonal; 1:200; Invitrogen), Paxillin (mouse monoclonal; 1:200; BD Biosciences), Rab11

(rabbit polyclonal; 1:200; BD Biosciences), FAK (rabbit polyclonal; 1:200; Santa Cruz Biotech), activate human β1 integrin clone 12G10 (mouse monoclonal; 1:200; Abcam), total human β1 integrin clone K20 (mouse monoclonal; 1:200; Santa Cruz), fibronectin antibody (rabbit polyclonal; 1:500; SIGMA), tyrosinated tubulin (rat monoclonal YL1/2; 1:20 dilution of culture supernatant), Golgi-GM31 (mouse monoclonal; 1:200; BD Biosciences), GFP (chicken polyclonal; 1:100; Chemicon-MilliPore) or Cy5/rhodamine-phalloidin (1:200; Cytoskeleton, Inc.). Secondary antibodies were purchased from Jackson ImmunoResearch Laboratories, Inc. and were absorbed to minimize cross-reaction with other species. Coverslips were mounted with Fluoromount-G (Southern Biotech, Birmingham, AL).

Cell migration experiments

Cells were plated at a subconfluent density (75%) on glass-bottom dishes and 24 h later growth medium was replaced by DMEM supplemented with 0.5% calf serum. The following day, cell monolayers were wounded with a pipette tip and incubated in DMEM containing 2% calf serum before imaging. Phase images were acquired after 12 and 24 hours post-wound using a 10X (NA 0.3) DLWD Plan Fluor objective and a CoolSNAP HQ CCD camera on a Nikon TE300 inverted microscope controlled by Metamorph (Molecular Devices, Sunnyvale, CA). Wound closure was calculated by the relative change in area between 0, 12 and 24 h.

Measurements of integrin activation

The activation state of endogenous α5β1 was assessed as described previously by measuring the binding of a recombinant soluble integrin-binding fragment of fibronectin containing the RGD- and the synergy-binding site for integrins (GST-FN9–11) (Hughes et al., 2002; Bouaouina et al., 2008; Bouaouina et al., 2012). For each preparation of biotinylated GST-FN9–11 the effective concentration to be used on the experiment was determined by titration. Briefly, cells were harvested by a brief trypsinization, followed by neutralization with the addition of complete

media. Following a brief centrifugation, cells were washed twice in ice cold Tyrode's buffer and suspended and incubated on ice with biotinylated GST FN9–11 for 30 min. After washing the cells with ice cold Tyrode's, cells were incubated on ice for another 30 min with Alexa Fluor 488-streptavidin (10µg/ml; Molecular Probes Inc.). The cells were then washed again in ice cold Tyrode's buffer and analyzed on a FACScan (Becton Dickinson) flow cytometer. The collected data were analyzed using *CellQuest* software (Becton Dickinson).

Western blotting

Cells were lysed in lysis buffer (1% NP-40, 50 mM Tris, pH 7.4, 150 mM NaCl, 2 mM $MgCl_2$, 1 mM EGTA, and protease and phosphatase inhibitors), boiled in 2x Laemmli sample buffer, and then separated by SDS-PAGE on 7.5 or 10% gels. Lysate protein concentration was determined by bicinchoninic acid assay and normalized for loading. Gels were transferred to nitrocellulose, blocked 1 h at room temperature in TBS buffer containing 5% BSA, and then incubated in 5% BSA/TBST overnight at 4°C with antibodies against Src (rabbit polyclonal; 1:500; Santa Cruz Biotech), Rab11 (rabbit polyclonal; 1:1,000; BD Biosciences), Paxillin pY118 (rabbit polyclonal; 1:1,000; Invitrogen), Paxillin (mouse monoclonal; 1:1,000; BD Biosciences) FAK (rabbit polyclonal; 1:500; Santa Cruz Biotech), pY397 FAK (rabbit polyclonal; 1:5,000; Invitrogen), vinculin (1:5,000), or tyrosinated tubulin (rat monoclonal YL1/2; 1:50,000) followed by the appropriate IR680- or IR800-conjugated secondary antibodies (1:5,000; Rockland Immunochemicals, Inc.). Quantification of bands was performed with an Odyssey imaging system (LI-COR Biosciences).

Microscopy

Immunofluorescently stained preparations were observed with an inverted microscope (TE2000-U; Nikon) using a 60x NA 1.45 Plan Apochromat objective and filter cubes optimized for coumarin, fluorescein/GFP, rhodamine, and Cy5 fluorescence. For TIRF microscopy,

preparations were observed using a TIRF illuminator and fiber optic–coupled laser illumination with three separate laser lines (Ar ion [488 nm] and HeNe [543 nm and 633 nm]) and filter cubes optimized for fluorescein/GFP, Cy3/Alexa Fluor 546, and Cy5 fluorescence (Chroma Technology Corp.). All Images were captured with a camera (OrcaIIER; Hamamatsu Photonics) using MetaMorph software (Molecular Devices, Sunnyvale, CA). Live cell imaging was performed with an inverted microscope (Nikon Eclipse Ti) equipped with motorized xyz stage to acquire multiple data points simultaneously using recording media (Gomes and Gundersen, 2006) and a temperature controller (37˚C). NIH3T3 cells stably expressing EGFP–paxillin were analyzed either by TIRF or DIC using a 60x NA 1.49 Apochromat objective. For TIRF microscopy preparations were observed using a TIRF illuminator and fibre optic–coupled laser illumination with an Ar ion [488] laser line. All images were captured with a camera (Andor iXon3 888, back illuminated EMCCD) controlled by NIS elements software.

Image quantifications

All images were background-subtracted before performing any type of measurement. To analyze the percentage of integrin signal in the ERC after FA disassembly we first defined a region of interest (ROI) highlighting the ERC (assessed by staining of endogenous Rab11). The integrin channel (assessed by transfection of α5 integrin-GFP) was then converted to binary and threshold was applied to get only the integrin signal. The total integrin binary area was then divided by the ROI to get the fraction of integrin signal localized to the Rab11 compartment.

To analyze the percentage of active integrin signal in the ERC after FA disassembly we defined a ROI highlighting the ERC (assessed by staining of endogenous Rab11). Then we used the 12G10 antibody to assess the amount of active β1 integrin signal (Sum intensity) present inside the Rab11 compartment (inside the ROI area). The active integrin Sum intensity was then divided by the ROI area drawn for each measurement.

To measure FA assembly and disassembly rates during wound healing we used cells stably expressing EGFP-paxillin and imaged them under TIRF microscopy. We defined ROIs at the cell leading edge where most of the FAs were concentrated and measured the Sum intensity in the GFP channel through the migration assay during treatment with the drugs (PF228 and PP2) and after drug washout. Moreover we also performed a more detailed measurement of the FA disassembly rate in a *per FA* basis. In this case each FA was highlighted with individual ROIs and the Sum intensity was measured through the time. The Sum intensity values for each FA were then divided by their individual ROI area.

Cell surface labeling and flow cytometry

Cell surface labeling was performed as described previously (Ezratty et al., 2009). Briefly, cells were harvested by trypsinization at several time points after MT regrowth and washed in cold PCN (1x PBS, 0.5% calf serum, and 0.1% NaN_3). Approximately 1×10^6 cells per sample were stained at 4°C without fixation. For the detection of α5 integrin in NIH3T3, PE-conjugated rat α-mouse CD49e monoclonal antibody (BD) was used at dilution of 1:100. After washes to remove unbound antibody, samples were fixed in cold 4% paraformaldehyde/PCN, and the distribution and mean fluorescence intensity of each sample was quantified using a FACScan (BD).

Transfection studies and plasmids

GFP-tagged FAK WT, FAK Y397F and HA-tagged FAK K454R were gifts from David Schlaepfer. GFP-tagged α5-integrin was a gift from Allan F. Horwitz and is exactly as described in Laukaitis et al., 2001 and Webb et al., 2007. Rab5 S34N, Rab11 S25N and Rab11 wt constructs were gifts from Jennifer Lipponcott-Schwartz. All constructs were transiently transfected with Lipofectamine Plus (Invitrogen) according to manufacturer's instructions and expressed for 24-48 hours before performing the FA disassembly assay. For siRNA knockdown

experiments 21-nucleotide RNA duplexes were purchased from Shanghai Gene Pharma (Shanghai, China) and resuspended in RNAase free water at a concentration of 20μM. NIH3T3 cells were transfected with 40 nM siRNA using Lipofectamine RNAiMAX (Invitrogen, Carlsbad, CA) according manufacturer's protocol. siRNAs were designed based on previously published sequences (Junutula et al., 2004) as follows: Rab11a: 5'-AATGTCAGACAGACGTGAAAA-3', Rab11b: 5'-AAGCACTTGACATAT GAGAAC-3'

Cell adhesion assay

Cells were trypsinized with 0.05% trypsin and 2 mM EDTA in PBS (2.5 min at 37°C). Trypsin was inactivated by the addition of 0.25 mg/ml soybean trypsin inhibitor in PBS. Cells were collected by centrifugation, resuspended in migration medium (DME with 0.5% BSA) and held in suspension at 37°C for 30 min. Acid-washed glass coverslips were coated with FN (1 or 2.5 μg/ml in PBS) overnight, 4°C, blocked with 1% BSA in PBS for 30 min, and pre-heated to 37°C before use in the experiments. Cells were evaluated for adhesion to FN-coated dishes following 15 min of plating by DAPI staining and subsequent counting.

Statistical analysis

A two-tailed unpaired Student's *t* test was used to evaluate two groups. Significance between multiple groups was determined by one-way analysis of variance (ANOVA) followed by Tukey's multiple comparison test.

Chapter 2: The Heterodimer Kif3AC is a Microtubule Motor for Polarized Integrin Trafficking in Migrating Cells

ABSTRACT

Integrin recycling has been generally accepted as a major component of cell migration. Surprisingly very little is known about the motors involved in integrin trafficking. After MT induced FA disassembly we noticed that integrin traffics to the Rab11 ERC before returning to the cell surface where it preferentially reassembles into FAs near the leading edge. Such long range transport suggests that a MT motor may be involved in returning integrin to the cell surface. We tested whether the kinesin II Kif3, which previously was shown to interact with a Rab11 adaptor protein (Schonteich et al., 2008), might be involved. Using the NZ washout assay as a model system to study integrin recycling we find that Kif3AC depletion affects FA reassembly without affecting FA disassembly, and that this is due to impaired recycling of α5-integrin back to the cell surface. Knockdown of the other Kif3 family member expressed in our cells (Kif3B) or the Kif3 adaptor protein, KAP3, did not affect FA reassembly, showing specificity in this transport. Consistent with a role in integrin trafficking, Kif3A- and Kif3C-depleted cells exhibited impaired migration. These results are the first to identify a MT-associated motor for polarized integrin trafficking to the cell leading edge that is important for FA formation and cell migration.

INTRODUCTION

I have found that FA reassembly is polarized towards the cell periphery/leading edge and that this event relies on Rab11-mediated integrin recycling (Chapter 1). These findings have important implications for cell migration and raise additional questions about the endocytic trafficking of integrins, for example: how does integrin move from the ERC to the cell surface? Is the return of integrin directed to the sites where FA reassembly occurs?

MTs have long been implicated in the migration of adherent cells (Vasiliev et al., 1970). It is possible that components specifically accumulated at MTs tips act as cofactors, along with cargo delivered by kinesins. For instance, there has been increasing evidence relating kinesins with FA dynamics. Krylyshkina et al., (2002) showed that kinesin-1 affects FA dynamics and similarly it was shown that Kif1C is enriched at a subset of MT-plus ends that contact podosomes and leads to podosome dissolution (Kopp et al., 2006). More recently, it was shown that CLIP-associated proteins (CLASPs) are necessary for efficient trafficking and deposition of KIF1C at the cell periphery and are critical components of podosome induction signaling (Efimova et al., 2014). Additionally, Kif1C has been recently shown to transport integrins to the cell rear for the proper maturation of trailing FAs thus facilitating directional migration (Theisen et al., 2012). Another study strongly suggesting a role for a kinesin in the dynamics of FAs showed that constitutively active Rab8 mutants induce MT1-matrix metalloproteinase collagen degradation and invasion in adenocarcinoma cells (Bravo-Cordero et al., 2007). Altogether, these data point to a critical role for MTs and MT motors in the regulation of major aspects of cell migration. Likewise we predict that long distance trafficking, such as would be required to move integrins from the pericentriollar ERC to the leading edge of migrating cells would involve kinesins (trafficking on

actin filaments is unlikely since they generally do not extend from the ERC to the plasma membrane).

In this chapter I sought to understand the relationship between the endocytic recycling of integrins and their roles as adhesion receptors in cell migration. More specifically I aimed to address whether there is a specific cytoskeletal mechanism to ensure that there is a polarized trafficking of internalized integrins as cell migrates. Interestingly I found a specific kinesin II motor to be involved in FA reassembly following endocytic disassembly. The kinesin II family comprises four members: Kif3A, Kif3B, Kif3C and Kif17 (not expressed in NIH 3T3 cells). Kif3 kinesins are heterodimers of Kif3A and either Kif3B or Kif3C; Kif17 kinesin is a homodimer. Kif3 kinesins frequently associate with Kif associated protein, KAP3, which acts as an adaptor for certain cargos (Hirokawa et al., 2009). Here we found that the heterodimer Kif3AC is involved in FA reassembly by recycling integrins back to the cell surface. This function was specific to this heterodimer since neither Kif3B nor KAP3 affected FA reassembly. Additionally Kif3A-depleted cells exhibited smaller FAs at steady state and impaired migration. To the best of our knowledge this is the first time that a MT-associated motor is shown to play a role in delivering integrin-containing vesicles to the cell front for polarized FA formation.

RESULTS

We have shown in Chapter 1 that integrin is recycled to the cell surface in a Rab11-dependent fashion and that this is required for FA reassembly. Likewise, our lab has unpublished data showing that dominant negative Rab11 blocks nuclear movement and that Kif3A depletion blocks centrosome orientation, two fundamental features of cell polarization/migration. Interestingly, Kif3 was reported to interact with a protein from the Rab11 *f*amily of *i*nteracting *p*roteins (Rab11-FIPs) and play a role in endocytic recycling (Schonteich et al., 2008). Together these results show that Kif3 plays important roles in cell migration and endocytic trafficking. These findings prompted us to test the involvement of this motor in integrin trafficking and cell motility.

We first used siRNA-mediated knockdown to deplete Kif3A in NIH 3T3 fibroblasts. The knockdown efficiency was close to 80% (Figure 24A). Interestingly, Kif3A-depleted cells displayed considerably smaller FAs after 3 days of knockdown when compared to non-coding siRNA-transfected cells (Figure 24B, C).

Next, we tested if Kif3A and other members of the kinsesin II family were required for FA reassembly using the NZ washout assay. Kif3A knockdown with two different siRNAs strongly inhibited FA reassembly (FA disassembly was not affected) (Figure 25A and B). As the members of kinesin II family exist either as Kif3A-Kif3B or Kif3A-Kif3C the depletion of Kif3A led to instability and degradation of Kif3B (Figure 25C). Thus we wanted to test if Kif3B was also involved in FA reassembly. Depletion of Kif3B (Figure 25D) did not affect FA disassembly or FA reassembly (Figure 25A, B). Finally we tested Kif3C, the other kinesin II member expressed in NIH3T3 fibroblasts. Similar to Kif3A, Kif3C depletion strongly inhibited FA reassembly without affecting FA disassembly (Figure 25A, B and E). Additionally, depletion

of KAP3 (Figure 26A) did not show any effect on FA disassembly or reassembly (Figure 26B, C). Collectively, these results show that Kif3AC is the specific kinesin II motor involved in FA reassembly.

To examine the involvement of Kif3A in FA reassembly with a different approach we microinjected a dominant negative tail construct of Kif3A (Kif3A-tail-GFP) (Hirokawa et al., 2009). Neither Kif3A-tail-GFP nor GFP microinjection affected FA disassembly. However, consistent with the knockdown data, microinjection of Kif3A-tail-GFP impaired FA reassembly when compared to GFP-microinjected cells (Figure 27). These results further support our previous data of an involvement of Kif3A in FA reassembly.

To test whether Kif3AC might be directly involved in the endocytic recycling of integrins, we localized Kif3A and examined the surface levels of α5 integrin after FA disassembly. Kif3A colocalized with endocytosed transferrin in the pericentriollar ERC both in migrating cells and in cells after MT-induced FA disassembly (Figure 28). Next we measured surface levels of α5 integrin during FA disassembly and reassembly triggered by MT regrowth. Kif3A depleted cells reduced their surface α5 integrin levels to the same extent as controls after FA disassembly (60 min NZ washout) but failed to return surface α5 integrin at the time of FA reassembly (Figure 29A). Consistent with its role in integrin recycling, Kif3A-depleted cells exhibited reduced wound closure (30-40% less) when compared to non-coding siRNA-transfected cells (Figure 29B, C). These results identify Kif3AC as a motor for integrin recycling in migrating cells.

DISCUSSION

Many cell types require the MT cytoskeleton to support cell polarity and directional cell migration. Interestingly, MTs are more important to the migration of large cells, while being dispensable for the locomotion of small cells (Kaverina and Straube, 2011). This is most likely due to their function as intracellular transport tracks, needed to efficiently deliver polarity factors to specific locations at the cell edge. In migrating cells, the MT cytoskeleton is usually asymmetrically arranged with the majority of MTs projecting toward the cell front (Miller et al., 2009). This front-biased MT cytoskeleton supports the directional transport of post-Golgi carriers, messenger RNAs, and recycling endosomes to the cell front, thereby supporting cell polarity and directional migration (Miller et al., 2009; Mingle et al., 2005; Palamidessi et al., 2008; Yadav et al., 2009).

Although it has been known for some time that trafficking of endocytosed transferrin depends in part on kinesin I (Lin et al., 2002) and on myosin-Vb (Lapierre et al., 2001; Provance et al., 2008), the motors involved in the trafficking and recycling of integrins remain to be determined. Interestingly, Kif1C (a kinesin-3) was shown to be involved in MT-dependent regulation of podosomes (Kopp et al., 2006). More recently Kif1C was shown to transport α5β1 integrins between the ERC and cell tails and disruption of this process led to impaired maturation of trailing adhesions causing defects in persistent cell migration (Theisen et al., 2012). On the other hand we identified Kif3A as the motor involved in polarized integrin trafficking towards the cell leading edge.

It is likely that there will be other kinesins involved in integrin transport during endocytic recycling and it will be important to screen for additional candidates involved in this event. Moreover, kinesins might be contributing to FA dynamics by indirect mechanisms. For instance,

they could traffic and deposit "disassembling factors" to FA sites, as shown for Kinesin-1 (Krylyshkina et al., 2002). Although we did not provide direct evidence that Kif3C is required for integrin recycling we strongly suggest that Kif3AC is the heterodimer transporting integrin-containing vesicles back to the plasma membrane prior to FA reassembly. The members of kinesin II family occur as a heterodimers. Thus the fact that Kif3A and Kif3C (but not Kif3B) are required for FA reassembly (Figure 25) along with the fact that Kif3A is critical for restoring integrin levels following endocytic recycling (Figure 29) and is localized in the ERC (Figure 28) strongly support the view that the heterodimer Kif3AC is the one responsible for integrin recycling in our system. To the best of our knowledge we are the first ones to identify a kinesin involved in the polarized transport of integrins to the cell front. Identifying the kinesin(s) involved in integrin endocytic recycling and return of integrin may provide the means to understand one of the links between the polarized organization of the MT network in a migrating cell and FA dynamics.

To unequivocally show that Kif3AC is the motor for integrin recycling I would suggest the following: 1) Show that Kif3AC accumulates in the ERC along with integrins after FA disassembly and that Kif3AC and integrin signals in the ERC are lost (or decreased) upon FA reassembly. 2) Demonstrate that α5 integrin-GFP accumulates in the ERC at 90-120 min after NZ washout in cells depleted for Kif3AC (due to impaired integrin recycling to the cell surface). 3) Perform direct imaging of Kif3A- or Kif3C-GFP during FA reassembly to visualize vesicles (presumably carrying integrin) coming from the ERC towards the cell periphery. Additionally, imaging studies using α5 integrin-GFP and Kif3A- or Kif3C-RFP during FA reassembly would provide direct evidence that Kif3AC is the motor for integrin recycling. 4) Perform co-

immunoprecipitation assays with endogenous or recombinant Kif3AC to show that Kif3AC-integrin interaction increases after FA disassembly.

FIGURES

Figure 24. Kif3A depleted NIH3T3 fibroblasts exhibit small FAs.

(A) Western blot analysis of Kif3A in NIH3T3 fibroblasts treated with non-coding (NC) or Kif3A siRNAs. Tubulin is a loading control. (B) Immunofluorescence images of paxillin-pY31 and vinculin in NIH3T3 fibroblasts treated with NC or Kif3A siRNAs and fixed after 120 min of NZ washout. Scale bar, 15 μm. (C) Data represent the distribution of FA area in Kif3A- and NC-treated cells. At least 160 FAs from 8 different cells were analyzed. **$p<0.01$ when comparing FA area between NC- and Kif3A-depleted cells.

A

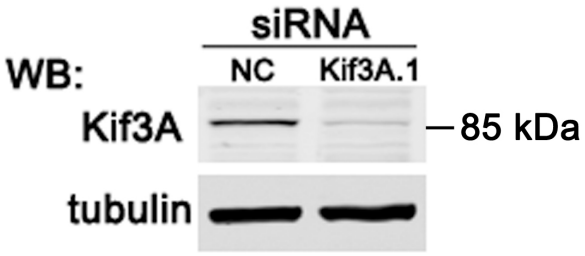
siRNA
NC
Kif3A.1
WB:
Kif3A
85 kDa
tubulin

B

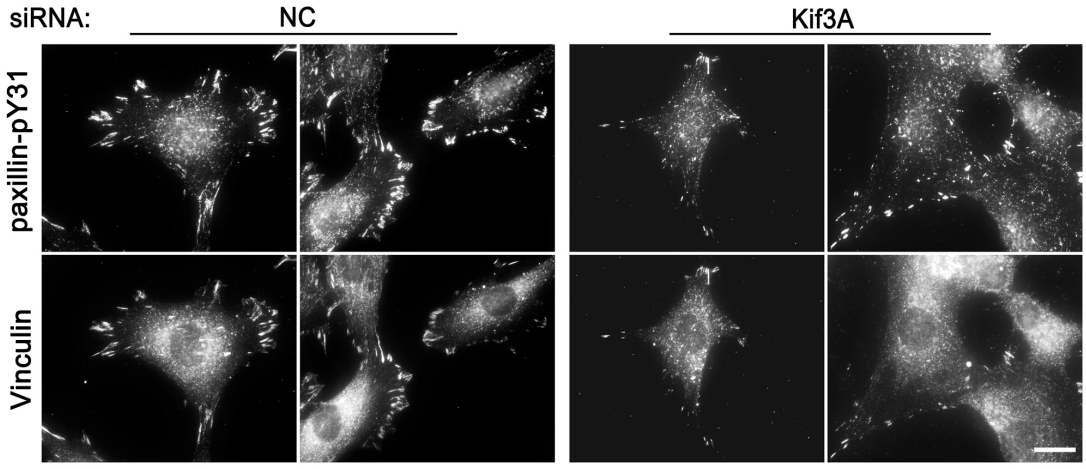
siRNA:
NC
Kif3A
paxillin-pY31
Vinculin

C

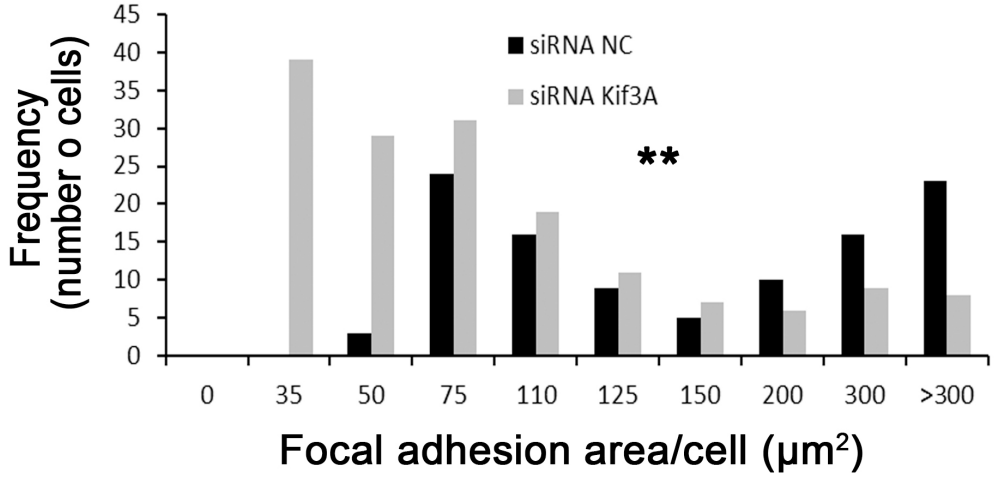
Frequency (number o cells)
45
40
35
30
25
20
15
10
5
0
siRNA NC
siRNA Kif3A
**
0
35
50
75
110
125
150
200
300
>300
Focal adhesion area/cell (μm²)

Figure 25. Kif3A and Kif3C but not Kif 3B are required for FA reassembly.

(A) Immunofluorescence images of paxillin in NIH3T3 fibroblasts treated with non-coding (NC), Kif3A, Kif3B or Kif3C siRNAs and fixed at the indicated times after NZ washout. Scale Bar, 10 μm. (B) Quantification of FA disassembly and reassembly in Kif3A-, Kif3B- or Kif3C-depleted cells at the indicate times after NZ washout. Bars are SD. At least 150 cells were analyzed in each experiment from a total of 5 independent experiments. (C-E) Western blot analysis of Kif3A, Kif3B or Kif3C in NIH3T3 fibroblasts treated with NC, Kif3A, Kif3B or Kif3C siRNAs. Tubulin is a loading control. Note that Kif3B protein levels go down after Kif3A depletion. **$p<0.01$, relative to NC 120 min after NZ washout. All the 60 min NZ washout values are not significantly different from control (NC).

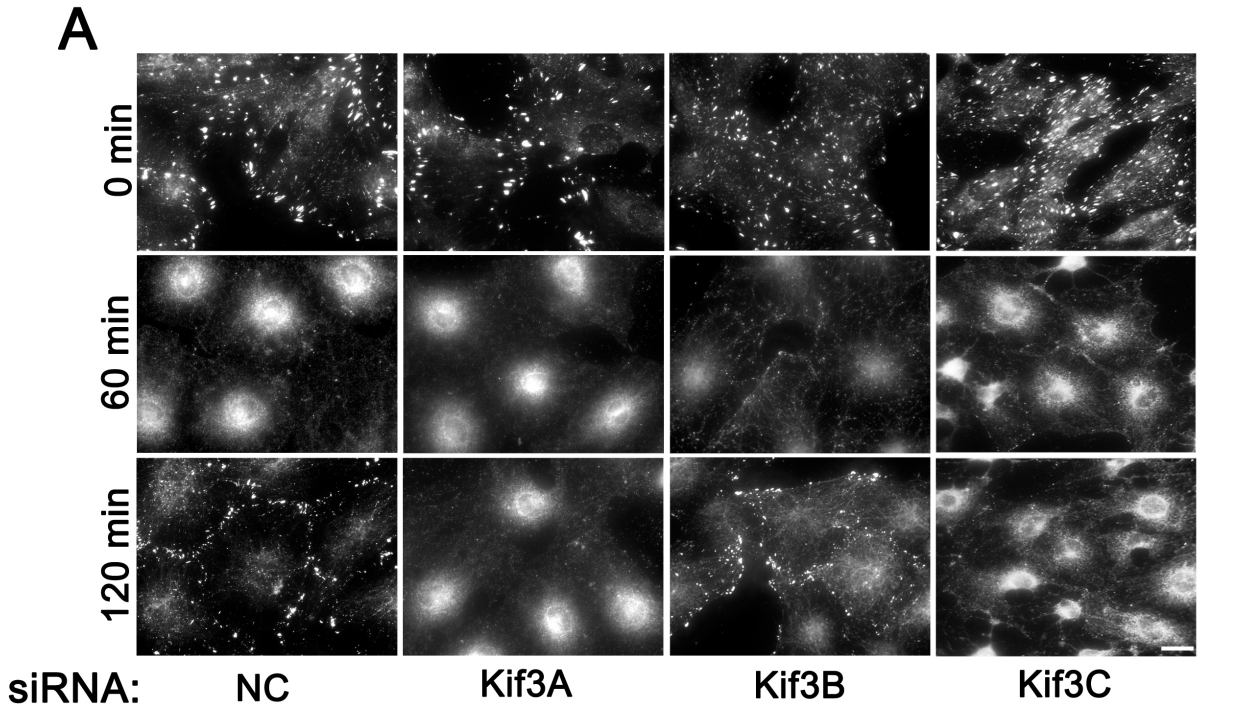
A
0 min
60 min
120 min
siRNA:
NC
Kif3A
Kif3B
Kif3C

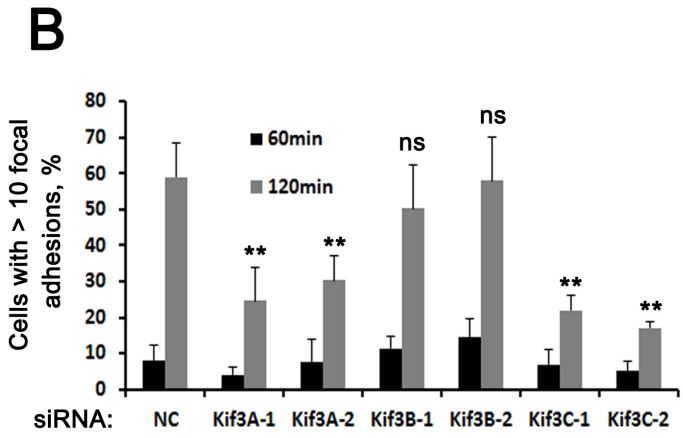
B
Cells with > 10 focal adhesions, %
60min
120min
ns
ns
**
**
**
**
siRNA:
NC
Kif3A-1
Kif3A-2
Kif3B-1
Kif3B-2
Kif3C-1
Kif3C-2

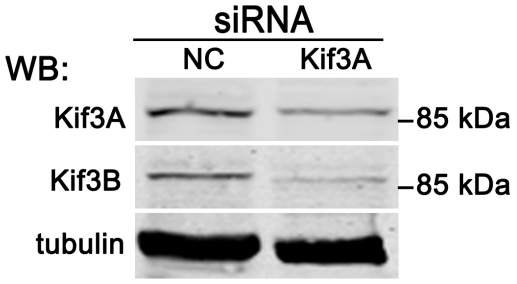
C
siRNA
WB:
NC
Kif3A
Kif3A
Kif3B
tubulin
85 kDa
85 kDa

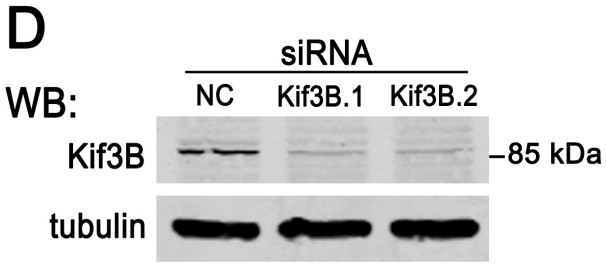
D
siRNA
WB:
NC
Kif3B.1
Kif3B.2
Kif3B
tubulin
85 kDa

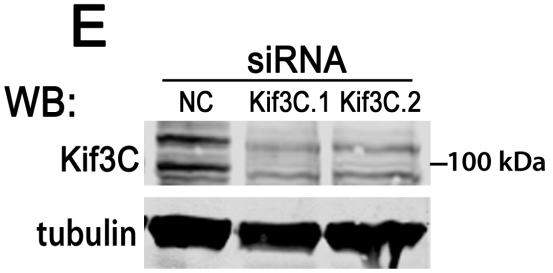
E
siRNA
WB:
NC
Kif3C.1
Kif3C.2
Kif3C
tubulin
100 kDa

Figure 26. KAP3 is not required for FA reassembly.

(A) Western blot analysis of KAP3 in NIH3T3 fibroblasts treated with non-coding (NC) or KAP3 siRNAs. Tubulin is a loading control. (B) Immunofluorescence images of paxillin and MTs in NIH3T3 fibroblasts treated with NC or KAP3 siRNAs and fixed at the indicated times after NZ washout. Scale Bar, 10 μm. (C) Quantification of FA disassembly and reassembly in KAP3-depleted cells at the indicated times after NZ washout. Bars are SD. At least 150 cells were analyzed in each experiment from a total of 3 independent experiments. All the 60 and 120 min NZ washout values are not significantly different from control.

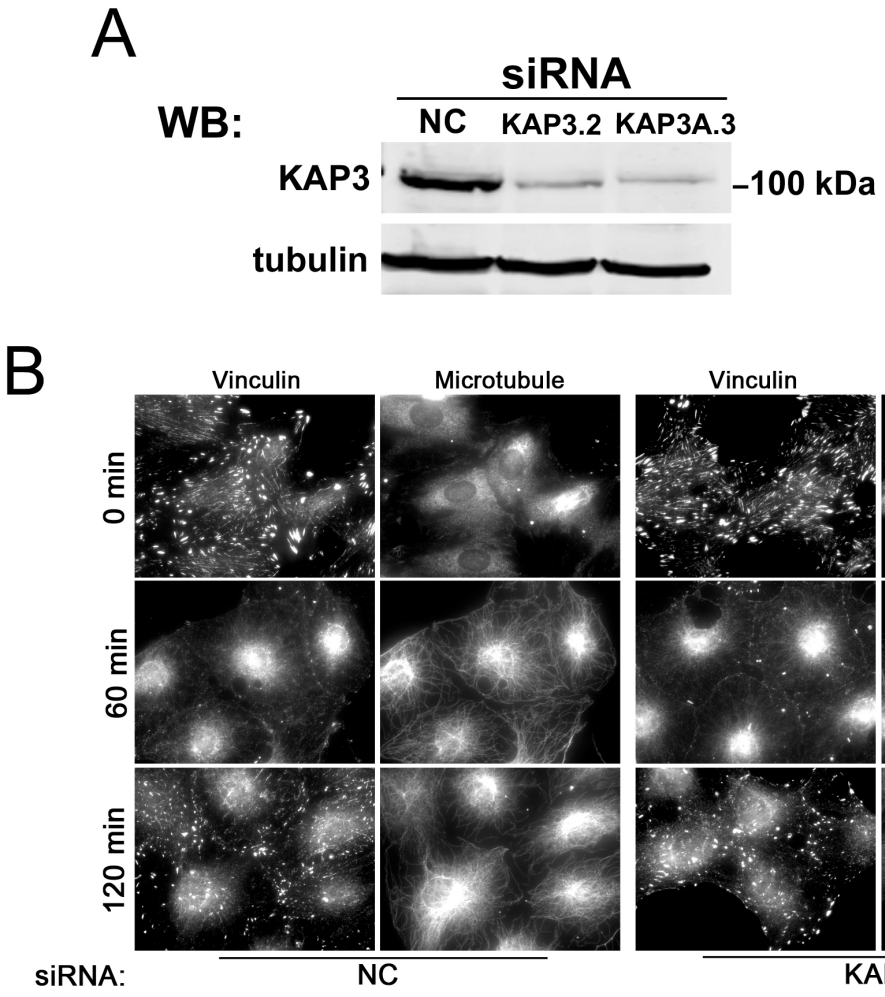
A
siRNA
WB:
NC
KAP3.2
KAP3A.3
KAP3
~100 kDa
tubulin
B
Vinculin
Microtubule
Vinculin
Microtubule
0 min
60 min
120 min
siRNA:
NC
KAP3
C
Cells with > 10 focal adhesions, %
90
80
70
60
50
40
30
20
10
0
NC
KAP3.2
KAP3A.3
ns
ns
ns
ns
60
120
NZ washout (min)

Figure 27. Kif3A-tail-microinjected NIH3T3 fibroblasts display impaired FA reassembly.

(A) Immunofluorescence images of Kif3A-tail (GFP), paxillin-pY118 and MTs in NIH3T3 fibroblasts expressing Kif3A-tail-GFP and fixed at the indicated times after NZ washout. Cells were microinjected with Kif3A-tail-GFP during NZ treatment. Arrows indicate microinjected cells. Scale Bar, 15 μm. (B) Quantification of FA disassembly and reassembly following NZ washout. At least 35 cells were analyzed in each experiment from a total of 3 independent experiments. Bars are SE. **$p<0.01$ relative to GFP-microinjected cells.

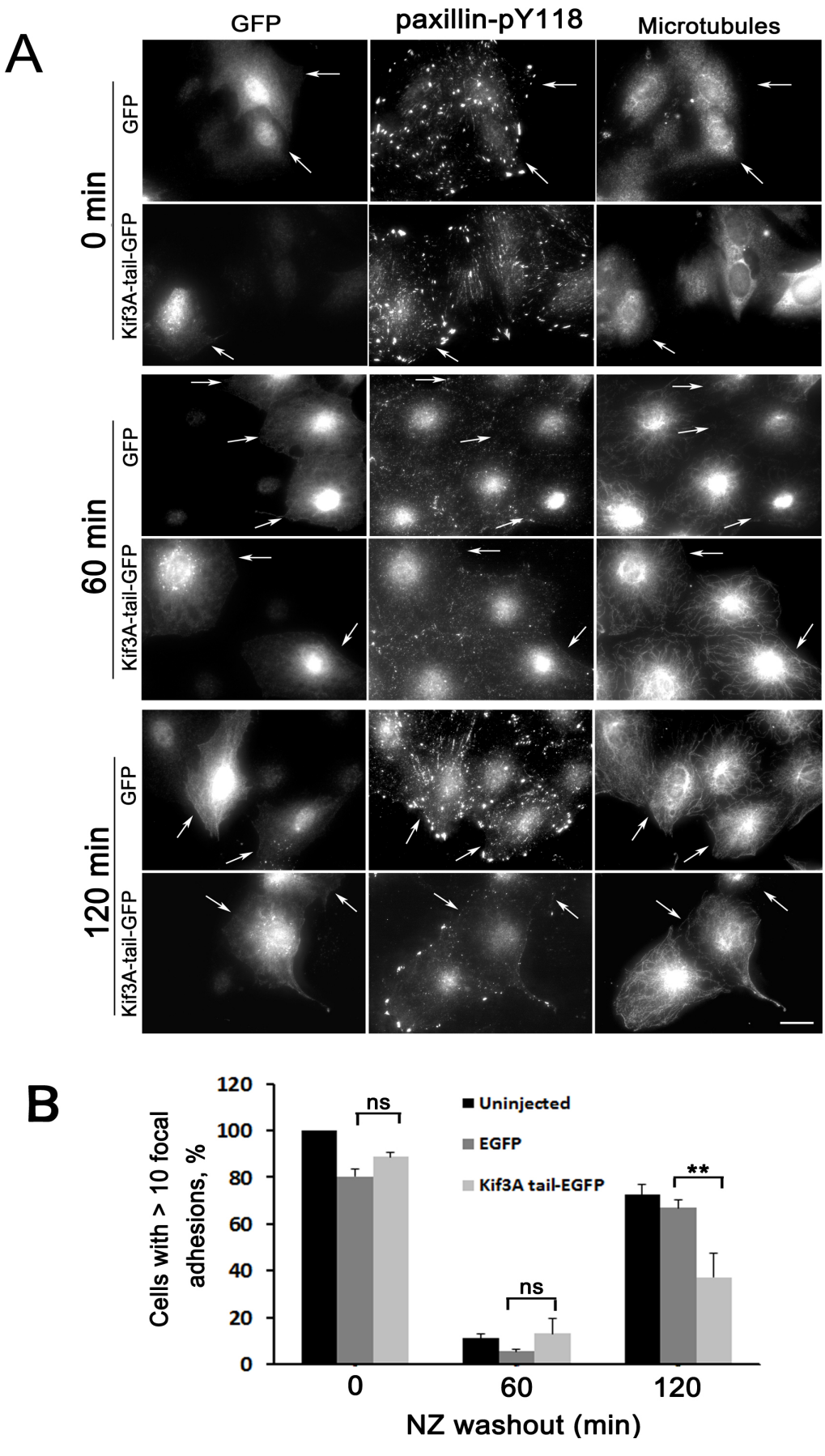
A
GFP
paxillin-pY118
Microtubules
0 min
60 min
120 min
GFP
Kif3A-tail-GFP
B
Cells with > 10 focal adhesions, %
120
100
80
60
40
20
0
ns
ns
**
Uninjected
EGFP
Kif3A tail-EGFP
0
60
120
NZ washout (min)

Figure 28. Kif3A localizes to the ERC after FA disassembly and during cell migration.

(Top) Immunofluorescence images of Kif3A and Alexa 649-conjugated transferrin in NIH3T3 fibroblasts fixed at 60 min after NZ washout. (Bottom) Immunofluorescence images of Kif3A and Alexa 649-conjugated transferrin in a wounded monolayer of NIH3T3 fibroblasts. Bar, 15 μm.

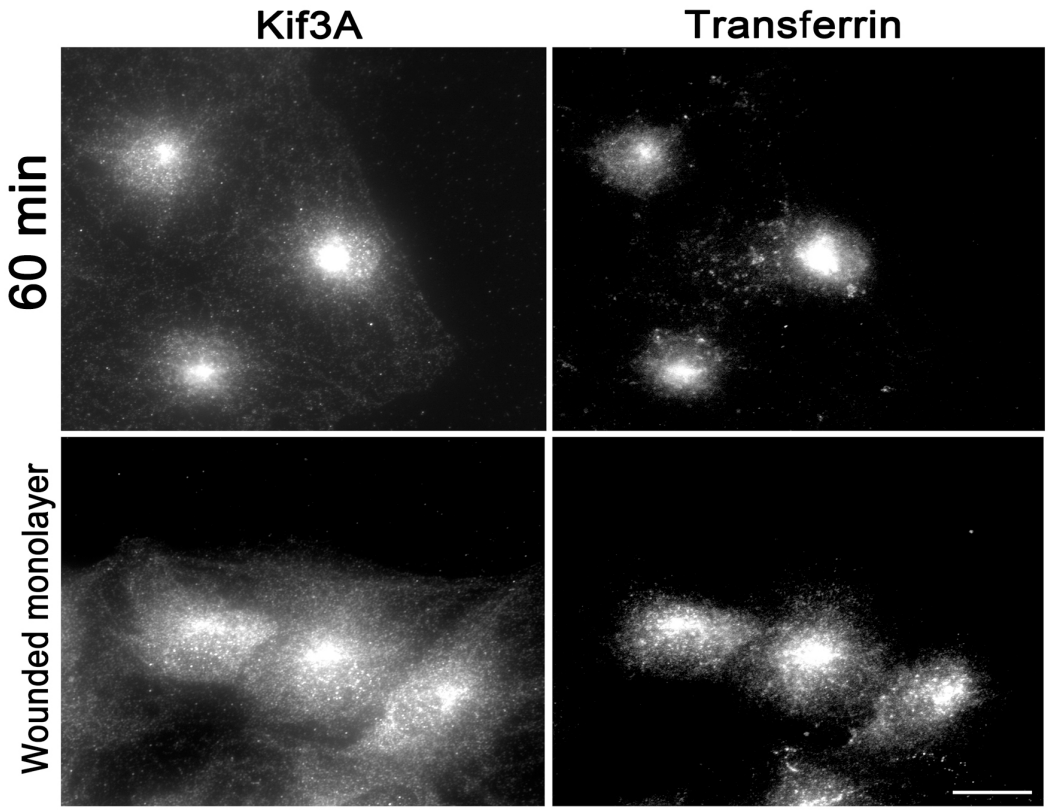
Kif3A
Transferrin
60 min
Wounded monolayer

Figure 29. Kif3A is a motor for integrin trafficking and is important for cell migration.

(A) Quantification of levels of α5 integrin measured by antibody labeling and flow cytometry at the indicated times after NZ washout for NIH3T3 fibroblasts treated with non-coding (NC) or Kif3A siRNAs. Data represent mean fluorescent intensity from seven independent experiments. Bars are SE. (B-C) Phase images and quantification of wound closure in NC-, Kif3A- and Kif3C-depleted cells. Bars are SE from 3 independent experiments. Scale bar, 50 μm. ** $p<0.01$ relative to control (NC) values; * $p<0.05$.

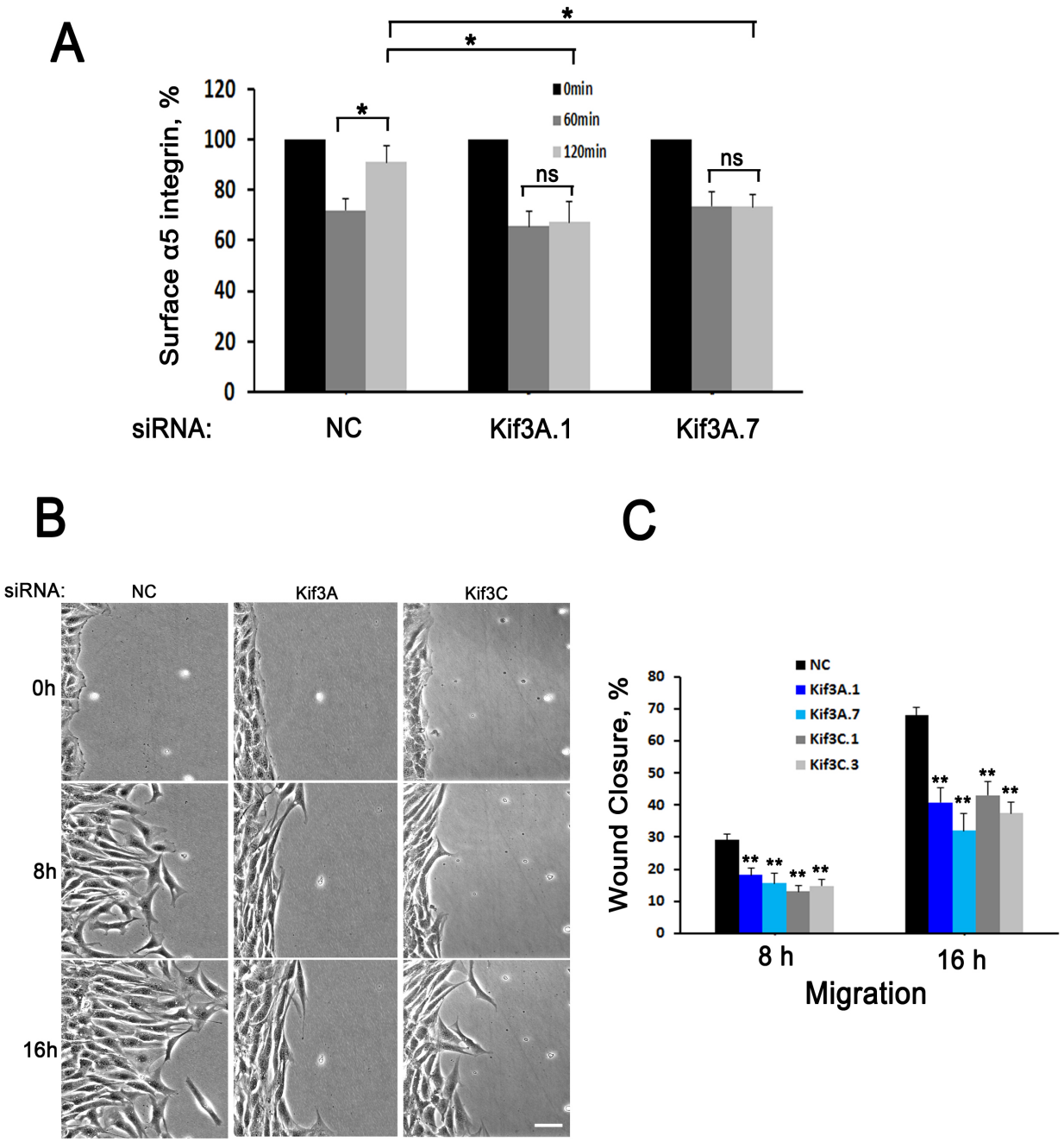
A
Surface α5 integrin, %
120
100
80
60
40
20
0
0min
60min
120min
*
*
*
ns
ns
siRNA:
NC
Kif3A.1
Kif3A.7
B
siRNA:
NC
Kif3A
Kif3C
0h
8h
16h
C
Wound Closure, %
80
70
60
50
40
30
20
10
0
NC
Kif3A.1
Kif3A.7
Kif3C.1
Kif3C.3
**
8 h
16 h
Migration

MATERIAL AND METHODS

Chemicals and cell culture

All chemicals were from Sigma unless otherwise noted. NIH 3T3 fibroblasts were cultured in DMEM and calf serum as previously described (Cook et al., 1998; Gundersen et al., 1994). For serum starvation, cells on acid-washed coverslips were grown to confluence (~2days) and transferred to serum-free medium (SFM; DMEM, 10mM HEPES, pH7.4) for 48 hour as previously described (Cook et al., 1998; Gundersen et al., 1994).

Plasmids, microinjection and transfection

Kif3A-tail-GFP was a generous gift from Dr. Geri Kreitzer. For microinjection, 10-50 μg/ml purified plasmid DNA in 10 mM HEPES, 140 mM KCl (pH 7.4) was pressure microinjected into nuclei of cells at the wounded edge using glass micropipettes and allowed to express for 1 hr. siRNAs (20 μM) were transfected with using Lipofectamine RNAiMAX (Invitrogen) according to manufacturer's instructions for reverse transfection. All siRNA oligonucleotides were from Shanghai GenePharma Co., Ltd (Shanghai, China). siRNAs were designed using Dharmacon algorithm (http://dharmacon.gelifesciences.com/design-center/). Sequences: Kif3A: 5'-TGTCATACTTGGAGATATA-3', 5'-CAGATAAGATGGTGGAAAT-3'and 5'-GGAAATAACATGAGGAAAC-3'; Kif3B: 5'-GAGCAGAAACGTCGAGAAA-3', 5'-GAAGAAGACCATTGGAAAT-3' and 5'-AGATAGAGCATGTGATGAA-3'; KAP3A: 5'-GAAGAAAGCTGTTGATGAA-3', 5'-GAGAAAGGATTATGACAAA-3'and 5'-AGAGAAGACTGGAAACAAA-3'; Kif3C:5'-CCGAAGAGGAAGATGATAA-3', 5'-GGCTAGAGCTGAAGGAGAA-3'; 5'-GGAGATTGCGGAACAGAAA-3'.

Focal adhesion disassembly and Immunofluorescence

Focal adhesion disassembly was performed as previously described (Ezratty et al., 2005). Briefly, NIH 3T3 cells were grown on glass coverslips and treated with 10 mM NZ for 3-4 hours

to completely depolymerize MTs. The drug was washed out with SFM, and MTs allowed to repolymerize for different intervals of time. For immunostaining cells were either fixed in 4% paraformaldehyde in PBS for 10 minutes followed by permeabilization with 0.3% Triton in PBS for 5 minutes and blocking with 5% normal goat serum (MP Biomedicals, Santa Ana, CA) before processing for immunofluorescence. Coverslips were mounted with Fluoromount-G (Southern Biotech, Birmingham, AL) after incubation with primary and secondary antibodies for 30 minutes each.

Western blotting and antibodies

Cells lysed in sample buffer were boiled for 5 min and then separated by SDS-PAGE on a 10% gel for all blots. Gels were transferred to nitrocellulose, blocked for 1 hour in NET buffer containing 5% BSA and then incubated overnight with different primary antibodies followed by 1 hour incubation with the appropriate IRDye-conjugated secondary antibodies (1:10,000 dilution, Li-cor, Lincoln, NE). After washing the membrane several times with TBS/Tween they were scanned and recorded with an Odyssey Infrared Imager (Li-cor). Antibodies used for Western Blot (WB) or Immunofluorescence (IF): pY118/31paxillin (rabbit polyclonal, 1:100 dilution for IF; Invitrogen), GFP (chicken polyclonal, 1:100 dilution for IF, EMD Millipore), Kif3A (mouse monoclonal, 1:1000 dilution for WB, BD Bioscience or rabbit polyclonal, 1:100 dilution for IF, Sigma), Kif3C (rabbit polyclonal, 1:1000 dilution for WB, Sigma), Kif3B (rabbit polyclonal, 1:1000 dilution for WB, Sigma), KAP3 (mouse monoclonal, 1:1000 dilution for WB, BD Bioscience), vinculin (mouse monoclonal, 1:100 dilution for IF; Sigma), tyrosinated tubulin (rat monoclonal YL1/2, 1/10 dilution of culture supernatant for IF and 1:50,000 dilution for WB). All secondary antibodies for immunofluorescence were from Jackson ImmunoResearch (West Grove, PA) and used at 1:200 dilution.

Epifluorescence and Phase contrast microscopy

Immunofluorescent stained preparations were observed with a Nikon Optiphot microscope using a 60X plan apo objective and filter cubes optimized for coumarin, fluorescein/GFP, rhodamine, and Cy5 fluorescence (Nikon). Images were captured with a MicroMax cooled CCD (Kodak KAF 1400 chip; Princeton Instruments, Trenton, NJ) using Metamorph software (Universal Imaging Corp., West Chester, PA). For wound healing assays phase contrast live cell movies were acquired with a 20X Planfluor objective (NA 0.45) and a CoolSNAP HQ CCD camera on a Nikon TE300 inverted microscope with temperature controller (37˚C) and motorized xyz stage to acquire multiple movies simultaneously using Metamorph's multi-dimensional acquisition application. Acquisition rate was 10 min per frame. AVI files and montage images were generated using Image J. controlled by Metamorph (Molecular Devices, Sunnyvale, CA) and processed with Image J (NIH, Bethesda, MD).

Cell surface labeling and flow cytometry

Cells were harvested by trypsinization at various timepoints during MT regrowth and FA disassembly, and washed in cold PCN (1x PBS, 0.5% Calf Serum, 0.1% NaN_3). Approximately $4x10^6$ cells per sample were stained without fixation at 4º. For detection of α5 integrin in NIH3T3 and HA1 fibroblasts, PE–conjugated rat α-mouse CD49e monoclonal antibody (BD Pharmingen) was used at dilution of 1:1500. After 3-4 washes to remove unbound antibody, samples were fixed in cold 4% paraformaldehyde/PCN and the distribution and mean fluorescence intensity of each sample was quantified using a Becton Dickson FACScan.

Statistical analysis

A two-tailed unpaired Student's *t* test was used to evaluate two groups. Significance between multiple groups was determined by one-way analysis of variance (ANOVA) followed by Tukey's multiple comparison test.

Chapter 3: Talin but not Other Integrin Activation Regulators is Required for Focal Adhesion Reassembly

INTRODUCTION

Given that FAK inhibition resulted in inactive integrin after recycling to the cell surface, we originally envisaged two scenarios: 1) FAK kinase activity was required to maintain integrin activation during endocytic recycling ("Always active" model-Figure 30A) or 2) FAK kinase activity was required to reactivate recycled integrin once they returned to the plasma membrane ("Surface activation" model-Figure 30B). In Chapter 1, I presented evidence that the "Always active" model is the more likely one. Specifically, I used conformation-specific antibodies for active integrins to demonstrate that FAK kinase activity is critical to keep integrins active during their endocytic recycling. Nevertheless, before reaching this conclusion, we made several attempts to test the "Surface activation" model. For instance, there are several proteins that interact with integrin α- and β-cytoplasmic tail and modulate integrin activation either positively or negatively (Bouvard et al., 2013; Morse et al., 2014). Thus in this chapter, we examined integrin activity regulators, which may also be FAK substrates, to determine if they played a role in the activation state of recycled integrin. This chapter is organized into three topics: integrin activators, phosphatidylinositol-4,5-bisphosphate generators and integrin inhibitors.

RESULTS AND DISCUSSION

Integrin activators

Since integrin return to the cell surface was unaffected by FAK inhibition but FA reassembly was still impaired due to lack of integrin activation (Figure 14, Chapter 1), we tested whether canonical integrin activators were involved in the activation of recycled integrin. To test this we knocked down talin1 and kindlin2, the two major integrin activators in most cells (Moser et al., 2009). Talin1 levels were reduced approximately 90% after transfecting NIH3T3 fibroblasts with three different siRNAs for talin1 (Figure 31A). Consistent with its role in integrin activation, talin1-depleted cells grown under sparse conditions or in wounded monolayers displayed considerably smaller and fewer FAs when compared to non-coding siRNA-transfected cells (Figure 31B). Next we conducted NZ washout assays with talin1-depleted cells to test its role in MT-induced FA disassembly and reassembly. Talin1-depleted cells displayed normal levels of FAs after NZ treatment and normal disassembly of FAs after NZ washout (Figure 31C and D). However, talin1-depleted cells exhibited impaired FA reassembly when compared to non-coding siRNA-treated cells (Figure 31C and D). This result was not surprising given talin's critical role in integrin activation. I should point out however that talin may be playing a role either during integrin recycling or right after their return to the plasma membrane (or maybe both). Further experimentation with talin-depleted cells and antibodies recognizing the active conformation of integrins may distinguish between these possibilities.

The level of talin expressed in cells determines the efficacy of kindlins in promoting integrin activation. For example, overexpressing kindlin2 in cells with relatively little talin has little or no effect on integrin affinity modulation and coexpression of the talin-head domain with kindlin1or kindlin2 results in a synergistic increase in αIIbβ3 affinity (Han et al., 2006). Conversely, talin depends on kindlins to promote integrin affinity because talin-head overexpression failed to

increase αIIbβ3 affinity in kindlin-depleted cells (Harburger et al., 2009; Harburger and Calderwood, 2009; Kloeker et al., 2004; Montanez et al., 2008; Ussar et al., 2008).

To test whether kindlin affected FA disassembly or reassembly, I knocked down kindlin2, the major isoform in fibroblasts, using three different siRNAs oligonucleotides (Figure 32A). Reduction of kindlin2 levels by knockdown did not affect either FA disassembly or reassembly following NZ washout (Figure 32B). Therefore although talin is critical for FA reassembly in our system, kindlin does not seem to play a crucial role.

To further test talin involvement in FA reassembly we used a talin1 head domain (residues 1-405) that was previously shown to bind to integrin β-subunit cytoplasmic tails and promote integrin activation (Bouaouina et al., 2008; Calderwood et al., 1999). We hypothesized that FAK kinase activity could be affecting talin activation, which involves an unfolding of the tail domain from the head domain (Moser et al., 2009). If this is correct, then the overexpression of talin head would bypass the requirement for FAK kinase activity and rescue FA reassembly in FAK-inhibited cells. As shown in figure 33, transient expression of full length talin or talin head did not have detectable effect on FA disassembly or reassembly in DMSO-treated cells. Neither full length talin nor talin head overexpression rescued FA reassembly in FAK-inhibited cells. This result was not completely unexpected as Zhang et al., (2008) had previously demonstrated that talin1 head activated β1 integrins but did not rescue FA formation in talin$^{-/-}$ cells. They concluded that integrin clustering into FAs depends on both the head and rod domains of talin.

Next we sought to test if talin binding to FAK was required for FA reassembly. To this end we used a FAK mutant that is defective in talin binding (FAK-E1015A) (Lawson et al., 2012) and tested whether it could rescue FA reassembly in FAK$^{-/-}$ cells (assuming it would rescue FA disassembly). As expected, FA disassembly was rescued in these cells and surprisingly FA

reassembly occurred normally (Figure 34A, C). Initially this suggested that talin binding to FAK is not critical for FA reassembly. However more careful analysis by Total Internal Reflection (TIRF) microscopy revealed that talin was being recruited normally to FAs in FAK-E1015A-transfected cells (Figure 34C). This is consistent with observations by Lawson et al. (2012) who showed that FAK-E1015A-talin colocalization in FAs increases at later time-points of cell spreading. This may reflect alternative FA targeting mechanisms for talin (Franco et al., 2006; Wang et al., 2011a).

Phosphatidylinositol-4,5-bisphosphate generators

We next explored the role of the type I phosphatidylinositol phosphate kinase isoform-γ90 (PIPKIγ90) in FA disassembly and reassembly. PIPKIγ90 generatesPtdIns(4,5)P_2 and is tyrosine phosphorylated by FAK-associated signaling, which increases its activity (Ling et al., 2002). Additionally, PIPKIγ90 was previously shown to be targeted to FAs by an association with talin (Di Paolo et al., 2002; Ling et al., 2002). Talin activation probably involves binding to PtdIns(4,5)P_2 since this lipid elicits a conformational change that disrupts the autoinhibitory head-tail interaction and enhances integrin-talin binding (Goksoy et al., 2008; Martel et al., 2001). Thus we hypothesized that integrins are not active in FAK-inhibited cells due to reduced levels of PtdIns(4,5)P_2 at plasma membrane sites, which would lead to impaired recruitment and activation of talin. To test this hypothesis, we transiently expressed PIPKIγ90 and PIPKIγ87 (an isoform that does not target to FAs) (Di Paolo et al., 2002; Ling et al., 2002) in NIH3T3 fibroblasts and conducted the FA disassembly/reassembly assay in the absence or presence of the FAK inhibitor PF228. PIPKIγ90 and PIPKIγ87 overexpression did not affect FA disassembly or reassembly in DMSO-treated cells (Figure 35A and B). Interestingly, PIPKIγ90 but not PIPKIγ87 partially rescued FA reassembly in PF228-treated cells (Figure 35), suggesting that PtdIns(4,5)P_2 levels might by an important factor modulating activation of recycled integrin.

Consistent with this hypothesis, adding PtdIns(4,5)P_2 to PF228-treated cells also partially rescued FA reassembly (Figure 36A, B). To investigate if FAK kinase activity was affecting the global cellular levels of PtdIns(4,5)P_2 we measured PtdIns(4,5)P_2 levels by high-performance liquid chromatography (HPLC) of lipid extracts prepared from cells during FA disassembly and reassembly. There were no significant changes in PtdIns(4,5)P_2 levels during FA disassembly or reassembly and PF228-treated cells displayed a slight (but statistically not significant) increase in PtdIns(4,5)P_2 levels (Figure 36C). These results suggest that FAK kinase activity does not modulate the activation of recycled integrin by affecting the global levels of PtdIns(4,5)P_2. The rescue of FA reassembly in PF228-treated cells transfected with PIPKIγ90 or treated with PtdIns(4,5)P_2 may reflect a gain of function. A similar gain of function in the reassembly of FAs is observed in PF228- and PP2-treated cells incubated with Rho activator II (Figure 37).

Integrin inhibitors

There are several integrin inhibitors that prevent integrin activation by binding to the cytoplasmic tails of either their α- or β-integrins (Bouvard et al., 2013). For example SHANK-associated RH domain-interacting protein (SHARPIN) was shown to bind to the α-integrin tail and prevent it from binding to the integrin activators talin and kindlin (Rantala et al., 2011). Likewise, filamin inhibits integrin activation by competing with talin for binding to β-integrin tails (Kiema et al., 2006). Interestingly, a kindlin binding protein known as migfilin (Brahme et al., 2013; Tu et al., 2003) was suggested to stimulate integrin activation by competing away filamin and promoting talin-integrin binding (Das et al., 2011; Ithychanda et al., 2009; Kiema et al., 2006; Lad et al., 2008; Musse et al., 2012). We first tested the possibility that FAK kinase activity is necessary to cause SHARPIN dissociation from integrin tails prior to FA reassembly. To verify this we knocked-down SHARPIN (Figure 38A) and performed the NZ washout assay in the presence of PF228. If our hypothesis is correct SHARPIN-depleted cells should

reassemble their FAs regardless of the presence of PF228. However, FA reassembly was still blocked in SHARPIN-depleted cells when the PF228 was present (Figure 38C). Furthermore, overexpression of a migfilin construct that localizes to stress fibers (migfilin 1-85aa) (Brahme et al., 2013) and promotes integrin activation by displacing filamin from integrin tails (Lad et al., 2008; Musse et al., 2012) did not rescue FA reassembly in PF228-treated cells (Figure 39). Together these results show that neither SHARPIN nor filamin are involved in the activation of recycled integrins.

Overall the results presented here strengthen the "Always active" model proposed in Chapter 1 (also see Figure 30) since all of the results to test the "Surface activation" model were negative. Nevertheless, the experiments do identify a role for talin1 in the reassembly of FAs from recycled integrins and it will be interesting to test whether talin1, like FAK, is required to maintain the activation state of integrins during their endocytic recycling.

FIGURES

Figure 30. Models for integrin (re)activation during endocytic recycling.

(A) “Always active model”: here we propose that recycled integrins never get deactivated during endocytic recycling. Thus once they get back to the plasma membrane they are ready to engage with the extracellular matrix to form new adhesions. (B) “Surface activation” model: here we suggest that at some point during the endocytic recycling integrins get deactivated and only after they are recycled back to the cell surface they are reactivated.

A

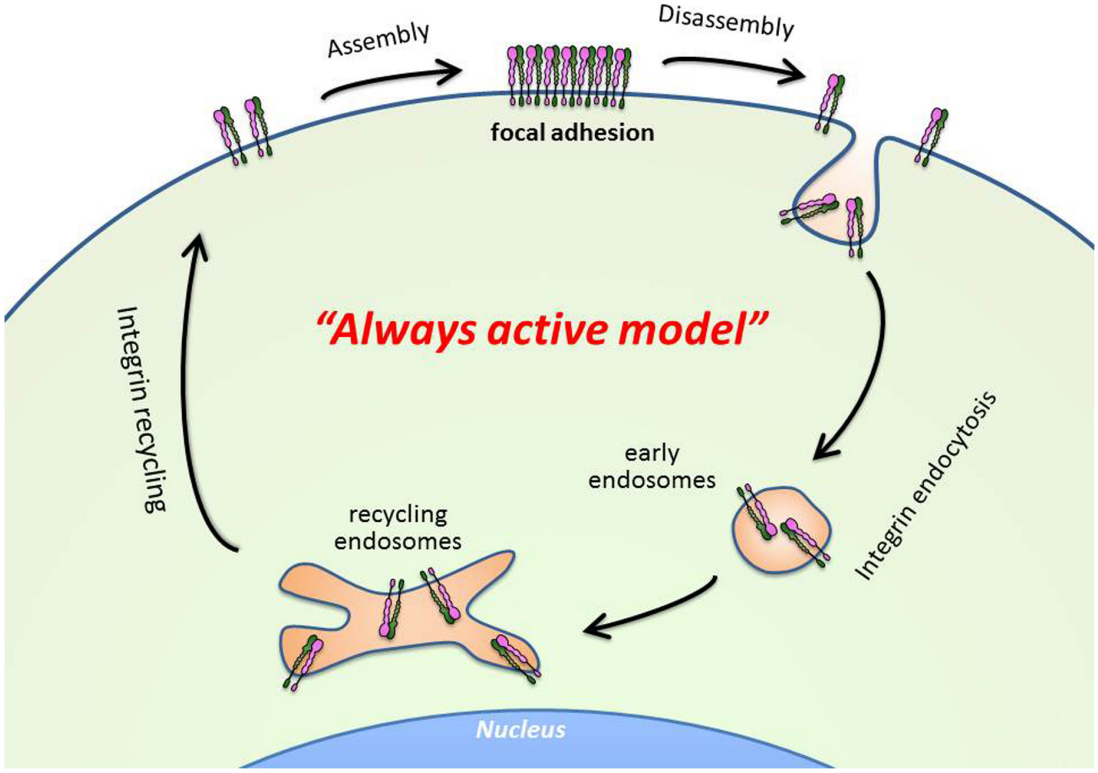
Assembly
Disassembly
focal adhesion
"Always active model"
Integrin recycling
early endosomes
Integrin endocytosis
recycling endosomes
Nucleus

B

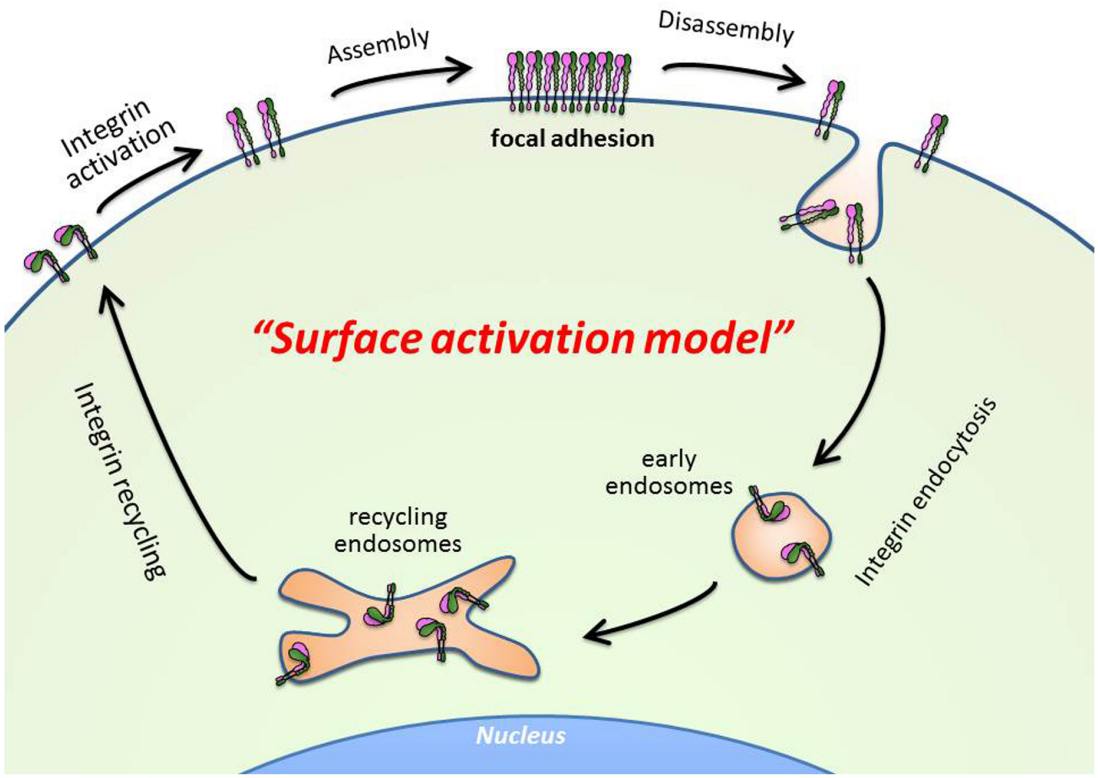
Assembly
Disassembly
Integrin activation
focal adhesion
"Surface activation model"
Integrin recycling
early endosomes
Integrin endocytosis
recycling endosomes
Nucleus

Figure 31. Talin1 is required for FA reassembly.

(A) Western blot analysis of talin1 in NIH3T3 fibroblasts treated with non-coding (NC) or talin1 siRNAs. Tubulin is a loading control. (B) Immunofluorescence images of vinculin in NIH3T3 fibroblasts treated with NC or talin1 siRNAs. Scale bar, 10 μm. (C) Immunofluorescence images of paxillin-pY31 and MTs in NIH3T3 fibroblasts treated with NC or talin1 siRNAs and fixed at the indicated times after NZ washout. Scale bar, 15 μm. (D) Quantification of FA disassembly and reassembly in talin1-depleted cells at the indicated times after NZ washout. Bars are SD. At least 150 cells were analyzed in each experiment from a total of 3 independent experiments. **$p<0.01$, relative to control (NC) values at 120 min after NZ washout.

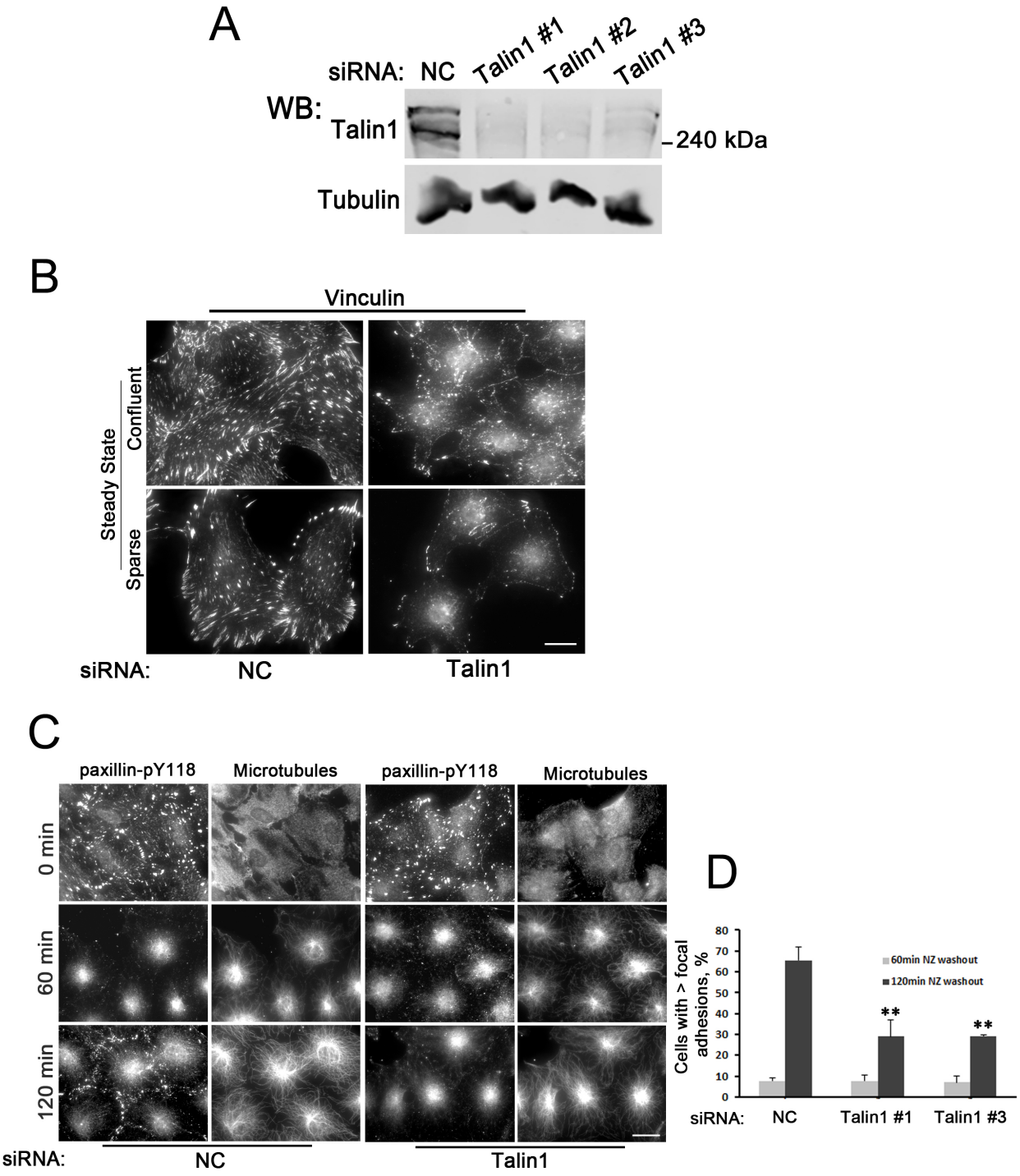
A
siRNA: NC Talin1 #1 Talin1 #2 Talin1 #3
WB: Talin1
240 kDa
Tubulin
B
Vinculin
Steady State
Confluent
Sparse
siRNA: NC Talin1
C
paxillin-pY118
Microtubules
paxillin-pY118
Microtubules
0 min
60 min
120 min
siRNA: NC Talin1
D
Cells with > focal adhesions, %
60min NZ washout
120min NZ washout
**
**
siRNA: NC Talin1 #1 Talin1 #3

Figure 32. Kindlin is not required for FA reassembly.

(A) Western blot analysis of kindlin2 in NIH3T3 fibroblasts treated with non-coding (NC) or kindlin2 siRNAs. Tubulin is a loading control. (B) Immunofluorescence images of paxillin-pY118 and MTs in NIH3T3 fibroblasts treated with NC or kindlin2 siRNAs and fixed at the indicated times after NZ washout. Scale bar, 15 μm. (C) Quantification of FA disassembly and reassembly in kindlin2-depleted cells at the indicated times after NZ washout. Bars are SD. At least 150 cells were analyzed in each experiment from a total of 3 independent experiments.

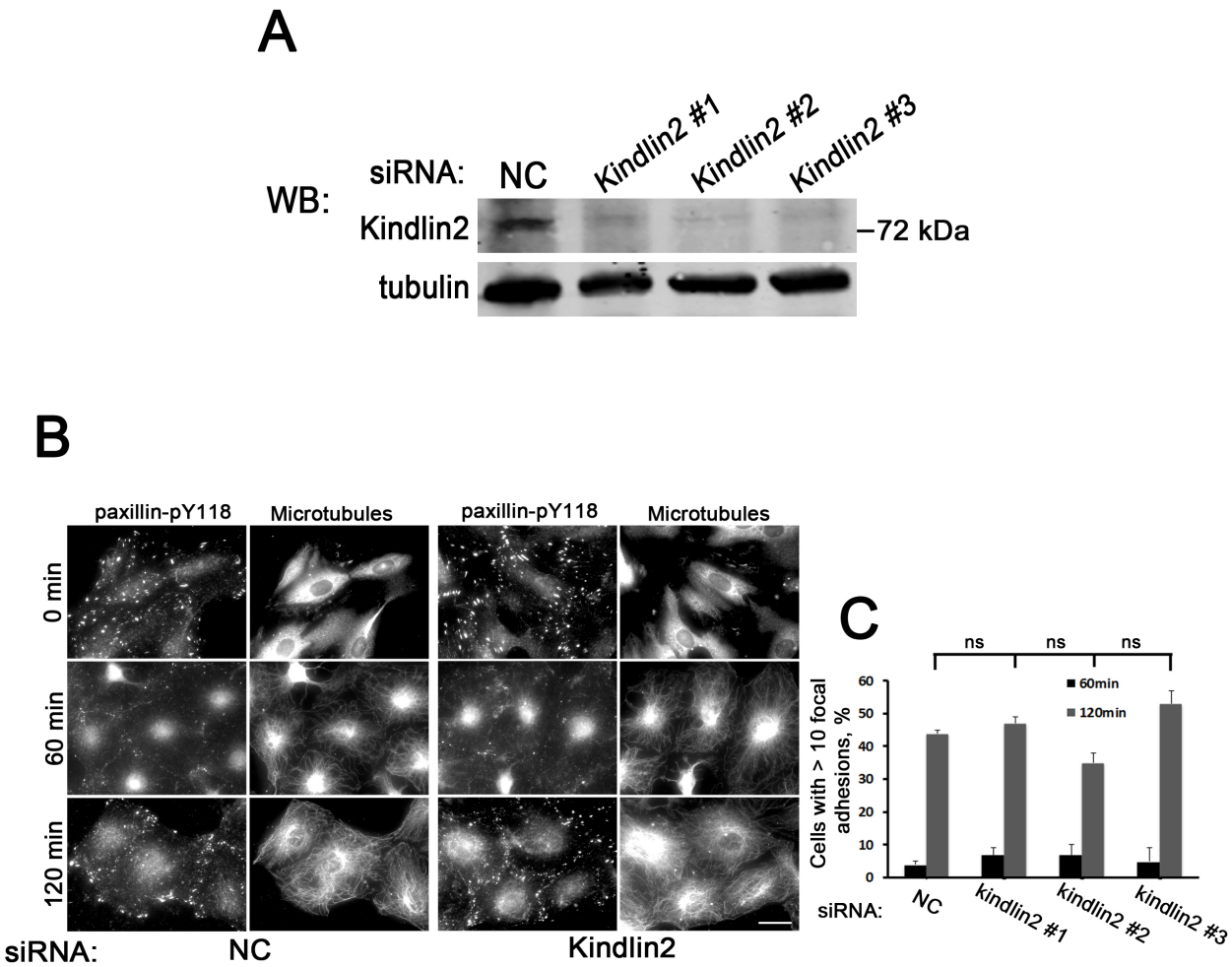
A
WB:
siRNA:
NC
Kindlin2 #1
Kindlin2 #2
Kindlin2 #3
Kindlin2
tubulin
72 kDa
B
paxillin-pY118
Microtubules
paxillin-pY118
Microtubules
0 min
60 min
120 min
siRNA:
NC
Kindlin2
C
ns
ns
ns
60min
120min
Cells with > 10 focal adhesions, %
0
10
20
30
40
50
60
siRNA:
NC
kindlin2 #1
kindlin2 #2
kindlin2 #3

Figure 33. Overexpression of full length talin or talin head (1-405) does not rescue FA reassembly in FAK-inhibited cells.

(A) Immunofluorescence images of talin (wt or head), vinculin and MTs in NIH3T3 fibroblasts expressing talin wt-EGFP or talin head (1-405aa)-EGFP and fixed at the indicated times after NZ washout in the presence of PF228 (10 μM) or vehicle (DMSO). Arrows point to the transfected cells. Scale bar, 15 μm. (B) Quantification of FA disassembly and reassembly in cells transfected with talin wt or talin-head (1-405) at the indicated times after NZ washout. Bars are SD. At least 150 cells were analyzed in each experiment from a total of 3 independent experiments. *** $p<0.001$.

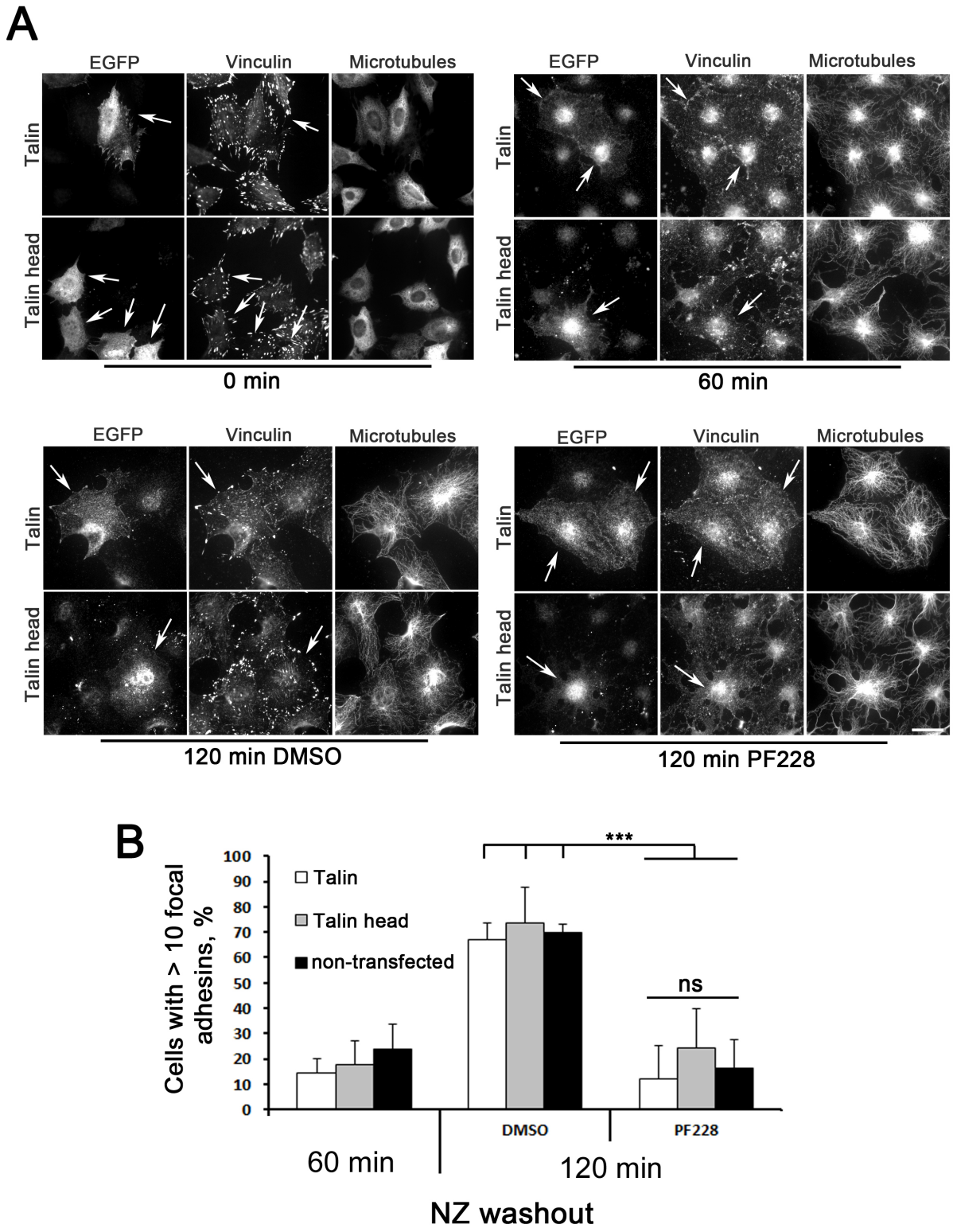
A
EGFP
Vinculin
Microtubules
Talin
Talin head
0 min
60 min
120 min DMSO
120 min PF228
B
Cells with > 10 focal adhesins, %
Talin
Talin head
non-transfected
***
ns
DMSO
PF228
60 min
120 min
NZ washout

Figure 34. Talin binding to FAK is not required for FA reassembly.

(A) Immunofluorescence images of FAK (talin binding mutant), vinculin and MTs in NIH3T3 fibroblasts expressing FAK-E1015A-GFP and fixed at the indicated times after NZ washout. Arrows point to the transfected cells. Scale bar, 15 μm. (B) Quantification of FA disassembly and reassembly in transfected cells at the indicated times after NZ washout. (C) Same as in "A" but the cells were analyzed by total internal reflection (TIRF) microscopy. Scale bar, 15 μm. At least 100 cells were analyzed in each experiment from a total of 3 independent experiments. Bars are SD. ** $p<0.01$, relative to 120 min after NZ washout.

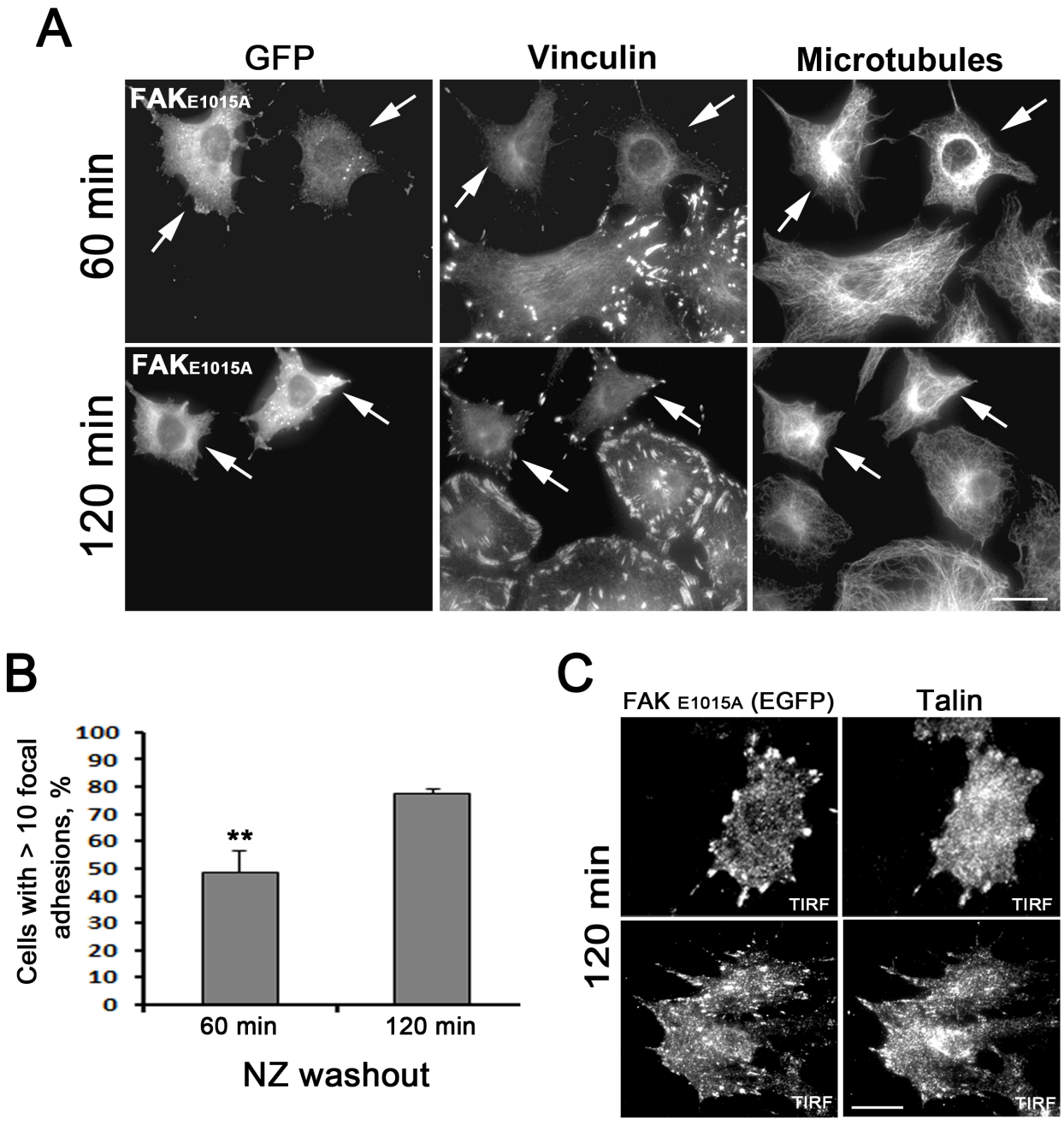
A
GFP
Vinculin
Microtubules
FAKE1015A
60 min
FAKE1015A
120 min
B
Cells with > 10 focal adhesions, %
100
90
80
70
60
50
40
30
20
10
0
**
60 min
120 min
NZ washout
C
FAK E1015A (EGFP)
Talin
120 min
TIRF
TIRF
TIRF
TIRF

Figure 35. Overexpression of PIPK1γ90 rescues FA reassembly in FAK-inhibited cells.

(A) Immunofluorescence images of PIPK1γ90 or PIPK1γ87, vinculin and MTs in NIH3T3 fibroblasts expressing either PIPK1γ90-GFP or PIPK1γ87-GFP and fixed at the indicated times after NZ washout in the presence of DMSO (vehicle) or PF228 (10 μM). Arrows point to the transfected cells. Scale bar, 20 μm. (B) Quantification of FA disassembly and reassembly in cells transfected with PIPK1γ90 or PIPK1γ87 at the indicated times of NZ washout. At least 150 cells were analyzed in each experiment from a total of 3 independent experiments. Bars are SD. *$p<0.05$; ** $p<0.01$.

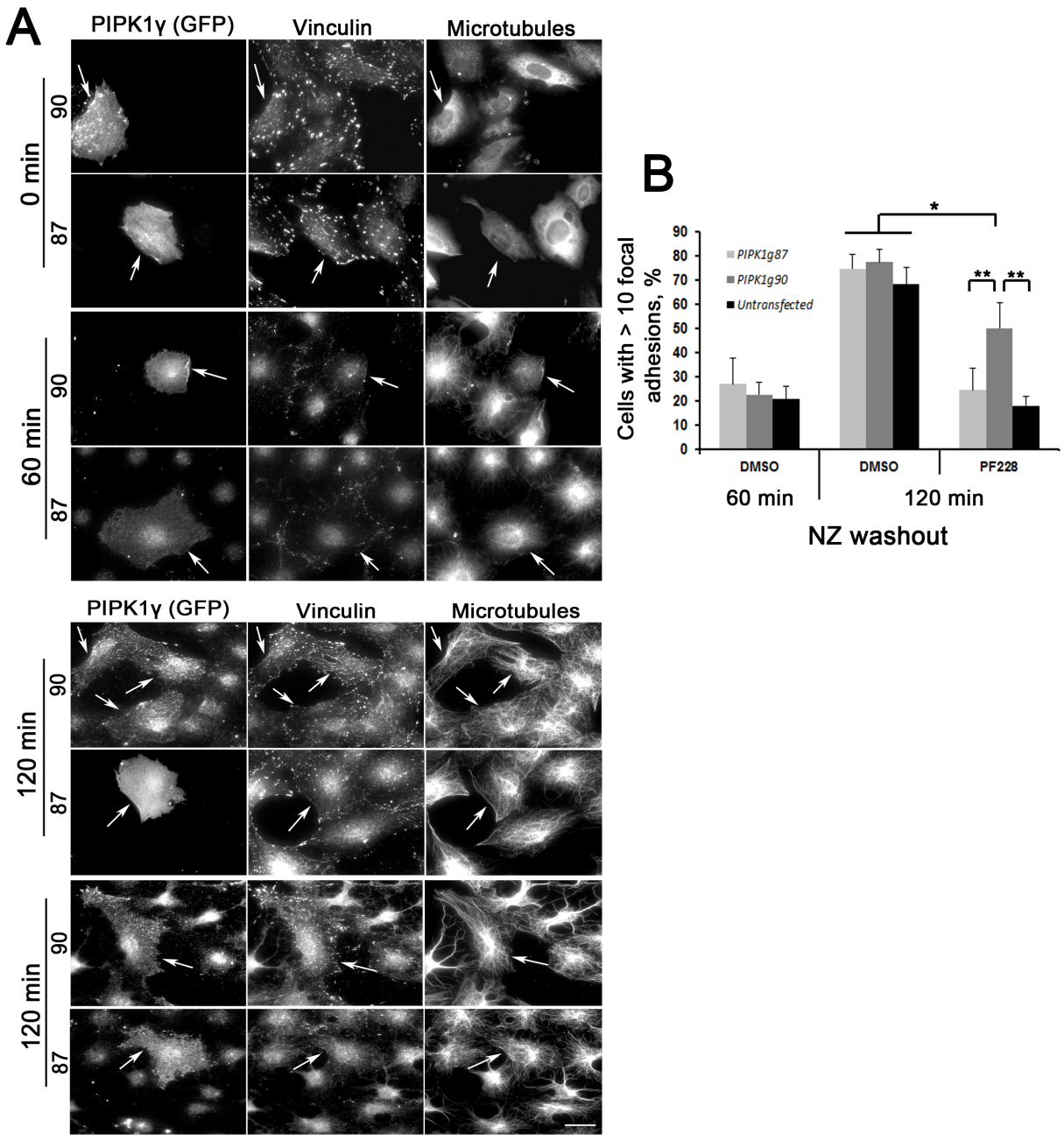
A
PIPK1γ (GFP)
Vinculin
Microtubules
0 min
60 min
120 min
90
87
B
Cells with > 10 focal adhesions, %
PIPK1g87
PIPK1g90
Untransfected
DMSO
DMSO
PF228
60 min
120 min
NZ washout
*
**
**

Figure 36. The phospholipid PI(4,5)P_2 rescues FA reassembly in FAK-inhibited cells but PI(4,5)P_2 levels remain unchanged.

(A) Immunofluorescence images of paxillin-pY118 and MTs in NIH3T3 fibroblasts treated with either PI(4,5)P_2 plus vehicle (neomycin sulfate) or vehicle only and fixed at 120 min after NZ washout. NZ washout was performed in the presence of either PF228 (10μM) or DMSO. Scale bar, 15 μm. (B) Quantification of FA reassembly after 120 min of NZ washout. At least 150 cells were analyzed in each experiment from a total of 3 independent experiments. (C) Data represent PI(4,5)P_2 levels measured by High-performance liquid chromatography (HPLC) in NIH3T3 fibroblasts harvested at the indicated times after NZ washout in the presence of PF228 (10μM) or DMSO. Bars are SD. ** $p < 0.01$.

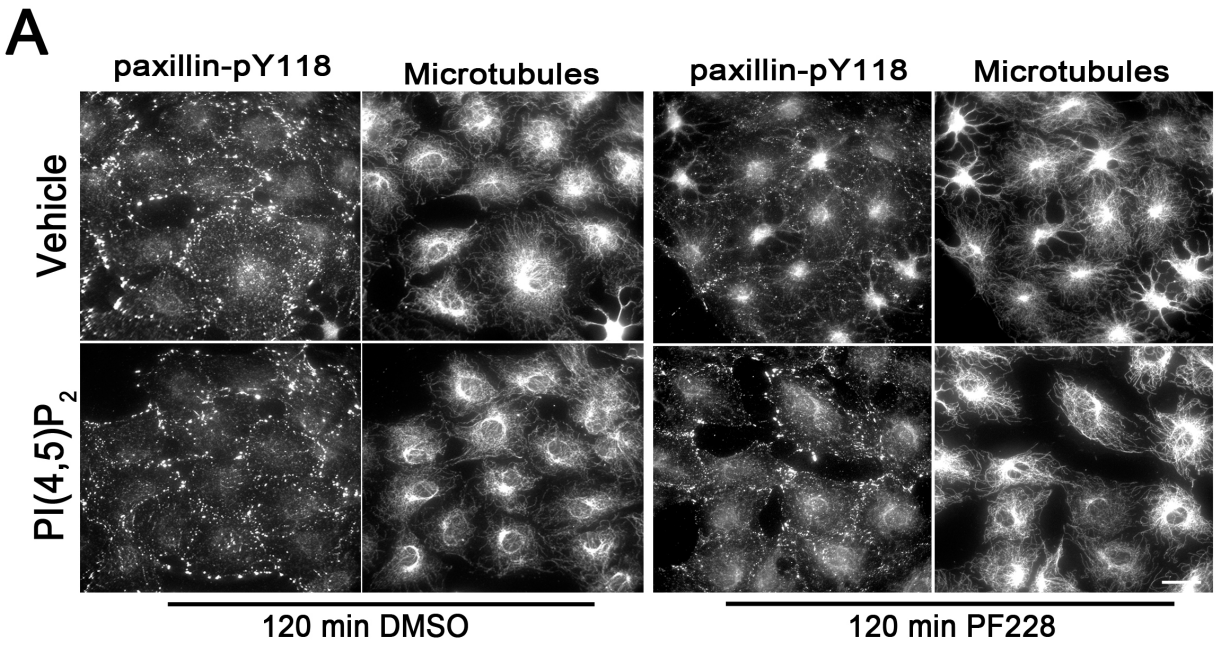
A
paxillin-pY118
Microtubules
paxillin-pY118
Microtubules
Vehicle
PI(4,5)P2
120 min DMSO
120 min PF228

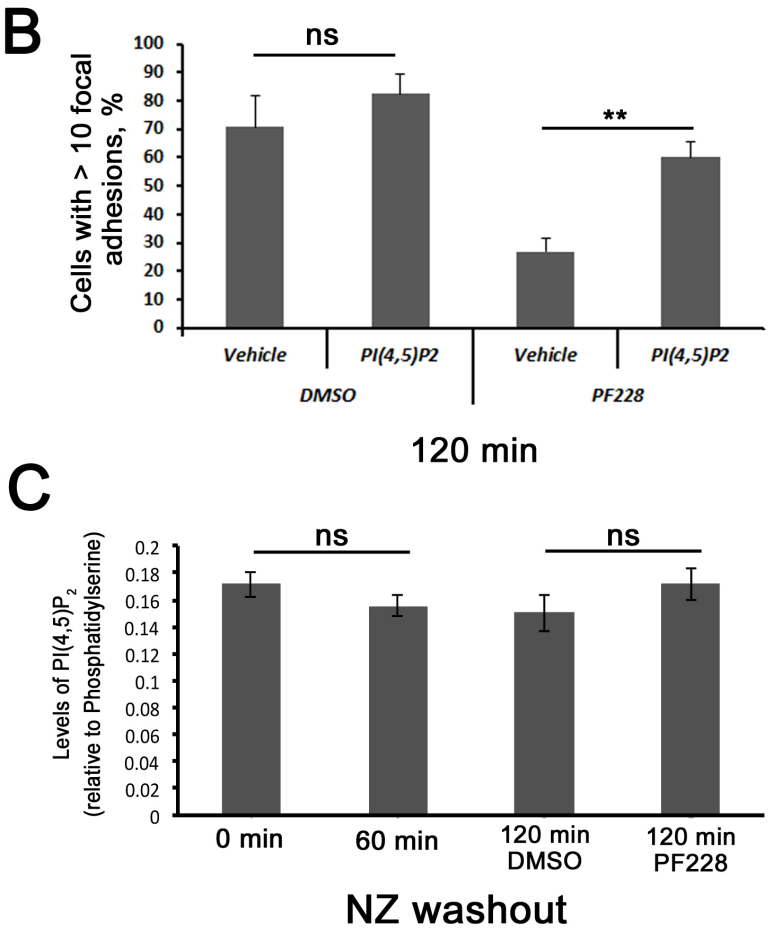
B
Cells with > 10 focal adhesions, %
ns
**
Vehicle
PI(4,5)P2
Vehicle
PI(4,5)P2
DMSO
PF228
120 min

C
Levels of PI(4,5)P2 (relative to Phosphatidylserine)
ns
ns
0 min
60 min
120 min DMSO
120 min PF228
NZ washout

Figure 37. Rho activator rescues FA reassembly in FAK-inhibited cells.

Immunofluorescence images of vinculin, rhodamine-phalloidin and MTs in NIH3T3 fibroblasts fixed at 120 min after NZ washout in the presence of PF228 (10 μM), SFKs inhibitor PP2 (10 μM) or DMSO. The Rho activator was added at 60 min after NZ washout. Scale bar, 15 μm.

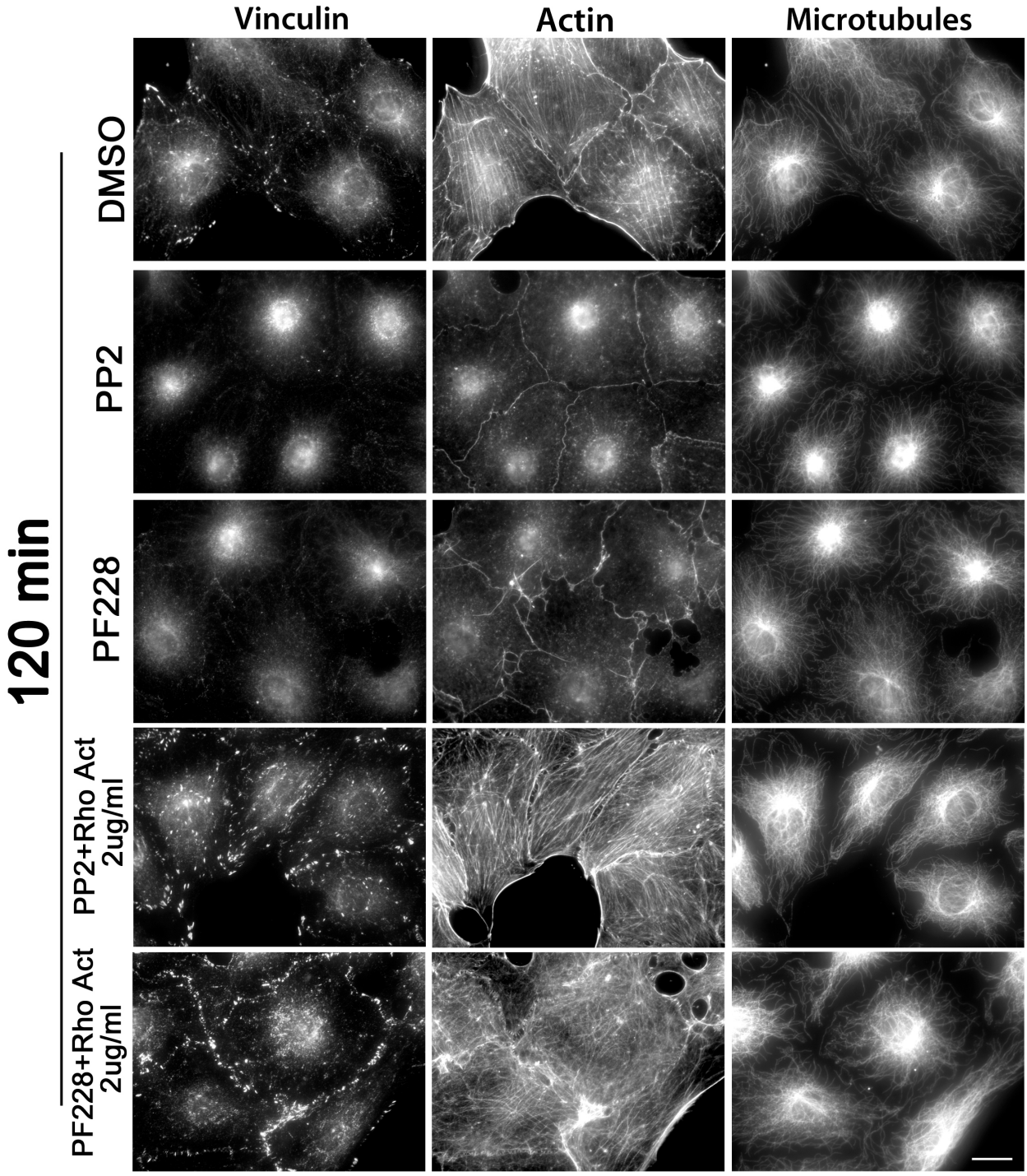
Vinculin
Actin
Microtubules
120 min
DMSO
PP2
PF228
PP2+Rho Act 2ug/ml
PF228+Rho Act 2ug/ml

Figure 38. SHARPIN depletion does not rescue FA reassembly in FAK-inhibited cells.

(A) Western blot analysis of SHARPIN in NIH3T3 fibroblasts treated with non-coding (NC) or SHARPIN siRNAs. Tubulin is a loading control. (B-C) Immunofluorescence images of paxillin and MTs in NIH3T3 fibroblasts treated with NC or SHARPIN siRNAs and fixed at the indicated times after NZ washout in the presence of PF228 (10 μM) or DMSO. Scale bars, 10 and 15 μm, respectively.

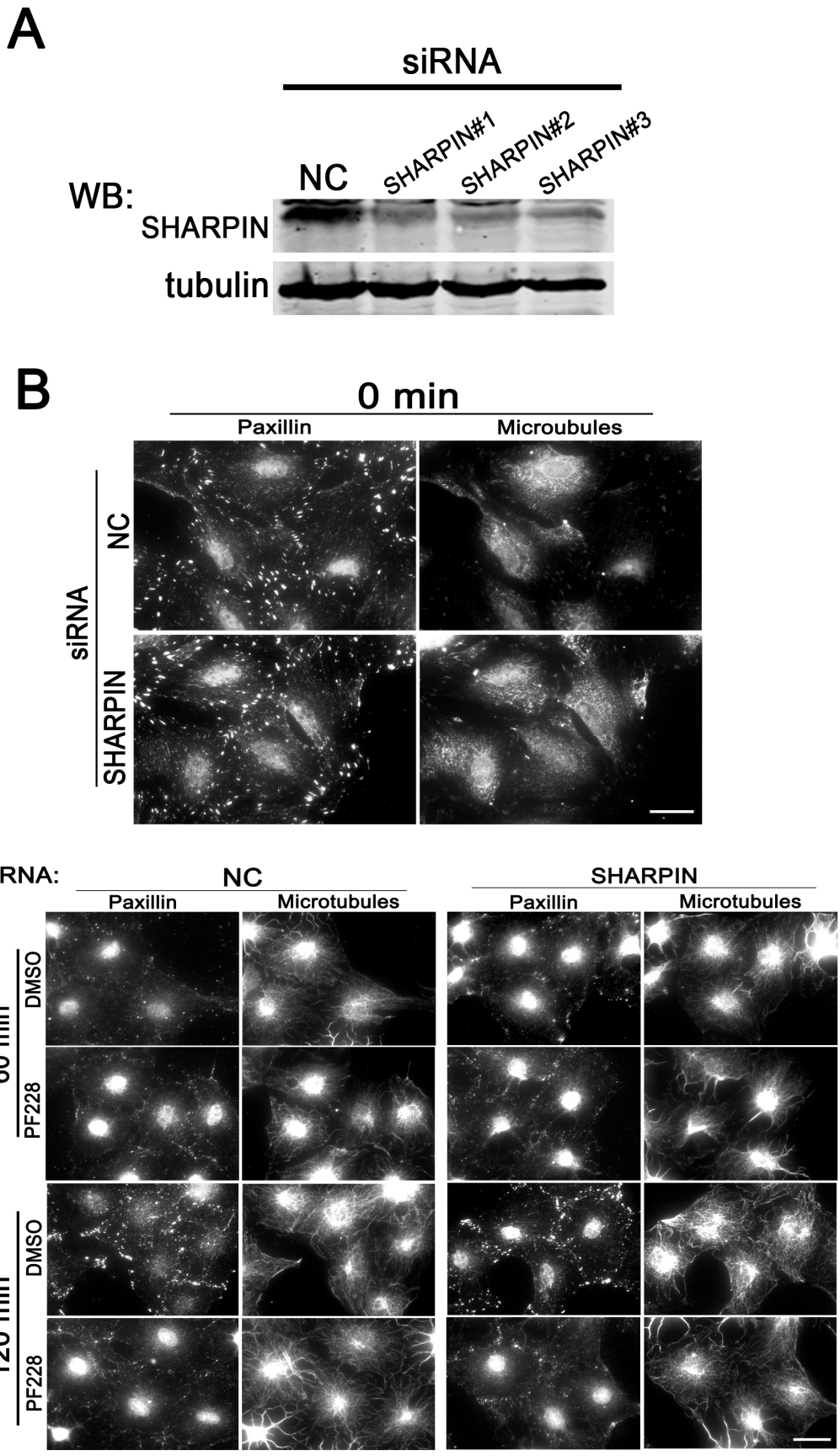
A
siRNA
NC
SHARPIN#1
SHARPIN#2
SHARPIN#3
WB:
SHARPIN
tubulin
B
0 min
Paxillin
Microubules
siRNA
NC
SHARPIN
C
siRNA:
NC
SHARPIN
Paxillin
Microtubules
Paxillin
Microtubules
60 min
DMSO
PF228
120 min
DMSO
PF228

Figure 39. Migfilin (1-85aa) overexpression does not rescue FA reassembly in FAK-inhibited cells. Immunofluorescence images of migfilin, paxillin-pY118 and MTs in NIH3T3 fibroblasts expressing the N-terminus of migfilin, Migfilin(1-85aa)-EGFP, and fixed at the indicated times after NZ washout in the presence of DMSO (vehicle) or PF228 (10 μM). Arrows point to the transfected cells. Scale bar, 15 μm.

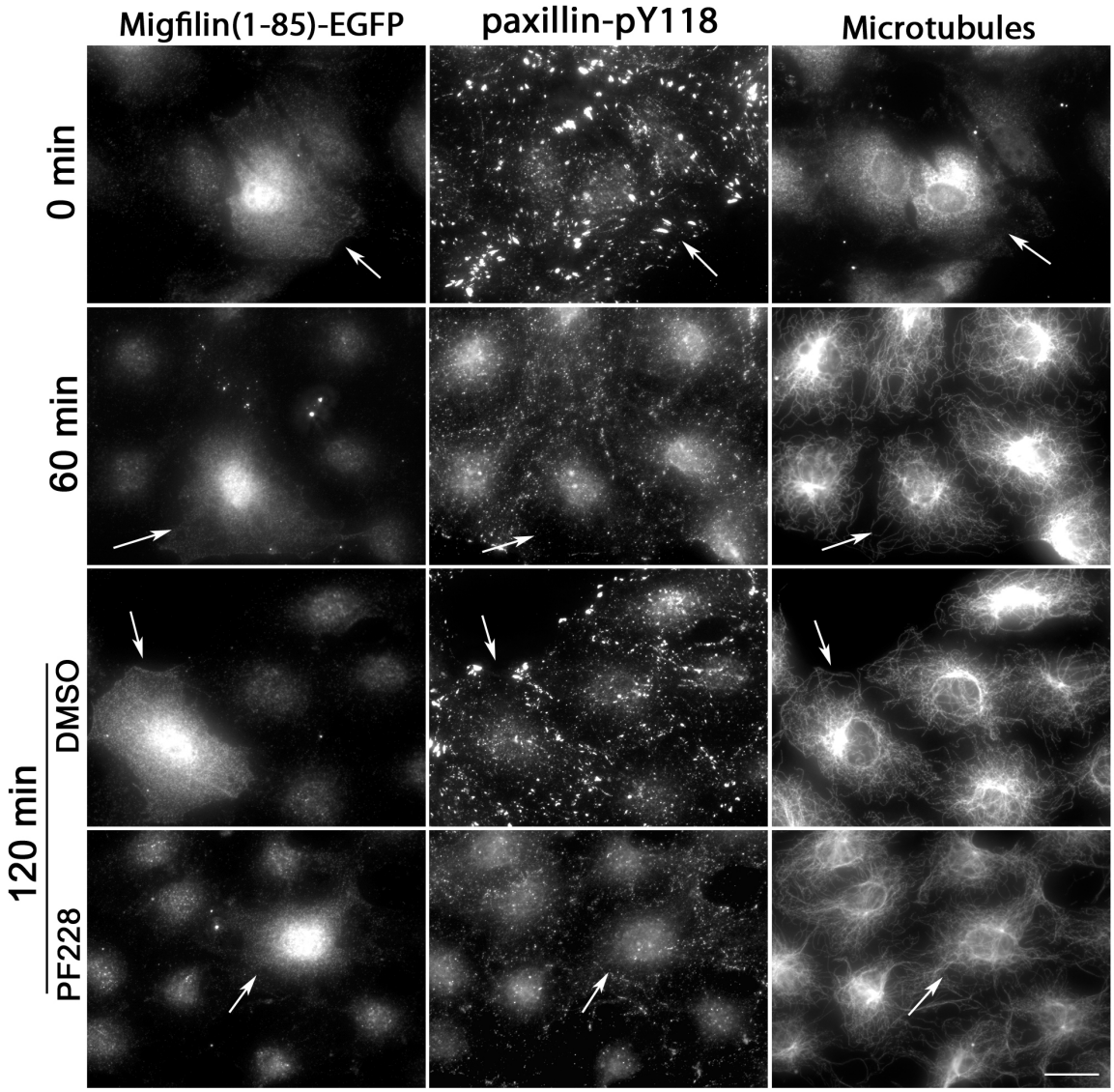
Migfilin(1-85)-EGFP
paxillin-pY118
Microtubules
0 min
60 min
120 min
DMSO
PF228

MATERIAL AND METHODS

Chemicals and cell culture

Nocodazole was purchased from Sigma. FAK inhibitor (PF228) was purchased from Tocris bioscience and Src family kinases inhibitor (PP2) was purchased from EMD Millipore Bioscience. The Rho Activator II was purchased from Cytoskeleton, Inc. The phospholipid PtdIns(4,5)P_2 was purchased from Echelon (Salt Lake city, UT). NIH 3T3 fibroblasts were cultured in DMEM and calf serum as previously described (Cook et al., 1998; Gundersen et al., 1994). For serum starvation, cells on acid-washed coverslips were grown to confluence (~2days) and transferred to serum-free medium (SFM; DMEM, 10mM HEPES, pH7.4) for 48 hour as previously described (Cook et al., 1998; Gundersen et al., 1994).

Plasmids and transfection

GFP-FAK-wt, GFP-FAK-Y397F, GFP-FAK-E1015A and HA-tagged FAK-K454R constructs were gifts from Dr. David Schlaepfer. EGFP-Talin1 wt, GFP-talin1-head (1-405aa) and EGFP-Migfilin (1-85aa) were gifts from Dr. David Calderwood. GFP-PIPKIγ90 and GFP-PIPKIγ87 were kindly provided by Dr. Di Paolo. All constructs were transiently transfected with Lipofectamine Plus reagent (Invitrogen) according to manufacturer's instructions and expressed for 24-48 hours before performing the FA disassembly assay. siRNAs (20 μM) were transfected with using Lipofectamine RNAiMAX (Invitrogen) according to manufacturer's instructions for reverse transfection. All siRNA oligonucleotides were from Shanghai GenePharma Co., Ltd (Shanghai, China). siRNAs were designed using Dharmacon algorithm (http://dharmacon.gelifesciences.com/design-center/). Sequences: Talin1: 5'-GGATGTAGCTGGTGGACTA-3', 5'-GCCAAAGAGACGTGGATAA-3' and 5'-TGACAAGGCCTGTGAATTT -3'; Kindlin2: 5'- GAGAAGAACUUAUUGGAAUUU -3', 5'-CGAGAAGAGUCCAGUGGUAUU-3' and 5'-UGACAAAGAAGUUGAUGAAUU-3';

SHARPIN: 5'-GCUCAAAUACCUAAAGCAAUU-3', 5'-CCAGAGAAGUUUCAGGACAUU -3'and 5'- GCUACAAGUCACAGUUGAAUU-3'.

Focal adhesion disassembly and Immunofluorescence

Focal adhesion disassembly was performed as previously described (Ezratty et al., 2005). Briefly, NIH 3T3 cells were grown on glass coverslips and treated with 10 mM NZ for 3-4 hours to completely depolymerize MTs. The drug was washed out with SFM, and MTs allowed to repolymerize for different intervals of time. For immunostaining cells were either fixed in 4% paraformaldehyde in PBS for 10 minutes followed by permeabilization with 0.3% Triton in PBS for 5 minutes and blocking with 5% normal goat serum (MP Biomedicals, Santa Ana, CA) before processing for immunofluorescence. Coverslips were mounted with Fluoromount-G (Southern Biotech, Birmingham, AL) after incubation with primary and secondary antibodies for 30 minutes each.

Western blotting and antibodies

Cells lysed in sample buffer were boiled for 5 min and then separated by SDS-PAGE on a 10% gel for all blots. Gels were transferred to nitrocellulose, blocked for 1 hour in NET buffer containing 5% BSA and then incubated overnight with different primary antibodies followed by 1 hour incubation with the appropriate IRDye-conjugated secondary antibodies (1:10,000 dilution, Li-cor, Lincoln, NE). After washing the membrane several times with TBS/Tween they were scanned and recorded with an Odyssey Infrared Imager (Li-cor). Antibodies used for Western Blot (WB) or Immunofluorescence (IF): pY118/31paxillin (rabbit polyclonal, 1:100 dilution for IF; Invitrogen), GFP (chicken polyclonal, 1:100 dilution for IF, EMD Millipore), vinculin (mouse monoclonal, 1:100 dilution for IF; Sigma), tyrosinated tubulin (rat monoclonal YL1/2, 1/10 dilution of culture supernatant for IF and 1:50,000 dilution for WB), paxillin (mouse monoclonal, 1:100 dilution for IF; BD Biosciences), HA.11 clone 16B12 (mouse monoclonal,

1:200 dilution for IF; Covance), SHARPIN (rabbit polyclonal, 1:500 dilution for WB; Santa Cruz Biotechnology, Inc.), Kindlin-2 (rabbit polyclonal, 1:1000 dilution for WB, Cell Signaling), Rhodamine-phalloidin (1:200 dilution, Molecular probes). All secondary antibodies for immunofluorescence were from Jackson ImmunoResearch (West Grove, PA) and used at 1:200 dilution.

Epifluorescence and TIRF microscopy

Immunofluorescent stained preparations were observed with a Nikon Optiphot microscope using a 60X plan apo objective and filter cubes optimized for coumarin, fluorescein/GFP, rhodamine, and Cy5 fluorescence (Nikon). Images were captured with a MicroMax cooled CCD (Kodak KAF 1400 chip; Princeton Instruments, Trenton, NJ) using Metamorph software (Universal Imaging Corp., West Chester, PA). For TIRF microscopy, preparations were observed using a 60X apo objective (NA=1.45) on a Nikon TE2000-U microscope equipped with a TIRF illuminator and fiber optic coupled laser illumination. Illumination was with three separate laser lines (Ar ion (488 nm); HeNe (543 nm and 633 nm)) and filter cubes optimized for flourescein/GFP, Cy3/Alexa 546 and Cy5 fluorescence (Chroma Technology, Rockingham, VT). Images were captured with a back-illuminated cooled CCD (1000X800 pixels; Princeton Instruments, Trenton, NJ) using Metamorph software (Universal Imaging Corp., West Chester, PA).

Preparation of cells for detection of phosphoinositides

Lipid Extraction

NIH 3T3 cells were grown to confluence in 10-cm dishes, and phospholipids were extracted as described by others (Nasuhoglu et al., 2002; Serunian et al., 1991). Solution was aspirated from culture dishes, 0.75 ml ice-cold MeOH:1 M HCl (1:1) was added, and the cells were scraped quickly from the dish. This suspension was transferred to a 2-ml microfuge tube

and vortexed vigorously. After addition of 0.38 ml chloroform, samples were agitated for 15 min and centrifuged at 1000g for 10 min. The lower phase was removed and washed with 1 ml of cold MeOH containing 2 mM oxalic acid. Finally, the chloroform phase was transferred to a new tube and dried with a stream of nitrogen.

Phospholipid deacylation and head group recovery

Phospholipids were deacylated with monomethylamine essentially as described by others (Bocckino et al., 1989). The reaction was carried out at 53°C for 50 min with 1 ml of reagent (42.8% of a 25% methylamine solution in water, 45.7% methanol, and 11.4% n-butanol). After centrifuging for 1 min at 1000g, the samples were dried in a Speed-Vac. The products were then resuspended in 0.5 ml water and extracted twice with an equal volume of n-butanol:petroleum ether:ethyl formate (20:4:1) to remove fatty acids. The aqueous phase was then dried in a Speed-Vac and resuspended in 33 ml of water. After centrifuging at 1000g to remove particulate matter, 30 ml of sample was used for analysis. When small amounts of pure phospholipids (<1 nmol) were deacylated, inclusion of 50 mM sodium dodecyl sulfate (SDS) with the phospholipid was found to increase recovery substantially.

Statistical analysis

A two-tailed unpaired Student's *t* test was used to evaluate two groups. Significance between multiple groups was determined by one-way analysis of variance (ANOVA) followed by Tukey's multiple comparison test.

Chapter 4: Kif4 Interacts with EB1 and Stabilizes Microtubules Downstream of Rho-mDia in Migrating Fibroblasts

Note: I am a co-first author of this work which was published in PLoSOne (2014) in collaboration with Edward Morris, Francesca Bartolini, Nagendran Ramalingam and Gregg Gundersen. My specific contribution to the results is indicated in each figure legend.

ABSTRACT

Selectively stabilized MTs form in the lamella of fibroblasts and contribute to cell migration. A Rho-mDia-EB1 pathway regulates the formation of stable MTs, yet how selective stabilization of MTs is achieved is unknown. Kinesin activity has been implicated in selective MT stabilization and a number of kinesins regulate MT dynamics both in vitro and in cells. Here, we show that the mammalian homolog of *Xenopus* XKLP1, Kif4, is both necessary and sufficient for the induction of selective MT stabilization in fibroblasts. Kif4 localized to the ends of stable MTs and participated in the Rho-mDia-EB1 MT stabilization pathway since Kif4 depletion blocked mDia- and EB1-induced selective MT stabilization and EB1 was necessary for Kif4 induction of stable MTs. Kif4 and EB1 interacted in cell extracts and binding studies revealed that the tail domain of Kif4 interacted directly with the N-terminal domain of EB1. Consistent with its role in regulating formation of stable MTs in interphase cells, Kif4 knockdown inhibited migration of cells into wounded monolayers. These data identify Kif4 as a novel factor in the Rho-mDia-EB1 MT stabilization pathway and cell migration.

INTRODUCTION

Rearrangements of MTs play a central role in the establishment of cell polarity in many systems (Li and Gundersen, 2008). In migrating cells, MTs contribute to the front-back polarity that is essential for directional migration of cells in a variety of environments. MTs are thought to provide the tracks for directional delivery of membrane precursors and actin regulators necessary for protrusion of the leading edge (Miller et al., 2009; Prigozhina and Waterman-Storer, 2004; Schmoranzer et al., 2003). MTs also regulate the turnover of FAs by stimulating the disassembly of FAs through endocytic processes (Chao and Kunz, 2009; Ezratty et al., 2009; Ezratty et al., 2005; Kaverina et al., 1999). In addition, MTs regulate myosin contraction in the cell rear in certain migrating cells such as neutrophils and T cells (Takesono et al., 2010; Xu et al., 2005).

To contribute to front-back polarity in migrating cells, the MT array itself becomes polarized. Several sources of MT polarization in migrating cells have been identified. Radial MT arrays are biased toward the front of many migrating cells by the specific orientation of the centrosome toward the leading edge (Luxton and Gundersen, 2011). The oriented centrosome positions the associated Golgi and endocytic recycling compartment to direct vesicular traffic toward the leading edge. The reorientation of the Golgi may also reinforce MT asymmetry toward the leading edge as the Golgi itself can nucleate MTs in certain cell types (Miller et al., 2009). Factors that interfere with centrosome orientation usually reduce the rate of cell migration (Gomes et al., 2005; Luxton et al., 2010; Schmoranzer et al., 2009), although direct laser ablation of the centrosome has modest-to-strong effects on cell migration depending on the cell type (Koonce et al., 1984; Wakida et al., 2010).

A second source of MT polarization is the selective stabilization of a subset of MTs oriented toward the cell's leading edge (Gundersen and Bulinski, 1988; Li and Gundersen, 2008). Because of their longevity, these selectively stabilized MTs become post-translationally modified by detyrosination and/or acetylation of tubulin. Even in situations where the centrosome does not orient toward the leading edge, for example, in a subset of fibroblasts migrating in 2D or in fibroblasts migrating on fibrillar 1D matrices, MT stabilization remains highly biased toward the front of the cell (Doyle et al., 2009; Gundersen and Bulinski, 1988; Palazzo et al., 2001b; Palazzo and N.D., 2001). Post-translationally modified MTs are longer-lived than their dynamic counterparts (Gundersen et al., 1987; Webster et al., 1987) and serve as preferred tracks for certain kinesin motors (Dunn et al., 2008; Konishi and Setou, 2009; Kreitzer et al., 1999; Liao and Gundersen, 1998; Lin et al., 2002; Reed et al., 2006). Thus, the generation of selectively stabilized MTs biases vesicle trafficking toward the leading edge in migrating cells.

Posttranslational modification of MTs may contribute to their stability (Peris et al., 2009), yet studies have shown that this is not likely responsible for the initial generation of stability of the long-lived MTs. Posttranslational modification of tubulin within MTs is relatively slow compared to dynamic turnover of MTs and in starved NIH3T3 fibroblasts stimulated with the serum factor lysophosphatidic acid (LPA), MTs are stabilized within minutes, long before the accumulation of posttranslational detyrosination (Cook et al., 1998). In addition, treatments that enhance the levels of detyrosinated or acetylated tubulin do not directly lead to stabilized MTs (Khawaja et al., 1988; Palazzo et al., 2003; Webster et al., 1990).

Factors have been identified that contribute to the selective stabilization of MTs in cells. Rho GTPase and its downstream effector the formin mDia are key factors in a MT stabilization

pathway that mediates the selective stabilization of MTs in migrating fibroblasts (Goulimari et al., 2005; Palazzo et al., 2003; Palazzo et al., 2001a) and other cell types (Andres-Delgado et al., 2012; Arakawa et al., 2003; Butler and Cooper, 2009; Kodama et al., 2003). Rho only stimulates mDia in the presence of integrin and FAK signaling, which may restrict the formation of stable MTs to the leading edge (Palazzo et al., 2004). mDia interacts with three MT +TIP proteins, EB1, APC and CLIP170 and the interactions with EB1 and APC have been implicated in MT stability (Butler and Cooper, 2009; Lewkowicz et al., 2008; Wen et al., 2004). In vitro, mDia2 binds directly to MTs and can stabilize them against cold-induced depolymerization, although it does not generate nondynamic MT ends typical of selectively stabilized MTs in vivo (see below) (Bartolini et al., 2008). mDia and other formins have recently emerged as MT regulators in addition to their role in regulating actin nucleation and elongation (Bartolini and Gundersen, 2009; Thurston et al., 2012). Other factors, including two other +TIPs CLASP and ACF7/MACF (Kodama et al., 2003; Lansbergen et al., 2006), actin capping protein (Bartolini et al., 2012), and the negative regulator moesin (Naghavi et al., 2007) and are also involved in the generation of selectively stabilized MTs. In addition to the Rho-mDia-EB1 MT stabilization pathway, other MT stabilization pathways have been described (Gundersen et al., 2004; Lansbergen and Akhmanova, 2006).

An unusual property of selectively stabilized MTs that may explain their longevity is the inability of their plus ends to add or lose tubulin subunits (Infante et al., 2000; Palazzo et al., 2001a; Palazzo et al., 2004; Webster et al., 1987). Indeed, these MTs behave as if their ends are capped, a property that may also explain their resistance to MT antagonists and to dilution after detergent permeabilization of cells (Infante et al., 2000; Khawaja et al., 1988). The nature of this putative cap is unknown. Some of the factors functioning in the MT stabilization pathway have

been localized to the ends of stable detyrosinated MTs (Wen et al., 2004), yet none of these factors have been shown to directly cap MTs to convert them to nondynamic MTs. A study with permeabilized cell models showed that the putative capping activity of stabilized MTs has characteristics of kinesin motor proteins, including inhibition by the non-hydrolyzable ATP analog AMP-PNP (Infante et al., 2000). Here we tested the possibility that kinesin motor proteins may be involved in the generation of selective MT stability in cells. Among a group of kinesins implicated in MT stability, we identify Kif4 as a novel factor in the selective stabilization of MTs in migrating cells and provide evidence that this protein functions downstream of other proteins in the Rho-mDia MT stabilization pathway and contributes to cell migration.

RESULTS

Kif4 motor domain induces stable MT formation in vivo

We first tested whether kinesins can induce the formation of selectively stabilized MTs by expressing motor domains of kinesins in serum-starved NIH3T3 fibroblasts that have low levels of stable MTs as judged by the lack of detyrosinated and NZ resistant MTs (Cook et al., 1998; Gundersen et al., 1994; Palazzo et al., 2001a; Wen et al., 2004). Throughout this paper we refer to stable MTs with high levels of detyrosinated tubulin as Glu MTs (reflecting the newly exposed glutamate residue formed by removal of tyrosine from the C-terminus of α-tubulin) and their dynamic counterparts as Tyr MTs. We tested kinesins that have been implicated in MT stability based upon: 1) their interaction with known MT stabilizing factors (Kif3, a kinesin 2 which binds APC) (Jimbo et al., 2002), 2) their ability to stabilize MTs in epithelial cells (Kif17, another kinesin 2) (Jaulin and Kreitzer, 2010); or 3) their ability to render MTs nondynamic in vitro (Kif4, a kinesin 4 and ortholog of Xenopus XKLP1) (Bieling et al., 2010; Bringmann et al., 2004) and in spindle midzone MTs (Hu et al., 2011). We were particularly interested in testing Kif4, because the motor domain of XKLP1 prevents tubulin subunit addition to or lose from MTs in biochemical studies (Bringmann et al., 2004). We chose not to explore a possible role for kinesin-8 motors (such as Kif18A), which also regulate MT dynamics, as they seem to primarily affect spindle MTs and do not appear to stabilize MTs against antagonists (Du et al., 2010; Stumpff et al., 2011; Weaver et al., 2011).

Green fluorescent protein (GFP)-tagged constructs encoding the motor domain of these kinesins were microinjected into nuclei of starved NIH3T3 fibroblasts bordering an in vitro wound and after 2 hr of expression, levels of Glu MTs were assessed in fixed cells by immunofluorescence. The motor domain of Kif4 induced Glu MTs in serum-starved NIH3T3 fibroblasts compared to uninjected neighboring cells (Figure 40A, B). The Kif4 motor domain

induced only a subset of the MTs to become Glu MTs and did not detectably alter the distribution of Tyr MTs, consistent with it selectively, rather than globally stabilizing MTs. Glu MTs in the Kif4 expressing cells were preferentially oriented toward the leading edge (as in Figure 40A) in 70 +/- 7% (N=3) of the cells, similar to the response of starved NIH3T3 fibroblasts to serum, LPA or active Rho (Cook et al., 1998; Gundersen et al., 1994). Kif3 or Kif17 motor domains did not induced the formation of Glu MTs above background levels when expressed in starved cells under identical conditions, even though the proteins were expressed at comparable levels to Kif4 as judged by GFP fluorescence (Figure 40A, B).

Glu MT staining is widely used as a marker for MT stability, but it was formally possible that Kif4 altered the enzymatic removal of tyrosine from α-tubulin instead of directly stabilizing MTs. To test this possibility and as an independent test of MT stabilization, cells expressing GFP-Kif4 motor domain were treated with NZ to depolymerize dynamic MTs and then stained for Glu tubulin. Starved NIH3T3 fibroblasts expressing GFP-Kif4 motor domain had numerous NZ-resistant Glu MTs whereas uninjected cells had only one or two short NZ-resistant MTs (Figure 40C, D). We conclude that the motor domain of Kif4, but not that of several other kinesins, is sufficient to induce the formation of stabilized and posttranslationally modified MTs in starved NIH3T3 fibroblasts.

Kif4 is required for LPA-induced formation of Glu MTs

To test whether Kif4 was necessary for formation of Glu MTs, we depleted Kif4 with small interfering RNAs (siRNAs) and then induced Glu MTs in serum-starved NIH3T3 fibroblasts by treating with the serum factor LPA. As controls, we depleted either glyceraldehyde 3-phosphate dehydrogenase (GAPDH) or Kif3A (we note that we were unable to test the role of Kif17, as it is not expressed in NIH3T3 fibroblasts-Figure 41). Kif4 depletion inhibited LPA-induced Glu MT formation while control siRNAs had no effect (Fig. 42A-C). Kif4 depletion had

no noticeable effects on Tyr MTs (Figure 42A), suggesting that it did not affect dynamic MTs. Knockdown of kinesins was verified by western blot, which showed that Kif4 and Kif3A were knocked down approximately 70% compared to GAPDH (control) siRNA-treated cells (Figure 42D, E). A second siRNA sequence to Kif4 also blocked Glu MT formation limiting the possibility that the effects of the Kif4 siRNAs were due to off-target effects (Figure 42C and Figure 43). While Kif4 depletion inhibited Glu MT formation, it did not affect LPA-induced actin stress fiber formation (Figure 44). These results show that Kif4 is necessary for LPA-induced formation of Glu MTs and suggest that it specifically regulates MTs rather than actin filaments downstream of LPA stimulation.

Endogenous Kif4 localizes to the ends of Glu MTs

We localized endogenous Kif4 to determine if it associated with Glu MTs. Kif4 has been described as a chromokinesin and much of Kif4 is localized in the nucleus before mitosis (Kurasawa et al., 2004; Mazumdar et al., 2004). Because of this, we first checked if Kif4 was present in the cytoplasm of serum-stimulated starved NIH3T3 fibroblast and whether its nuclear localization was regulated during the cell cycle. In starved cells or at early times after serum stimulation, there was little detectable Kif4 in the nucleus and diffuse staining of Kif4 in the cytoplasm; at 12-24 hours of serum stimulation, corresponding to late G1/S and G2 phases, Kif4 appeared in both the cytoplasm and the nucleus suggesting that Kif4's nuclear localization is cell cycle regulated (Figure 45A). The cytoplasmic staining of Kif4 in unstimulated cells, which mostly appeared punctate, was dramatically reduced by siRNA–mediated depletion of Kif4 (Figure 46), indicating that the signal detected with the Kif4 antibody was specific. In LPA-treated cells, Kif4 cytoplasmic staining appeared to increase coincident with the formation of Glu MTs and in some cells appeared as linear accumulations that paralleled MTs (Figure 45B).

To address Kif4's localization further and in particular to probe whether Kif4 might be associated with Glu MTs, we used total internal reflection fluorescence (TIRF) microscopy. Most of the Kif4 puncta observed by TIRF microscopy were associated with MTs with linear accumulations detected on both Glu and Tyr MTs (Figure 45C). We were particularly interested in the ends of Glu MTs, because localization at this site is readily quantifiable and because other factors in the Rho-mDia pathway are localized on the ends of Glu (Butler and Cooper, 2009; Wen et al., 2004). In serum-stimulated NIH3T3 fibroblasts, Kif4 puncta were detected on a number of Glu MT ends and also along their length (Figure 45D, E). In contrast, fewer Kif4 puncta were localized on Tyr MT ends (Figure 45E). To account for random localization, we determined the number of Kif4 puncta on Glu and Tyr MTs ends before and after shifting the Kif4 image relative to the MT images: for both types of MTs, shifting the images eliminated the colocalization with the ends, indicating that the Kif4 localization on MT ends was not due to random overlap of Kif4 puncta with MT ends. A similar analysis of Kif4 localization in TC-7 cells, which have particularly distinct Glu MTs, also revealed specific localization of Kif4 on Glu MT ends (Figure 47). These results show that endogenous Kif4 specifically accumulates on some Glu MTs ends, consistent with a direct involvement of Kif4 in MT stabilization.

Kif4 is required for induction of Glu MTs by factors in the Rho-mDia-EB1 MT stabilization pathway

To test the relationship between Kif4 and the Rho-mDia-EB1 MT stabilization pathway, we asked if Kif4 was necessary for the induction of Glu MTs stimulated by known intracellular activators of the pathway. The formation of Glu MTs in serum starved NIH3T3 fibroblasts can be stimulated by expressing the Dia autoregulatory domain (DAD) of mDia, which relieves the autoinhibition of the formin and activates it toward both actin and MTs (Palazzo et al., 2001a; Palazzo et al., 2004). Microinjection of GST-DAD into serum-starved NIH3T3 fibroblasts

depleted of Kif4 did not induce Glu MT formation, whereas it did when introduced into control (GAPDH) depleted cells (Figure 48A, B). While GST-DAD failed to induce Glu MTs in Kif4 depleted cells, it still stimulated actin cable formation showing that Kif4 depletion did not prevent DAD from activating mDia (Figure 48C).

To test further whether Kif4 functioned downstream of mDia in the formation of Glu MTs, we tested whether Kif4 was necessary for the induction of Glu MTs in serum starved NIH3T3 fibroblasts treated with LiCl, an inhibitor of GSK-3β. Activation of mDia by Rho leads to the inhibition of GSK-3β and this is necessary for the formation of Glu MTs in NIH3T3 fibroblasts (Eng et al., 2006). LiCl treatment of NIH3T3 fibroblasts depleted of Kif4 failed to induce the formation of Glu MTs, whereas similar treatment of control (GAPDH) depleted cells did (Figure 48D, E). Combined, these results suggest that Kif4 functions downstream of mDia in Glu MT formation and that Kif4 is not involved in mDia's stimulatory effect on actin filaments. Consistent with this interpretation, we did not detect a significant alteration in the distribution of mDia1 or EB1 in GFP-Kif4 motor expressing cells (Figure 49).

Kif4 and EB1 require each other to generate stable MTs

EB1 functions downstream of mDia in the MT stabilization pathway and overexpression of EB1 induces the formation of stable MTs in serum-starved NIH3T3 fibroblasts (Wen et al., 2004). We tested if the induction of Glu MTs by Kif4 and/or EB1 expression in starved NIH3T3 fibroblasts depended on each other. Kif4 or control (GAPDH) depleted serum-starved NIH3T3 fibroblasts were microinjected with GST-EB1 and the formation of Glu MTs was assessed. GST-EB1 induced Glu MTs in control cells, but not in Kif4 depleted cells (Figure 50A, B). Similarly, expression of either GFP-tagged Kif4 motor domain or Kif4 full length in starved cells knocked down for EB1 (Figure 51), which inhibits Glu MTs induced by LPA (Wen et al., 2004), did not

induce Glu MTs (Figure 50C, D). These results suggest that Kif4 and EB1 are mutually dependent for inducing stable MTs.

Kif4 interacts directly with EB1

Given the mutual dependence of Kif4 and EB1 in inducing Glu MTs, we tested whether the proteins might interact. Immunoprecipitation of endogenous EB1 revealed that endogenous Kif4 associated with EB1 in NIH3T3 fibroblast lysates (Figure 52A). Kif4 has predicted N-terminal motor, central stalk with coiled coils domains and C-terminal tail domains (Figure 52B) (Sekine et al., 1994). Using purified recombinant proteins, we found that EB1 interacted directly with the tail of Kif4, but not the motor domain; there was also a weak interaction of EB1 with the stalk domain of Kif4 (Figure 52C). Using fragments of EB1, we found that Kif4 tail bound to the N-terminal domain of EB1, but not the C-terminal domain (Figure 52C). These results show that Kif4 associates directly with one of the previously established factors in the pathway for selective stabilization of MTs.

Kif4 is necessary for efficient migration of cells

Selectively stabilized MTs have been implicated in cell migration (Akhmanova et al., 2001; Gundersen and Bulinski, 1988; Wen et al., 2004). To test whether Kif4 contributed to cell migration, we knocked it down and measured rates of migration of NIH3T3 fibroblasts into in vitro wounds. Cells depleted of Kif4 still formed a normal confluent monolayer, but migration into the wound was reduced about 40% (Figure 53A, B). Analysis of the cell aspect ratio, a measure of overall cell polarization, revealed that Kif4 depleted cells had a significantly reduced aspect ratio compared to controls (Figure 53C). These results are consistent with earlier studies suggesting that stable MTs in the lamella contribute to cell migration by enhancing cell polarization and strengthen the notion that Kif4 has non-mitotic functions.

DISCUSSION

Previous studies revealed that long-lived Glu MTs in TC-7 cells and NIH3T3 fibroblasts exhibit the unusual property of not growing or shrinking for long intervals (Infante et al., 2000; Palazzo et al., 2001a; Webster et al., 1990; Wen et al., 2004). This nondynamic behavior of Glu MTs contrasts with the bulk of the MTs, which undergo dynamic instability and exhibit much more rapid turnover. Glu MTs in detergent extracted TC-7 cell models behave as if they are capped at their plus ends by an ATP-sensitive activity that has characteristics of kinesin motors (Infante et al., 2000). In this study, we identified Kif4 as a kinesin that is necessary and sufficient for the induction of Glu MTs and NZ resistant MTs in NIH3T3 fibroblasts. Our results indicate that Kif4 functions in the Rho-mDia-EB1 MT stabilization pathway because Kif4 depletion prevented the formation of Glu MTs in response to extracellular (LPA) and intracellular factors (DAD, LiCl and EB1) that activate this pathway, overexpression of Kif4 motor domain was sufficient to induce Glu MTs and Kif4 interacted with EB1, a previously identified factor in the pathway. Kif4 also localized to Glu MT ends where other factors in this pathway have been localized (Wen et al., 2004). Our data suggest a model in which Kif4 contributes to the nondynamic behavior and stability of Glu MTs potentially by accumulating on Glu MT ends. Because only a subset of Glu MT ends had detectable Kif4 localization, we cannot rule out a model in which Kif4 may act more transiently, perhaps by transporting another factor in the pathway.

How does Kif4 stabilize MTs? Studies have identified two activities for Kif4. A motor function for Kif4 in the delivery of L1 cell adhesion molecule was described in studies of rat neurons (Bisbal et al., 2009; Peretti et al., 2000). Kif4 also appears to be required for transporting Gag protein from murine leukemia virus and HIV (Kim et al., 1998; Martinez et al., 2008), the

ribosomal protein P0 (Bisbal et al., 2009), and the mitotic protein PRC1 (Zhu and Jiang, 2005). A MT stabilizing activity of the *Xenopus* Kif4, XKLP1 was identified in in vitro studies (Bringmann et al., 2004). In this study, the motor domain of XKLP1 alone was shown to prevent the assembly and disassembly of dynamic MTs in vitro. Three pieces of data from our study are consistent with Kif4 generating nondynamic stabilized MTs through its predicted stabilizing activity: 1) induction of stabilized MTs by Kif4 motor domain, 2) localization of Kif4 on Glu MT ends, and 3) the ability of Kif4 to function downstream of other factors in the Rho-mDia MT stabilization pathway. Such a role would also be consistent with Kif4's reported role in cytokinesis where it contributes to the stability and nondynamic nature of midzone MTs (Hu et al., 2011; Kurasawa et al., 2004; Zhu and Jiang, 2005). Additional studies will be needed to test whether mammalian Kif4 exhibits the direct MT stabilization activity of XKLP1 and/or whether Kif4 transport activity is necessary for MT stabilization.

Given the potent stabilizing activity of the Kif4 motor domain shown in the study of XKLP1, an interesting question arises in the context of selective stabilization of interphase MTs: how is the stabilizing activity of the motor regulated so that it selectively stabilizes only a subset of MTs in vivo? One possibility is that other factors in the Rho-mDia-EB1 pathway restrict its activity to specific locations. Rho is activated near the leading edge of migrating fibroblasts (Pertz et al., 2006), but as yet there is no evidence that Rho or mDia interact with Kif4. Another possibility is that EB1 interaction with Kif4 may regulate its stabilizing activity. The yeast EB1, Mal3, interacts with the kinesin Tea2, and this interaction activates its motor activity (Browning and Hackney, 2005). The mammalian kinesin-2, Kif17, stabilizes MTs in epithelial cells in part by binding to EB1(Jaulin and Kreitzer, 2010). A number of destabilizing kinesin-13s also interact with EBs and this interaction targets their activity to the MT plus end (Su et al., 2012).

Perhaps, the stabilizing activity of Kif4 needs to be targeted to or retained on MT plus ends and this is accomplished by EB1. We note that in addition to this possible role for EB1, it is likely that EB1 plays a Kif4-independent role in MT stabilization, since EB1 interacts with a number of other components implicated in MT stabilization including mDia (Wen et al., 2004) and CLASPs (Mimori-Kiyosue et al., 2005).

Kif4 may also be regulated by phosphorylation, as has been shown for other kinesins (Hirokawa et al., 2009). PKCε is activated and GSK3β is inactivated downstream of mDia activation in fibroblasts and both contribute to formation of stabilized Glu MTs (Eng et al., 2006). The downstream substrates of these kinases in the Rho-mDia stabilization pathway have not been identified. Kif4 has 12 known phosphorylation sites as shown by mass spectroscopy and two of these are predicted to be sites for GSK3β (S1017 and S1186; http://scansite.mit.edu/) (Nousiainen et al., 2006). Kif4 was recently shown to be activated by Aurora B phosphorylation in mitotic cells (Nunes Bastos et al., 2013). It would be interesting to test whether it is phosphorylated by one of these kinases during generation of stable MTs in LPA stimulated cells.

Kif4 has a well characterized role in cell division but there is growing evidence that Kif4 has roles in non-dividing cells (see references above). Our results show that even in serum-starved cells in G_0 there is a small pool of cytoplasmic Kif4 and that cytoplasmic Kif4 increases with either LPA or serum stimulation. Consistent with a role in regulating interphase MT stability, we find that the axial polarization and migration of serum-stimulated cells was inhibited by Kif4 knockdown. Kif4 has a predicted nuclear localization sequence, yet we observed that nuclear accumulation of Kif4 was delayed for 12-24 h after serum-stimulation, suggesting that its nuclear localization is regulated in a cell cycle dependent fashion.

Members of the kinesin superfamily have been recognized for some time to participate in the regulation of MT dynamics in addition to their well-established role in acting as molecular transporters. Indeed, a subset of the kinesins, those in the kinesin-13 subfamily of which MCAK/Kif2 has been most intensively studied, are well-established MT depolymerases that recognize and promote the curved protofilament structure of depolymerizing MTs (Ems-McClung and Walczak, 2010; Wordeman, 2005). The kinesin-8 family has also been implicated in regulating MT dynamics (Gardner et al., 2008). There are fewer kinesins that have been implicated in stabilizing MTs to generate long-lived and post-translationally modified MTs. Indeed, other than Kif4/XKLP1 the only other kinesin that has been reported to enhance MT longevity is Kif-17(Jaulin and Kreitzer, 2010). In our study, we found that Kif17 was not expressed in NIH3T3 fibroblasts and expression of its motor domain did not induce MT stability in starved fibroblasts. Since the same construct induced MT stability in epithelial cells (Jaulin and Kreitzer, 2010), these results suggest that different kinesins may be used to regulate MT stability in different cell types. It will be interesting to explore other kinesin subfamilies to determine whether there are other kinesins with the ability to generate long-lived, stable MTs.

FIGURES

Figure 40. Kif4 motor domain induces the formation of stable Glu MTs in starved NIH3T3 fibroblasts.

(A) Immunofluorescence of Glu MTs and Tyr MTs in starved NIH3T3 fibroblasts expressing the indicated GFP-tagged kinesin motor constructs. Arrows indicate expressing cells. (B) Quantification of Glu MT formation in starved NIH3T3 fibroblasts expressing the indicated kinesin motors. n>70 cells; error bars, SEM from at least 6 experiments. (C)* Immunofluorescence staining of Glu MTs in GFP-Kif4 motor expressing NIH3T3 fibroblasts treated with 10 μM NZ for 1 hr. The expressing cell (arrow) has NZ-resistant Glu MTs. (D)* Quantification of cells with NZ resistant Glu MTs. Error bars, SEM from 3 experiments. Scale bars, 10 μm.

*My contribution

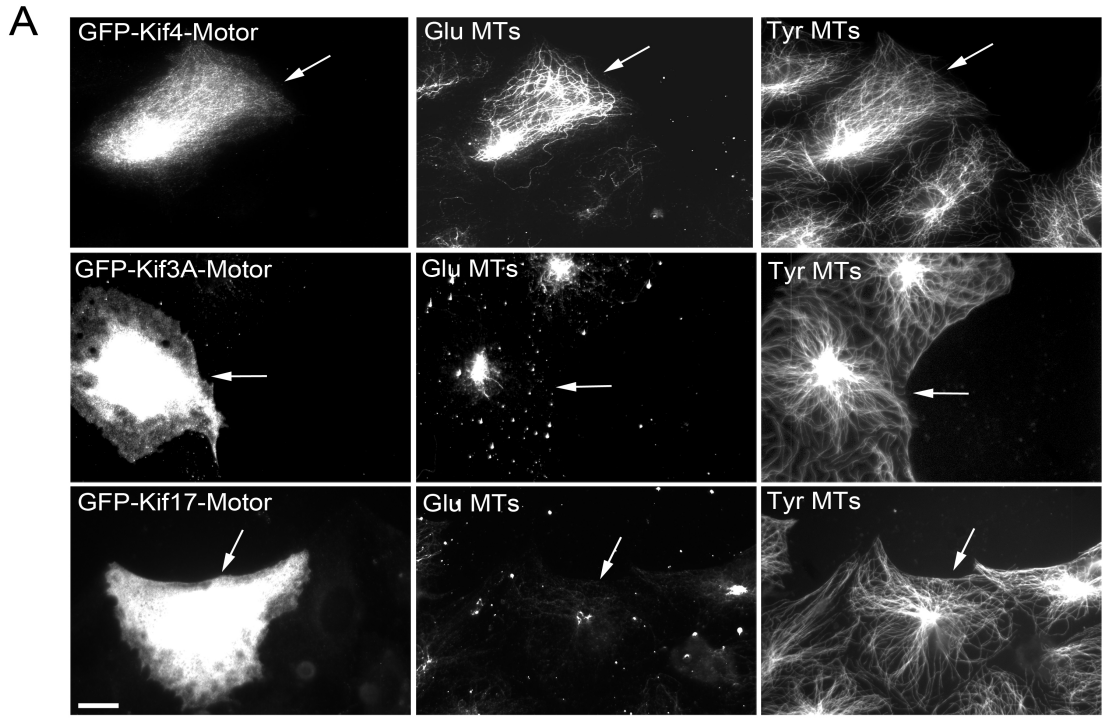
A
GFP-Kif4-Motor
Glu MTs
Tyr MTs
GFP-Kif3A-Motor
Glu MTs
Tyr MTs
GFP-Kif17-Motor
Glu MTs
Tyr MTs

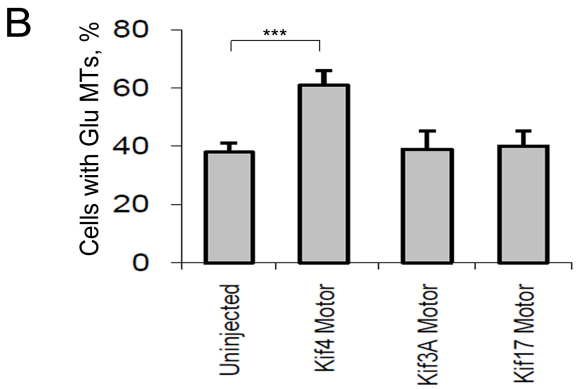
B
Cells with Glu MTs, %
80
60
40
20
0
***
Uninjected
Kif4 Motor
Kif3A Motor
Kif17 Motor

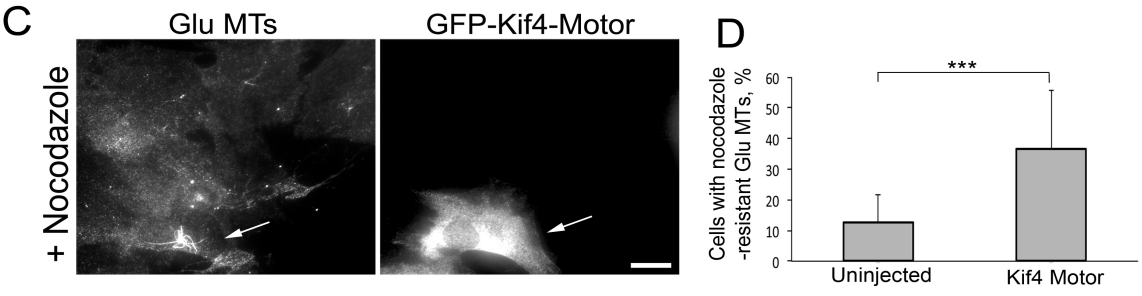
C
Glu MTs
GFP-Kif4-Motor
+ Nocodazole
D
Cells with nocodazole -resistant Glu MTs, %
60
50
40
30
20
10
0
***
Uninjected
Kif4 Motor

Figure 41. Analysis of Kif17 expression in NIH3T3 fibroblasts.

(A)* Western blot analysis of Kif17 in MDCK cell and NIH3T3 fibroblast lysates. Tubulin is shown as a loading control. **(B)** RT-PCR analysis of Kif17 expression in mouse brain and NIH3T3 fibroblasts. Kif16B is shown as a positive control.

*My contribution

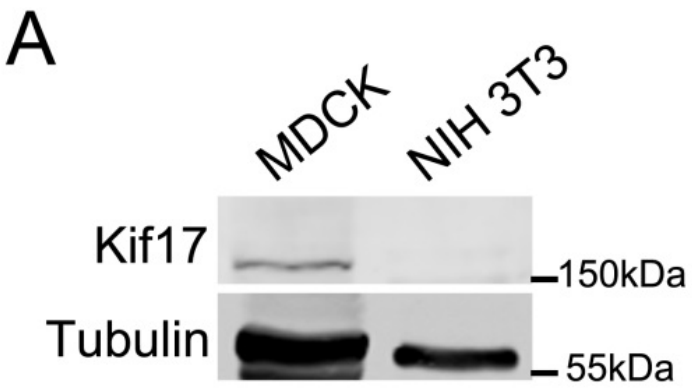
A
MDCK
NIH 3T3
Kif17
150kDa
Tubulin
55kDa

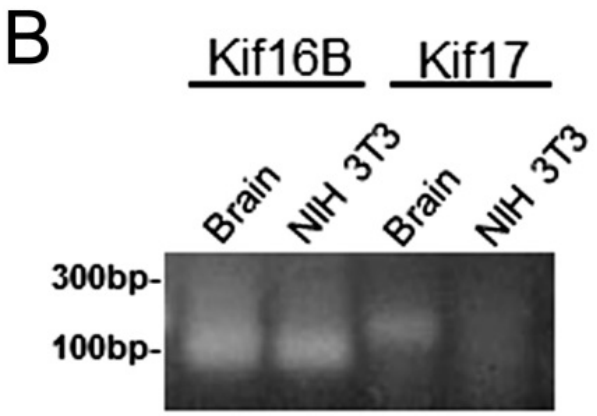
B
Kif16B
Kif17
Brain
NIH 3T3
Brain
NIH 3T3
300bp-
100bp-

Figure 42. Knockdown of Kif4 inhibits LPA-induced formation of Glu MTs in NIH3T3 fibroblasts. (A,B) Glu MT and Tyr MT staining of LPA-stimulated NIH3T3 fibroblasts transfected with the indicated siRNAs. (C) Quantification of the percent of siRNA-treated cells that scored positive for Glu MTs. Two different siRNAs targeting Kif4 (#1 and #2) gave similar results. n>100 cells; error bars, SEM from at least 5 experiments. (D, E) Western blots of NIH3T3 fibroblasts treated with indicated siRNAs and blotted for the indicated proteins. Quantification of the bands revealed over 70% knockdown of the indicated kinesins. Scale bars, 20 µm.

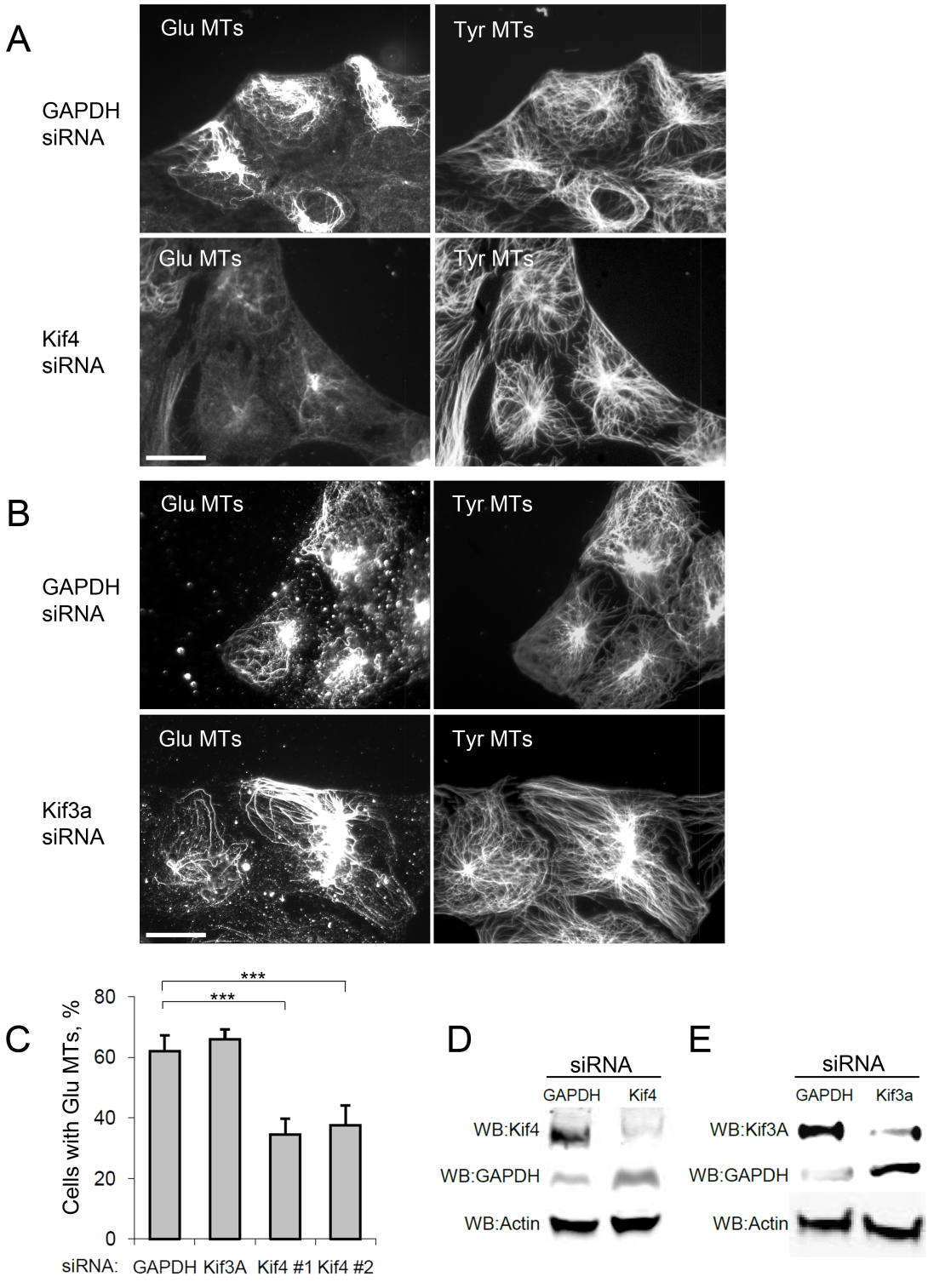
A
GAPDH siRNA
Glu MTs
Tyr MTs
Kif4 siRNA
Glu MTs
Tyr MTs
B
GAPDH siRNA
Glu MTs
Tyr MTs
Kif3a siRNA
Glu MTs
Tyr MTs
C
Cells with Glu MTs, %
80
60
40
20
0
***
***
siRNA: GAPDH Kif3A Kif4 #1 Kif4 #2
D
siRNA
GAPDH Kif4
WB:Kif4
WB:GAPDH
WB:Actin
E
siRNA
GAPDH Kif3a
WB:Kif3A
WB:GAPDH
WB:Actin

Figure 43. Western blot of Kif4 knockdown using a second siRNA.

NIH3T3 fibroblasts treated with noncoding GAPDH or Kif4 siRNA #2 were analyzed by western blot. Actin was used as a loading control.

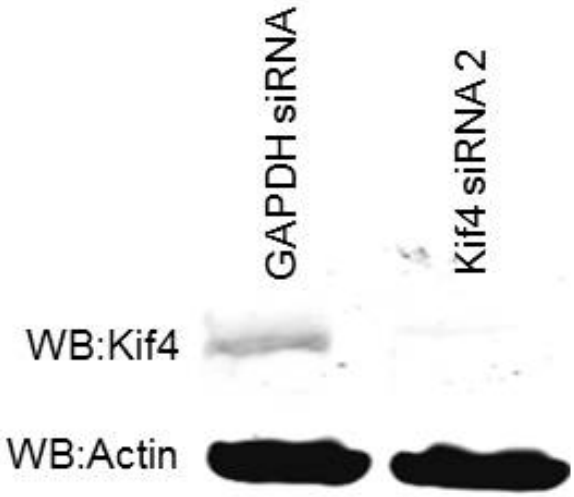
GAPDH siRNA
Kif4 siRNA 2
WB:Kif4
WB:Actin

Figure 44. LPA stimulates normal actin fiber formation in Kif4 siRNA-treated NIH3T3 fibroblasts. Fluorescence images of F-actin stained with rhodamine phalloidin in LPA stimulated NIH3T3 fibroblasts that had previously been treated with control (GAPDH) or Kif4 siRNAs. Scale bar, 10 μm.

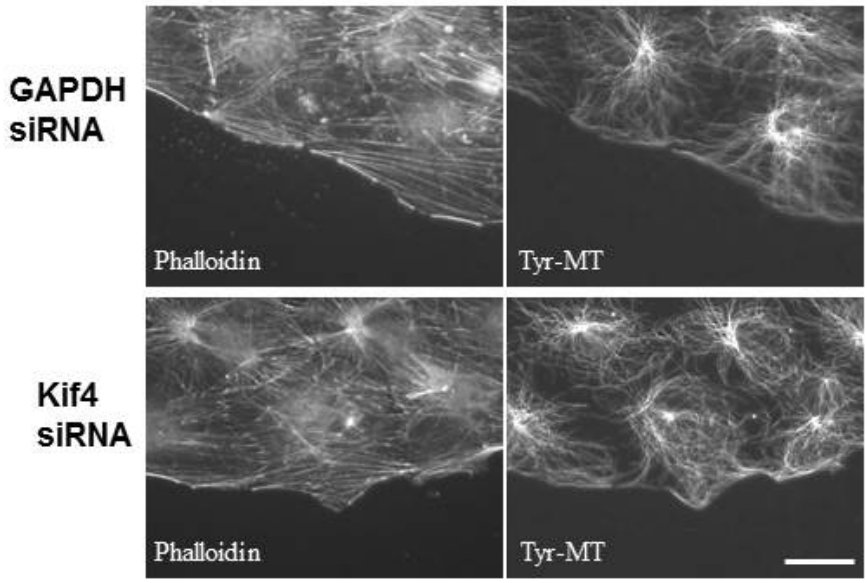
GAPDH
siRNA
Phalloidin
Tyr-MT
Kif4
siRNA
Phalloidin
Tyr-MT

Figure 45. Localization of endogenous Kif4 in interphase cells.

(A) Immunofluorescence images of Kif4, cyclin B and Tyr MTs in serum-starved NIH3T3 fibroblasts (0h) and in cells stimulated with serum for 12 and 24h. **(B)** Immunofluorescence images of Kif4, Glu and Tyr MTs in serum-starved NIH3T3 fibroblasts (0 min) and in cells stimulated with LPA for 30 and 60 min. Arrowheads indicate linear accumulations of Kif4 that coaligned with Glu and Tyr MTs. **(C)** TIRF immunofluorescence images of Kif4, Glu and Tyr MTs in serum-stimulated NIH3T3 fibroblasts. Linear accumulations of Kif4 on Glu MTs are indicted by arrowheads; on Tyr MTs by arrows. **(D)*** TIRF immunofluorescence images of Kif4 localization on Glu MT ends. The boxed region in the merged image is shown at higher magnification in the right panels. **(E)** Quantification of Kif4 on Glu and Tyr MT ends in serum-stimulated NIH3T3 fibroblasts. To account for random colocalization, overlaid Kif4 images were shifted relative to Glu MT images and then recounted. n>50 ends, error bars, SEM from three experiments. Scale bars, A, B, 20 µm; C, 5 µm. D, 10 µm; 5 µm (high mag).

*My contribution

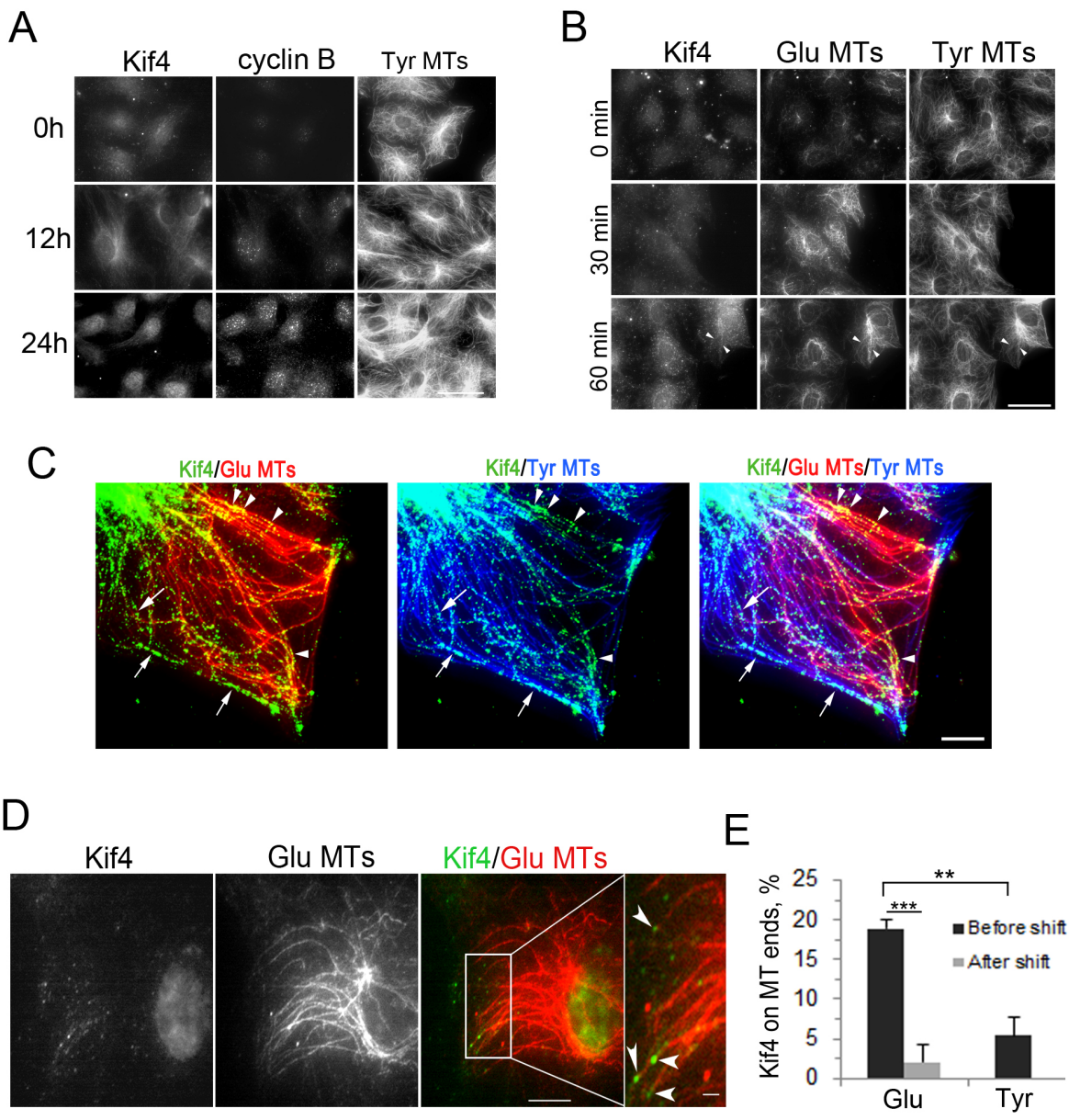
A
Kif4
cyclin B
Tyr MTs
0h
12h
24h
B
Kif4
Glu MTs
Tyr MTs
0 min
30 min
60 min
C
Kif4/Glu MTs
Kif4/Tyr MTs
Kif4/Glu MTs/Tyr MTs
D
Kif4
Glu MTs
Kif4/Glu MTs
E
Kif4 on MT ends, %
25
20
15
10
5
0
**
***
Before shift
After shift
Glu
Tyr

Figure 46*. Immunofluorescence images of Kif4 and Tyr MTs in noncoding (NC) and Kif4 siRNA-treated cells.

NIH3T3 fibroblasts were stimulated for 60 min with LPA. Note the reduction in cytoplasmic Kif4 immunostaining in cells treated with Kif4 siRNA. Scale bar, 20 µm.

*My contribution

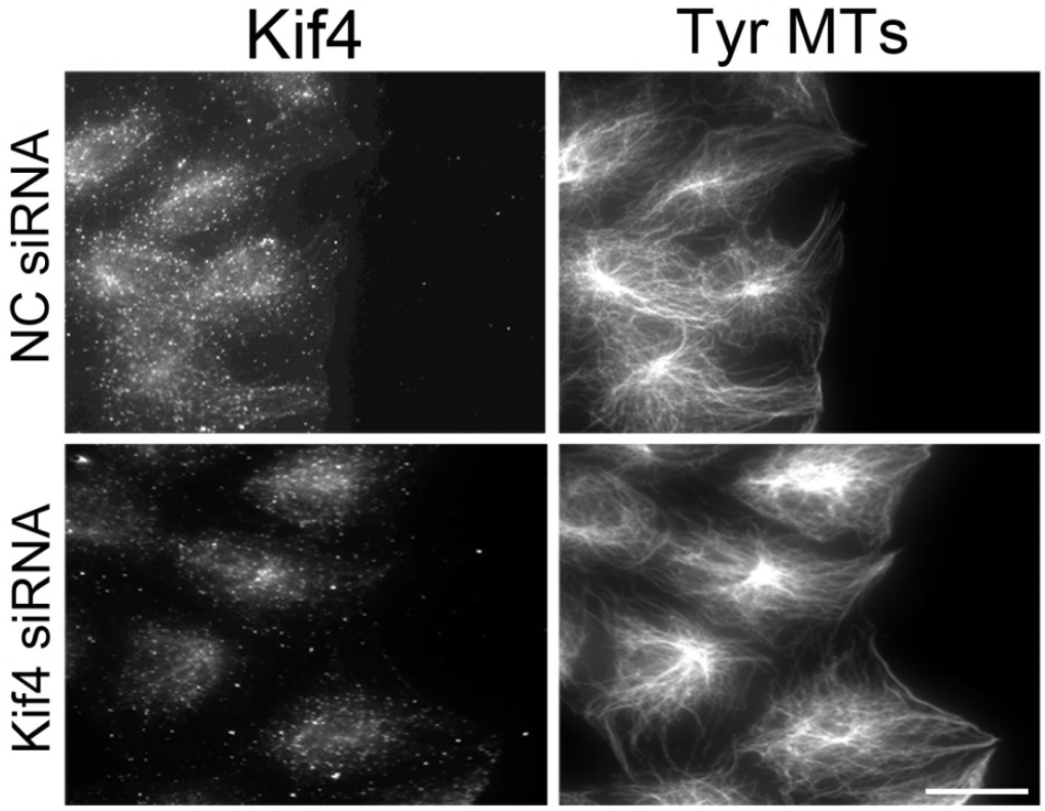
Kif4
Tyr MTs
NC siRNA
Kif4 siRNA

Figure 47. Kif4 localization on Glu MT ends in TC-7 cells.

(A) Immunofluorescence images of Kif4 and Glu MTs in TC-7 cells showing typical examples of localization of Kif4 on the ends of Glu MTs (arrows). **(B)** Quantification of the percentage of Glu MTs ends that exhibit Kif4 puncta before and after shifting the Glu MT and Kif4 images relative to each other. n>20 ends, error bars are SEM from at least 3 experiments. Scale bar, 0.5 µm.

A

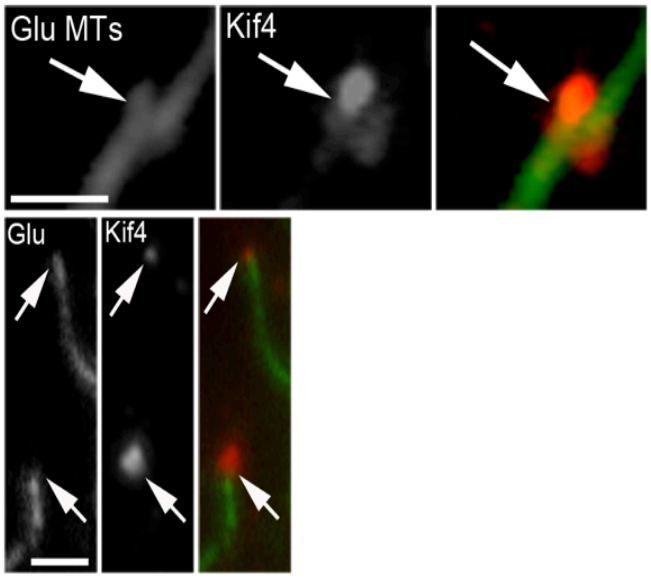
Glu MTs
Kif4
Glu
Kif4

B

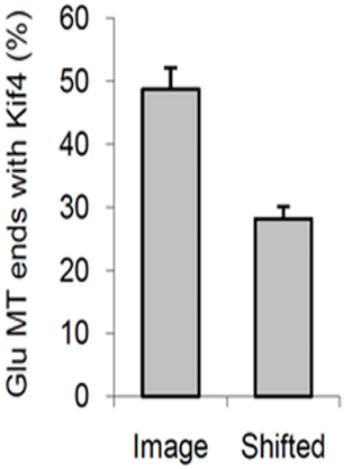
Glu MT ends with Kif4 (%)
60
50
40
30
20
10
0
Image
Shifted

Figure 48. Kif4 functions downstream of mDia in the Rho-mDia-EB1 MT stabilization pathway.

(A) Immunofluorescence staining of Tyr MTs and Glu MTs in NIH3T3 fibroblasts treated with GAPDH (control) siRNA or Kif4 siRNA and microinjected with GST-DAD. Arrows indicate injected cells. **(B)** Quantification of GST-DAD induction of Glu MTs in siRNA treated cells. n>50 cells; error bars, SEM from at least 4 experiments. **(C)** Immunofluorescence staining of GST-DAD and phalloidin staining of F-actin in NIH3T3 fibroblasts treated with GAPDH (control) or Kif4 siRNA and microinjected with GST-DAD (arrows). **(D)** Immunofluorescence staining of Kif4 and Glu MTs in starved NIH3T3 fibroblasts treated with indicated siRNAs and 10 mM LiCl for 2 hr. **(E)** Quantification of LiCl-induced Glu MTs in GAPDH control and Kif4 siRNA cells. n>50 cells; error bars, SEM from at least 4 experiments. Scale bars, A,D 10 μm; C 20 μm.

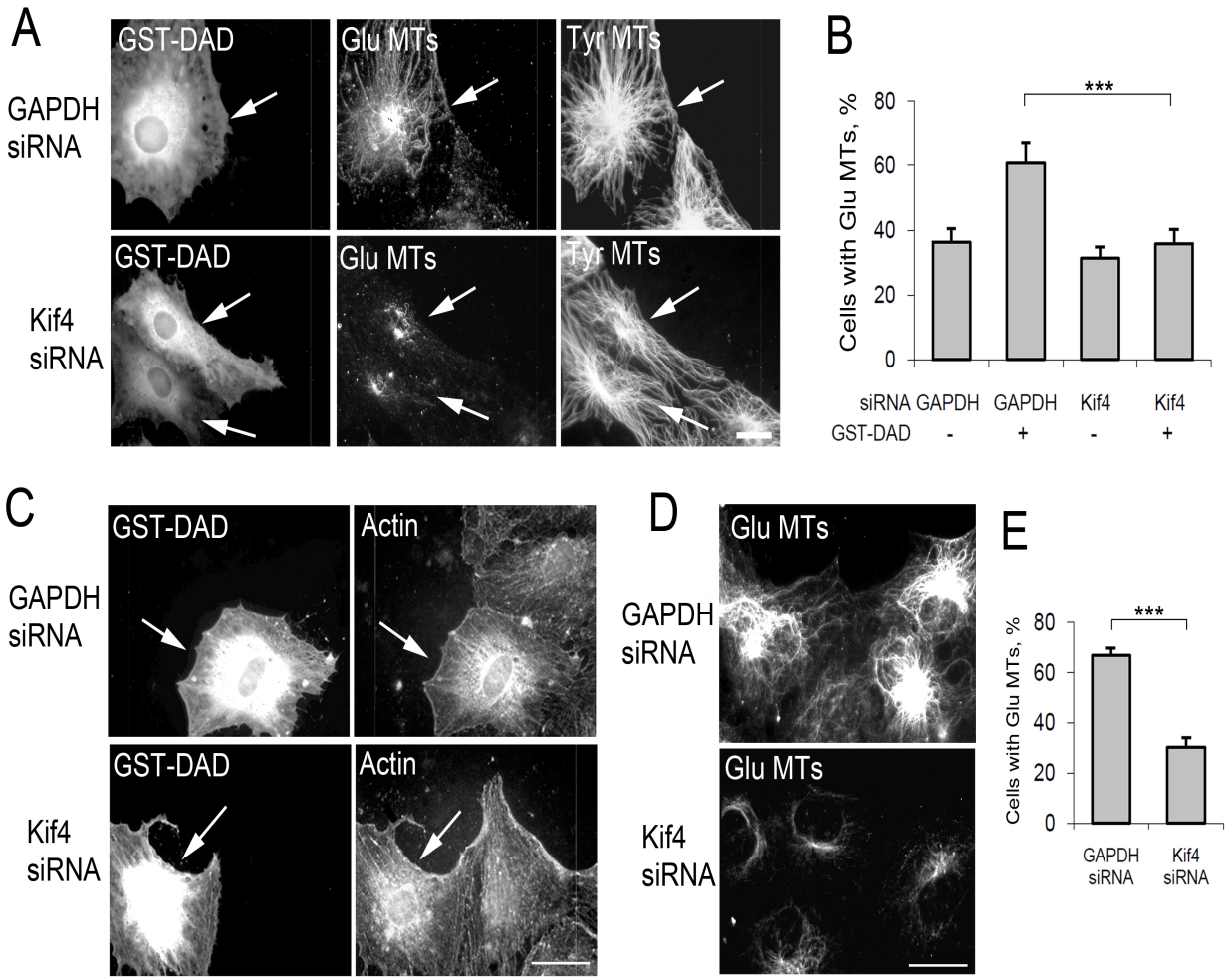
A
GST-DAD
Glu MTs
Tyr MTs
GAPDH siRNA
Kif4 siRNA
B
Cells with Glu MTs, %
***
siRNA GAPDH GAPDH Kif4 Kif4
GST-DAD - + - +
C
Actin
D
E

Figure 49*. GFP-Kif4 motor expression does not change the distribution of mDia1 or EB1.

Immunofluorescence of GFP, mDia1 and Glu MTs (top) and EB1 and Tyr MTs (bottom) in starved NIH3T3 fibroblasts expressing GFP-Kif4 motor. Arrows indicate GFP-Kif4 motor expressing cells. Scale bar, 10 μm.

* My contribution

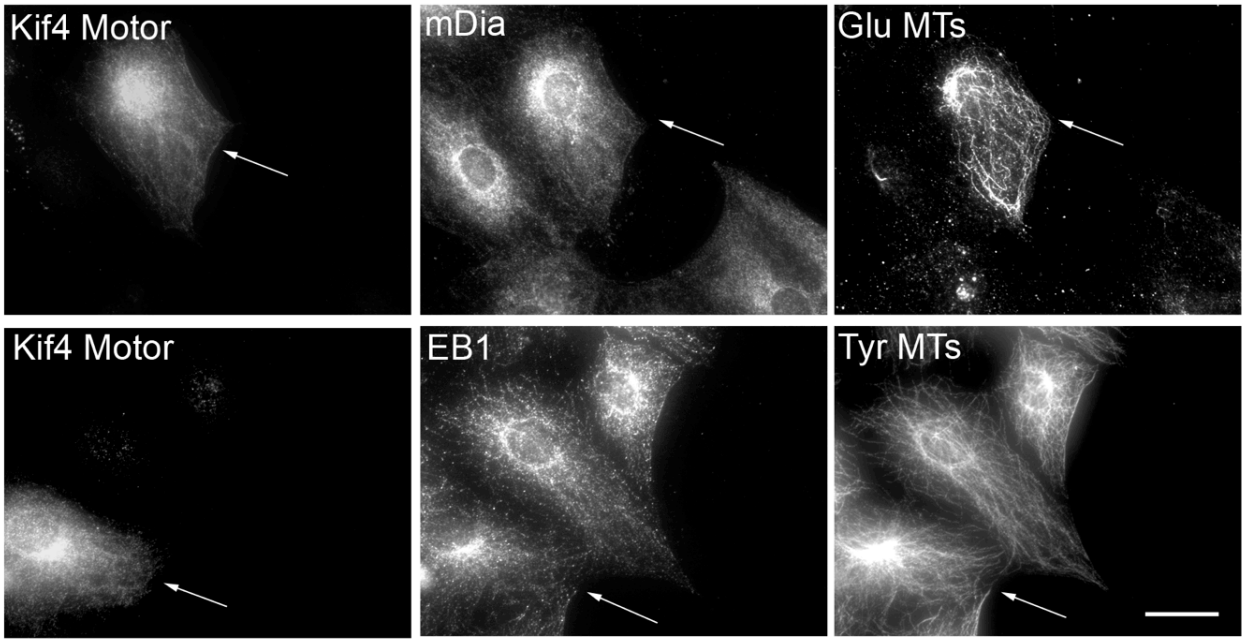
Kif4 Motor
mDia
Glu MTs
Kif4 Motor
EB1
Tyr MTs

Figure 50. Expressed Kif4 and EB1 require each other to induce Glu MTs.

(A) Immunofluorescence staining of Glu MTs in starved NIH3T3 fibroblasts treated with control (GAPDH) siRNA or Kif4 siRNA and microinjected with GST-EB1 (arrows). Human IgG (IgG) was used as an injection marker for GST-EB1 injected cells. Arrows indicate injected cells. **(B)** Quantification of the percentage of siRNA-treated cells exhibiting Glu MTs after injection with GST-EB1 protein. n>100 cells; error bars are SEM from 4 experiments. **(C)*** Immunofluorescence staining of Glu MTs in starved NIH3T3 fibroblasts treated with control (noncoding) siRNA or EB1 siRNA and expressing GFP-Kif4 motor (arrows). **(D)*** Quantification of the percentage of siRNA-treated cells exhibiting Glu MTs after expression of GFP-Kif4 full length (FL) or motor (M) constructs. n>100 cells; error bars, SEM from at least 4 experiments. Scale bars, 10 μm.

*My contribution

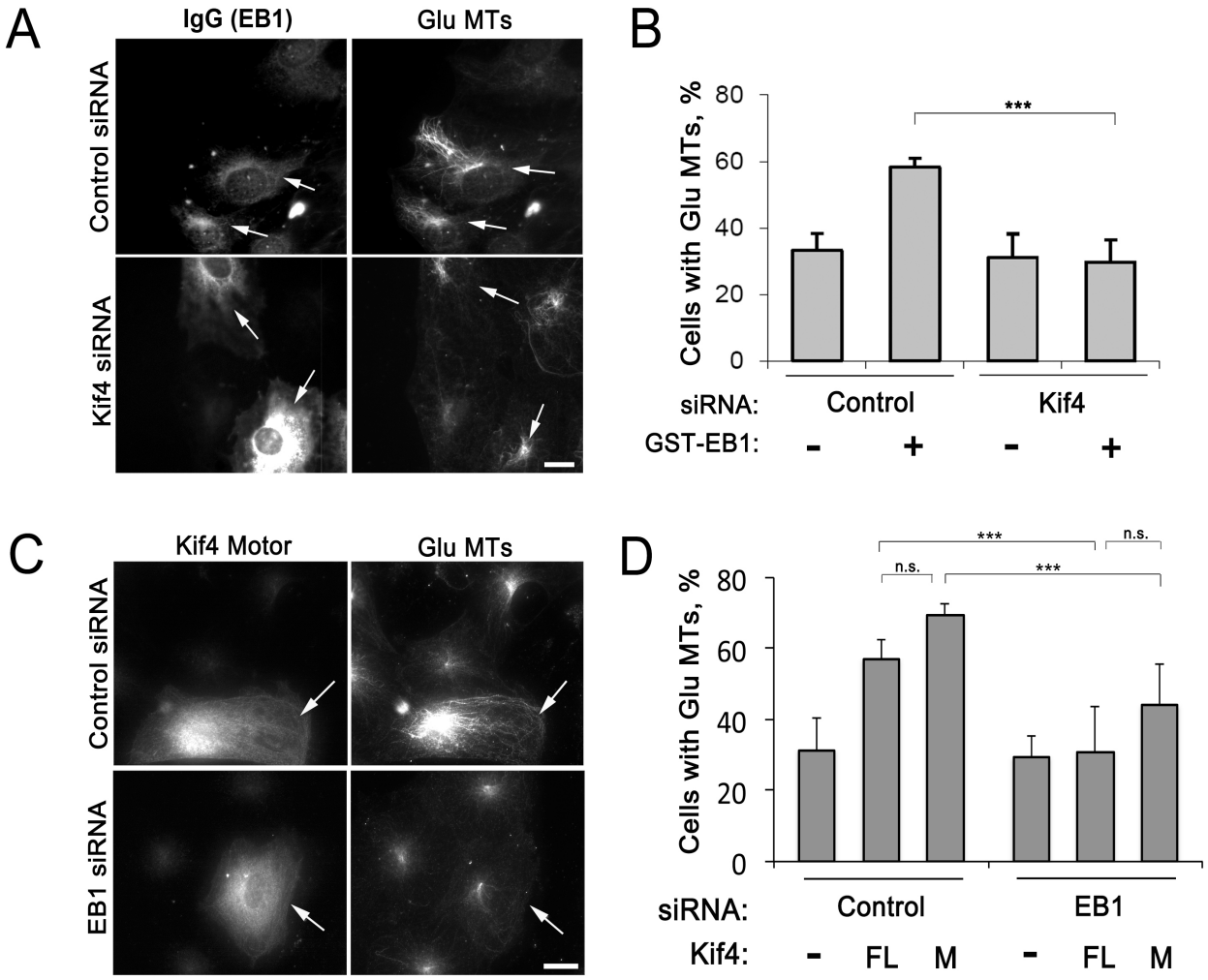
A
IgG (EB1)
Glu MTs
Control siRNA
Kif4 siRNA
B
Cells with Glu MTs, %
80
60
40
20
0
***
siRNA:
Control
Kif4
GST-EB1:
-
+
-
+
C
Kif4 Motor
Glu MTs
Control siRNA
EB1 siRNA
D
Cells with Glu MTs, %
80
60
40
20
0
***
n.s.
n.s.
***
siRNA:
Control
EB1
Kif4:
-
FL
M
-
FL
M

Figure 51*. Western blot of EB1 knockdown using EB1 siRNA.

NIH3T3 fibroblasts treated with noncoding (NC) or EB1 siRNA were analyzed by western blot. Tubulin was used as a loading control.

*My contribution

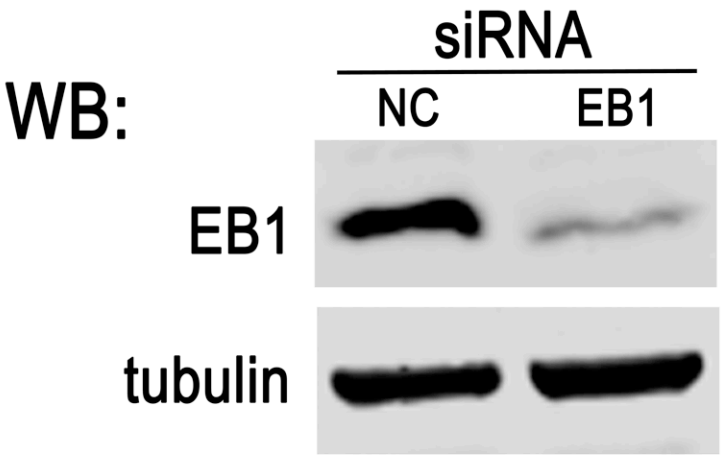
siRNA
WB:
NC
EB1
EB1
tubulin

Figure 52. Kif4 interacts directly with EB1.

(A) Kif4 coimmunoprecipitates with EB1 from NIH3T3 fibroblast lysates. EB1 or control IgG immunoprecipitates were western blotted for EB1 and Kif4. **(B)** Diagram of Kif4 protein fragments used for binding studies. **(C)** Pull-down of recombinant proteins. Equal amounts of GST or the indicated GST-EB1 proteins on glutathione-Sepharose were used to pull down MBP-tagged Kif4 proteins. Bound proteins were analyzed by western blotting as indicated.

A

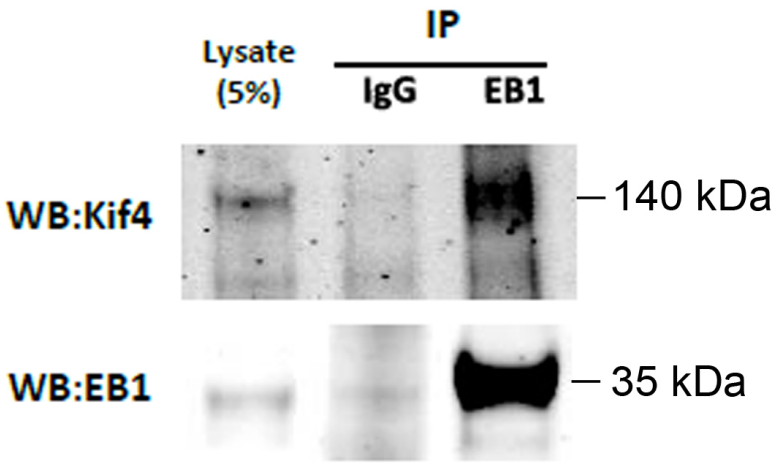
Lysate
(5%)
IP
IgG
EB1
WB:Kif4
140 kDa
WB:EB1
35 kDa

B

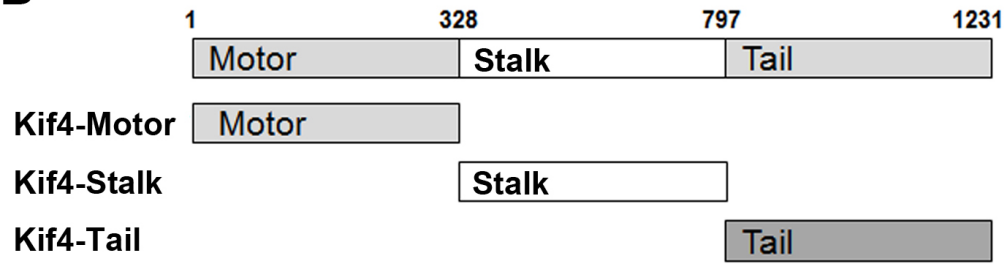
1
328
797
1231
Motor
Stalk
Tail
Kif4-Motor
Motor
Kif4-Stalk
Stalk
Kif4-Tail
Tail

C

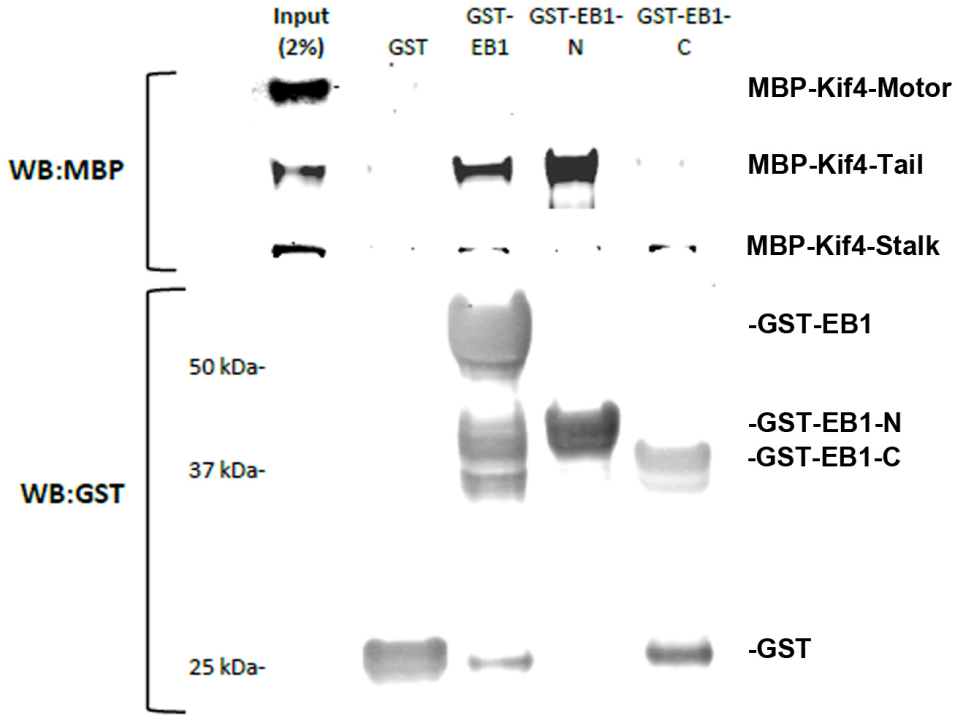
Input
(2%)
GST
GST-
EB1
GST-EB1-
N
GST-EB1-
C
WB:MBP
MBP-Kif4-Motor
MBP-Kif4-Tail
MBP-Kif4-Stalk
WB:GST
50 kDa-
37 kDa-
25 kDa-
-GST-EB1
-GST-EB1-N
-GST-EB1-C
-GST

Figure 53*. Kif4 knockdown inhibits cell migration into wounded monolayers.

(A) Panels from phase movies of wounded monolayers of NIH3T3 fibroblast treated with noncoding (NC) or Kif4 siRNAs. Scale bar, 15 μm. **(B)** Quantification of the migration of NIH3T3 fibroblast monolayers after treating with noncoding (NC) or Kif4 siRNAs. **(C)** Quantification of the cellular aspect ratio of wound edge NIH3T3 fibroblast treated with noncoding (NC) or Kif4 siRNAs and allowed to migrate for indicated times. Histograms in B, C are based on data from 3 experiments; error bars are SD.

*My contribution

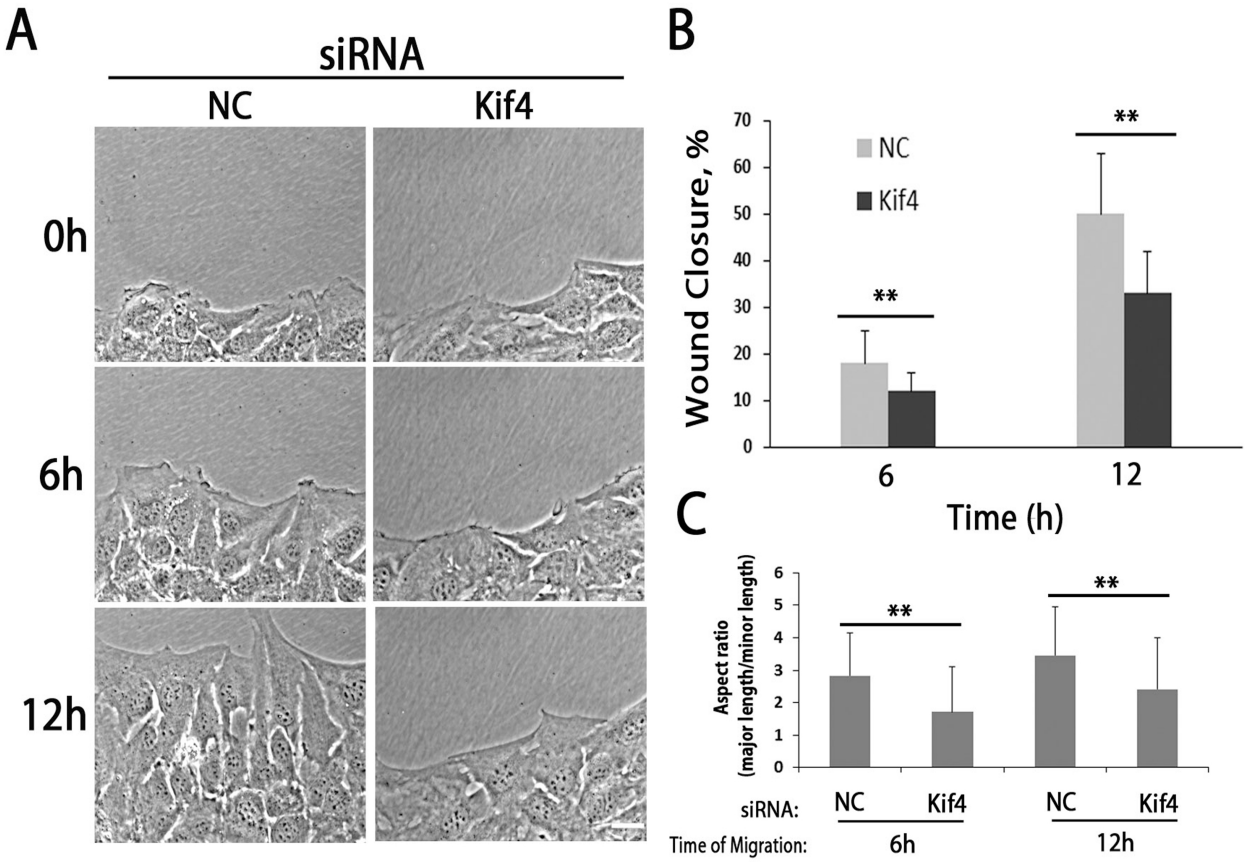
A
siRNA
NC
Kif4
0h
6h
12h
B
Wound Closure, %
NC
Kif4
**
**
70
60
50
40
30
20
10
0
6
12
Time (h)
C
Aspect ratio
(major length/minor length)
**
**
6
5
4
3
2
1
0
siRNA:
NC
Kif4
NC
Kif4
Time of Migration:
6h
12h

MATERIAL AND METHODS

Cell culture and chemicals

NIH3T3 cells (ATCC) were used throughout unless otherwise noted and were cultured in 10% calf serum in DMEM (Gibco BRL) as previously described (Cook et al., 1998; Palazzo et al., 2001a). TC-7 cells (ATCC) were cultured as described previously (Infante et al., 2000). MDCK cell lysate and Kif17 antibody (Sigma) were kind gifts from G. Kreitzer (Weill Cornell Medical College, NY). All chemicals were from Sigma-Aldrich unless otherwise noted.

Cell starvation and LPA and serum treatments

NIH3T3 cells were passaged onto glass coverslips and after growing to confluency, were starved for two days in serum-free DMEM plus 10 mM Hepes, pH 7.4 (Cook et al., 1998; Gundersen et al., 1994; Palazzo et al., 2001a). After wounding with a jeweler's screwdriver, MT stabilization was induced by adding 5 μM LPA for 2 hr. To examine Kif4 localization, starved NIH3T3 cells were stimulated for various times with either 5 μM LPA or 10% calf serum.

Microinjection

Serum-starved NIH3T3 fibroblasts at the edge of wounded monolayers were pressure-microinjected with a micromanipulator (Narshige International). DNA (50 μg/ml) was injected into nuclei and recombinant protein (90 μM) was injected into the cytoplasm. After microinjection, the injected plasmid was allowed to express for 2 hr before fixation or further treatment with LPA.

cDNA Constructs. Human GFP-Kif4 motor (residues 1-356), GFP-Kif3A motor (residues 1-354) and GFP-Kif17 motor (residues 1-335) were kind gifts of G. Kreitzer (Weil Cornell Medical College, NY). Mouse Kif4 full length was obtained from Open Biosystems and cloned into the Clontech GFP-C1 vector to prepare mouse GFP-Kif4. Human Kif4 fragments were

subcloned into a maltose binding protein (MBP) vector pMAL-c2E (New England Biolabs) from the GFP-C1 vector after digesting with EcoRI and SalI and were verified by sequencing.

Binding of purified proteins

Recombinant GST-EB1, GST-EB1-N and GST-EB1-C proteins were previously described (Wen et al., 2004). MBP-tagged Kif4 proteins were expressed in Rosetta-2 bacteria (EMD Biosciences) and purified according to manufacturer's recommendations except using a different buffer (20 mM Hepes buffer, 150 mM NaCl, pH 7.5). Binding studies were performed by incubating 0.3 μM MBP-tagged Kif4 proteins in RIPA buffer (20 mM Tris pH 7.5, 150 mM NaCl, 1% Nonidet-P40, 1% sodium deoxycholate, 0.1% SDS) with 0.3 μM GST-tagged EB1 proteins on glutathione-agarose overnight at 4ºC. After washing, bound proteins were eluted with SDS sample buffer and western blotted.

Immunoprecipitation

Immunoprecipitation was performed overnight at 4ºC using pre-cleared NIH3T3 fibroblast lysates in 10% RIPA buffer plus protease inhibitor cocktail (Sigma Aldrich) and MG132 (A.G. Scientific) and 1 μg rabbit anti-EB1 antibody (Santa Cruz Biotechnology) or non-immune rabbit IgG as a control. MG132 was critical to prevent degradation of Kif4 during the incubation. Immunoprecipitates were recovered with Protein A/G beads (1:1 mix), washed, and the bound protein eluted with SDS sample buffer and analyzed by western blotting.

siRNA transfection

Cells were transfected with siRNA (5 μM) using Lipofectamine RNAiMax (Invitrogen) according to manufacturer's instructions and plating cells directly into the transfection media. After overnight transfection, cells were serum-starved for 2 days. siRNAs were designed using the BIOPREDsi website (www.biopredsi.org/) and were obtained from Shanghai GenePharma.

siRNA sequences were as follows: GAPDH, 5'-AAAGUUGUCAUGGAUGACCTT-3'; Kif4#1, 5'-GGAACUGGAGGGUCAAAUATT-3'; Kif4#2, 5'-GCAGAUUGAAAGCCUAGAGTT-3'; KIF3A, 5'-CAGGAAAUAACAUGAGGAATT-3'; EB1, 5'-CUGCCAGACAAGGUCAAGAAA-3' *Fixation*. For routine immunofluorescence and for staining Kif4 in NIH3T3 fibroblasts, cells on glass coverslips were fixed in methanol for 5 min at -20˚ C. To detect Kif4 on the ends of MTs in TC-7 cells, cells were cryofixed in isopentane cooled in a dry ice-liquid nitrogen bath with constant stirring until it started to become gel-like, which corresponds to approximately -200˚C (Oliver and Jamur, 2010). After one min in isopentane, the cells were freeze substituted in a 6:4 acetone:methanol on dry ice and then transferred to -80˚C for 2 days. The cryofixed cells were gradually warmed by placing them in an insulated container at -20˚C container for 4 hr and then transferred to TBS buffer (20 mM Tris pH 7.4, 150 mM NaCl) and stained with antibodies.

Immunofluorescence staining

Rabbit anti-Glu-tubulin antibody (dilution 1:400) was described previously(Gundersen et al., 1984). Rat anti-Tyr tubulin (dilution 1:10 of culture supernatant) was from European Collection of Animal Cell Cultures. Kif4 monoclonal antibody (dilution 1:50) was described previously (Bisbal et al., 2009) and was a gift from A. Caceres or was from Sigma-Aldrich. Mouse anti-GFP antibody (dilution 1:200) was from Sigma-Aldrich. Cyclin B antibody (dilution 1:100) was from Santa Cruz. Secondary antibodies, absorbed to minimize interspecies cross reactivity, were from Jackson ImmunoResearch and were used as described previously (Palazzo et al., 2001a). Because most serum-starved NIH3T3 fibroblasts have a small number of Glu MTs before LPA stimulation, we scored cells as positive for Glu MTs if they had more than five brightly and continuously labeled Glu MTs that extended toward the cell periphery (Cook et al., 1998; Gundersen et al., 1994). The stability of MTs in cells expressing kinesin motors was tested by

treating cells with 10 μM NZ for 30 min as described previously (Cook et al., 1998; Gurland and Gundersen, 1995).

Western Blotting

Samples were run on 4-15% polyacrylamide SDS gels and transferred to nitrocellulose. Blots were incubated with the following antibodies: anti-Kif4 mAb (1:500), anti-beta-catenin (1;1000), anti-actin (Ab-5; 1:10,000), anti-Kif3A (1:100; BD Transduction Laboratories), anti-EB1 (1:10,000), anti-Kif17 (1:1000) or anti-GAPDH (1;6000). After incubation with fluorescent IR680- or IR800-conjugated secondary antibodies (1:5,000, Rockland Immunochemicals), reactivity was documented with an Odyssey scanner (Li-Cor Biosciences).

Analysis of Kif4 localization at Glu MT ends

NIH3T3 fibroblasts or TC-7 cells immunofluorescently stained for Glu tubulin, Tyr tubulin and Kif4 were mounted in TBS and imaged by TIRF microscopy on a Nikon TE2000 microscope with a 60X, 1.45 objective and an Orca II ER CCD (Hamamatsu) controlled by MetaMorph software. To unambiguously identify Glu MT ends, we overlaid Glu and Tyr MT images and considered only ends of Glu MTs in which the Glu tubulin staining abruptly stopped and was not "continued" with Tyr tubulin staining. Circles (10 pixels in diameter) were then drawn on the Glu MT ends and the overlaid on the corresponding image of Kif4 staining. Kif4 puncta inside circles that also contacted Glu MT ends were counted positive; those lacking Kif4 were counted negative. To control for random overlap of Kif4 puncta with Glu MTs, the circles were shifted 10 pixels in the x- and y-axes and the number of Kif4 puncta appearing in the circles was determined.

Analysis of Cell Migration

Wounded monolayers of NIH3T3 fibroblasts treated with noncoding or Kif4 siRNAs were imaged with a 20X ELWD Plan Fluor objective (NA 0.45) at multiple positions every 10 min for

12 h on a Nikon TE300 microscope with a temperature controller (37^{o} C) and motorized xyz stage. The extent of cell migration was measured as percentage of wound closure. The polarization of the cells was measured by determining their aspect ratio (major axis/minor axis) using Image J software.

Statistical Anaylsis

Statistical significance was assessed by Chi square analysis for non-parametric data and paired t-test for parametric data. P values are indicated in the figures as: *, $p<0.05$; **, $p<0.01$; ***, $p< 0.001$.

DISCUSSION

In this work I sought to answer the following questions:

- Do FA components traffic with internalized integrins and affect their trafficking?

- Do integrins engaged in FAs traffic through a specific endocytic pathway?

- Is there a relationship between integrin recycling and FA formation?

- When are recycled integrins reactivated?

- Is membrane trafficking coupled to a specific cytoskeletal mechanism to ensure that internalized integrins are trafficked in a polarized fashion?

Molecular mechanisms of migration have been extensively studied over the past decades (Pollard and Borisy, 2003; Ridley et al., 2003; Vicente-Manzanares et al., 2005) and FA turnover is a major aspect of persistent cell migration (Webb et al., 2002). FA disassembly occurs in a common cytoplasm along with FA formation, which makes it difficult to separately study the mechanisms underlying these events. Ezratty et al., (2005) developed a model system that kinetically separate FA disassembly from FA reassembly and showed that FA disassembly involves integrin endocytosis that is dependent on dynamin, GRB2, FAK, clathrin and clathrin adaptors (Dab2 and ARH). Therefore FA disassembly was characterized as an endocytic process.

Integrin endocytosis and recycling was previously shown to be important for cell migration (Caswell et al., 2008; Caswell et al., 2007; Pellinen et al., 2006). These studies report the overall pathways taken by bulk integrins but do not provide information about the recycling

of integrins that were previously resident in FAs. Therefore they could not address the relationship between integrin endocytosis and FA disassembly/reassembly. This prompted us to ask the following question: Do FA-derived integrins travel through the same recycling pathways as bulk integrins? Importantly, my findings strongly support the view that FA-derived integrins traffic through different pathways when compared to bulk integrins.

I identified unanticipated roles for SFKs in the recycling of integrins (previously resident at FAs) from the ERC and for FAK in the maintenance of integrin activation during their recycling to the cell surface (Figure 54). More specifically, I found that FA-derived endocytosed integrin localizes to the Rab5 and then to the Rab11 compartment in an active state. Additionally, FAK also localized to the Rab5 endosomes and both FAK and Src colocalized at the Rab11 ERC along with active integrins. This particular integrin population is then recycled back to the plasma membrane in a Rab11-, SFKs- and Kif3AC-dependent fashion (Figure 54). I anticipate that Kif3AC will play an important role in determining where exocytosis of endocytosed integrin occurs. Polarized integrin trafficking would be a critical aspect of persistent cell migration since our findings predict that recycled integrins are active and therefore ready to engage with the ECM to rapidly form new FAs.

My study shows that α5β1 integrins are kept active during endocytic recycling in a FAK-dependent fashion since FAK-inhibited cells displayed reduced staining for active integrins following FA disassembly (Figure 18). Therefore, we suggest that FAK and SFKs are critical regulators of integrin endocytic trafficking by escorting them throughout the recycling pathway and maintaining them active. But how do FAK and SFKs maintain integrins active during recycling? Are there other proteins (possibly FAK/SFKs substrates) involved in this step?

Although possible, it is unlikely that inactive (or bulk) integrins will be associated with

FA components during their recycling. We have observed FAK and active integrin in Rab5 and Rab11 endosomes (Figure 18). It is probable that endocytosed integrins that have not been previously in FAs will travel on endosomes that do not have FAK or other FA proteins associated with them. In this case we suggest that these integrins are inactive and further experimentation will be required to answer whether or not, and if so, how these integrin-containing vesicles are (re)sorted for recycling.

How might FAK maintain the activation state of endocytosed integrin? One possibility is that direct FAK binding to integrin tails may be involved. FAK has been shown to bind to β1 integrin tail (Chen et al., 2000; Schaller et al., 1995). Alternatively, FAK kinase activity may be important to target other proteins to the integrin tail, e.g., talin. Immunoprecipitation of active integrin at 60 min after NZ washout (and therefore resident at the ERC) to detect its binding partners and also imaging studies of talin and active integrins would shed some light on this topic. Additionally, talin phosphorylation has been proposed as a mechanism for its activation (Moser et al., 2009), thus it will be interesting to immunoprecipitate talin and analyze its phosphotyrosine levels in the presence and absence of PF228 and PP2 during FA reassembly. Consistent with a role for talin in integrin activation, depletion of talin blocked FA reassembly (Figure 31). We do not know however, how talin is contributing to FA reassembly and we envisage two scenarios that are not mutually exclusive: 1) talin is required to keep integrins active at the plasma membrane after they are exocytosed-in this case we propose there will be a switch between FAK and talin for binding to the integrin tail and/or 2) talin is required (along with FAK/SFKs) to keep integrins active during their endocytic recycling. Hypothesis "1" would be in complete concurrence with the canonical role for talin in integrin activation (Moser et al., 2009). On the other hand, hypothesis "2" would reveal a new role for talin as until now this FA

component has not been shown to play a role during endocytic trafficking. In agreement with this hypothesis, talin localized to the ERC following FA disassembly (data not shown). Further experimentation is needed to test these hypotheses.

As mentioned above, I found that SFKs are required for integrin recycling from the ERC. SFKs may play a role in the budding of vesicles from the ERC or in the attachment of Kif3AC or an adaptor protein to the integrin-containing vesicles derived from the ERC. Kif3AC immunoprecipitation assays after MT-induced FA disassembly in PP2-treated may shed some light on the potential partners of Kif3AC that are being modulated by SFKs activities.

In addition to their role in promoting trafficking from the ERC to the plasma membrane, SFKs may also contribute to maintaining the activation of endocytosed integrins. The observation that Mn^{2+} rescued FA reassembly in $FAK^{-/-}$ cells transfected with FAK-Y397 (Figure 15D and E), suggests that Src binding to FAK is not required for integrin recycling from the ERC and further implies that SFKs (along with FAK) play a role in integrin activation at the level of the plasma membrane. Consistent with this, I have preliminary results showing that when PF228 is washed out (after integrin has returned to the cell surface) and PP2 is added, FAs do not reassemble. Further experimentation using assays that measure integrin surface levels in cells transfected with FAK kinase mutants would test this hypothesis.

Another major regulator of integrin activation is kindlin (Moser et al., 2009). It was recently shown that the binding of SNX17 to the MD NPxY motif of β1 integrin (which is also the binding site for kindlin2) early on after endocytosis is critical for the recycling of this receptor to the cell surface (Bottcher et al., 2012; Steinberg et al., 2012). Similarly, two studies reported that kindlin2 binding to this same motif was important to regulate β1 integrin surface levels by different mechanisms. Whereas one study showed that kindlin2 is required to prevent

β1 integrin degradation (Margadant et al., 2012) the other group found that it is rather required to regulate β1 integrin mRNA levels but not its recycling or degradation (Bottcher et al., 2012). In agreement with the findings of Botcher et al., (2012) my results indicate that kindlin2 is not required for integrin recycling as kindlin2-depleted cells displayed normal FA reassembly (Figure 32). The mechanisms of how kindlins regulate β1 integrin surface expression will clearly require further analysis.

The heterodimer α5β1 was shown to recycle via the Rab11-dependent, long-loop pathway and Rab4 disruption had no effect (Powelka et al., 2004). My studies of FA-derived α5β1 are consistent with this as their recycling was dependent on Rab11 (Figure 6G). On the other hand, PDGF-stimulated recycling of bulk αvβ3 integrin was shown to occur via the Rab4-dependent, short-loop pathway, suggesting alternative pathways for integrins for different integrins (Roberts et al., 2001). Interestingly, α5β1 and αvβ3 integrins were recently shown to exhibit distinct dynamic nanoscale organizations inside FAs (Rossier et al., 2012). Therefore, it will be interesting for future studies to characterize the trafficking pathways taken by integrin αvβ3 after MT-induced FA disassembly to see whether they follow similar pathways to the ones here characterized for the α5β1 heterodimer. Likewise it will be important to determine whether there are different proteins affecting the recycling of the integrin αvβ3.

Active and inactive integrins were shown to have distinct net endocytic rates. The active β1 integrins endocytosis is higher when compared to the endocytosis of the inactive β1 integrin, which is counteracted by rapid recycling to the plasma membrane via a Rab4-dependent pathway (Arjonen et al., 2012). Additionally, it has been shown that FN and integrins colocalize in late endosomal compartments (Lobert et al., 2010) suggesting that active, FN-engaged integrins are directed to degradation. An important consideration in this study is that the cells were incubated

with soluble recombinant FN prior to stimulate endocytosis. Therefore the intracellular FN they detected was not derived from the ECM. Thus it is unlikely that the integrins associated with this FN were previously in FAs. It may be that integrin attached to the soluble ligand is efficiently degraded as observed (Lobert et al., 2010) and in my case I speculate that FA-derived integrin is separated from FN upon endocytosis. Consistent with this hypothesis, intracellular FN did not colocalize with active integrin in the Rab11 ERC after FA disassembly (Figure 18I) and FA-derived integrins were accessible to the FN fragment (Figure 18J), which would be unlikely to occur if this integrin population was still bound to FN. Another important point is that I am looking at integrins derived from FAs, and as suggested above, it is likely that this integrin population may be associated with FA components, what may alter its trafficking while keeping it active.

Given the considerations above, new questions arise: Is ECM-derived FN that is associated with FA-integrins endocytosed along with integrins during FA disassembly? If not, what are the mechanisms by which FN is detached during endocytosis? Detachment might occur by three different ways: 1) Mechanically, by the force of endocytosis, analogous to the force of endocytosis helping Notch cleavage (Musse et al., 2012); this could be tested by using a FN FRET-biosensor that would stretch upon integrin endocytosis. 2) By MMP-mediated ECM degradation during FA disassembly (Stehbens et al., 2014; Wang et al., 2012). Although this is an attractive hypothesis, I have preliminary results that MMPs inhibitors do not block MT-induced FA disassembly. 3) By sorting after endocytosis (ligand uncoupling). If this hypothesis is correct, ECM-derived FN should not be found in Rab5 endosomes following MT-induced FA disassembly. These mechanisms are not mutually exclusive so it is possible a combination of them may contribute to removal of FN from integrins endocytosed during FA disassembly.

Active integrins have been previously shown to localize to different Rab compartments (Arjonen et al., 2012; Chao and Kunz, 2009). In these studies, cells were pre-incubated with antibodies that detect active-conformation integrins and then integrin endocytosis was triggered either by MT-induced FA disassembly (Chao and Kunz, 2009) or by incubating the cells at 37^{o}C with serum-containing medium, which stimulates the endocytosis of not only antibody-bound but also bulk integrins (Arjonen et al., 2012). One major concern about these studies is that these conformation-specific antibodies may lock integrins in their active conformation (Byron et al., 2009 and Calderwood, personal communication). In contrast, in my studies I fixed the cells at different times after NZ washout and only then I used an antibody that recognizes active integrins (12G10). My imaging studies showed that the integrin pool endocytosed from FAs after MT regrowth localizes to the Rab5 and Rab11 ERC in an active state (Figure 18). Importantly, I also detected other FA components (including Src and active FAK) in the same compartment (Figures 4, 9, 11 and 13). Previously, FAK was reported to localize at the perinuclear region of highly invasive cytotrophoblasts (Ilic et al., 2001).

The endocytic trafficking pathways followed by different FA components have just started to be elucidated, therefore the real significance of their distinct intracellular localizations remains elusive. Here we speculate that the localization of several FA components to the ERC following FA disassembly suggests the existence of an intracellular "FA signaling module" that might be critical to drive integrin recycling and to keep it from being directed to degradation. In agreement with this idea, it was recently suggested that endocytosed active integrins may signal from the endosomes via an "inside-in" mechanism (Bouvard et al., 2013) and here we further suggest that this will ultimately influence integrin recycling and FA formation. Moreover it might be that additional FA components traffic with the integrin endocytosed from FAs. Indeed,

in preliminary experiments I have found that two additional FA components, paxillin and vinculin, localized to the ERC after FA disassembly (Figure 55).

Several actin-associated molecular motors play a role in integrin trafficking. For instance, actin-based motors, such as myosin-10, regulate integrin-mediated cell adhesion in filopodia (Zhang et al., 2004) and myosin-6 promotes the internalization of ligand-bound α5β1 integrin (Valdembri et al., 2009). However a comprehensive characterization of the MT-associated molecular machinery regulating integrin trafficking was missing. Collectively, our findings indicate that plasma membrane delivery of endocytosed integrins from the ERC is important for FA reassembly and in turn imply that MTs and kinesins may contribute to this event. Consistent with these ideas, I have found data supporting the idea that the heterodimer Kif3AC transports active integrins from the ERC to the cell leading edge for polarized FA reassembly. Interestingly, Kif1C was recently shown to transport integrins to the cell rear and to play an important role in persistent cell migration (Theisen et al., 2012). In contrast, I identified Kif3AC as a kinesin committed to polarized integrin trafficking towards the cell front. This would keep a cycling pool of integrins in a restricted cell region for proper FA dynamics and cell migration, as suggested previously (Caswell et al., 2009). Identifying a motor engaged in integrin recycling constituted a significant finding as until now there was no evidence linking a molecular motor with polarized integrin trafficking during cell migration. It will be interesting for future studies to determine if Kif3AC directly transports integrin from the Rab11 ERC to the cell surface and to determine the relationship between integrin exocytic sites and FA reassembly sites.

The exact pathway of integrin trafficking depends not only on the integrin activation state, but also on cell type, composition of the integrin heterodimer and extracellular stimuli (Caswell and Norman, 2006). Likewise, different integrin heterodimers exhibit distinct trafficking

kinetics (Caswell et al., 2009) and this suggests diverse molecular requirements for the trafficking (Teckchandani et al., 2009). In this context, it is likely that distinct kinesins will be committed to transport different integrin heterodimers and affect FA dynamics through different mechanisms. For instance, kinesin-1 was suggested to affect FA disassembly by the delivery of a hypothetical "relaxing factor" to FAs (Krylyshkina et al., 2002). Similarly, Kif15 (a member of the kinesin-12 family) was recently proposed to regulate α2 integrin internalization by controlling the cell-surface localization of Dab2 (Eskova et al., 2014). Surprisingly, several regulators of α2 integrin trafficking were related to FA formation and epithelial cell migration (Simpson et al., 2008; Winograd-Katz et al., 2009), further indicating a functional crosstalk between integrin trafficking, FA dynamics and cell motility. Of note, KIF15 was shown to be overexpressed in various tumors (Bidkhori et al., 2013). Therefore, it is clear that it will be important to screen for additional motors engaged in the recycling of different integrin heterodimers in different cell types to ultimately prevent cell migration in the context of cancer progression and tumor spreading.

Importantly, our model system based on MT-induced FA disassembly allowed us to identify critical steps and regulators of integrin recycling dependent-FA reassembly. More specifically it allowed us to characterize the different endosomal compartments through which FA-integrins travel following endocytosis and also allowed to unveil the molecules playing critical roles during integrin endocytic trafficking. This model system however is artificial since in order to stimulate FA disassembly in a synchronous fashion we treat the cells with NZ for several hours. Therefore it was crucial to test if our findings would also apply to migrating cells, in a NZ-free context. In order to test this I made several predictions about the behavior of integrins in migrating cells based on the findings gleaned with the MT-induced FA disassembly assay: 1) FAs should disassemble but not reassemble in migrating cells treated with either FAK

or SFKs inhibitors. 2) Integrin recycling should be blocked in SFKs-inhibited cells but not in FAK-inhibited cells. 3) FA reassembly should occur faster in FAK-inhibited cells than in SFKs-inhibited cells upon drug release. 4) Manganese should rescue FA reassembly in FAK- but not SFKs-inhibited cells. Importantly all these predictions were verified (Figure 22), strongly supporting the view that the major steps and players characterized with the NZ washout assay will contribute to the understanding of the basic mechanisms of cell migration. Additional tests of the model in migrating cells would be to examine the role of Kif3AC in integrin trafficking and the FA disassembly/reassembly cycle.

It will also be interesting to determine the implications and relevance of our model in the context of collective cell migration. This mode differs from single cell migration in that cells remain connected as they move, which results in migrating cohorts. Collective migration of cohesive cell groups *in vivo* is particularly prevalent during embryogenesis and drives the formation of many complex tissues and organs. For instance, it plays an essential role in the branching morphogenesis of mammary ducts, in border cell migration in the *Drosophila* egg chamber and in vascular sprouting during angiogenesis (Friedl and Gilmour, 2009).

A hallmark of collective cell migration is the distinction of the cell cohort into "leader" cells that guide the "followers" cells at their rear. Leader cells in the front row display polarized morphologies, detect extracellular guidance cues and generate greater cytoskeletal dynamics than follower cells. Moreover leader cells display distinct integrin heterodimer expression and a polarized localization towards the leading edge. Significantly, many invasive tumor types display a similar collective behavior and configuration. They can move as isolated groups or clusters that migrate through tissue after they detach from their origins (Friedl and Gilmour, 2009). It is likely that polarized integrin recycling/trafficking and the activation state of these receptors will be

much more critical for the leader cells than to the followers ones. Therefore it will be interesting to test if our findings are relevant in the context of collective migration of cancer and other cells. For instance, can we prevent cell migration and tumor metastasis by specifically targeting integrin activation in the leader cells?

In conclusion, my work has established unprecedented findings that revealed key aspects of integrin recycling and FA formation during cell migration and showed that these two basic cellular events are intimately connected. Until now it was uncertain whether or not recycled integrins previously resident in FAs remained active during their endocytic trafficking. Besides, little is known about the molecules controlling integrin trafficking and here we identified FAK and SFKs as major components of this event. Importantly, we are the first to identify a FA component playing a role during integrin recycling (namely FAK). FAK has been known as the "activatable scaffolding kinase" (Schwartz, 2001) that has two major functions: it can act as a signaling platform where other adaptor proteins and kinases bind and transduce downstream signals or it can act as a kinase by directly phosphorylating substrates. It has been known for some time now that FAK knockout cells exhibit enlarged FAs, so FAK has been generally considered to be required for FA disassembly but not for FA assembly (Ezratty et al., 2005; Ilic et al., 1995; Ren et al., 2000; Sieg et al., 1999). Surprisingly I revealed an unanticipated role for FAK kinase activity in FA reassembly. Whereas I found that FAK activity is dispensable for FA disassembly I showed it is crucial for FA reassembly by keeping integrins active during endocytic recycling. Importantly, FAK scaffolding function had been previously shown to be required for FA disassembly (Ezratty et al., 2005). Additionally, SFKs have been implicated in FA reassembly as *Src, Yes,* and *Fyn* knockout cells (*SYF* cells) displayed impaired FA reassembly after NZ washout (Yeo et al., 2006). Also, Src has been known to localize to the ERC and

suggested to regulate endosomal trafficking (Kaplan et al., 1992) but until now its precise roles in this compartment were undefined. Here I gathered evidence showing that SFKs modulate integrin recycling from the ERC. Such long-range traffic implies that there must be a MT-associated motor transporting integrins back to the plasma membrane for polarized FA formation. Here I identified the heterodimer Kif3AC, a kinesin II family member, as a critical player in this event. In the near future the relationship here established between integrin recycling, integrin activation and FA (re)formation will certainly provide alternative ways to better interfere with deregulated cell migration during tumor cell motility and metastasis *in vivo*.

Figure 54. Proposed model for polarized FA reassembly mediated by a kinesin II-driven integrin trafficking.

MT-induced-FA disassembly is dependent on integrin endocytosis mediated by FAK, GRB2, dynamin2, clathrin, clathrin adaptors (Dab2 and ARH) and PIPk1β. Following endocytosis, integrins remain associated with Rab5-positive early endosomes that also contain FAK and possibly Src, and this maintains integrins in an active conformation. Active integrins are then trafficked to the Rab11 endocytic recycling compartment where FAK and Src are also present. The recycling of integrins back to the cell surface is dependent on Rab11, SFKs activity and the kinesin II family member Kif3AC. Whether these proteins function in one or multiple steps in returning integrin from the ERC is unclear. Of note, FA reassembly will rapidly occur following exocytosis of integrin-containing vesicles since recycled integrins are active and therefore ready to engage with the extracellular matrix. The labels in red represent my findings whereas those in black refer to previous findings.

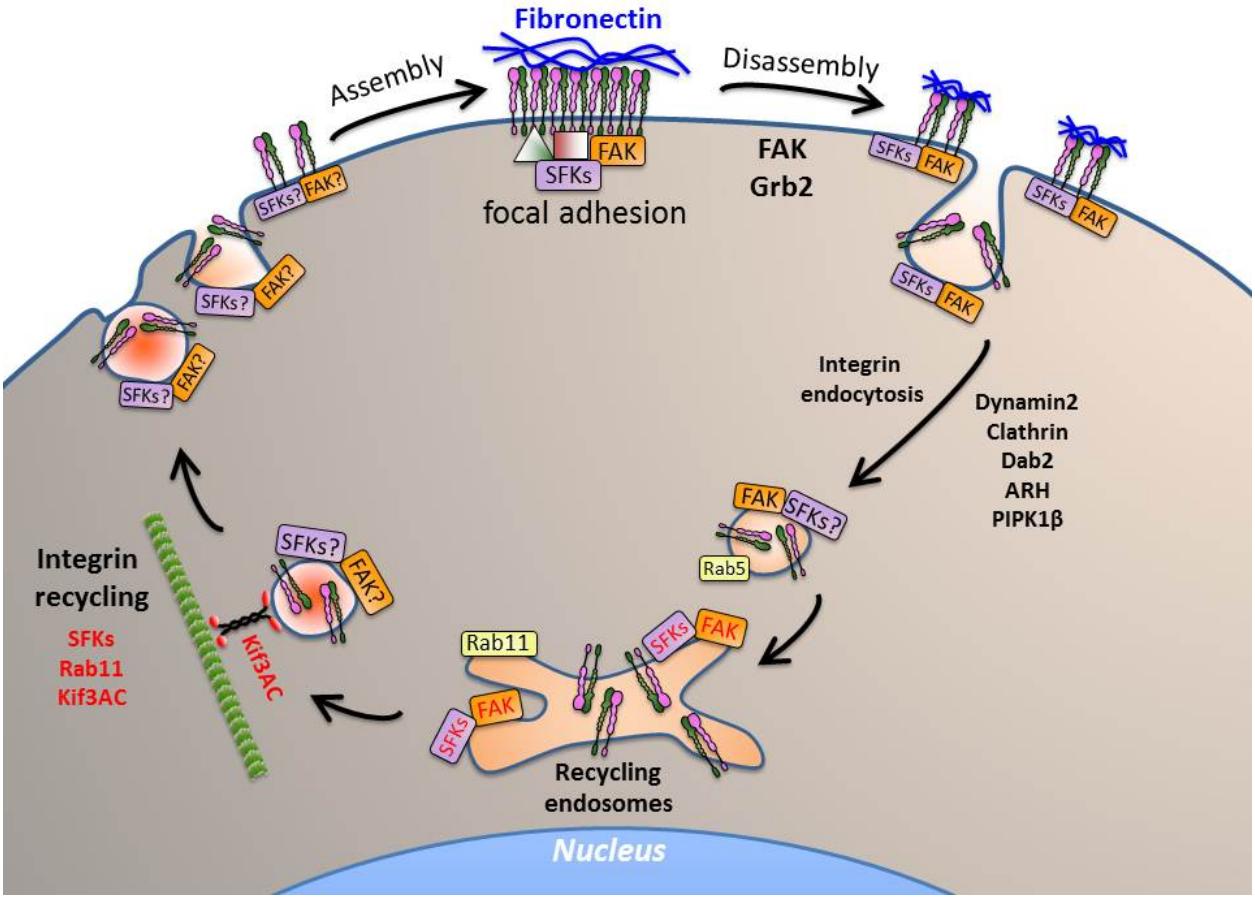
Fibronectin
Assembly
Disassembly
FAK
SFKs
focal adhesion
FAK
Grb2
SFKs?
FAK?
SFKs
FAK
Integrin
endocytosis
Dynamin2
Clathrin
Dab2
ARH
PIPK1β
FAK
SFKs?
Rab5
Rab11
SFKs
FAK
Recycling
endosomes
Nucleus
Integrin
recycling
SFKs
Rab11
Kif3AC
Kif3AC

Figure 55. Different FA markers localize to the ERC following FA disassembly.

Immunofluorescence images of vinculin, Rab11, paxillin and FAK-pY397 in NIH3T3 fibroblasts fixed at 60 min of NZ washout. Arrows indicate colocalization between vinculin and Rab11 or between paxillin and FAK-pY397. Scale bar, 10 μm.

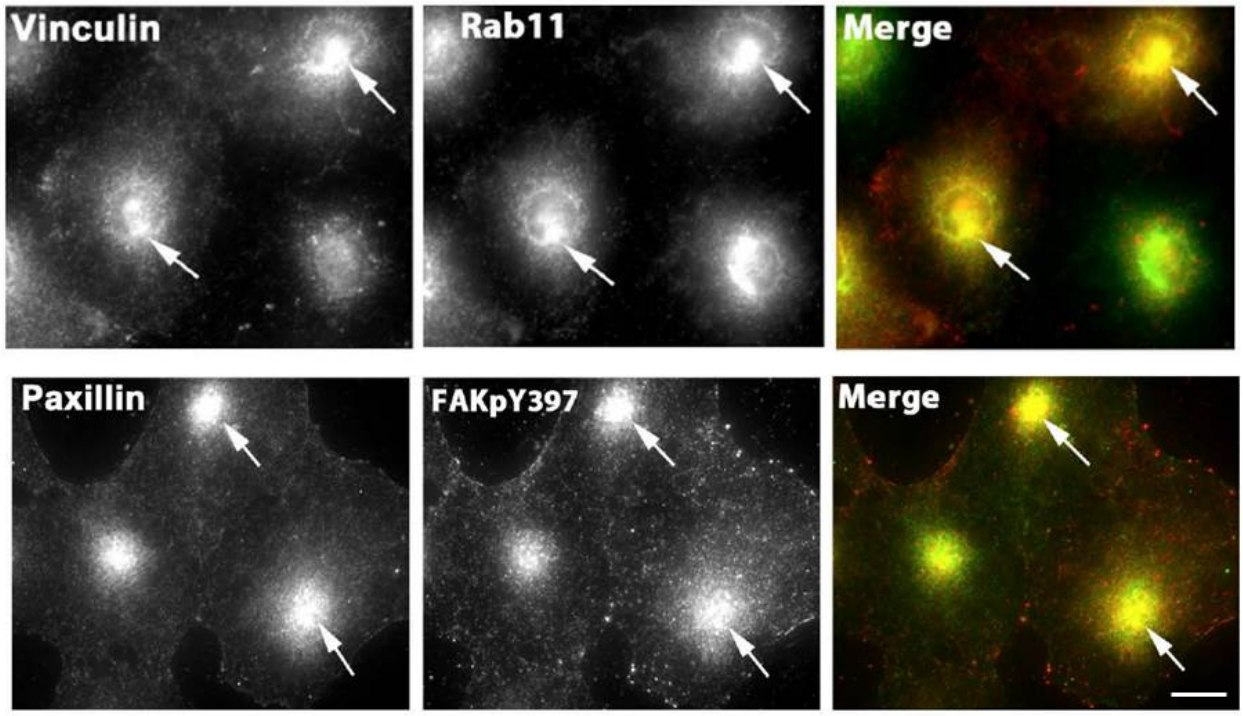
Vinculin
Rab11
Merge
Paxillin
FAKpY397
Merge

BIBLIOGRAPHY

Abercrombie, M. 1978. Fibroblasts. *Journal of clinical pathology. Supplement*. 12:1-6.

Abercrombie, M., and G.A. Dunn. 1975. Adhesions of fibroblasts to substratum during contact inhibition observed by interference reflection microscopy. *Exp Cell Res*. 92:57-62.

Abercrombie, M., G.A. Dunn, and J.P. Heath. 1977. The shape and movement of fibroblasts in culture. *Society of General Physiologists series*. 32:57-70.

Abercrombie, M., J.E. Heaysman, and S.M. Pegrum. 1971. The locomotion of fibroblasts in culture. IV. Electron microscopy of the leading lamella. *Exp Cell Res*. 67:359-367.

Akhmanova, A., C.C. Hoogenraad, K. Drabek, T. Stepanova, B. Dortland, T. Verkerk, W. Vermeulen, B.M. Burgering, C.I. De Zeeuw, F. Grosveld, and N. Galjart. 2001. Clasps are CLIP-115 and -170 associating proteins involved in the regional regulation of microtubule dynamics in motile fibroblasts. *Cell*. 104:923-935.

Amano, M., M. Ito, K. Kimura, Y. Fukata, K. Chihara, T. Nakano, Y. Matsuura, and K. Kaibuchi. 1996. Phosphorylation and activation of myosin by Rho-associated kinase (Rho-kinase). *J Biol Chem*. 271:20246-20249.

Andres-Delgado, L., O.M. Anton, F. Bartolini, A. Ruiz-Saenz, I. Correas, G.G. Gundersen, and M.A. Alonso. 2012. INF2 promotes the formation of detyrosinated microtubules necessary for centrosome reorientation in T cells. *J Cell Biol*. 198:1025-1037.

Anthis, N.J., K.L. Wegener, F. Ye, C. Kim, B.T. Goult, E.D. Lowe, I. Vakonakis, N. Bate, D.R. Critchley, M.H. Ginsberg, and I.D. Campbell. 2009. The structure of an integrin/talin complex reveals the basis of inside-out signal transduction. *EMBO J*. 28:3623-3632.

Arakawa, Y., H. Bito, T. Furuyashiki, T. Tsuji, S. Takemoto-Kimura, K. Kimura, K. Nozaki, N. Hashimoto, and S. Narumiya. 2003. Control of axon elongation via an SDF-1alpha/Rho/mDia pathway in cultured cerebellar granule neurons. *J Cell Biol*. 161:381-391.

Arjonen, A., J. Alanko, S. Veltel, and J. Ivaska. 2012. Distinct recycling of active and inactive beta1 integrins. *Traffic*. 13:610-625.

Arthur, W.T., L.A. Petch, and K. Burridge. 2000. Integrin engagement suppresses RhoA activity via a c-Src-dependent mechanism. *Curr Biol*. 10:719-722.

Askari, J.A., P.A. Buckley, A.P. Mould, and M.J. Humphries. 2009. Linking integrin conformation to function. *Journal of cell science*. 122:165-170.

Askari, J.A., C.J. Tynan, S.E. Webb, M.L. Martin-Fernandez, C. Ballestrem, and M.J. Humphries. 2010. Focal adhesions are sites of integrin extension. *The Journal of cell biology*. 188:891-903.

Barsukov, I.L., A. Prescot, N. Bate, B. Patel, D.N. Floyd, N. Bhanji, C.R. Bagshaw, K. Letinic, G. Di Paolo, P. De Camilli, G.C. Roberts, and D.R. Critchley. 2003. Phosphatidylinositol phosphate kinase type 1gamma and beta1-integrin cytoplasmic domain bind to the same region in the talin FERM domain. *J Biol Chem*. 278:31202-31209.

Bartolini, F., and G.G. Gundersen. 2009. Formins and microtubules. *Biochim Biophys Acta*.

Bartolini, F., J.B. Moseley, J. Schmoranzer, L. Cassimeris, B.L. Goode, and G.G. Gundersen. 2008. The formin mDia2 stabilizes microtubules independently of its actin nucleation activity. *J Cell Biol*. 181:523-536.

Bartolini, F., N. Ramalingam, and G.G. Gundersen. 2012. Actin-capping protein promotes microtubule stability by antagonizing the actin activity of mDia1. *Mol Biol Cell*. 23:4032-4040.

Bellis, S.L., J.T. Miller, and C.E. Turner. 1995. Characterization of tyrosine phosphorylation of paxillin in vitro by focal adhesion kinase. *The Journal of biological chemistry*. 270:17437-17441.

Beningo, K.A., M. Dembo, I. Kaverina, J.V. Small, and Y.L. Wang. 2001. Nascent focal adhesions are responsible for the generation of strong propulsive forces in migrating fibroblasts. *J Cell Biol*. 153:881-888.

Berginski, M.E., E.A. Vitriol, K.M. Hahn, and S.M. Gomez. 2011. High-resolution quantification of focal adhesion spatiotemporal dynamics in living cells. *PloS one*. 6:e22025.
Bershadsky, A., A. Chausovsky, E. Becker, A. Lyubimova, and B. Geiger. 1996. Involvement of microtubules in the control of adhesion-dependent signal transduction. *Curr Biol*. 6:1279-1289.
Bershadsky, A.D., N.Q. Balaban, and B. Geiger. 2003. Adhesion-dependent cell mechanosensitivity. *Annual review of cell and developmental biology*. 19:677-695.
Bidkhori, G., Z. Narimani, S. Hosseini Ashtiani, A. Moeini, A. Nowzari-Dalini, and A. Masoudi-Nejad. 2013. Reconstruction of an integrated genome-scale co-expression network reveals key modules involved in lung adenocarcinoma. *PloS one*. 8:e67552.
Bieling, P., I.A. Telley, and T. Surrey. 2010. A minimal midzone protein module controls formation and length of antiparallel microtubule overlaps. *Cell*. 142:420-432.
Bisbal, M., J. Wojnacki, D. Peretti, A. Ropolo, J. Sesma, I. Jausoro, and A. Caceres. 2009. KIF4 mediates anterograde translocation and positioning of ribosomal constituents to axons. *J Biol Chem*. 284:9489-9497.
Bocckino, S.B., P. Wilson, and J.H. Exton. 1989. An enzymatic assay for picomole levels of phosphatidate. *Analytical biochemistry*. 180:24-27.
Borisy, G.G., and T.M. Svitkina. 2000. Actin machinery: pushing the envelope. *Curr Opin Cell Biol*. 12:104-112.
Bottcher, R.T., C. Stremmel, A. Meves, H. Meyer, M. Widmaier, H.Y. Tseng, and R. Fassler. 2012. Sorting nexin 17 prevents lysosomal degradation of beta1 integrins by binding to the beta1-integrin tail. *Nat Cell Biol*. 14:584-592.
Bouaouina, M., B.T. Goult, C. Huet-Calderwood, N. Bate, N.N. Brahme, I.L. Barsukov, D.R. Critchley, and D.A. Calderwood. 2012. A conserved lipid-binding loop in the kindlin FERM F1 domain is required for kindlin-mediated alphaIIbbeta3 integrin coactivation. *The Journal of biological chemistry*. 287:6979-6990.
Bouaouina, M., Y. Lad, and D.A. Calderwood. 2008. The N-terminal domains of talin cooperate with the phosphotyrosine binding-like domain to activate beta1 and beta3 integrins. *The Journal of biological chemistry*. 283:6118-6125.
Bouvard, D., J. Pouwels, N. De Franceschi, and J. Ivaska. 2013. Integrin inactivators: balancing cellular functions in vitro and in vivo. *Nature reviews. Molecular cell biology*. 14:430-442.
Brahme, N.N., D.S. Harburger, K. Kemp-O'Brien, R. Stewart, S. Raghavan, M. Parsons, and D.A. Calderwood. 2013. Kindlin binds migfilin tandem LIM domains and regulates migfilin focal adhesion localization and recruitment dynamics. *The Journal of biological chemistry*. 288:35604-35616.
Bravo-Cordero, J.J., R. Marrero-Diaz, D. Megias, L. Genis, A. Garcia-Grande, M.A. Garcia, A.G. Arroyo, and M.C. Montoya. 2007. MT1-MMP proinvasive activity is regulated by a novel Rab8-dependent exocytic pathway. *EMBO J*. 26:1499-1510.
Bretscher, M.S. 1989. Endocytosis and recycling of the fibronectin receptor in CHO cells. *The EMBO journal*. 8:1341-1348.
Bretscher, M.S. 1992. Circulating integrins: alpha 5 beta 1, alpha 6 beta 4 and Mac-1, but not alpha 3 beta 1, alpha 4 beta 1 or LFA-1. *The EMBO journal*. 11:405-410.
Bretscher, M.S., and C. Aguado-Velasco. 1998. Membrane traffic during cell locomotion. *Current opinion in cell biology*. 10:537-541.
Bridgewater, R.E., J.C. Norman, and P.T. Caswell. 2012. Integrin trafficking at a glance. *J Cell Sci*. 125:3695-3701.
Bringmann, H., G. Skiniotis, A. Spilker, S. Kandels-Lewis, I. Vernos, and T. Surrey. 2004. A kinesin-like motor inhibits microtubule dynamic instability. *Science*. 303:1519-1522.
Browning, H., and D.D. Hackney. 2005. The EB1 homolog Mal3 stimulates the ATPase of the kinesin Tea2 by recruiting it to the microtubule. *J Biol Chem*. 280:12299-12304.
Burridge, K., M. Chrzanowska-Wodnicka, and C. Zhong. 1997. Focal adhesion assembly. *Trends in cell biology*. 7:342-347.

Butler, B., and J.A. Cooper. 2009. Distinct roles for the actin nucleators Arp2/3 and hDia1 during NK-mediated cytotoxicity. *Curr Biol*. 19:1886-1896.

Byron, A., J.D. Humphries, J.A. Askari, S.E. Craig, A.P. Mould, and M.J. Humphries. 2009. Anti-integrin monoclonal antibodies. *J Cell Sci*. 122:4009-4011.

Calderwood, D.A. 2004a. Integrin activation. *J Cell Sci*. 117:657-666.

Calderwood, D.A. 2004b. Talin controls integrin activation. *Biochem Soc Trans*. 32:434-437.

Calderwood, D.A., Y. Fujioka, J.M. de Pereda, B. Garcia-Alvarez, T. Nakamoto, B. Margolis, C.J. McGlade, R.C. Liddington, and M.H. Ginsberg. 2003. Integrin beta cytoplasmic domain interactions with phosphotyrosine-binding domains: a structural prototype for diversity in integrin signaling. *Proc Natl Acad Sci U S A*. 100:2272-2277.

Calderwood, D.A., B. Yan, J.M. de Pereda, B.G. Alvarez, Y. Fujioka, R.C. Liddington, and M.H. Ginsberg. 2002. The phosphotyrosine binding-like domain of talin activates integrins. *J Biol Chem*. 277:21749-21758.

Calderwood, D.A., R. Zent, R. Grant, D.J. Rees, R.O. Hynes, and M.H. Ginsberg. 1999. The Talin head domain binds to integrin beta subunit cytoplasmic tails and regulates integrin activation. *J Biol Chem*. 274:28071-28074.

Caswell, P., and J. Norman. 2008. Endocytic transport of integrins during cell migration and invasion. *Trends Cell Biol*. 18:257-263.

Caswell, P.T., M. Chan, A.J. Lindsay, M.W. McCaffrey, D. Boettiger, and J.C. Norman. 2008. Rab-coupling protein coordinates recycling of alpha5beta1 integrin and EGFR1 to promote cell migration in 3D microenvironments. *The Journal of cell biology*. 183:143-155.

Caswell, P.T., and J.C. Norman. 2006. Integrin trafficking and the control of cell migration. *Traffic*. 7:14-21.

Caswell, P.T., H.J. Spence, M. Parsons, D.P. White, K. Clark, K.W. Cheng, G.B. Mills, M.J. Humphries, A.J. Messent, K.I. Anderson, M.W. McCaffrey, B.W. Ozanne, and J.C. Norman. 2007. Rab25 associates with alpha5beta1 integrin to promote invasive migration in 3D microenvironments. *Developmental cell*. 13:496-510.

Caswell, P.T., S. Vadrevu, and J.C. Norman. 2009. Integrins: masters and slaves of endocytic transport. *Nature reviews. Molecular cell biology*. 10:843-853.

Chao, W.T., F. Ashcroft, A.C. Daquinag, T. Vadakkan, Z. Wei, P. Zhang, M.E. Dickinson, and J. Kunz. 2010. Type I phosphatidylinositol phosphate kinase beta regulates focal adhesion disassembly by promoting beta1 integrin endocytosis. *Mol Cell Biol*. 30:4463-4479.

Chao, W.T., and J. Kunz. 2009. Focal adhesion disassembly requires clathrin-dependent endocytosis of integrins. *FEBS letters*. 583:1337-1343.

Chen, B.H., J.T. Tzen, A.R. Bresnick, and H.C. Chen. 2002. Roles of Rho-associated kinase and myosin light chain kinase in morphological and migratory defects of focal adhesion kinase-null cells. *J Biol Chem*. 277:33857-33863.

Chen, L.M., D. Bailey, and C. Fernandez-Valle. 2000. Association of beta 1 integrin with focal adhesion kinase and paxillin in differentiating Schwann cells. *The Journal of neuroscience : the official journal of the Society for Neuroscience*. 20:3776-3784.

Chen, R., O. Kim, M. Li, X. Xiong, J.L. Guan, H.J. Kung, H. Chen, Y. Shimizu, and Y. Qiu. 2001. Regulation of the PH-domain-containing tyrosine kinase Etk by focal adhesion kinase through the FERM domain. *Nat Cell Biol*. 3:439-444.

Cheng, K.W., J.P. Lahad, W.L. Kuo, A. Lapuk, K. Yamada, N. Auersperg, J. Liu, K. Smith-McCune, K.H. Lu, D. Fishman, J.W. Gray, and G.B. Mills. 2004. The RAB25 small GTPase determines aggressiveness of ovarian and breast cancers. *Nature medicine*. 10:1251-1256.

Choi, C.K., M. Vicente-Manzanares, J. Zareno, L.A. Whitmore, A. Mogilner, and A.R. Horwitz. 2008. Actin and alpha-actinin orchestrate the assembly and maturation of nascent adhesions in a myosin II motor-independent manner. *Nat Cell Biol*. 10:1039-1050.

Chrzanowska-Wodnicka, M., and K. Burridge. 1996. Rho-stimulated contractility drives the formation of stress fibers and focal adhesions. *The Journal of cell biology*. 133:1403-1415.

Cook, T.A., T. Nagasaki, and G.G. Gundersen. 1998. Rho guanosine triphosphatase mediates the selective stabilization of microtubules induced by lysophosphatidic acid. *J Cell Biol*. 141:175-185.

Critchley, D.R. 2005. Genetic, biochemical and structural approaches to talin function. *Biochem Soc Trans*. 33:1308-1312.

Crowley, E., and A.F. Horwitz. 1995. Tyrosine phosphorylation and cytoskeletal tension regulate the release of fibroblast adhesions. *The Journal of cell biology*. 131:525-537.

Curtis, A.S. 1964. The Mechanism of Adhesion of Cells to Glass. A Study by Interference Reflection Microscopy. *The Journal of cell biology*. 20:199-215.

Das, M., S.S. Ithychanda, J. Qin, and E.F. Plow. 2011. Migfilin and filamin as regulators of integrin activation in endothelial cells and neutrophils. *PloS one*. 6:e26355.

Di Paolo, G., L. Pellegrini, K. Letinic, G. Cestra, R. Zoncu, S. Voronov, S. Chang, J. Guo, M.R. Wenk, and P. De Camilli. 2002. Recruitment and regulation of phosphatidylinositol phosphate kinase type 1 gamma by the FERM domain of talin. *Nature*. 420:85-89.

Doyle, A.D., F.W. Wang, K. Matsumoto, and K.M. Yamada. 2009. One-dimensional topography underlies three-dimensional fibrillar cell migration. *J Cell Biol*. 184:481-490.

Dozynkiewicz, M.A., N.B. Jamieson, I. Macpherson, J. Grindlay, P.V. van den Berghe, A. von Thun, J.P. Morton, C. Gourley, P. Timpson, C. Nixon, C.J. McKay, R. Carter, D. Strachan, K. Anderson, O.J. Sansom, P.T. Caswell, and J.C. Norman. 2012. Rab25 and CLIC3 collaborate to promote integrin recycling from late endosomes/lysosomes and drive cancer progression. *Developmental cell*. 22:131-145.

Du, Y., C.A. English, and R. Ohi. 2010. The kinesin-8 Kif18A dampens microtubule plus-end dynamics. *Curr Biol*. 20:374-380.

Dunn, S., E.E. Morrison, T.B. Liverpool, C. Molina-Paris, R.A. Cross, M.C. Alonso, and M. Peckham. 2008. Differential trafficking of Kif5c on tyrosinated and detyrosinated microtubules in live cells. *J Cell Sci*. 121:1085-1095.

Efimova, N., A. Grimaldi, A. Bachmann, K. Frye, X. Zhu, A. Feoktistov, A. Straube, and I. Kaverina. 2014. Podosome-regulating kinesin KIF1C translocates to the cell periphery in a CLASP-dependent manner. *J Cell Sci*.

Ems-McClung, S.C., and C.E. Walczak. 2010. Kinesin-13s in mitosis: Key players in the spatial and temporal organization of spindle microtubules. *Semin Cell Dev Biol*. 21:276-282.

Emsley, J., C.G. Knight, R.W. Farndale, M.J. Barnes, and R.C. Liddington. 2000. Structural basis of collagen recognition by integrin alpha2beta1. *Cell*. 101:47-56.

Eng, C.H., T.M. Huckaba, and G.G. Gundersen. 2006. The formin mDia regulates GSK3beta through novel PKCs to promote microtubule stabilization but not MTOC reorientation in migrating fibroblasts. *Mol Biol Cell*. 17:5004-5016.

Eskova, A., B. Knapp, D. Matelska, S. Reusing, A. Arjonen, T. Lisauskas, R. Pepperkok, R. Russell, R. Eils, J. Ivaska, L. Kaderali, H. Erfle, and V. Starkuviene. 2014. An RNAi screen identifies KIF15 as a novel regulator of the endocytic trafficking of integrin. *Journal of cell science*. 127:2433-2447.

Etienne-Manneville, S. 2013. Microtubules in cell migration. *Annu Rev Cell Dev Biol*. 29:471-499.

Etienne-Manneville, S., and A. Hall. 2001. Integrin-mediated activation of Cdc42 controls cell polarity in migrating astrocytes through PKCzeta. *Cell*. 106:489-498.

Evers, E.E., G.C. Zondag, A. Malliri, L.S. Price, J.P. ten Klooster, R.A. van der Kammen, and J.G. Collard. 2000. Rho family proteins in cell adhesion and cell migration. *Eur J Cancer*. 36:1269-1274.

Ezratty, E.J., C. Bertaux, E.E. Marcantonio, and G.G. Gundersen. 2009. Clathrin mediates integrin endocytosis for focal adhesion disassembly in migrating cells. *The Journal of cell biology*. 187:733-747.

Ezratty, E.J., M.A. Partridge, and G.G. Gundersen. 2005. Microtubule-induced focal adhesion disassembly is mediated by dynamin and focal adhesion kinase. *Nature cell biology*. 7:581-590.

Fincham, V.J., M. Unlu, V.G. Brunton, J.D. Pitts, J.A. Wyke, and M.C. Frame. 1996. Translocation of Src kinase to the cell periphery is mediated by the actin cytoskeleton under the control of the Rho family of small G proteins. *The Journal of cell biology*. 135:1551-1564.

Fletcher, S.J., and J.Z. Rappoport. 2010. Moving forward: polarised trafficking in cell migration. *Trends in cell biology*. 20:71-78.

Franco, S., B. Perrin, and A. Huttenlocher. 2004a. Isoform specific function of calpain 2 in regulating membrane protrusion. *Experimental cell research*. 299:179-187.

Franco, S.J., M.A. Rodgers, B.J. Perrin, J. Han, D.A. Bennin, D.R. Critchley, and A. Huttenlocher. 2004b. Calpain-mediated proteolysis of talin regulates adhesion dynamics. *Nature cell biology*. 6:977-983.

Franco, S.J., M.A. Senetar, W.T. Simonson, A. Huttenlocher, and R.O. McCann. 2006. The conserved C-terminal I/LWEQ module targets Talin1 to focal adhesions. *Cell motility and the cytoskeleton*. 63:563-581.

Friedl, P., and D. Gilmour. 2009. Collective cell migration in morphogenesis, regeneration and cancer. *Nature reviews. Molecular cell biology*. 10:445-457.

Gailit, J., and E. Ruoslahti. 1988. Regulation of the fibronectin receptor affinity by divalent cations. *The Journal of biological chemistry*. 263:12927-12932.

Galbraith, C.G., K.M. Yamada, and M.P. Sheetz. 2002. The relationship between force and focal complex development. *J Cell Biol*. 159:695-705.

Gardel, M.L., I.C. Schneider, Y. Aratyn-Schaus, and C.M. Waterman. 2010. Mechanical integration of actin and adhesion dynamics in cell migration. *Annual review of cell and developmental biology*. 26:315-333.

Gardner, M.K., D.J. Odde, and K. Bloom. 2008. Kinesin-8 molecular motors: putting the brakes on chromosome oscillations. *Trends Cell Biol*. 18:307-310.

Geiger, B., A. Bershadsky, R. Pankov, and K.M. Yamada. 2001. Transmembrane crosstalk between the extracellular matrix--cytoskeleton crosstalk. *Nat Rev Mol Cell Biol*. 2:793-805.

Geiger, B., J.P. Spatz, and A.D. Bershadsky. 2009. Environmental sensing through focal adhesions. *Nature reviews. Molecular cell biology*. 10:21-33.

Geneste, O., J.W. Copeland, and R. Treisman. 2002. LIM kinase and Diaphanous cooperate to regulate serum response factor and actin dynamics. *J Cell Biol*. 157:831-838.

Glading, A., D.A. Lauffenburger, and A. Wells. 2002. Cutting to the chase: calpain proteases in cell motility. *Trends Cell Biol*. 12:46-54.

Goksoy, E., Y.Q. Ma, X. Wang, X. Kong, D. Perera, E.F. Plow, and J. Qin. 2008. Structural basis for the autoinhibition of talin in regulating integrin activation. *Molecular cell*. 31:124-133.

Golubovskaya, V.M., F.A. Kweh, and W.G. Cance. 2009. Focal adhesion kinase and cancer. *Histol Histopathol*. 24:503-510.

Gomes, E.R., S. Jani, and G.G. Gundersen. 2005. Nuclear movement regulated by Cdc42, MRCK, myosin, and actin flow establishes MTOC polarization in migrating cells. *Cell*. 121:451-463.

Gottschalk, K.E. 2005. A coiled-coil structure of the alphaIIbbeta3 integrin transmembrane and cytoplasmic domains in its resting state. *Structure*. 13:703-712.

Goulimari, P., T.M. Kitzing, H. Knieling, D.T. Brandt, S. Offermanns, and R. Grosse. 2005. Galpha12/13 is essential for directed cell migration and localized Rho-Dia1 function. *J Biol Chem*. 280:42242-42251.

Grant, B.D., and J.G. Donaldson. 2009. Pathways and mechanisms of endocytic recycling. *Nature reviews. Molecular cell biology*. 10:597-608.

Gu, Z., E.H. Noss, V.W. Hsu, and M.B. Brenner. 2011. Integrins traffic rapidly via circular dorsal ruffles and macropinocytosis during stimulated cell migration. *J Cell Biol*. 193:61-70.

Gundersen, G.G., and J.C. Bulinski. 1988. Selective stabilization of microtubules oriented toward the direction of cell migration. *Proc Natl Acad Sci U S A*. 85:5946-5950.

Gundersen, G.G., E.R. Gomes, and Y. Wen. 2004. Cortical control of microtubule stability and polarization. *Curr Opin Cell Biol*. 16:106-112.

Gundersen, G.G., M.H. Kalnoski, and J.C. Bulinski. 1984. Distinct populations of microtubules: tyrosinated and nontyrosinated alpha tubulin are distributed differently in vivo. *Cell*. 38:779-789.
Gundersen, G.G., S. Khawaja, and J.C. Bulinski. 1987. Postpolymerization detyrosination of alpha-tubulin: a mechanism for subcellular differentiation of microtubules. *J Cell Biol*. 105:251-264.
Gundersen, G.G., I. Kim, and C.J. Chapin. 1994. Induction of stable microtubules in 3T3 fibroblasts by TGF-beta and serum. *J Cell Sci*. 107:645-659.
Guo, F., M. Debidda, L. Yang, D.A. Williams, and Y. Zheng. 2006. Genetic deletion of Rac1 GTPase reveals its critical role in actin stress fiber formation and focal adhesion complex assembly. *J Biol Chem*. 281:18652-18659.
Gurland, G., and G.G. Gundersen. 1995. Stable, detyrosinated microtubules function to localize vimentin intermediate filaments in fibroblasts. *J Cell Biol*. 131:1275-1290.
Han, J., C.J. Lim, N. Watanabe, A. Soriani, B. Ratnikov, D.A. Calderwood, W. Puzon-McLaughlin, E.M. Lafuente, V.A. Boussiotis, S.J. Shattil, and M.H. Ginsberg. 2006. Reconstructing and deconstructing agonist-induced activation of integrin alphaIIbbeta3. *Current biology : CB*. 16:1796-1806.
Hanke, J.H., J.P. Gardner, R.L. Dow, P.S. Changelian, W.H. Brissette, E.J. Weringer, B.A. Pollok, and P.A. Connelly. 1996. Discovery of a novel, potent, and Src family-selective tyrosine kinase inhibitor. Study of Lck- and FynT-dependent T cell activation. *The Journal of biological chemistry*. 271:695-701.
Hanks, S.K., L. Ryzhova, N.Y. Shin, and J. Brabek. 2003. Focal adhesion kinase signaling activities and their implications in the control of cell survival and motility. *Front Biosci*. 8:d982-996.
Harburger, D.S., M. Bouaouina, and D.A. Calderwood. 2009. Kindlin-1 and -2 directly bind the C-terminal region of beta integrin cytoplasmic tails and exert integrin-specific activation effects. *The Journal of biological chemistry*. 284:11485-11497.
Harburger, D.S., and D.A. Calderwood. 2009. Integrin signalling at a glance. *Journal of cell science*. 122:159-163.
Hendey, B., C.B. Klee, and F.R. Maxfield. 1992. Inhibition of neutrophil chemokinesis on vitronectin by inhibitors of calcineurin. *Science*. 258:296-299.
Hirokawa, N., Y. Noda, Y. Tanaka, and S. Niwa. 2009. Kinesin superfamily motor proteins and intracellular transport. *Nat Rev Mol Cell Biol*. 10:682-696.
Horgan, C.P., and M.W. McCaffrey. 2011. Rab GTPases and microtubule motors. *Biochem Soc Trans*. 39:1202-1206.
Hsia, D.A., S.K. Mitra, C.R. Hauck, D.N. Streblow, J.A. Nelson, D. Ilic, S. Huang, E. Li, G.R. Nemerow, J. Leng, K.S. Spencer, D.A. Cheresh, and D.D. Schlaepfer. 2003. Differential regulation of cell motility and invasion by FAK. *J Cell Biol*. 160:753-767.
Hu, C.K., M. Coughlin, C.M. Field, and T.J. Mitchison. 2011. KIF4 regulates midzone length during cytokinesis. *Curr Biol*. 21:815-824.
Hu, K., L. Ji, K.T. Applegate, G. Danuser, and C.M. Waterman-Storer. 2007. Differential transmission of actin motion within focal adhesions. *Science*. 315:111-115.
Hughes, P.E., F. Diaz-Gonzalez, L. Leong, C. Wu, J.A. McDonald, S.J. Shattil, and M.H. Ginsberg. 1996. Breaking the integrin hinge. A defined structural constraint regulates integrin signaling. *J Biol Chem*. 271:6571-6574.
Humphries, J.D., P. Wang, C. Streuli, B. Geiger, M.J. Humphries, and C. Ballestrem. 2007. Vinculin controls focal adhesion formation by direct interactions with talin and actin. *J Cell Biol*. 179:1043-1057.
Hynes, R.O. 2002. Integrins: bidirectional, allosteric signaling machines. *Cell*. 110:673-687.
Ilic, D., Y. Furuta, S. Kanazawa, N. Takeda, K. Sobue, N. Nakatsuji, S. Nomura, J. Fujimoto, M. Okada, and T. Yamamoto. 1995. Reduced cell motility and enhanced focal adhesion contact formation in cells from FAK-deficient mice. *Nature*. 377:539-544.

Ilic, D., O. Genbacev, F. Jin, E. Caceres, E.A. Almeida, V. Bellingard-Dubouchaud, E.M. Schaefer, C.H. Damsky, and S.J. Fisher. 2001. Plasma membrane-associated pY397FAK is a marker of cytotrophoblast invasion in vivo and in vitro. *The American journal of pathology*. 159:93-108.

Infante, A.S., M.S. Stein, Y. Zhai, G.G. Borisy, and G.G. Gundersen. 2000. Detyrosinated (Glu) microtubules are stabilized by an ATP-sensitive plus-end cap. *J Cell Sci*. 113 (Pt 22):3907-3919.

Ithychanda, S.S., D. Hsu, H. Li, L. Yan, D.D. Liu, M. Das, E.F. Plow, and J. Qin. 2009. Identification and characterization of multiple similar ligand-binding repeats in filamin: implication on filamin-mediated receptor clustering and cross-talk. *The Journal of biological chemistry*. 284:35113-35121.

Izzard, C.S., and L.R. Lochner. 1976. Cell-to-substrate contacts in living fibroblasts: an interference reflexion study with an evaluation of the technique. *Journal of cell science*. 21:129-159.

Izzard, C.S., and L.R. Lochner. 1980. Formation of cell-to-substrate contacts during fibroblast motility: an interference-reflexion study. *Journal of cell science*. 42:81-116.

Jaulin, F., and G. Kreitzer. 2010. KIF17 stabilizes microtubules and contributes to epithelial morphogenesis by acting at MT plus ends with EB1 and APC. *J Cell Biol*. 190:443-460.

Jimbo, T., Y. Kawasaki, R. Koyama, R. Sato, S. Takada, K. Haraguchi, and T. Akiyama. 2002. Identification of a link between the tumour suppressor APC and the kinesin superfamily. *Nat Cell Biol*. 4:323-327.

Jones, M.C., P.T. Caswell, and J.C. Norman. 2006. Endocytic recycling pathways: emerging regulators of cell migration. *Curr Opin Cell Biol*. 18:549-557.

Kaplan, K.B., J.R. Swedlow, H.E. Varmus, and D.O. Morgan. 1992. Association of p60c-src with endosomal membranes in mammalian fibroblasts. *The Journal of cell biology*. 118:321-333.

Kasahara, K., Y. Nakayama, A. Kihara, D. Matsuda, K. Ikeda, T. Kuga, Y. Fukumoto, Y. Igarashi, and N. Yamaguchi. 2007. Rapid trafficking of c-Src, a non-palmitoylated Src-family kinase, between the plasma membrane and late endosomes/lysosomes. *Experimental cell research*. 313:2651-2666.

Katz, B.Z., E. Zamir, A. Bershadsky, Z. Kam, K.M. Yamada, and B. Geiger. 2000. Physical state of the extracellular matrix regulates the structure and molecular composition of cell-matrix adhesions. *Mol Biol Cell*. 11:1047-1060.

Kaverina, I., O. Krylyshkina, and J.V. Small. 1999. Microtubule targeting of substrate contacts promotes their relaxation and dissociation. *The Journal of cell biology*. 146:1033-1044.

Kaverina, I., K. Rottner, and J.V. Small. 1998. Targeting, capture, and stabilization of microtubules at early focal adhesions. *The Journal of cell biology*. 142:181-190.

Kaverina, I., and A. Straube. 2011. Regulation of cell migration by dynamic microtubules. *Seminars in cell & developmental biology*. 22:968-974.

Kharbanda, S., A. Saleem, Z. Yuan, Y. Emoto, K.V. Prasad, and D. Kufe. 1995. Stimulation of human monocytes with macrophage colony-stimulating factor induces a Grb2-mediated association of the focal adhesion kinase pp125FAK and dynamin. *Proceedings of the National Academy of Sciences of the United States of America*. 92:6132-6136.

Khawaja, S., G.G. Gundersen, and J.C. Bulinski. 1988. Enhanced stability of microtubules enriched in detyrosinated tubulin is not a direct function of detyrosination level. *J Cell Biol*. 106:141-149.

Kiema, T., Y. Lad, P. Jiang, C.L. Oxley, M. Baldassarre, K.L. Wegener, I.D. Campbell, J. Ylanne, and D.A. Calderwood. 2006. The molecular basis of filamin binding to integrins and competition with talin. *Molecular cell*. 21:337-347.

Kim, C., F. Ye, and M.H. Ginsberg. 2011. Regulation of integrin activation. *Annu Rev Cell Dev Biol*. 27:321-345.

Kim, M., C.V. Carman, and T.A. Springer. 2003. Bidirectional transmembrane signaling by cytoplasmic domain separation in integrins. *Science*. 301:1720-1725.

Kim, W., Y. Tang, Y. Okada, T.A. Torrey, S.K. Chattopadhyay, M. Pfleiderer, F.G. Falkner, F. Dorner, W. Choi, N. Hirokawa, and H.C. Morse, 3rd. 1998. Binding of murine leukemia virus Gag polyproteins to KIF4, a microtubule-based motor protein. *J Virol*. 72:6898-6901.

Kimura, K., M. Ito, M. Amano, K. Chihara, Y. Fukata, M. Nakafuku, B. Yamamori, J. Feng, T. Nakano, K. Okawa, A. Iwamatsu, and K. Kaibuchi. 1996. Regulation of myosin phosphatase by Rho and Rho-associated kinase (Rho-kinase). *Science*. 273:245-248.

Kloeker, S., M.B. Major, D.A. Calderwood, M.H. Ginsberg, D.A. Jones, and M.C. Beckerle. 2004. The Kindler syndrome protein is regulated by transforming growth factor-beta and involved in integrin-mediated adhesion. *The Journal of biological chemistry*. 279:6824-6833.

Kodama, A., I. Karakesisoglou, E. Wong, A. Vaezi, and E. Fuchs. 2003. ACF7. An essential integrator of microtubule dynamics. *Cell*. 115:343-354.

Konishi, Y., and M. Setou. 2009. Tubulin tyrosination navigates the kinesin-1 motor domain to axons. *Nat Neurosci*. 12:559-567.

Koonce, M.P., R.A. Cloney, and M.W. Berns. 1984. Laser irradiation of centrosomes in newt eosinophils: evidence of centriole role in motility. *J Cell Biol*. 98:1999-2010.

Kopp, P., R. Lammers, M. Aepfelbacher, G. Woehlke, T. Rudel, N. Machuy, W. Steffen, and S. Linder. 2006. The kinesin KIF1C and microtubule plus ends regulate podosome dynamics in macrophages. *Mol Biol Cell*. 17:2811-2823.

Kreitzer, G., G. Liao, and G.G. Gundersen. 1999. Detyrosination of tubulin regulates the interaction of intermediate filaments with microtubules in vivo via a kinesin-dependent mechanism. *Mol Biol Cell*. 10:1105-1118.

Krylyshkina, O., I. Kaverina, W. Kranewitter, W. Steffen, M.C. Alonso, R.A. Cross, and J.V. Small. 2002. Modulation of substrate adhesion dynamics via microtubule targeting requires kinesin-1. *The Journal of cell biology*. 156:349-359.

Kurasawa, Y., W.C. Earnshaw, Y. Mochizuki, N. Dohmae, and K. Todokoro. 2004. Essential roles of KIF4 and its binding partner PRC1 in organized central spindle midzone formation. *EMBO J*. 23:3237-3248.

Lad, Y., P. Jiang, S. Ruskamo, D.S. Harburger, J. Ylanne, I.D. Campbell, and D.A. Calderwood. 2008. Structural basis of the migfilin-filamin interaction and competition with integrin beta tails. *The Journal of biological chemistry*. 283:35154-35163.

Lansbergen, G., and A. Akhmanova. 2006. Microtubule plus end: a hub of cellular activities. *Traffic*. 7:499-507.

Lansbergen, G., I. Grigoriev, Y. Mimori-Kiyosue, T. Ohtsuka, S. Higa, I. Kitajima, J. Demmers, N. Galjart, A.B. Houtsmuller, F. Grosveld, and A. Akhmanova. 2006. CLASPs attach microtubule plus ends to the cell cortex through a complex with LL5beta. *Dev Cell*. 11:21-32.

Lapierre, L.A., R. Kumar, C.M. Hales, J. Navarre, S.G. Bhartur, J.O. Burnette, D.W. Provance, Jr., J.A. Mercer, M. Bahler, and J.R. Goldenring. 2001. Myosin vb is associated with plasma membrane recycling systems. *Molecular biology of the cell*. 12:1843-1857.

Lau, T.L., V. Dua, and T.S. Ulmer. 2008. Structure of the integrin alphaIIb transmembrane segment. *J Biol Chem*. 283:16162-16168.

Lauffenburger, D.A., and A.F. Horwitz. 1996. Cell migration: a physically integrated molecular process. *Cell*. 84:359-369.

Laukaitis, C.M., D.J. Webb, K. Donais, and A.F. Horwitz. 2001. Differential dynamics of alpha 5 integrin, paxillin, and alpha-actinin during formation and disassembly of adhesions in migrating cells. *The Journal of cell biology*. 153:1427-1440.

Lawson, C., S.T. Lim, S. Uryu, X.L. Chen, D.A. Calderwood, and D.D. Schlaepfer. 2012. FAK promotes recruitment of talin to nascent adhesions to control cell motility. *The Journal of cell biology*. 196:223-232.

Lawson, M.A., and F.R. Maxfield. 1995. Ca(2+)- and calcineurin-dependent recycling of an integrin to the front of migrating neutrophils. *Nature*. 377:75-79.

Lee, J., A. Ishihara, G. Oxford, B. Johnson, and K. Jacobson. 1999. Regulation of cell movement is mediated by stretch-activated calcium channels. *Nature*. 400:382-386.

Lewkowicz, E., F. Herit, C. Le Clainche, P. Bourdoncle, F. Perez, and F. Niedergang. 2008. The microtubule-binding protein CLIP-170 coordinates mDia1 and actin reorganization during CR3-mediated phagocytosis. *J Cell Biol*. 183:1287-1298.

Li, F., and H.N. Higgs. 2003. The mouse Formin mDia1 is a potent actin nucleation factor regulated by autoinhibition. *Curr Biol*. 13:1335-1340.

Li, J., B.A. Ballif, A.M. Powelka, J. Dai, S.P. Gygi, and V.W. Hsu. 2005a. Phosphorylation of ACAP1 by Akt regulates the stimulation-dependent recycling of integrin beta1 to control cell migration. *Developmental cell*. 9:663-673.

Li, R., and G.G. Gundersen. 2008. Beyond polymer polarity: how the cytoskeleton builds a polarized cell. *Nat Rev Mol Cell Biol*. 9:860-873.

Li, S., J.L. Guan, and S. Chien. 2005b. Biochemistry and biomechanics of cell motility. *Annu Rev Biomed Eng*. 7:105-150.

Liao, G., and G.G. Gundersen. 1998. Kinesin is a candidate for cross-bridging microtubules and intermediate filaments. Selective binding of kinesin to detyrosinated tubulin and vimentin. *J Biol Chem*. 273:9797-9803.

Liao, G., T. Nagasaki, and G.G. Gundersen. 1995. Low concentrations of nocodazole interfere with fibroblast locomotion without significantly affecting microtubule level: implications for the role of dynamic microtubules in cell locomotion. *Journal of cell science*. 108 (Pt 11):3473-3483.

Lim, Y., I. Han, J. Jeon, H. Park, Y.Y. Bahk, and E.S. Oh. 2004. Phosphorylation of focal adhesion kinase at tyrosine 861 is crucial for Ras transformation of fibroblasts. *J Biol Chem*. 279:29060-29065.

Lin, S.X., G.G. Gundersen, and F.R. Maxfield. 2002. Export from pericentriolar endocytic recycling compartment to cell surface depends on stable, detyrosinated (glu) microtubules and kinesin. *Mol Biol Cell*. 13:96-109.

Ling, K., R.L. Doughman, A.J. Firestone, M.W. Bunce, and R.A. Anderson. 2002. Type I gamma phosphatidylinositol phosphate kinase targets and regulates focal adhesions. *Nature*. 420:89-93.

Lobert, V.H., A. Brech, N.M. Pedersen, J. Wesche, A. Oppelt, L. Malerod, and H. Stenmark. 2010. Ubiquitination of alpha 5 beta 1 integrin controls fibroblast migration through lysosomal degradation of fibronectin-integrin complexes. *Dev Cell*. 19:148-159.

Luo, B.H., C.V. Carman, J. Takagi, and T.A. Springer. 2005. Disrupting integrin transmembrane domain heterodimerization increases ligand binding affinity, not valency or clustering. *Proc Natl Acad Sci U S A*. 102:3679-3684.

Luo, B.H., T.A. Springer, and J. Takagi. 2004. A specific interface between integrin transmembrane helices and affinity for ligand. *PLoS Biol*. 2:e153.

Luxton, G.W., E.R. Gomes, E.S. Folker, E. Vintinner, and G.G. Gundersen. 2010. Linear arrays of nuclear envelope proteins harness retrograde actin flow for nuclear movement. *Science*. 329:956-959.

Luxton, G.W., and G.G. Gundersen. 2011. Orientation and function of the nuclear-centrosomal axis during cell migration. *Curr Opin Cell Biol*. 23:579-588.

Ma, Y.Q., J. Qin, C. Wu, and E.F. Plow. 2008. Kindlin-2 (Mig-2): a co-activator of beta3 integrins. *J Cell Biol*. 181:439-446.

Machacek, M., L. Hodgson, C. Welch, H. Elliott, O. Pertz, P. Nalbant, A. Abell, G.L. Johnson, K.M. Hahn, and G. Danuser. 2009. Coordination of Rho GTPase activities during cell protrusion. *Nature*. 461:99-103.

Margadant, C., R.A. Charafeddine, and A. Sonnenberg. 2010. Unique and redundant functions of integrins in the epidermis. *FASEB J*. 24:4133-4152.

Margadant, C., M. Kreft, D.J. de Groot, J.C. Norman, and A. Sonnenberg. 2012. Distinct roles of talin and kindlin in regulating integrin alpha5beta1 function and trafficking. *Curr Biol*. 22:1554-1563.

Margadant, C., H.N. Monsuur, J.C. Norman, and A. Sonnenberg. 2011. Mechanisms of integrin activation and trafficking. *Curr Opin Cell Biol*. 23:607-614.

Margadant, C., K. Raymond, M. Kreft, N. Sachs, H. Janssen, and A. Sonnenberg. 2009. Integrin alpha3beta1 inhibits directional migration and wound re-epithelialization in the skin. *J Cell Sci*. 122:278-288.

Martel, V., C. Racaud-Sultan, S. Dupe, C. Marie, F. Paulhe, A. Galmiche, M.R. Block, and C. Albiges-Rizo. 2001. Conformation, localization, and integrin binding of talin depend on its interaction with phosphoinositides. *The Journal of biological chemistry*. 276:21217-21227.

Martinez, N.W., X. Xue, R.G. Berro, G. Kreitzer, and M.D. Resh. 2008. Kinesin KIF4 regulates intracellular trafficking and stability of the human immunodeficiency virus type 1 Gag polyprotein. *J Virol*. 82:9937-9950.

Mazumdar, M., S. Sundareshan, and T. Misteli. 2004. Human chromokinesin KIF4A functions in chromosome condensation and segregation. *J Cell Biol*. 166:613-620.

Meves, A., C. Stremmel, K. Gottschalk, and R. Fassler. 2009. The Kindlin protein family: new members to the club of focal adhesion proteins. *Trends Cell Biol*. 19:504-513.

Mikhailov, A., and G.G. Gundersen. 1998. Relationship between microtubule dynamics and lamellipodium formation revealed by direct imaging of microtubules in cells treated with nocodazole or taxol. *Cell motility and the cytoskeleton*. 41:325-340.

Miller, P.M., A.W. Folkmann, A.R. Maia, N. Efimova, A. Efimov, and I. Kaverina. 2009. Golgi-derived CLASP-dependent microtubules control Golgi organization and polarized trafficking in motile cells. *Nat Cell Biol*. 11:1069-1080.

Mimori-Kiyosue, Y., I. Grigoriev, G. Lansbergen, H. Sasaki, C. Matsui, F. Severin, N. Galjart, F. Grosveld, I. Vorobjev, S. Tsukita, and A. Akhmanova. 2005. CLASP1 and CLASP2 bind to EB1 and regulate microtubule plus-end dynamics at the cell cortex. *J Cell Biol*. 168:141-153.

Mingle, L.A., N.N. Okuhama, J. Shi, R.H. Singer, J. Condeelis, and G. Liu. 2005. Localization of all seven messenger RNAs for the actin-polymerization nucleator Arp2/3 complex in the protrusions of fibroblasts. *Journal of cell science*. 118:2425-2433.

Mitra, S.K., D.A. Hanson, and D.D. Schlaepfer. 2005. Focal adhesion kinase: in command and control of cell motility. *Nature reviews. Molecular cell biology*. 6:56-68.

Mohl, C., N. Kirchgessner, C. Schafer, B. Hoffmann, and R. Merkel. 2012. Quantitative mapping of averaged focal adhesion dynamics in migrating cells by shape normalization. *Journal of cell science*. 125:155-165.

Montanez, E., S. Ussar, M. Schifferer, M. Bosl, R. Zent, M. Moser, and R. Fassler. 2008. Kindlin-2 controls bidirectional signaling of integrins. *Genes Dev*. 22:1325-1330.

Morse, E.M., N.N. Brahme, and D.A. Calderwood. 2014. Integrin cytoplasmic tail interactions. *Biochemistry*. 53:810-820.

Moser, M., K.R. Legate, R. Zent, and R. Fassler. 2009. The tail of integrins, talin, and kindlins. *Science*. 324:895-899.

Moser, M., B. Nieswandt, S. Ussar, M. Pozgajova, and R. Fassler. 2008. Kindlin-3 is essential for integrin activation and platelet aggregation. *Nat Med*. 14:325-330.

Murphy, D.A., and S.A. Courtneidge. 2011. The 'ins' and 'outs' of podosomes and invadopodia: characteristics, formation and function. *Nat Rev Mol Cell Biol*. 12:413-426.

Musse, A.A., L. Meloty-Kapella, and G. Weinmaster. 2012. Notch ligand endocytosis: mechanistic basis of signaling activity. *Seminars in cell & developmental biology*. 23:429-436.

Naghavi, M.H., S. Valente, T. Hatziioannou, K. de Los Santos, Y. Wen, C. Mott, G.G. Gundersen, and S.P. Goff. 2007. Moesin regulates stable microtubule formation and limits retroviral infection in cultured cells. *EMBO J*. 26:41-52.

Nakano, K., K. Takaishi, A. Kodama, A. Mammoto, H. Shiozaki, M. Monden, and Y. Takai. 1999. Distinct actions and cooperative roles of ROCK and mDia in Rho small G protein-induced reorganization of the actin cytoskeleton in Madin-Darby canine kidney cells. *Mol Biol Cell*. 10:2481-2491.

Nasuhoglu, C., S. Feng, J. Mao, M. Yamamoto, H.L. Yin, S. Earnest, B. Barylko, J.P. Albanesi, and D.W. Hilgemann. 2002. Nonradioactive analysis of phosphatidylinositides and other anionic

phospholipids by anion-exchange high-performance liquid chromatography with suppressed conductivity detection. *Analytical biochemistry*. 301:243-254.
Nieswandt, B., M. Moser, I. Pleines, D. Varga-Szabo, S. Monkley, D. Critchley, and R. Fassler. 2007. Loss of talin1 in platelets abrogates integrin activation, platelet aggregation, and thrombus formation in vitro and in vivo. *J Exp Med*. 204:3113-3118.
Nishimura, T., and K. Kaibuchi. 2007. Numb controls integrin endocytosis for directional cell migration with aPKC and PAR-3. *Dev Cell*. 13:15-28.
Nobes, C.D., and A. Hall. 1995. Rho, rac, and cdc42 GTPases regulate the assembly of multimolecular focal complexes associated with actin stress fibers, lamellipodia, and filopodia. *Cell*. 81:53-62.
Nousiainen, M., H.H. Sillje, G. Sauer, E.A. Nigg, and R. Korner. 2006. Phosphoproteome analysis of the human mitotic spindle. *Proc Natl Acad Sci U S A*. 103:5391-5396.
Nunes Bastos, R., S.R. Gandhi, R.D. Baron, U. Gruneberg, E.A. Nigg, and F.A. Barr. 2013. Aurora B suppresses microtubule dynamics and limits central spindle size by locally activating KIF4A. *J Cell Biol*. 202:605-621.
Oliver, C., and M.C. Jamur. 2010. Immunocytochemical methods and protocols. *Methods Mol Biol*. 588:iv-v.
Palamidessi, A., E. Frittoli, M. Garre, M. Faretta, M. Mione, I. Testa, A. Diaspro, L. Lanzetti, G. Scita, and P.P. Di Fiore. 2008. Endocytic trafficking of Rac is required for the spatial restriction of signaling in cell migration. *Cell*. 134:135-147.
Palazzo, A., B. Ackerman, and G.G. Gundersen. 2003. Cell biology: Tubulin acetylation and cell motility. *Nature*. 421:230.
Palazzo, A.F., T.A. Cook, A.S. Alberts, and G.G. Gundersen. 2001a. mDia mediates Rho-regulated formation and orientation of stable microtubules. *Nat Cell Biol*. 3:723-729.
Palazzo, A.F., C.H. Eng, D.D. Schlaepfer, E.E. Marcantonio, and G.G. Gundersen. 2004. Localized stabilization of microtubules by integrin- and FAK-facilitated Rho signaling. *Science*. 303:836-839.
Palazzo, A.F., H.L. Joseph, Y.J. Chen, D.L. Dujardin, A.S. Alberts, K.K. Pfister, R.B. Vallee, and G.G. Gundersen. 2001b. Cdc42, dynein, and dynactin regulate MTOC reorientation independent of Rho-regulated microtubule stabilization. *Curr Biol*. 11:1536-1541.
Palazzo, R.E., and D. N.D. 2001. Centrosomes and Spindle Pole Bodies. Academic Press.
Pankov, R., E. Cukierman, B.Z. Katz, K. Matsumoto, D.C. Lin, S. Lin, C. Hahn, and K.M. Yamada. 2000. Integrin dynamics and matrix assembly: tensin-dependent translocation of alpha(5)beta(1) integrins promotes early fibronectin fibrillogenesis. *J Cell Biol*. 148:1075-1090.
Papagrigoriou, E., A.R. Gingras, I.L. Barsukov, N. Bate, I.J. Fillingham, B. Patel, R. Frank, W.H. Ziegler, G.C. Roberts, D.R. Critchley, and J. Emsley. 2004. Activation of a vinculin-binding site in the talin rod involves rearrangement of a five-helix bundle. *EMBO J*. 23:2942-2951.
Parsons, J.T. 2003. Focal adhesion kinase: the first ten years. *J Cell Sci*. 116:1409-1416.
Parsons, J.T., A.R. Horwitz, and M.A. Schwartz. 2010. Cell adhesion: integrating cytoskeletal dynamics and cellular tension. *Nat Rev Mol Cell Biol*. 11:633-643.
Partridge, A.W., S. Liu, S. Kim, J.U. Bowie, and M.H. Ginsberg. 2005. Transmembrane domain helix packing stabilizes integrin alphaIIbbeta3 in the low affinity state. *J Biol Chem*. 280:7294-7300.
Pellinen, T., A. Arjonen, K. Vuoriluoto, K. Kallio, J.A. Fransen, and J. Ivaska. 2006. Small GTPase Rab21 regulates cell adhesion and controls endosomal traffic of beta1-integrins. *The Journal of cell biology*. 173:767-780.
Pellinen, T., and J. Ivaska. 2006. Integrin traffic. *Journal of cell science*. 119:3723-3731.
Peretti, D., L. Peris, S. Rosso, S. Quiroga, and A. Caceres. 2000. Evidence for the involvement of KIF4 in the anterograde transport of L1-containing vesicles. *J Cell Biol*. 149:141-152.
Peris, L., M. Wagenbach, L. Lafanechere, J. Brocard, A.T. Moore, F. Kozielski, D. Job, L. Wordeman, and A. Andrieux. 2009. Motor-dependent microtubule disassembly driven by tubulin tyrosination. *J Cell Biol*. 185:1159-1166.

Pertz, O., L. Hodgson, R.L. Klemke, and K.M. Hahn. 2006. Spatiotemporal dynamics of RhoA activity in migrating cells. *Nature*. 440:1069-1072.
Petrich, B.G., P. Marchese, Z.M. Ruggeri, S. Spiess, R.A. Weichert, F. Ye, R. Tiedt, R.C. Skoda, S.J. Monkley, D.R. Critchley, and M.H. Ginsberg. 2007. Talin is required for integrin-mediated platelet function in hemostasis and thrombosis. *J Exp Med*. 204:3103-3111.
Pierini, L.M., M.A. Lawson, R.J. Eddy, B. Hendey, and F.R. Maxfield. 2000. Oriented endocytic recycling of alpha5beta1 in motile neutrophils. *Blood*. 95:2471-2480.
Pletjushkina, O.J., A.M. Belkin, O.J. Ivanova, T. Oliver, J.M. Vasiliev, and K. Jacobson. 1998. Maturation of cell-substratum focal adhesions induced by depolymerization of microtubules is mediated by increased cortical tension. *Cell Adhes Commun*. 5:121-135.
Pollard, T.D., and G.G. Borisy. 2003. Cellular motility driven by assembly and disassembly of actin filaments. *Cell*. 112:453-465.
Powelka, A.M., J. Sun, J. Li, M. Gao, L.M. Shaw, A. Sonnenberg, and V.W. Hsu. 2004. Stimulation-dependent recycling of integrin beta1 regulated by ARF6 and Rab11. *Traffic*. 5:20-36.
Prigozhina, N.L., and C.M. Waterman-Storer. 2004. Protein kinase D-mediated anterograde membrane trafficking is required for fibroblast motility. *Curr Biol*. 14:88-98.
Provance, D.W., Jr., E.J. Addison, P.R. Wood, D.Z. Chen, C.M. Silan, and J.A. Mercer. 2008. Myosin-Vb functions as a dynamic tether for peripheral endocytic compartments during transferrin trafficking. *BMC cell biology*. 9:44.
Rainero, E., and J.C. Norman. 2013. Late endosomal and lysosomal trafficking during integrin-mediated cell migration and invasion: cell matrix receptors are trafficked through the late endosomal pathway in a way that dictates how cells migrate. *Bioessays*. 35:523-532.
Rantala, J.K., J. Pouwels, T. Pellinen, S. Veltel, P. Laasola, E. Mattila, C.S. Potter, T. Duffy, J.P. Sundberg, O. Kallioniemi, J.A. Askari, M.J. Humphries, M. Parsons, M. Salmi, and J. Ivaska. 2011. SHARPIN is an endogenous inhibitor of beta1-integrin activation. *Nature cell biology*. 13:1315-1324.
Rappoport, J.Z., and S.M. Simon. 2003. Real-time analysis of clathrin-mediated endocytosis during cell migration. *J Cell Sci*. 116:847-855.
Reed, N.A., D. Cai, T.L. Blasius, G.T. Jih, E. Meyhofer, J. Gaertig, and K.J. Verhey. 2006. Microtubule acetylation promotes kinesin-1 binding and transport. *Curr Biol*. 16:2166-2172.
Ren, X.D., W.B. Kiosses, D.J. Sieg, C.A. Otey, D.D. Schlaepfer, and M.A. Schwartz. 2000. Focal adhesion kinase suppresses Rho activity to promote focal adhesion turnover. *J Cell Sci*. 113 (Pt 20):3673-3678.
Ridley, A.J., and A. Hall. 1992. The small GTP-binding protein rho regulates the assembly of focal adhesions and actin stress fibers in response to growth factors. *Cell*. 70:389-399.
Ridley, A.J., H.F. Paterson, C.L. Johnston, D. Diekmann, and A. Hall. 1992. The small GTP-binding protein rac regulates growth factor-induced membrane ruffling. *Cell*. 70:401-410.
Ridley, A.J., M.A. Schwartz, K. Burridge, R.A. Firtel, M.H. Ginsberg, G. Borisy, J.T. Parsons, and A.R. Horwitz. 2003. Cell migration: integrating signals from front to back. *Science*. 302:1704-1709.
Roberts, M., S. Barry, A. Woods, P. van der Sluijs, and J. Norman. 2001. PDGF-regulated rab4-dependent recycling of alphavbeta3 integrin from early endosomes is necessary for cell adhesion and spreading. *Current biology : CB*. 11:1392-1402.
Roberts, M.S., A.J. Woods, T.C. Dale, P. Van Der Sluijs, and J.C. Norman. 2004. Protein kinase B/Akt acts via glycogen synthase kinase 3 to regulate recycling of alpha v beta 3 and alpha 5 beta 1 integrins. *Molecular and cellular biology*. 24:1505-1515.
Rossier, O., V. Octeau, J.B. Sibarita, C. Leduc, B. Tessier, D. Nair, V. Gatterdam, O. Destaing, C. Albiges-Rizo, R. Tampe, L. Cognet, D. Choquet, B. Lounis, and G. Giannone. 2012. Integrins beta1 and beta3 exhibit distinct dynamic nanoscale organizations inside focal adhesions. *Nature cell biology*. 14:1057-1067.
Rottner, K., A. Hall, and J.V. Small. 1999. Interplay between Rac and Rho in the control of substrate contact dynamics. *Curr Biol*. 9:640-648.

Sandilands, E., V.G. Brunton, and M.C. Frame. 2007. The membrane targeting and spatial activation of Src, Yes and Fyn is influenced by palmitoylation and distinct RhoB/RhoD endosome requirements. *Journal of cell science*. 120:2555-2564.

Sandilands, E., C. Cans, V.J. Fincham, V.G. Brunton, H. Mellor, G.C. Prendergast, J.C. Norman, G. Superti-Furga, and M.C. Frame. 2004. RhoB and actin polymerization coordinate Src activation with endosome-mediated delivery to the membrane. *Developmental cell*. 7:855-869.

Sandilands, E., and M.C. Frame. 2008. Endosomal trafficking of Src tyrosine kinase. *Trends in cell biology*. 18:322-329.

Schaller, M.D. 2001. Biochemical signals and biological responses elicited by the focal adhesion kinase. *Biochim Biophys Acta*. 1540:1-21.

Schaller, M.D., C.A. Otey, J.D. Hildebrand, and J.T. Parsons. 1995. Focal adhesion kinase and paxillin bind to peptides mimicking beta integrin cytoplasmic domains. *The Journal of cell biology*. 130:1181-1187.

Schaller, M.D., and J.T. Parsons. 1995. pp125FAK-dependent tyrosine phosphorylation of paxillin creates a high-affinity binding site for Crk. *Molecular and cellular biology*. 15:2635-2645.

Schlaepfer, D.D., C.R. Hauck, and D.J. Sieg. 1999. Signaling through focal adhesion kinase. *Progress in biophysics and molecular biology*. 71:435-478.

Schlaepfer, D.D., and T. Hunter. 1996. Evidence for in vivo phosphorylation of the Grb2 SH2-domain binding site on focal adhesion kinase by Src-family protein-tyrosine kinases. *Molecular and cellular biology*. 16:5623-5633.

Schlaepfer, D.D., S.K. Mitra, and D. Ilic. 2004. Control of motile and invasive cell phenotypes by focal adhesion kinase. *Biochimica et biophysica acta*. 1692:77-102.

Schmoranzer, J., J.P. Fawcett, M. Segura, S. Tan, R.B. Vallee, T. Pawson, and G.G. Gundersen. 2009. Par3 and dynein associate to regulate local microtubule dynamics and centrosome orientation during migration. *Curr Biol*. 19:1065-1074.

Schmoranzer, J., G. Kreitzer, and S.M. Simon. 2003. Migrating fibroblasts perform polarized, microtubule-dependent exocytosis towards the leading edge. *J Cell Sci*. 116:4513-4519.

Schonteich, E., G.M. Wilson, J. Burden, C.R. Hopkins, K. Anderson, J.R. Goldenring, and R. Prekeris. 2008. The Rip11/Rab11-FIP5 and kinesin II complex regulates endocytic protein recycling. *J Cell Sci*. 121:3824-3833.

Schwartz, M.A. 2001. Integrin signaling revisited. *Trends Cell Biol*. 11:466-470.

Sekine, Y., Y. Okada, Y. Noda, S. Kondo, H. Aizawa, R. Takemura, and N. Hirokawa. 1994. A novel microtubule-based motor protein (KIF4) for organelle transports, whose expression is regulated developmentally. *J Cell Biol*. 127:187-201.

Serunian, L.A., K.R. Auger, and L.C. Cantley. 1991. Identification and quantification of polyphosphoinositides produced in response to platelet-derived growth factor stimulation. *Methods in enzymology*. 198:78-87.

Shattil, S.J., C. Kim, and M.H. Ginsberg. 2010. The final steps of integrin activation: the end game. *Nat Rev Mol Cell Biol*. 11:288-300.

Shi, F., and J. Sottile. 2011. MT1-MMP regulates the turnover and endocytosis of extracellular matrix fibronectin. *J Cell Sci*. 124:4039-4050.

Sieg, D.J., C.R. Hauck, D. Ilic, C.K. Klingbeil, E. Schaefer, C.H. Damsky, and D.D. Schlaepfer. 2000. FAK integrates growth-factor and integrin signals to promote cell migration. *Nature cell biology*. 2:249-256.

Sieg, D.J., C.R. Hauck, and D.D. Schlaepfer. 1999. Required role of focal adhesion kinase (FAK) for integrin-stimulated cell migration. *Journal of cell science*. 112 (Pt 16):2677-2691.

Simpson, K.J., L.M. Selfors, J. Bui, A. Reynolds, D. Leake, A. Khvorova, and J.S. Brugge. 2008. Identification of genes that regulate epithelial cell migration using an siRNA screening approach. *Nature cell biology*. 10:1027-1038.

Slack-Davis, J.K., K.H. Martin, R.W. Tilghman, M. Iwanicki, E.J. Ung, C. Autry, M.J. Luzzio, B. Cooper, J.C. Kath, W.G. Roberts, and J.T. Parsons. 2007. Cellular characterization of a novel focal adhesion kinase inhibitor. *The Journal of biological chemistry*. 282:14845-14852.

Small, J.V., T. Stradal, E. Vignal, and K. Rottner. 2002. The lamellipodium: where motility begins. *Trends Cell Biol*. 12:112-120.

Smilenov, L.B., A. Mikhailov, R.J. Pelham, E.E. Marcantonio, and G.G. Gundersen. 1999. Focal adhesion motility revealed in stationary fibroblasts. *Science*. 286:1172-1174.

Steffen, A., G. Le Dez, R. Poincloux, C. Recchi, P. Nassoy, K. Rottner, T. Galli, and P. Chavrier. 2008. MT1-MMP-dependent invasion is regulated by TI-VAMP/VAMP7. *Curr Biol*. 18:926-931.

Stehbens, S.J., M. Paszek, H. Pemble, A. Ettinger, S. Gierke, and T. Wittmann. 2014. CLASPs link focal-adhesion-associated microtubule capture to localized exocytosis and adhesion site turnover. *Nat Cell Biol*. 16:561-573.

Steinberg, F., K.J. Heesom, M.D. Bass, and P.J. Cullen. 2012. SNX17 protects integrins from degradation by sorting between lysosomal and recycling pathways. *J Cell Biol*. 197:219-230.

Streblow, D.N., J. Vomaske, P. Smith, R. Melnychuk, L. Hall, D. Pancheva, M. Smit, P. Casarosa, D.D. Schlaepfer, and J.A. Nelson. 2003. Human cytomegalovirus chemokine receptor US28-induced smooth muscle cell migration is mediated by focal adhesion kinase and Src. *J Biol Chem*. 278:50456-50465.

Stumpff, J., Y. Du, C.A. English, Z. Maliga, M. Wagenbach, C.L. Asbury, L. Wordeman, and R. Ohi. 2011. A tethering mechanism controls the processivity and kinetochore-microtubule plus-end enrichment of the kinesin-8 Kif18A. *Mol Cell*. 43:764-775.

Su, X., R. Ohi, and D. Pellman. 2012. Move in for the kill: motile microtubule regulators. *Trends Cell Biol*. 22:567-575.

Takesono, A., S.J. Heasman, B. Wojciak-Stothard, R. Garg, and A.J. Ridley. 2010. Microtubules regulate migratory polarity through Rho/ROCK signaling in T cells. *PLoS One*. 5:e8774.

Takino, T., H. Saeki, H. Miyamori, T. Kudo, and H. Sato. 2007. Inhibition of membrane-type 1 matrix metalloproteinase at cell-matrix adhesions. *Cancer Res*. 67:11621-11629.

Takino, T., Y. Watanabe, M. Matsui, H. Miyamori, T. Kudo, M. Seiki, and H. Sato. 2006. Membrane-type 1 matrix metalloproteinase modulates focal adhesion stability and cell migration. *Exp Cell Res*. 312:1381-1389.

Tanaka, E., T. Ho, and M.W. Kirschner. 1995. The role of microtubule dynamics in growth cone motility and axonal growth. *The Journal of cell biology*. 128:139-155.

Tanji, M., T. Ishizaki, S. Ebrahimi, Y. Tsuboguchi, T. Sukezane, T. Akagi, M.C. Frame, N. Hashimoto, S. Miyamoto, and S. Narumiya. 2010. mDia1 targets v-Src to the cell periphery and facilitates cell transformation, tumorigenesis, and invasion. *Molecular and cellular biology*. 30:4604-4615.

Teckchandani, A., N. Toida, J. Goodchild, C. Henderson, J. Watts, B. Wollscheid, and J.A. Cooper. 2009. Quantitative proteomics identifies a Dab2/integrin module regulating cell migration. *J Cell Biol*. 186:99-111.

Theisen, U., E. Straube, and A. Straube. 2012. Directional persistence of migrating cells requires Kif1C-mediated stabilization of trailing adhesions. *Dev Cell*. 23:1153-1166.

Thurston, S.F., W.A. Kulacz, S. Shaikh, J.M. Lee, and J.W. Copeland. 2012. The ability to induce microtubule acetylation is a general feature of formin proteins. *PLoS One*. 7:e48041.

Toutant, M., A. Costa, J.M. Studler, G. Kadare, M. Carnaud, and J.A. Girault. 2002. Alternative splicing controls the mechanisms of FAK autophosphorylation. *Mol Cell Biol*. 22:7731-7743.

Traub, L.M. 2009. Tickets to ride: selecting cargo for clathrin-regulated internalization. *Nat Rev Mol Cell Biol*. 10:583-596.

Tu, Y., S. Wu, X. Shi, K. Chen, and C. Wu. 2003. Migfilin and Mig-2 link focal adhesions to filamin and the actin cytoskeleton and function in cell shape modulation. *Cell*. 113:37-47.

Ussar, S., M. Moser, M. Widmaier, E. Rognoni, C. Harrer, O. Genzel-Boroviczeny, and R. Fassler. 2008. Loss of Kindlin-1 causes skin atrophy and lethal neonatal intestinal epithelial dysfunction. *PLoS genetics*. 4:e1000289.

Vadali, K., X. Cai, and M.D. Schaller. 2007. Focal adhesion kinase: an essential kinase in the regulation of cardiovascular functions. *IUBMB Life*. 59:709-716.
Valdembri, D., P.T. Caswell, K.I. Anderson, J.P. Schwarz, I. Konig, E. Astanina, F. Caccavari, J.C. Norman, M.J. Humphries, F. Bussolino, and G. Serini. 2009. Neuropilin-1/GIPC1 signaling regulates alpha5beta1 integrin traffic and function in endothelial cells. *PLoS biology*. 7:e25.
van der Flier, A., and A. Sonnenberg. 2001. Function and interactions of integrins. *Cell Tissue Res*. 305:285-298.
Vasiliev, J.M., I.M. Gelfand, L.V. Domnina, O.Y. Ivanova, S.G. Komm, and L.V. Olshevskaja. 1970. Effect of colcemid on the locomotory behaviour of fibroblasts. *J Embryol Exp Morphol*. 24:625-640.
Veale, K.J., C. Offenhauser, S.P. Whittaker, R.P. Estrella, and R.Z. Murray. 2010. Recycling endosome membrane incorporation into the leading edge regulates lamellipodia formation and macrophage migration. *Traffic*. 11:1370-1379.
Vicente-Manzanares, M., X. Ma, R.S. Adelstein, and A.R. Horwitz. 2009. Non-muscle myosin II takes centre stage in cell adhesion and migration. *Nature reviews. Molecular cell biology*. 10:778-790.
Vicente-Manzanares, M., D.J. Webb, and A.R. Horwitz. 2005. Cell migration at a glance. *Journal of cell science*. 118:4917-4919.
Wakida, N.M., E.L. Botvinick, J. Lin, and M.W. Berns. 2010. An intact centrosome is required for the maintenance of polarization during directional cell migration. *PLoS One*. 5:e15462.
Wang, P., C. Ballestrem, and C.H. Streuli. 2011a. The C terminus of talin links integrins to cell cycle progression. *The Journal of cell biology*. 195:499-513.
Wang, Y., H. Cao, J. Chen, and M.A. McNiven. 2011b. A direct interaction between the large GTPase dynamin-2 and FAK regulates focal adhesion dynamics in response to active Src. *Molecular biology of the cell*. 22:1529-1538.
Wang, Y., and M.A. McNiven. 2012. Invasive matrix degradation at focal adhesions occurs via protease recruitment by a FAK-p130Cas complex. *J Cell Biol*. 196:375-385.
Weaver, L.N., S.C. Ems-McClung, J.R. Stout, C. LeBlanc, S.L. Shaw, M.K. Gardner, and C.E. Walczak. 2011. Kif18A uses a microtubule binding site in the tail for plus-end localization and spindle length regulation. *Curr Biol*. 21:1500-1506.
Webb, D.J., J.T. Parsons, and A.F. Horwitz. 2002. Adhesion assembly, disassembly and turnover in migrating cells -- over and over and over again. *Nature cell biology*. 4:E97-100.
Webster, D.R., G.G. Gundersen, J.C. Bulinski, and G.G. Borisy. 1987. Differential turnover of tyrosinated and detyrosinated microtubules. *Proc Natl Acad Sci U S A*. 84:9040-9044.
Webster, D.R., J. Wehland, K. Weber, and G.G. Borisy. 1990. Detyrosination of alpha tubulin does not stabilize microtubules in vivo [published erratum appears in J Cell Biol 1990 Sep;111(3):1325-6]. *J Cell Biol*. 111:113-122.
Wen, Y., C.H. Eng, J. Schmoranzer, N. Cabrera-Poch, E.J. Morris, M. Chen, B.J. Wallar, A.S. Alberts, and G.G. Gundersen. 2004. EB1 and APC bind to mDia to stabilize microtubules downstream of Rho and promote cell migration. *Nat Cell Biol*. 6:820-830.
Wiesner, C., J. Faix, M. Himmel, F. Bentzien, and S. Linder. 2010. KIF5B and KIF3A/KIF3B kinesins drive MT1-MMP surface exposure, CD44 shedding, and extracellular matrix degradation in primary macrophages. *Blood*. 116:1559-1569.
Winograd-Katz, S.E., S. Itzkovitz, Z. Kam, and B. Geiger. 2009. Multiparametric analysis of focal adhesion formation by RNAi-mediated gene knockdown. *The Journal of cell biology*. 186:423-436.
Wordeman, L. 2005. Microtubule-depolymerizing kinesins. *Curr Opin Cell Biol*. 17:82-88.
Worthylake, R.A., and K. Burridge. 2003. RhoA and ROCK promote migration by limiting membrane protrusions. *J Biol Chem*. 278:13578-13584.
Wozniak, M.A., L. Kwong, D. Chodniewicz, R.L. Klemke, and P.J. Keely. 2005. R-Ras controls membrane protrusion and cell migration through the spatial regulation of Rac and Rho. *Mol Biol Cell*. 16:84-96.

Wu, X., A. Kodama, and E. Fuchs. 2008. ACF7 regulates cytoskeletal-focal adhesion dynamics and migration and has ATPase activity. *Cell*. 135:137-148.

Wu, X., S. Suetsugu, L.A. Cooper, T. Takenawa, and J.L. Guan. 2004. Focal adhesion kinase regulation of N-WASP subcellular localization and function. *The Journal of biological chemistry*. 279:9565-9576.

Xu, J., F. Wang, A. Van Keymeulen, P. Herzmark, A. Straight, K. Kelly, Y. Takuwa, N. Sugimoto, T. Mitchison, and H.R. Bourne. 2003. Divergent signals and cytoskeletal assemblies regulate self-organizing polarity in neutrophils. *Cell*. 114:201-214.

Xu, J., F. Wang, A. Van Keymeulen, M. Rentel, and H.R. Bourne. 2005. Neutrophil microtubules suppress polarity and enhance directional migration. *Proceedings of the National Academy of Sciences of the United States of America*. 102:6884-6889.

Yadav, S., S. Puri, and A.D. Linstedt. 2009. A primary role for Golgi positioning in directed secretion, cell polarity, and wound healing. *Molecular biology of the cell*. 20:1728-1736.

Yeo, M.G., M.A. Partridge, E.J. Ezratty, Q. Shen, G.G. Gundersen, and E.E. Marcantonio. 2006. Src SH2 arginine 175 is required for cell motility: specific focal adhesion kinase targeting and focal adhesion assembly function. *Molecular and cellular biology*. 26:4399-4409.

Yoon, S.O., S. Shin, and A.M. Mercurio. 2005. Hypoxia stimulates carcinoma invasion by stabilizing microtubules and promoting the Rab11 trafficking of the alpha6beta4 integrin. *Cancer Res*. 65:2761-2769.

Zaidel-Bar, R., M. Cohen, L. Addadi, and B. Geiger. 2004. Hierarchical assembly of cell-matrix adhesion complexes. *Biochemical Society transactions*. 32:416-420.

Zaidel-Bar, R., S. Itzkovitz, A. Ma'ayan, R. Iyengar, and B. Geiger. 2007. Functional atlas of the integrin adhesome. *Nature cell biology*. 9:858-867.

Zamir, E., and B. Geiger. 2001. Molecular complexity and dynamics of cell-matrix adhesions. *Journal of cell science*. 114:3583-3590.

Zhai, J., H. Lin, Z. Nie, J. Wu, R. Canete-Soler, W.W. Schlaepfer, and D.D. Schlaepfer. 2003. Direct interaction of focal adhesion kinase with p190RhoGEF. *J Biol Chem*. 278:24865-24873.

Zhang, H., J.S. Berg, Z. Li, Y. Wang, P. Lang, A.D. Sousa, A. Bhaskar, R.E. Cheney, and S. Stromblad. 2004. Myosin-X provides a motor-based link between integrins and the cytoskeleton. *Nature cell biology*. 6:523-531.

Zhu, C., and W. Jiang. 2005. Cell cycle-dependent translocation of PRC1 on the spindle by Kif4 is essential for midzone formation and cytokinesis. *Proc Natl Acad Sci U S A*. 102:343-348.